

Controlled Synthesis of Acrylic Polymers

A Thesis

Submitted to the

University of Pune

*In Partial Fulfillment of the Requirements
for the Degree of*

DOCTOR OF PHILOSOPHY

in

CHEMISTRY

by

ANUJ MITTAL

Division of Polymer Chemistry

National Chemical Laboratory

PUNE - 411 008

June 2006

Dedicated to

My parents, for making it possible to embark on this journey.

&

My wife, for making it possible to conclude it.

Acknowledgements

*Firstly, let me deeply pray and thank **Almighty** to shower me such a wonderful life with family and friends. A journey is easier when you travel together. Interdependence is certainly better than independence. Pursuing a Ph.D. is both painful and enjoyable experience. It's just like climbing a high peak, step-by-step, accompanied with hardships, frustration, encouragement, trust and with so many people's kind help. This thesis is a result of seven years of work whereby many people supported me. It is a pleasant aspect that I have now the opportunity to express my gratitude for all of them.*

First of all, I would like to give my sincere thanks to my honorific mentor, Dr. S. Sivaram, who accepted me as his Ph.D. student without any hesitation. It was those days when my mentor Prof. (Late) K. Kishore (Indian Institute of Science, IISc, Bangalore) left me un-groomed in the field of research. Dr. S. Sivaram mentorship was paramount in providing me consistent advice, patiently supervising me in right direction to target long-term career goals. He encouraged me not only to grow as an experimentalist and a chemist but also as an instructor and an independent thinker. His overly enthusiasm and integral view on research and his mission for providing 'only high-quality work and not less', has made a deep impression on me, without his help I could not have finished my work successfully. I owe him lots of gratitude for having me shown this way of research. He could not even realize how much I have learned from him. For everything you have done for me, Dr. Sivaram, my sincere thanks to you. I also express my deep gratitude to Dr. (Mrs.) Rama Sivaram for consistent moral boosting during the times of ill health.

I am also deeply indebted to my promotor Dr. D. Baskaran whose timely help, stimulating suggestions and consistent encouragement helped me all the time during the moments of stress and while writing my thesis. At last stage of my thesis, he enlightened my way of thinking ability through conversations, improvements and discussions. It is not sufficient to express my gratitude with only a few words for him.

My sincere thanks to Dr. M. G. Kulkarni, head Polymer Science and Engineering division, for providing me access to the facilities in the division. Additionally, I am very grateful to all the cooperation I received from other scientists, namely, Dr. P. P. Wadgaonkar, Dr. R. P. Singh, Dr. C. Ramesh, Dr. C. V. Avadhani, Dr. P. R. Rajamohanan (NMR facility), Dr. T. P. Mohandas, Mr. S. K. Menon and Mrs. D. A. Dhoble, of division is gratefully acknowledged. I am also thankful to all the members of PSE division NCL, for maintaining a cordial atmosphere. Myself will be failing in my duty if I do not mention the laboratory staff and administrative staff of NCL for their timely help. Needless to say, I would like to thank everyone who has helped me directly or indirectly in executing my work at NCL, only I am responsible for any inconsistencies, errors and other shortcomings.

I wish myself would never forget the company I had from my fellow research scholars, Subarna, Saptirishi, Mahua, Rajesh, Subramanyam, Arvind, Mahesh, Ravi, Manash, Shailendra, Shrojal, and Gnaneshwar). My special thanks to my labmates cum friends (Kedar and Mukesh) of my division and some of friends, Anupam (Telco), Sushanto (IBM), Tarun (Parametric), Swant (Kanbay), Savitha (α -metals), Pratiksha (HCL), Arun (Aldrich) and Soumen (HEMRL) for their love and cooperation.

Finally, and most importantly, I would like to thank my family for their life-long invaluable love, support, faith and allowing me to be ambitious, as I wanted. I especially owe to my parents for their sacrifices in bringing me to this stage, their consistent encouragements, and making me realize the value of hard work. It was under their watchful eye that I have gained so much drive and ability that has affected me to be steadfast and tackle challenges head on. My mom and dad I love you a lot and miss you every moment of time.

Last but not least, I am showered with a lovely loving friend cum wife, Prerna. We got tied together on 22nd April 2006, and I am greatly indebted to her who forms my backbone and origin of my happiness since past six years and will now be forever. Her constant love and support without any complaint has enabled me to complete my Ph.D. work successfully. Her understanding is well understood from the fact that she without any hesitation allowed me to leave for my thesis work immediately after my marriage day. I must say thanks to my in-laws, Dr. Prabhakar. P. Jadhav and Prabhavati who liked me and ushered with their blessings. I owe my every achievement to my parents and my wife.

Finally, I thank CSIR for the senior research fellowship and the Director, NCL for allowing me to carry out this work at this esteemed laboratory.

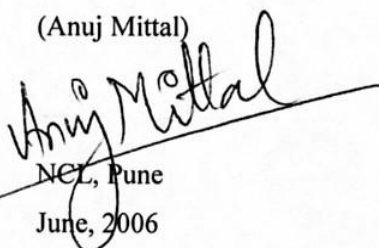
Anuj Mittal

June, 2006

Declaration

The research work presented in this thesis entitled "**Controlled Synthesis of Acrylic Polymers**" has been carried out at National Chemical Laboratory, Pune. This work is original and has not been submitted for any other institute or university for any other degree.

(Anuj Mittal)



NCL, Pune
June, 2006



राष्ट्रीय रासायनिक प्रयोगशाला
डॉ. होमी भाभा मार्ग, पुणे - 411 008.भारत
NATIONAL CHEMICAL LABORATORY
Dr. Homi Bhabha Road, Pune - 411 008 India.

डॉ. शिवराम

देशक

S. Sivaram

Director

CERTIFICATE

The research work presented in this thesis entitled “Controlled Synthesis of Acrylic Polymers” has been carried out under my supervision and is bonafide work of Mr. Anuj Mittal. This work is original and has not been submitted for any other degree or diploma of this or any other University.

Place: Pune

Date: 17-06-2006

(Dr. S. Sivaram)

(Research Guide)

Contents

Abstract	i
Abbreviations	iv
List of Tables	vi
List of Figures	ix
List of Schemes	xiii

Chapter 1: Introduction

	1
1. Introduction	
1.1. Polymers	1
1.2. Free radical polymerization	1
1.3. Living polymerization: prerequisites	2
1.4. Understanding and controlling radical polymerization	2
1.4.1. Criteria of “livingness” in radical polymerization	3
1.4.2. Reversible activation-deactivation equilibrium	4
1.5. Evolution of controlled radical polymerization (CRP)	4
1.5.1. Introduction	4
1.5.2. Classification of controlled radical polymerization	9
1.6. Atom transfer radical polymerization (ATRP)	11
1.6.1. Introduction	11
1.6.2. Atom transfer radical addition (ATRA)/ Kharasch addition in organic chemistry	11

1.6.2.1. Atom transfer radical addition (ATRA) to atom transfer radical polymerization (ATRP)	12
1.6.3. Tuning in ATRP-a multicomponent system	14
1.6.3.1. Catalysts	14
1.6.3.2. Ligands	16
1.6.3.3. Monomers	21
1.6.3.4. Initiators	22
1.6.4. Reverse ATRP	23
1.6.5. Perspectives and future Prospects	24
1.7. Scope and objectives of this thesis	24
1.8. References	25

Chapter 2: Experimental methods

2.1. Materials	29
2.2. Purification	30
2.2.1. Nitrogen or argon gas	30
2.2.2. Solvents	30
2.2.3. Monomers	31
2.2.4. Copper (I) halides	31
2.3. Synthesis of ligands	31
2.3.1. N- (<i>n</i> -propyl)-pyridylmethanimine (NPPI)	31
2.3.2. N,N'-dibenzylidene-ethane-1,2-diamine (NBED)	32
2.3.3. N,N'- <i>bis</i> (pyridin-2-ylmethylene)-ethane-1,2-diamine (NPMED)	33
2.3.4. N,N'- <i>bis</i> (1-phenylethylidene)-1,2-ethanediamine (NPEED)	34

2.3.5.	N,N'-dibenzylidene-ethane-1,2-diamine (NDBED)	35
2.3.6.	N,N'-bis(<i>n</i> -pentyl)-2,6-pyridylmethanimine (NBPPI)	35
2.3.7.	2,6-bis[1-(2,6-diisopropyl phenyl imino) ethyl] pyridine (BPIEP)	36
2.3.8.	N-((1E)-1-{6-[(1E)-N-phenylethanimidoyl]pyridin-2-yl}ethylidene) aniline) (NPEPEA)	38
2.3.9.	(N-((1E)-1-{6-[N-(aminophenyl)ethanimidyl]pyridin-2-yl}ethylidene)-N'-dimethyl benzene-1,4-diamine (NAPPDBD)	39
2.3.10.	2,6-bis[1-(2,6-diisopropyl-4-nitrophenylimino)ethylpyridine (BPNPIEP)	40
2.3.10.1.	Protection of amino group of 2,6-diisopropylaniline	41
2.3.10.2.	Nitration of protected amine	42
2.3.10.3.	Hydrolysis of protected amine	42
2.3.10.4.	Synthesis of imine ligand (BPNPIEP)	43
2.3.11.	2,6-bis[1-(2,6-diisopropyl,4-(N,N'-dimethylamino) phenylimino) ethyl] pyridine (BPDAPIEP)	44
2.3.11.1.	Reduction of protected nitro amine	44
2.3.11.2.	N-alkylation of protected nitro amine	45
2.3.11.3.	Hydrolysis of protected N-alkylated amine	46
2.3.11.4.	Synthesis of imine ligand (BPDAPIEP)	47
2.3.12.	2,6-bis(4,4-dimethyl-2-oxazolin-2-yl)pyridine (<i>dm</i> PYBOX)	47
2.3.12.1.	Synthesis of N,N'-(1,1-dimethyl-2-hydroxyethyl) pyridine-2,6-dicarboxamide)	47
2.3.12.2.	Synthesis of bisoxazoline (<i>dm</i> PYBOX)	49
2.4.	Synthesis of initiators	50
2.4.1.	1-phenylethyl bromide (1-PEBr)	50
2.4.2.	Benzyl thiocyanate (BzSCN)	51
2.4.3.	Ethyl-2-methyl-2-thiocyanatopropanoate (EMTP)	52
2.4.4.	3-bromo-3-methyl-butanone-2 (MBB)	53

2.4.5.	3-(bromomethyl)-4-methylfuran-2,5-dione (BMFD)	54
2.5.	Electrochemical studies of copper complexes	55
2.6.	General procedure for ATRP	56
2.6.1.	Polymerization of methyl methacrylate (MMA) in toluene	56
2.6.2.	Polymerization of styrene	56
2.6.3.	Polymerization of <i>t</i> -butylacrylate (<i>t</i> -BA)	57
2.6.4.	Polymerization of glycidylmethacrylate (GMA)	57
2.6.5.	Bulk polymerization of methyl methacrylate (MMA)	57
2.6.6.	Reverse ATRP of MMA	58
2.6.7.	Kinetics of polymerization and estimation of rate constants	58
2.6.8.	Free radical polymerization of methylvinylketone (MVK)	59
2.6.9.	ATRP of MVK	59
2.6.10.	Reverse ATRP of MVK	59
2.6.11.	Copolymerization of MVK and MMA by reverse ATRP	60
2.7.	Characterization techniques	60
2.8.	References	61

Chapter 3: Atom transfer radical polymerization of methyl methacrylate using 2,6-*bis*[1-(2,6-diisopropyl phenyl imino) ethyl] pyridine (BPIEP)- A tridentate ligand

3.1.	Introduction	62
3.2.	Results and discussion	63
3.2.1.	ATRP of MMA using BPIEP as ligand and EB <i>i</i> B as initiator	63
3.2.2.	Kinetics of bulk polymerization of MMA with BPIEP ligand	64
3.2.3.	Kinetics of polymerization of MMA with BPIEP ligand	65

3.2.3.1. Effect of ligand concentration	65
3.2.3.2. Effect of initiator concentration	67
3.2.3.3. Effect of solvent	68
3.2.3.4. Effect of solvent volume	70
3.2.3.5. Effect of temperature	72
3.2.3.6. Effect of initiator structure	74
3.2.3.7. Effect of catalyst concentration	76
3.2.3.8. Effect of [M]/ [I] ratios	76
3.2.3.9. Effect of ageing of the catalyst	77
3.2.3.10. Polymerization of glycidylmethacrylate (GMA), methyl acrylate (MA), styrene, and <i>t</i> -butylacrylate (<i>t</i> -BA).	78
3.2.3.11. Chain extension experiments	79
3.2.4. Kinetics of ATRP of MMA using bidentate and tridentate Schiff base imines.	80
3.2.5. Reverse ATRP of MMA in solution and bulk using BPIEP as ligand, CuX ₂ as catalyst and AIBN as initiator	83
3.3. Conclusions	86
3.4. References	87

Chapter 4: Influence of steric and electronic effects around the metal center in ATRP of MMA using *bis*(iminopyridine) ligand and EBiB as initiator.

4.1. Introduction	90
4.2. Results and discussion	92
4.2.1. Nature of tridentate ligand	92
4.2.2. Influence of steric crowding around metal center on the ATRP of MMA.	93

4.2.2.1. ATRP of MMA in toluene at 90 °C using tridentate N-donor as ligands and EB <i>i</i> B as initiator	93
4.2.3. Influence of electronic effects around metal center on the ATRP of MMA.	94
4.2.3.1. ATRP of MMA in toluene at 90 °C using tridentate N-donor as ligands and EB <i>i</i> B as initiator	94
4.2.4. Kinetic study of ATRP of MMA in toluene at 90 °C using NPEPEA as ligand and EB <i>i</i> B as initiator	96
4.3. Conclusions	98
4.4. References	98

Chapter 5: Influence on the nature of ligands on ATRP of MMA using Cu^IX as catalyst and EB*i*B as initiator.

5.1. Introduction	100
5.2. Results and discussion	103
5.2.1. ATRP of MMA in toluene at 90 °C with unconjugated α -diimines as ligands, CuBr as catalyst and EB <i>i</i> B as initiator.	103
5.2.1.1. ATRP of MMA using multidentate amines as ligands, CuBr as catalyst and EB <i>i</i> B as initiator.	104
5.2.1.2. ATRP of MMA in toluene at using tridentate N-donor as ligand, CuBr as catalyst and EB <i>i</i> B as initiator	105
5.3. Conclusions	106
5.4. References	106

Chapter 6: Study of novel initiators for ATRP of MMA

6.1. Introduction	109
6.2. Results and discussion	110
6.2.1 ATRP of MMA in toluene at 90 °C with different N-donors as ligands, CuBr as catalyst, and 3-bromo-3-methyl-butanone-2 (MBB) as initiator.	110
6.2.1.1. Influence of different N-donors as ligands on polymerization of MMA using MBB as initiator	110
6.2.1.2. Kinetic study of ATRP of MMA in toluene at 90 °C using BPIEP as ligand, CuBr as catalyst and MBB as initiator.	113
6.2.2 ATRP of MMA in toluene at 90 °C with BPIEP/CuBr as catalyst system, and BMFD as initiator.	114
6.2.2.1. ATRP of MMA in toluene at 90 °C using different N-donors as ligand, CuBr as catalyst, and BMFD as initiator	116
6.2.2.2. Structure of PMMA obtained using BMFD as initiator, BPIEP/CuBr as catalyst system	117
6.2.2.3. Analysis of the polymer end-groups	121
6.2.3 ATRP of MMA in toluene at 90 °C using tridentate N-donor, BPIEP, as ligand, CuBr as catalyst, and BPN as initiator.	123
6.2.3.1. Kinetic study of ATRP of MMA in toluene at 90 °C using BPIEP as ligand, CuBr as catalyst and BPN as initiator	124
6.3. Conclusions	126
6.4. References	126

Chapter 7: Atom transfer radical polymerization of methyl methacrylate using different N-donors as ligands, Cu^IX (X= Br, Cl, SCN) as catalyst and ethyl-2-methyl-2-thiocyanatopropanoate as initiator

7.1. Introduction	128
7.2. Results and discussion	130
7.2.1. Effect of nature of counterion.	130
7.2.2. Cyclic Voltammetry studies of the Cu ^I thiocyanate complexes in acetonitrile at room temperature	130
7.2.3. ATRP of styrene in diphenylether using <i>dn</i> Nbpy as ligand, Cu ^I X (X = Br, SCN) as catalyst and different initiation systems (R-SCN).	132
7.2.4. ATRP of MMA at 90 °C in toluene using unconjugated α-diimines, and NPPI as ligands, CuSCN as catalyst and ethyl-2-methyl-2-thiocyanatopropanoate (EMTP) as initiator.	134
7.2.5. ATRP of MMA at 90 °C in toluene using NPEED as ligand, Cu ^I X (X = Br, Cl, SCN) and EB <i>i</i> B as initiator.	135
7.2.6. ATRP of MMA at 90 °C in toluene using NPPI as ligands, Cu ^I X (X = Br, Cl, SCN) as catalyst and EMTP as initiator	136
7.3. Conclusions	137
7.4. References	137

Chapter 8: Atom transfer radical polymerization of methyl vinyl ketone

8.1. Introduction	139
8.2. Results and discussion	140
8.2.1. Free radical polymerization of MVK using AIBN	140
8.2.2. Polymerization of MVK using ATRP and reverse ATRP	142
8.2.3. Evidences for the coordination of copper halide and MVK	143
8.2.4. Copolymerization of MMA and MVK using reverse ATRP	149
8.3. Conclusions	150
8.4. References	150

Chapter 9: Summary and Conclusions

9.1. Summary and conclusions	152
9.2. Scope for future work	153

Controlled Synthesis of Acrylic Polymers

Abstract

Compared to living anionic polymerization, the use of radical polymerization methods appears more attractive from the point of view of ease of practice and the number of monomers capable of being polymerized. The evolution of techniques of controlled radical polymerization in recent years is an attempt to control the termination and transfer reaction leading to greater control over chain ends and polydispersity. Atom transfer radical polymerization (ATRP) has rapidly become one of the versatile methods in polymer synthesis. Copper catalyzed ATRP has been successively used in controlling polymerization of many styrenes, acrylates, methacrylates and several other relatively reactive monomers such as acrylamides, vinyl pyridines, and acrylonitrile. The objective of the present study is to examine the ATRP of methyl methacrylate (MMA) and other acrylates including styrene using Schiff base imines as N-donor ligands complexed with copper halide in conjunction with suitable initiators in order to achieve a controlled polymerization system. The study also involves a detailed investigation of a new tridentate N-donor ligand comprising batch, kinetic studies involving solvent, temperature, aging and substituents effects differing in electronic and steric property in ATRP. The other part of the study involves the use of novel initiators for ATRP. In the course of this investigation, ATRP of a vinyl ketone monomer, namely, methyl vinyl ketone was examined using an initiator which has structural similarity to the propagating radical.

- † The efficacy of a tridentate ligand, namely 2,6-*bis*[1-(2,6-diisopropylphenylimino)ethyl] pyridine (BPIEP) on ATRP of MMA was studied. The optimum condition for BPIEP ligand was found to be 100: 1: 1: 2 ([MMA]: [EBiB]: [CuBr]: [BPIEP]) ratio at 90 °C in anisole as well as toluene (33 %, v/v) resulted in well-defined PMMA with a narrow molecular weight distribution. Systematic studies were performed with respect to nature and volume of the solvent, initiator concentration, and temperature. The tridentate ligand, BPIEP, resulted in higher polymerization rates and initiator efficiencies at lower solvent volume. The rate of polymerization was slower with the tridentate ligand compared to a well-known

bidentate ligand, namely, N-(*n*-propyl)-2-pyridylmethanimine (NPPI). The reverse ATRP of MMA using Cu^{II}/AIBN system showed good control in solution as well as bulk. The ligand was also successfully used for the ATRP of methyl acrylate and glycidyl methacrylate.

- † The steric and electronic effects around metal center in atom transfer radical polymerization of methylmethacrylate at 90 °C using *bis*(imino) pyridine ligand was studied. Various tridentate N-donor molecules, having different steric and electronic environment were synthesized and characterized. Reducing the steric bulk on the ligand (BPIEP) results in loss of control in the polymerization of MMA. Kinetic studies of ATRP of MMA in toluene at 90 °C using N-((1E)-1-{6-[(1E)-N-phenylethanimidoyl]pyridin-2-yl}ethylidene)aniline) (NPEPA) resulted in curvature in the first order plot indicating termination reaction during the polymerization. However, using BPIEP as ligand resulted in PMMA ($[M]/[I] = 800$) with $M_{n,SEC} = 15,600$ with PDI = 1.16 and high initiator efficiency of 0.85. Thus, the favorable effects of steric and electronic effect of the ligand on ATRP could be demonstrated.
- † Four different unconjugated α -diimines, and a bisoxazoline were examined as N-donor ligands in the ATRP of MMA in toluene at 90 °C using CuBr as catalyst and EB*i*B as initiator. None of the unconjugated α -diimines gave acceptable polymerization behavior. A tridentate, bisoxazoline ligand (*dm*PYBOX) showed reasonable polymerization control for MMA under defined conditions.
- † 2-bromopropionitrile (BPN), 3-bromo-3-methyl-2-butanone (MBB) and 3-(bromomethyl)-4-methylfuran-2,5-dione (BMFD) were explored as initiators for ATRP of MMA. All the three initiators gave controlled polymerization of MMA. The apparent rate constant (k_{app}) and initiator efficiency (I_{eff}) decreased in the order BPN > MBB > EB*i*B. MBB works efficiently with a bulky tridentate N-donor ligand, namely, BPIEP. However, when used with well-known ligands such as, NPPI and *dn*Nbpy, the polymerization results are not satisfactory.
- † The efficacy of softer pseudo halogen (SCN⁻) as counterion in the initiator (R-X) as well as for catalyst (Cu^I-X) in copper catalyzed ATRP of MMA was studied. The chemistry of using thiocyanate both as counter ion for copper salt, CuSCN, and

initiator, R-SCN, was based on the premise that CuSCN forms stable complexes with bidentate ligands. The redox potentials obtained for copper complexes were in the range suitable for ATRP catalysts. However, the catalyst system RSCN/CuSCN was ineffective for controlled polymerization of MMA and styrene.

- † The feasibility of ATRP of methylvinylketone (MVK) was examined by varying the nature of ligands as well as initiators. Inability to polymerize MVK in the presence of copper catalyst was attributed to the presence of extended coordination of MVK with copper.

Abbreviations

ATRA	Atom transfer radical addition
ATRP	Atom transfer radical polymerization
BMFD	3-(bromomethyl)-4-methylfuran-2,5-dione
BPIEP	2,6- <i>bis</i> [1-(2,6-diisopropylphenylimino) ethyl] pyridine
BPN	2-bromopropionitrile
BzSCN	Benzyl thiocyanate
CRP	Controlled radical polymerization
<i>t</i> -BA	<i>tert</i> -butylacrylate
DCM	Dichloromethane
DAP	2,6-Diacetyl pyridine
DIPA	2,6-Diisopropyl aniline
DMF	Dimethylformamide
<i>dm</i> PYBOX	2,6- <i>bis</i> (4,4-dimethyl-2-oxazolin-2-yl) pyridine
<i>dn</i> Nbpy	4,4'-di (<i>n</i> -nonyl) 2,2'-bipyridine
DPE	Diphenyl ether
E_a	Activation energy
EB <i>i</i> B	Ethyl-2-bromoisobutyrate
EMTP	Ethyl-2-methyl-2-thiocyanatopropanoate
GMA	Glycidyl methacrylate
GC	Gas chromatography
GPC	Gel permeation chromatography
HMTETA	1,1,4,7,10,10-hexamethyl triethylenetetramine
k_{app}	Apparent rate constant of propagation

MA	Methyl acrylate
MALDI-TOF MS	Matrix assisted laser desorption/ionization-time of flight mass spectrometry
MBB	3-bromo-3-methyl-butanone-2
MMA	Methyl methacrylate
MWD	Molecular weight distribution
NPPI	N-(<i>n</i> -propyl)-2pyridylmethanimine
PDI	Polydispersity index
PMDETA	N,N,N',N',N''-pentamethyldiethylenetriamine
PMMA	Poly(methyl methacrylate)
PS	Polystyrene
PTSA	<i>p</i> -Toluene sulfonic acid
RAFT	Reversible addition fragmentation chain-transfer polymerization
SEC	Size exclusion chromatography
TBAF	Tetra butyl ammonium flouride
TGA	Thermogravimetric analysis
THF	Tetrahydrofuran

List of Tables

Table	Page no.
1.1 Comparison of NMP, ATRP and degenerative transfer systems	8
1.2 Kinetic parameters for various CRPs	10
1.3 Copper Based N-donors employed in CRP	18
3.1 ATRP of MMA in toluene using 2,6-bis[1-(2,6-diisopropyl phenyl imino) ethyl pyridine (BPIEP) as ligand	63
3.2 Kinetic data of bulk ATRP of MMA at 90 °C using BPIEP as ligand	65
3.3 Effect of ligand concentration in ATRP of MMA in toluene at 90 °C.	67
3.4 ATRP of MMA in toluene at 90 °C	68
3.5 Effect of solvents in batch ATRP of MMA at 90 °C	69
3.6 Kinetic study of the effect of solvents in ATRP of MMA at 90 °C	70
3.7 Kinetic data for ATRP of MMA in toluene (33%, v/v) at different polymerization temperatures	72
3.8 Effect of initiators in ATRP of MMA in toluene (66%, v/v) using CuBr/BPIEP as catalyst system at 90 °C	75
3.9 ATRP of MMA in toluene (66%, v/v) with different catalyst concentration	76
3.10 ATRP of MMA at different DP values	77
3.11 Ageing of the BPIEP/CuBr complex using different concentration of solvent in ATRP of MMA at 90 °C	77
3.12 ATRP of different monomers using BPIEP as ligand, CuBr as catalyst and α -bromo compounds as initiators	79
3.13 Kinetic studies of ATRP of MMA at 90 °C using CuBr/ N-(<i>n</i> -propyl)-2 pyridylmethanimine as ligand	81
3.14 Comparison of type of ligands in ATRP of MMA in different solvents	83
3.15 Reverse ATRP of MMA using different N-donors at 70 °C	85

3.16	Summarized kinetic data for bidentate and tridentate ligand in ATRP of MMA	86
4.1	Effect of steric bulk in ligand structure and catalyst in ATRP of MMA	94
4.2	Effect of electronic properties of ligand on ATRP of MMA	95
4.3	Electronic effect of ligands on ATRP of MMA at different [M]/[I] ratios	95
4.4	Effect of ligand structure complexed with CuX in ATRP of MMA	97
5.1	Literature data for ATRP of MMA using CuBr/L as catalyst system and EBiB as initiator.	101
5.2	Literature data for TON obtained for PMMA by ATRP	102
5.3	ATRP of MMA with unconjugated α -diimines as ligands	104
5.4	ATRP of MMA with multidentate amine as ligands	105
5.5	ATRP of MMA with different N-donor as ligand	106
6.1	ATRP of MMA using MBB as initiator at 90 °C/5.5 h	111
6.2	Kinetic study of ATRP of MMA at 90 °C using MBB	113
6.3	Batch ATRP of MMA using BMFD as initiator/5.5 h	115
6.4	ATRP of MMA using BMFD as initiator at 90 °C/ 5.5 h	117
6.5	Batch ATRP of MMA at 90 °C using BPN as initiator	124
6.6	Kinetic study of ATRP of MMA at 90 °C using BPN	126
6.7	Comparison of apparent rate constant in ATRP of MMA	126
7.1	Redox potentials of Cu ^I SCN- bidentate imine complexes in acetonitrile at room temperature	131
7.2	ATRP of Styrene using Cu ^I X (X = Br, SCN)/ <i>dn</i> Nbpy as catalyst system	133
7.3	ATRP of MMA using EMTP as initiator and CuSCN as catalyst and different ligands	134
7.4	Color of the CuSCN Complex	135
7.5	ATRP of MMA using NPEED as ligand, EBiB as initiator and various catalysts	136
7.6	ATRP of MMA using NPPI as ligand, EMTP as initiator and various copper salts	136

8.1	Unsuccessful polymerization of methyl vinyl ketone using copper mediated ATRP and reverse ATRP processes	142
8.2	IR, UV and ^1H NMR shifts on mixing methyl vinyl ketone and copper bromide	145

List of Figures

Figure		Page no.
1.1	Schematic effect of slow initiation, transfer, termination and exchange on: a) kinetics, b) molecular weights for CRP systems	9
2.1	Structures of bidentate Schiff base imines	31
2.2	¹ H-NMR spectrum of N- (<i>n</i> -propyl)-2-pyridylmethanimine in CDCl ₃	32
2.3	¹ H-NMR spectrum of N, N'-dibenzylidene-ethane-1, 2-diamine in CDCl ₃	33
2.4	¹ H-NMR spectrum N,N'- <i>bis</i> -pyridin-2-yl-methylene-ethane-1,2-diamine in CDCl ₃	34
2.5	¹ H-NMR spectrum N,N'- <i>bis</i> (1-phenylethylidene)-1,2-ethanediamine in CDCl ₃	34
2.6	¹ H-NMR spectrum N, N'-dibenzylidene-ethane-1, 2-diamine in acetone-D ₆	35
2.7	¹ H-NMR spectrum N, N'- <i>bis</i> -(<i>n</i> -pentyl)-2,6-pyridylmethanimine in CDCl ₃	36
2.8	Schiff base imine condensation using Dean Stark apparatus	37
2.9	¹ H-NMR spectrum 2,6- <i>bis</i> [1-(2,6-diisopropylphenylimino)ethyl]pyridine in CDCl ₃	38
2.10	¹ H-NMR spectrum of N-((1E)-1-{6-[(1E)-N-phenylethanimidoyl]pyridin-2-yl} ethylidene) aniline in CDCl ₃	38
2.11	¹³ C-NMR spectrum of N-((1E)-1-{6-[(1E)-N-phenylethanimidoyl] pyridin-2-yl} ethylidene) aniline in CDCl ₃	39
2.12	¹ H-NMR spectrum of (N-((1E)-1-{6-[N-(aminophenyl)ethanimidoyl] pyridin-2-yl} ethylidene)-N',N'-dimethyl benzene -1,4-diamine in CDCl ₃	40
2.13	¹³ C-NMR spectrum of (N-((1E)-1-{6-[N-(aminophenyl)ethanimidoyl]pyridin-2-yl} ethylidene)-N',N'-dimethyl benzene -1,4-diamine in CDCl ₃	40
2.14	¹ H-NMR spectrum of protected amino of 2,6-DIPA in DMSO-D ₆	41
2.15	¹ H-NMR spectrum of 8 in CDCl ₃	42
2.16	¹ H-NMR spectrum after hydrolysis of <i>p</i> -nitro-protected-2,6-DIPA in CDCl ₃	43
2.17	¹ H-NMR spectrum of 2,6- <i>bis</i> [1-(2,6-diisopropyl-4-nitrophenylimino)ethyl]pyridine in CDCl ₃	43
2.18	¹ H-NMR spectrum of 10 in CDCl ₃	45
2.19	¹ H-NMR spectrum of 11 in CDCl ₃	46

2.20	¹ H-NMR spectrum of 12 in CDCl ₃	46
2.21	¹ H-NMR spectrum of 2,6-bis[1-(2,6-diisopropyl,4-(N,N'-dimethylamino)phenylimino) ethyl] pyridine in CDCl ₃	47
2.22	¹ H-NMR spectrum of N,N'-(1,1-dimethyl-2-hydroxyethyl)pyridine-2,6-dicarboxamide in CDCl ₃	48
2.23	¹ H-NMR spectrum of 2,6-bis(4,4-dimethyl-2-oxazolin-2-yl)pyridine in CDCl ₃	49
2.24	¹³ C-NMR spectrum of 2,6-bis(4,4-dimethyl-2-oxazolin-2-yl)pyridine in CDCl ₃	49
2.25	¹ H-NMR spectrum of 1-phenylethyl bromide in CDCl ₃	51
2.26	¹ H-NMR spectrum of benzyl thiocyanate (BzSCN) in CDCl ₃	52
2.27	¹ H-NMR spectrum of ethyl 2-methyl-2-thiocyanatopropanoate in CDCl ₃	53
2.28	¹ H-NMR of 3-bromo-3-methyl-2-butanone in CDCl ₃	54
2.29	¹³ C-NMR of 3-bromo-3-methyl-2-butanone in CDCl ₃	54
2.30	¹ H-NMR of 3-(bromomethyl)-4-methylfuran-2,5-dione in CDCl ₃	55
2.31	¹³ C-NMR of 3-(bromomethyl)-4-methylfuran-2,5-dione in CDCl ₃	55
3.1	First order kinetic plot for the bulk ATRP of MMA at 90 °C. [MMA] = 3.12 M. [MMA]: [EB <i>i</i> B]: [CuBr]: [BPIEP] = 100: 1: 1: 2.	64
3.2	Dependence of molecular weight and polydispersity on conversion for the bulk ATRP of MMA at 90 °C with [EB <i>i</i> B] = 0.0312M. Open symbols represent polydispersities and filled symbol represents <i>M_n</i> -(GPC).	64
3.3	Semi logarithmic kinetic plots for the ATRP of MMA at 90 °C in toluene (66 %, v/v). [MMA] = 3.12 M. [MMA]: [EB <i>i</i> B]: [CuBr]: [BPIEP] = 100: 1: 1: X	66
3.4	Plot of <i>k_{app}</i> as a function of increasing ligand concentration (BPIEP) at constant CuBr concentration for the solution ATRP of MMA in toluene at 90 °C. [EB <i>i</i> B] = [CuBr] = 0.0312 M	66
3.5	Semi logarithmic kinetic plot for the solution ATRP of MMA at 90 °C where [MMA] = 3.12 M. [MMA]: [EB <i>i</i> B]: [CuBr]: [BPIEP] = 100: 0.5: 1: 2	68
3.6	Semi logarithmic kinetic plots for the ATRP of MMA at 90 °C in toluene and anisole. [MMA] = 3.12 M. [MMA]: [EB <i>i</i> B]: [CuBr]: [BPIEP] = 100: 1: 1: 2	72
3.7	Dependence of molecular weight and polydispersity on conversion in the solution ATRP of MMA at 90 °C with [EB <i>i</i> B] = 0.0312M. Open symbols represent polydispersities and filled symbol represents <i>M_n</i> -(GPC).	72

3.8	First order kinetic plots showing the effect of the polymerization temperature on ATRP of MMA in toluene. [MMA] = 3.12 M; [MMA]: [EB <i>i</i> B]: [CuBr]: [BPIEP] = 100: 1: 1: 2	73
3.9	Temperature effect on the molecular weight and polydispersity with respect to conversion in the solution ATRP of MMA at 90 °C with [EB <i>i</i> B] = 0.0312M. Open symbols represent polydispersities and filled symbol represents M_n -(GPC).	73
3.10	Plot of $\ln k_{app}$ vs 1/T for ATRP of MMA initiated by EB <i>i</i> B with CuBr/BPIEP as ligand in toluene. [MMA] = 3.12 M. [MMA]: [EB <i>i</i> B]: [CuBr]: [BPIEP] = 100: 1: 1: 2	74
3.11	Gel Permeation chromatograms of PMMA-Br (before and after chain extension) by ATRP initiated by EB <i>i</i> B with CuBr/BPIEP as catalyst in toluene. [MMA] = 3.12 M. [MMA]: [EB <i>i</i> B]: [CuBr]: [BPIEP] = 100: 1: 1: 2	80
3.12	Semi logarithmic kinetic plots for the ATRP of MMA in toluene (66 %, v/v) at 90 °C. [MMA] = 3.12 M. [MMA]: [EB <i>i</i> B]: [CuBr]: [NPPI] = 100: 1: 1: 2.	82
3.13	Dependence of molecular weight and polydispersity on conversion for the ATRP of MMA in toluene (66 %, v/v) at 90 °C with [EB <i>i</i> B] = 0.0312M. Open symbols represent polydispersities and filled symbol represents M_n -(GPC).	82
4.1	Tridentate imines as N-donors in ATRP	91
4.2	Semi logarithmic kinetic plots for the ATRP of MMA in toluene at 90 °C using EB <i>i</i> B as initiator. [MMA] = 3.12 M. [MMA]: [EB <i>i</i> B]: [CuBr]: [Ligand] = 100: 1: 1: 2	98
4.3	Dependence of molecular weight and polydispersity on conversion in the solution ATRP of MMA at 90 °C with [EB <i>i</i> B] = 0.0312M	98
5.1	Structures of various Schiff base imines used in ATRP	103
6.1	Structure of the initiators employed in ATRP	110
6.2	Semi logarithmic kinetic plot for the ATRP of MMA in toluene at 90 °C using MBB as initiator. [MMA] = 4.68 M. [MMA]: [MBB]: [CuBr]: [BPIEP] = 100: 1: 1: 2	114
6.3	Dependence of molecular weight and polydispersity on conversion in the solution ATRP of MMA at 90 °C with [MBB] = 0.0468 M. Open symbols represent M_n -(GPC).	114
6.4	Reaction of PMDETA with BMFD (2)	116
6.5	GPC eluogram of PMMA (Run 3, Table 6.3)	118
6.6	GPC eluogram of PMMA (Run 3, Table 6.4)	118
6.7	¹ H NMR (500 MHz) spectrum of PMMA (Run 3, Table 6.3) in CDCl ₃	118

6.8	^{13}C NMR in CDCl_3 of PMMA (Run 3, Table 6.3) obtained by ATRP	119
6.9	DEPT spectrum of PMMA (Run 3, Table 6.3) obtained by ATRP in CDCl_3	119
6.10	FT-IR of low molecular weight PMMA using KBr pellet	120
6.11	GPC eluograms of the precursor PMMA, PEG_OMe and PMMA- <i>co</i> -PEG_OMe after 48 h.	123
6.12	GPC eluograms showing the formation of PMMA- <i>co</i> -PEG_OMe during the reaction at 16 h and 48 h.	123
6.13	^1H NMR of the PMMA- <i>co</i> -PEG_OMe after 48 h in CDCl_3	123
6.14	Semi logarithmic kinetic plot for the ATRP of MMA in toluene at 90 °C using BPN as initiator. $[\text{MMA}] = 4.68 \text{ M}$. $[\text{MMA}]: [\text{BPN}]: [\text{CuBr}]: [\text{BPIEP}] = 100: 1: 1: 2$.	125
6.15	Dependence of molecular weight and polydispersity on conversion in the solution ATRP of MMA at 90 °C with $[\text{BPN}] = 0.0468 \text{ M}$. Open symbols represent polydispersities and filled symbol represents M_n -(GPC).	125
8.1	Copolymer of poly (VAc- <i>co</i> -MVK) (a) SEC eluogram (i) before oxidation and (ii) after oxidation of PMVK and (b) ^1H NMR spectrum in CDCl_3	141
8.2	^1H -NMR spectra of admixture residue after removing excess MVK in CDCl_3 (a) neat MVK, (b) residue of 1:1 mixture of MVK and CuBr, and (c) residue of CuBr mixed with excess of MVK.	144
8.3	(a) FTIR spectra showing stretching frequencies of MVK and (b) MVK-CuBr over KBr pellet	146
8.4	Solutions of CuBr (a) homogeneous in excess of MVK (4 mg/ mL) and (b) heterogeneous in excess MMA (5 mg/ mL)	146
8.5	TGA of viscous residue of $(\text{MVK})_m\text{-(CuBr)}_n$ admixture after removing all free MVK under vacuum. The calculation indicates 0.97:0.30 mole ratio of MVK:CuBr in the complex. This supports the extended coordination of MVK with CuBr through vinyl as well as carbonyl groups	147
8.6	Proposed extended-coordinative structure of $(\text{MVK})_m\text{-(CuBr)}_n$ based on X-ray crystal structure of MVK-CuCl. Note that the structure shows both trans-conformation, inter and intra molecular MVK coordination with CuX dimer	148
8.7	The order of monomer coordination with copper halide	148
8.8	^{13}C NMR spectrum of the poly (MMA- <i>co</i> -MVK) obtained by reverse ATRP in CDCl_3	149

List of Schemes

Scheme		Page no.
1.1	Reversible activation-deactivation equilibrium	4
1.2	Examples of controlled radical polymerization	7
1.3	Schematic description of different mechanisms involving controlled radical polymerization	10
1.4	Atom or group transfer in ATRP	11
1.5	Atom transfer radical addition chain reaction	12
1.6	Repetitive cycle of radical addition in ATRP: ATRA to ATRP	13
1.7	Copper catalyzed atom transfer radical polymerization (ATRP)	13
1.8	Possible geometries of the copper bipyridine complex in two different oxidation states. (a) T: <i>Tetrahedral</i> , (b) SP: <i>Square planar</i> , (c) Oh: <i>Octahedral</i> , and (d) tbp: <i>Trigonal bipyramidal</i>	16
1.9	ATRP equilibrium with a copper halide complex containing two 2,2'-bipyridine units as ligands	17
2.1	Structures of tridentate Schiff base imines	37
2.2	Synthesis of 4-nitro-2,6-diisopropyl aniline	41
2.3	Synthetic route to prepare 4-N,N-dimethyl- 2,6-diisopropyl aniline	44
2.4	Synthetic route to 2,6- <i>bis</i> (4,4-dimethyl-2-oxazolin-2-yl)pyridine	48
2.5	Reaction of water with phosphorous tribromide	50
2.6	Synthesis of 3-bromo-3-methyl-butanone-2	53
4.1	Structures of various Schiff base imines utilized for ATRP of MMA	93
6.1	Structural features of a polymer chain prepared by ATRP	109
6.2	ATRP of MMA using BMFD as initiator	119
6.3	Mechanism of intramolecular ring closure	121
7.1	Structures of possible CuBr/dNbpy complexes in solution	128
8.1	Synthesis of poly (vinyl acetate) copolymers with controlled molecular weight using post-polymer analogous reactions of poly (methyl vinyl ketone)	140

Chapter 1. Introduction

1. Introduction

1.1. Polymers

Plastic, derived from the Greek '*plassein*' meaning '*to mold*' or '*to shape*', is often used extensively to denote the class of polymer materials as a whole. Polymers belong to some of the nature's most sophisticated molecules and are the material of choice for a wide variety of applications. Polymers provided man with replacement of scarce materials like silk, wool, wood and metals. Today they are indispensable to human kind providing man with a range of materials ranging from soft rubber like materials to tough plastics, from silk like fibers to fibers with the tenacity of steel.¹⁻⁴ Only during the last few decades it was recognized that polymers can also be endowed with functional properties beyond the scope of traditional structural materials like wood, metals and ceramics. Just 'making macromolecules' is no longer sufficient rather the aspects of design in the synthesis of macromolecules is gaining increasing importance. Using a set of monomer(s) one can create a variety of polymer architectures with differing macroscopic properties by tailoring the chain length distribution, monomer sequence distribution, tacticity, nature of functionality and degree of branching.

1.2. Free radical polymerization

Free radical polymerization is the most important and the oldest method for synthesizing polymers. Approximately, 50% of all synthetic polymers are prepared via radical process.^{5,6} The success of free radical polymerization is due to the fact that a large number of monomers are amenable for polymerization by this method. Furthermore, free radical polymerization is more forgiving with regard to adventitious impurities.⁵ Despite its tremendous utility, radical polymerization has been considered difficult to control because of low selectivity and high reactivity of the propagating radical species. Radicals are neutral, in contrast to their ionic counterparts, and, thus, have pronounced tendency to undergo recombination or disproportionation reaction. A significant drawback of free radical polymerizations is that they yield polymers with uncontrolled molecular weights and high

polydispersities. Therefore, defining suitable conditions for a well controlled free radical polymerization has been one of the long-standing goals in polymer chemistry.

1.3. Living polymerization: prerequisites

Living anionic polymerization was first defined by Szwarc ⁷ as a chain growth process without chain breaking reactions ⁸ (i.e. transfer and termination). Such a polymerization provides end-group control and enables the synthesis of block copolymers by sequential monomer addition. Additional requirements of living polymerization includes the complete consumption of initiator at early stages ($k_i \gg k_p$) of the polymerization and the exchange between the species of various reactivities should be fast in comparison to propagation.⁹⁻¹¹ The number of active sites during polymerization is constant and is equal to the number of initiator molecules used for initiation of the reaction. As a consequence, the number average degree of polymerization is determined by the molar ratio of monomer converted to initiator, i.e., $DP_n = \Delta[M]/[I]_o$, under such conditions, polydispersity is close to a Poisson distribution ¹² ($M_w/M_n \approx 1 + 1/DP$).

1.4. Understanding and controlling radical polymerization

Free radical polymerizations, wherein, the incidence of transfer and termination are substantially low are termed as *controlled* polymerization. Greszta *et. al* defined controlled radical polymerization as one in which the amount of terminated chains does not exceed 5 % relative to the total number of chains present in the system. ¹³

1.4.1. Criterion of “livingness” in radical polymerization

In a conventional radical polymerization systems a chain is born, grows, and dies within approximately 1s; during this time it is not possible to perform any synthetic manipulations such as chain extension, end-functionalization etc. On the other hand, under controlled radical polymerization, chains grow during several hours enabling precise macromolecular engineering. Long lifetime of chain requires sufficiently low concentration of growing radicals but also sufficiently high concentration of propagating chains, i.e., (a) concentration of growing radicals ($<10^{-7}M$) or R_t/R_p should be low, and (b) polymer chains

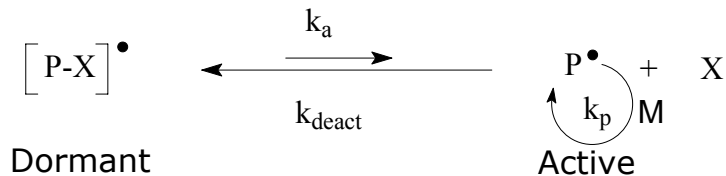
are kept to short lengths (ν).¹³ The ratio of rate of termination to that of propagation is given as,

$$\frac{R_t}{R_p} = \frac{k_t[P^\bullet]^2}{k_p[M][P^\bullet]} = \frac{k_t[P^\bullet]}{k_p[M]} = \frac{1}{\nu} \quad (1.1)$$

From equation 1.1, the ratio of rate of propagation to that of termination (also termed as “livingness”) decreases with increase in $[P^\bullet]$ because termination is second order ($k_t[P^\bullet]^2$) and propagation is first order ($k_p[M][P^\bullet]$) with respect to growing radical. Therefore, the contribution of termination reaction and the proportion of terminated chains increase with the concentration of free radicals. Also, it has been shown that the proportion of terminated chains can be reduced when polymer chains are kept to short lengths (ν).¹³ Thus, well-defined polymers from radical polymerization may be formed only if chains are relatively short and concentration of free radicals is low. These two criterion are in apparent contradiction but can be accommodated via reversible deactivation of growing free radicals in a way similar to the deactivation of growing carbocations.¹⁴ Thus, the dynamics of equilibrium between a growing radical and a dormant species defines the “extent of livingness” of the propagating radical.

1.4.2. Reversible activation-deactivation equilibrium^{13,14}

In ionic reactions, active species with various reactivities coexist (free ions, ions pairs, aggregates, covalent species, etc.). If they propagate simultaneously but with different rate constants, a polymodal molecular weight distribution may result. Polydispersity will depend on the rate of exchange between these species. In case where exchange is much faster than propagation, narrow polydispersities can be expected. When one of the species involved in equilibrium is stable enough that it does not undergo propagation the two-state system can be called a *reversible deactivation* system, based on the reversible formation of inactive or ‘dormant’ species. Thermodynamically, the equilibrium must lie towards the side of dormant chain ends. Kinetically this exchange should be very fast. Dormant species are covalent in nature and active species can be ions, ion-pairs, or radicals.



Scheme 1.1. Reversible activation-deactivation equilibrium

In general, the above criteria of livingness can be achieved only if there exist a fast equilibrium between dormant-active species ($k_{\text{act}} \cdot [P-X] = k_{\text{deact}} \cdot [P^{\bullet}]$), and the equilibrium always lies towards the side of dormant species ($k_{\text{act}} \approx 0.1-1 \times 10^{-3} \text{ s}^{-1}$ and $k_{\text{deact}} \approx 10-10^3 \text{ s}^{-1}$). The establishment of above equilibrium results in a low, persistent concentration of radicals. Therefore, the chain length will depend on the sum of concentration of active and dormant species, i.e., initiator, $DP_n = \Delta[M]/([P-X]^{\bullet} + [P^{\bullet}])$. Overall, the three basic requirements for achieving controlled radical polymerization are given as,

- a. Fast exchange between dormant and growing radicals ($k_{\text{deact}} > k_{\text{act}}$)
- b. A small proportion of chains involved in chain breaking reactions, and
- c. Fast and quantitative initiation ($k_i \geq k_p$)

1.5. Evolution of controlled radical polymerization (CRP)

In spite of two major chain-breaking reactions, free radical polymerization is still one of the most important commercial processes for the synthesis of a variety of useful polymers. Also, free radical polymerization occurs at 25 to 100 °C and most often in water, as suspension, solution or emulsion. This is in contrast to ionic polymerization that often requires expensive organic solvents, complete removal of moisture and oxygen (< 10 ppm) and temperatures lower than ambient. Therefore, there exists a strong motivation for extending the concept of controlled polymerization from ionic to radical processes.

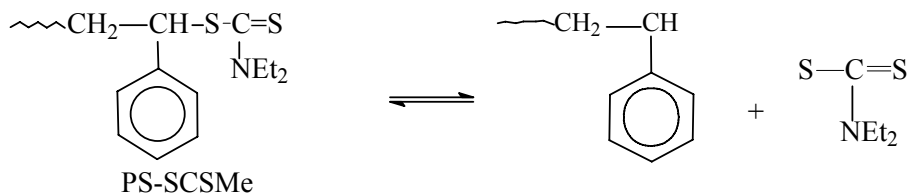
1.5.1 Introduction

The first demonstration of the possibility of controlled radical polymerization was the use of 3,3,4,4-tetraphenylhexane (TPH) as an initiator in the polymerization of methyl methacrylate and styrene.¹⁵ The initiator efficiencies were very low and the polydispersities

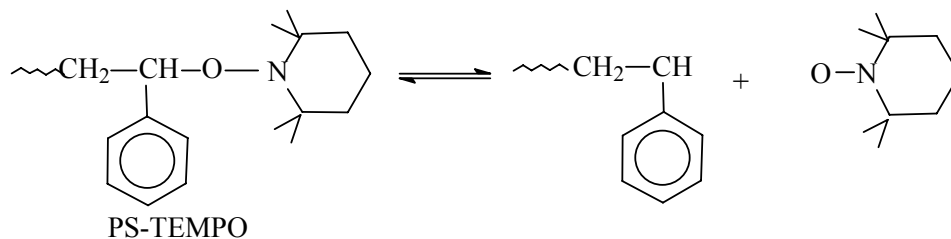
of polymers obtained were relatively high. Also, the increase in molecular weight was much higher than predicted by $DP_n = \Delta[M]/[I]_0$. Although Borsig *et al.*¹⁶ did not specifically call this polymerization a controlled polymerization, yet this was the first demonstration of using a counter radical to reversibly deactivate a growing polymer chains. He also demonstrated that these macroinitiators could be used in the preparation of block copolymers. Similarly, Lee *et al.*¹⁷ reported that polymerization of methyl methacrylate (MMA) initiated by benzoylperoxide (BPO) in presence of chromium (III) acetate resulted in an increase of molecular weight with conversion. They also reported the formation of block copolymers. Though the idea of controlled radical polymerization using stable or persistent radicals first appeared in 1969¹⁶ and 1979¹⁷, it was not recognized until later that persistent radical effect^{18,19} was the operative mechanism in these polymerizations. Other examples of controlled radical polymerization by forming stable persistent radicals include the use of organoaluminum compound and the formation of hypervalent phosphoranyl radicals. Mardare *et al.* reported controlled polymerization of vinyl acetate using an $AlR_3/bpy/TEMPO$ system.²⁰

Otsu *et al.*²¹ introduced the use of the term “living radical polymerization” during his work on the use of disulfides to polymerize styrene and methylmethacrylate. These disulfides photochemically dissociate resulting in the formation of S-centered radicals, which not only polymerize but also reversibly terminate growing radicals. Additionally, the formed radicals can also participate in transfer processes. Such compounds were termed as *iniferters* (*initiator*, *transfer* agent, and *terminating* agent) and allow the synthesis of block copolymers.²² A practical drawback of this system is the occurrence of side reactions which lead to the loss of chain-end functionality.²³ However, later Druliner and coworkers²⁴ developed a system where a long-living oxygen centered radicals, formed by reaction with electron acceptors, enable acrylate block copolymer synthesis. Arvanitopoulos *et al.*²⁵ used cobalttoximes in “living” radical polymerization under photochemical conditions. To polymerize acrylates, the procedure reported by Arvanitopoulos was modified by Wayland *et al.*²⁶

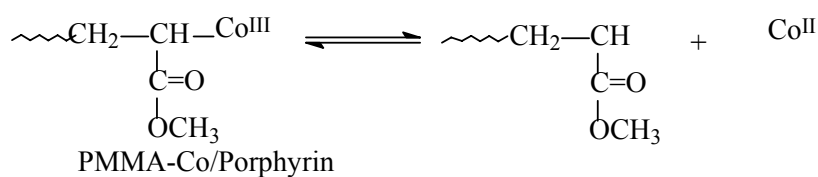
a). " Iniferter " Polymerization (Otsu et al., 1982)



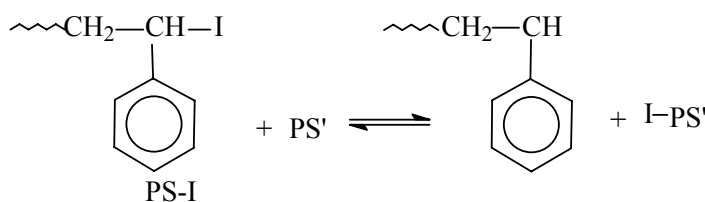
b). " NMP " (Solomon et al. 1985 ; Georges et al. 1993)



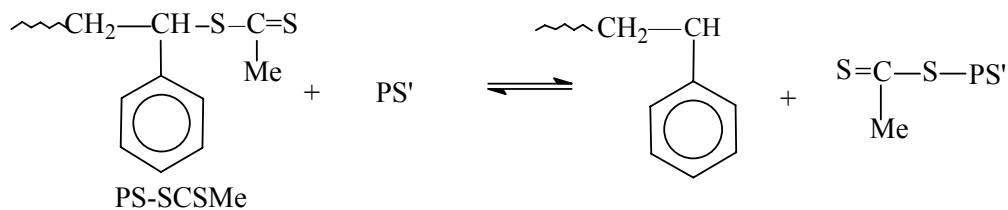
c). Cobalt/ Phorphyrin Complexes (Wayland et al. 1994)



d). " Iodine Transfer " (Tatemoto et al. 1991; Sawamoto et al. 1994; Matyjaszewski et al. 1995)

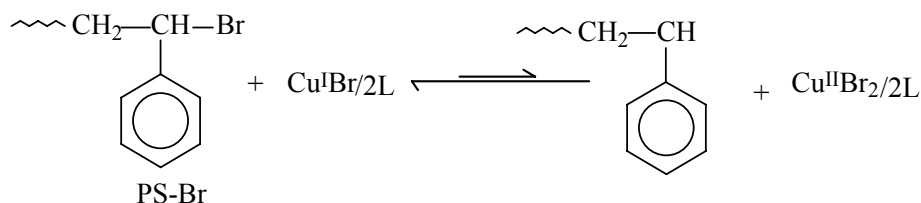


e). " RAFT " (Moad et al. 1998)

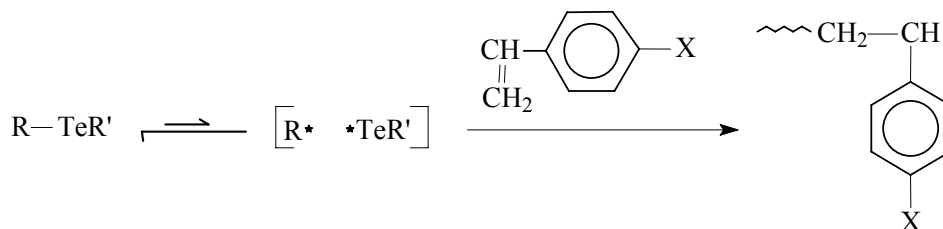


contd

f). " ATRP " (Sawamoto et al.1995 ; Matyjaszewski et al. 1995)



g). " TERP " (Yamago et al. 2002)



Scheme 1.2: Examples of controlled radical polymerizations

One of the more promising and thoroughly studied “living” radical polymerization techniques is the nitroxide-mediated polymerization (NMP), which was first reported by Solomon and Rizzardo,²⁷ and Georges *et al.*²⁸ NMP requires long reaction time for obtaining high conversions. Also the removal of nitroxyl group from the polymer chain end is not easy, making the synthesis of functional polymers more difficult.

In 1998 another method, namely, reversible addition-fragmentation chain transfer (RAFT) polymerization²⁹ was reported for controlled free radical polymerization. A feature of the RAFT process is that it can be applied to virtually any monomer, regardless of the functional groups present. Atom transfer radical polymerization (ATRP) was first reported in 1995 for controlled radical polymerizations.^{30,31} Table 1.1 summarizes the distinguishing features of these three major classes of CRP.

Recently, Yamago and coworkers reported that organotellurium compounds undergo reversible carbon-tellurium bond cleavage upon thermolysis and photolysis,³² and that the resulting carbon-centered radicals can react with variety of radical acceptors. The method was named as organotellurium mediated “living” radical polymerization (TERP).

Table 1.1: Comparison of NMP, ATRP and degenerative transfer systems

Feature	Systems		
	NMP	ATRP	RAFT
Monomers	-Styrenes for TEMPO Also acrylates & acryl amides for new nitroxides -NO methacrylates	Nearly all monomers with activated double bonds - No vinyl acetate, VC	-Nearly all monomers
Conditions	-Elevated temp (>120 °C for TEMPO) -Water borne systems -Sensitive to O ₂	-Large range of temperature (-30 °C to 150 °C) Water born systems -Tolerance to O ₂ and inhibitor with M _t ^o	-Elevated temperatures for less reactive monomers. -Water borne systems -Sensitive to O ₂
End-groups	Alkoxyamines Requires radical chem. for transformations -Relatively expensive -Thermally unstable	Alkyl(pseudo)halides Either S _N , E or radical chem.. for transformation Inexpensive and available Thermally and photostable Halogen exchange for enhanced cross propagation	Dithioesters, iodides & methacrylates Radical chem.. for transformation (S _N for RI) -Relatively expensive -Thermally & photochemically less stable -Color/odorless
Additives	None -NMP may be accelerated with acyl compounds	Transition metal catalysts -Should be removed / recycled.	Conventional radical initiator -May decrease end-functionality -May produce too many new chains.

TERP is a new addition to the armoury of CRP methods and is applicable to variety of monomers. The activation process was at first believed to be reversible thermolysis of the C-Te bond due to the similarity of the bond dissociation energies for alkyl methyltellanyl (R-TeCH₃) and TEMPO compounds with the same alkyl groups. It was later found that

TERP is mainly driven by a degenerative transfer (DT) mechanism with some contribution of thermal dissociation mechanism (DC).³³

1.5.2 Classification of controlled radical polymerization

Basically, each type of controlled radical polymerization is based on the principle of dynamic equilibrium between dormant and active species (Scheme 1.1). Well-controlled systems should provide,

- A linear first order semilogarithmic plot of $\ln([M]_0/[M]_t)$ versus time passing through origin. Intercept on abscissa indicates induction period. Acceleration on such plot indicates slow initiation and deceleration indicates termination or deactivation of catalyst (Figure 1.1(a)).
- Linear plot of M_n versus conversion; molecular weights lower than predicted by $\Delta[M]/[I]_0$ ratios indicates, transfer and, molecular weights higher than predicted by $\Delta[M]/[I]_0$ ratios indicates inefficient initiation or chain coupling. (Figure 1.1(b)).

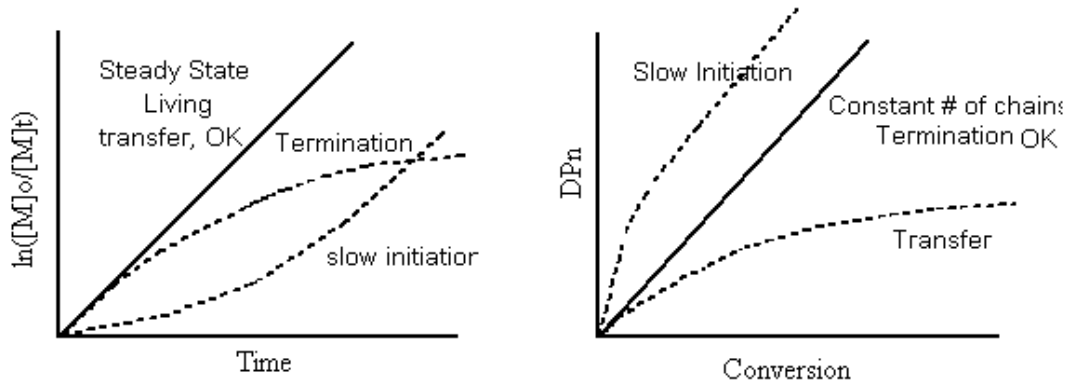
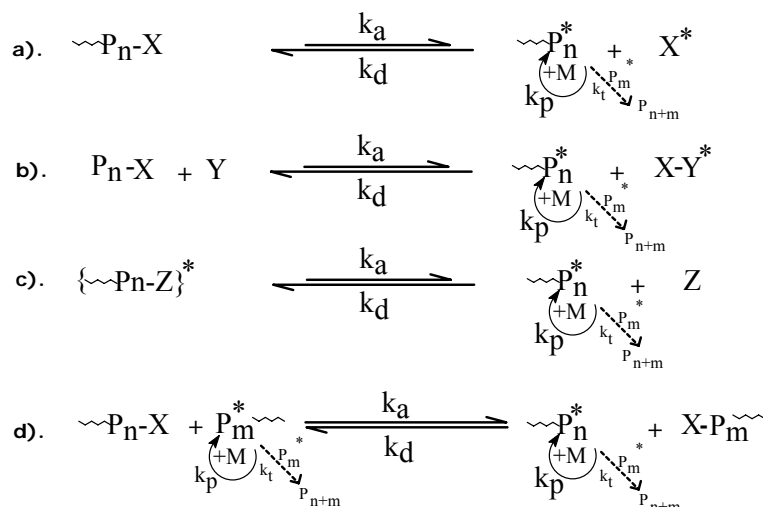


Fig. 1.1: Schematic effect of slow initiation, transfer, termination and exchange on: a) kinetics, b) molecular weights for CRP systems.

- Polydispersity increases with conversion when contribution of chain breaking reactions is significant, whereas decreases with conversion for systems with slow initiation and slow exchange.
- End functionalities are reduced in presence of chain breaking reactions, and not affected by slow initiation and exchange.



Scheme 1.3: Schematic description of different mechanisms involving controlled radical polymerization

Table 1.2: Kinetic parameters for various CRPs

S.No	Technique	Kinetic Law	DP _n	M _w /M _n
1	NMP/ TEMPO	$R_p = k_p K_{eq}[I]_o/[X^*]$	$\Delta[M]/[I]_o$	$1+(2/p-1)(k_p[I]_o)/(k_d[X^*])$
2	ATRP	$R_p = k_p K_{eq}[I]_o[Y]/[XY^*]$	$\Delta[M]/[I]_o$	$1+(2/p-1)(k_p[I]_o)/(k_d[XY^*])$
3	-	$R_p = k_p K_{eq}[I]_o/[Z]$	$\Delta[M]/[I]_o$	$1+(2/p-1)(k_p[I]_o)/(k_d[Z])$
4	RAFT/ Degenerative Transfer	$R_p = k_p f [M]k_d (k_t)^{-1/2} ([I]_o)^{1/2}$	$\Delta[M]/([P-X]^* + [P^*])$	$1+(2/p-1)(k_p/k_d)$

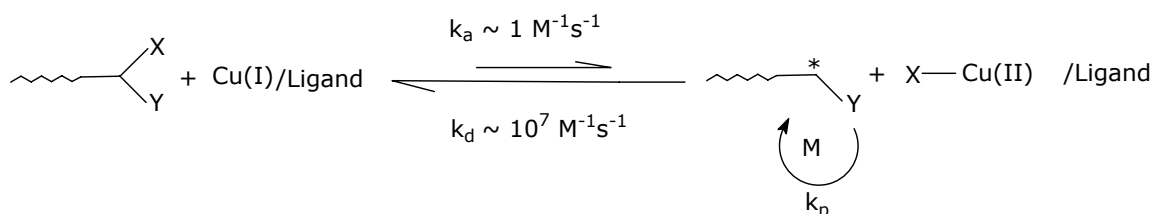
Thus, mechanistically, controlled radical polymerization may be classified in terms of four different cases shown collectively in Scheme 1.3. The dormant species are *alkoxy amines* in stable free radical polymerization (SFRP) or more conveniently called as nitroxide mediated radical polymerization (NMP: in Scheme 1.3a), *thioesters* in reversible addition fragmentation chain transfer polymerization (RAFT: in Scheme 1.3d), *alkyl halides* in atom transfer radical polymerization (ATRP: in Scheme 1.3b) or degenerative transfer polymerization (DT: in Scheme 1.3d) and an *organometallic species* in transition metal mediated polymerization. Free radicals are generated by a spontaneous thermal process in

NMP, reversible degenerative exchange process in DT and RAFT and by a catalyzed reaction in ATRP. The typical kinetic law and expressions for all four cases are summarized in Table 1.2.

1.6. Atom transfer radical polymerization (ATRP)

1.6.1. Introduction

ATRP was first reported by Wang and Matyjaszewski³⁰ who used copper as transition metal and bipyridine or substituted bipyridines as ligands. Sawamoto³¹ and coworkers used ruthenium/organic phosphorous compounds as catalyst systems for ATRP. Since its discovery, ATRP is one of the most successful member of the CRP family. It effectively utilizes the concept of equilibrium between dormant and active centers to control the radical polymerization of vinyl monomers. The polymerization is initiated by homolytic cleavage of an atom (X or group) from initiator via redox reaction by transition metal complex. The resulting radical can begin to initiate radical polymerization as shown by Scheme 1.4

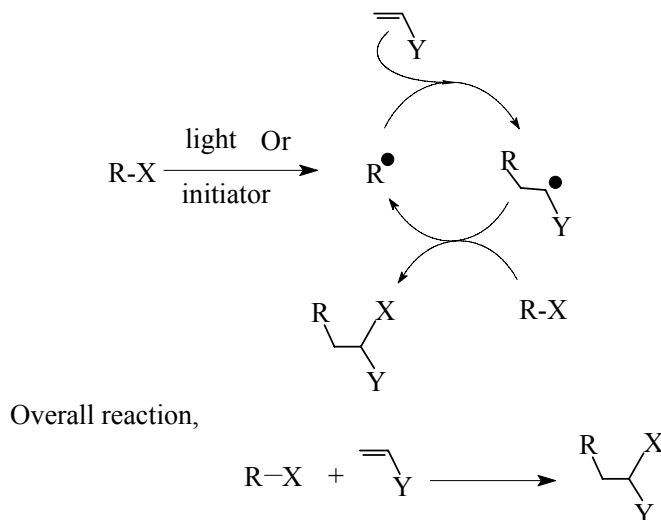


Scheme 1.4: Atom or group transfer in ATRP

1.6.2. Atom transfer radical addition (ATRA)/ Kharasch addition in organic chemistry

Addition of free radicals to alkenes is a fundamental reaction in organic and polymer synthesis.^{34,35} The earliest example of this class of reactions is the addition of halogenated methanes to olefins. The reaction became known as atom transfer radical addition (ATRA) or Kharasch addition and is accepted to occur via a free-radical mechanism. The reaction involves an atom transfer from an organic halide to a transition metal complex to generate the reactive radicals (Scheme 1.5). The reaction is highly exothermic and rapid due to the loss of one π bond and formation of σ bond. Being fast and unselective, it was considered

difficult to control organic radical reactions, which suffer from low yields of desired products caused by several side reactions.^{34,35}

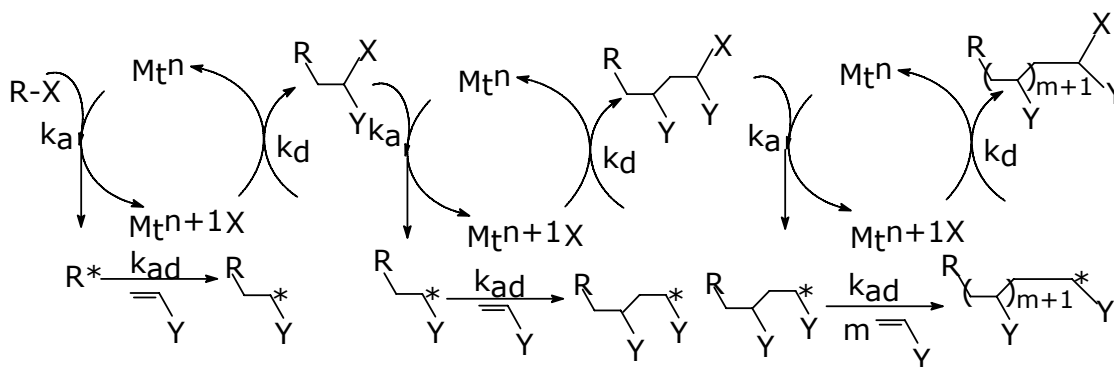


Scheme 1.5: Atom transfer radical addition chain reaction

The fast rate of radical reactions as well as its tolerance to many functionalities prove its importance in synthetic chemistry. However, the Kharasch addition of alkyl halides to alkenes initiated by small amount of peroxides or light,³⁵ and atom transfer radical addition catalyzed by transition metals led to highly chemoselective 1:1 adducts in high yields.^{34,35}

1.6.2.1. Atom transfer radical addition (ATRA) to atom transfer radical polymerization (ATRP)

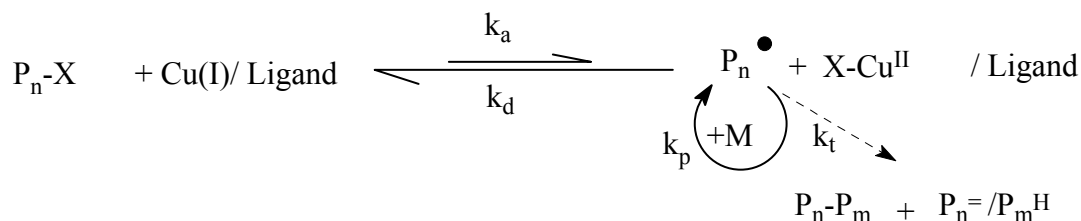
ATRA adds one monomer to the starting organic halide in a similar fashion to the chain propagation during a radical polymerization. ATRA can be extended to ATRP provided more than one addition step occurs. The substrates chosen for ATRA are such that, the addition product is much less stable than the initiating radical followed by irreversible addition to the oxidized transition metal complex (acting as a persistent radical) to give the required product molecule. Therefore, *if the starting and product radicals are of similar reactivity it is possible to repeat the catalytic cycle possessing multiple additions of unsaturated monomers leading to a polymerization reaction* (Scheme 1.6).



Scheme 1.6: Repetitive cycle of radical addition in ATRP: ATRA to ATRP

ATRA usually provides excellent yields, and side reactions such as radical coupling are rarely observed. This suggests that the concentration of reactive radicals in ATRA is low enough to suppress bimolecular coupling. However, addition of several monomer molecules during one activation step decides the relative rates of propagation and deactivation and affects polydispersity of the obtained polymers.

The concept of atom transfer radical addition (ATRA) or Kharasch addition in organic chemistry has been extended to polymerization reaction resulting in the development of "atom transfer radical polymerization" (ATRP).^{30,31} The technique is based on transition metal catalyzed reversible cleavage of covalent bond in dormant species through a redox process given in Scheme 1.7 as,



Scheme 1.7: Copper catalyzed atom transfer radical polymerization (ATRP)

The technique rests on the iteration of the Kharasch reaction, in which a transition metal catalyst acts as a carrier of the halogen atom in a reversible redox process. Control is achieved in ATRP because the relative rates of activation and deactivation (i.e., equilibrium constant) are of the order of 10^{-7} . Thus, the concentration of growing radicals is sufficiently low ($\sim 10^{-8}$ M) to effectively eliminate bimolecular termination. The most important parameter in ATRP is the dynamics of exchange and, especially, the relative rates of

deactivation. However, the actual kinetics in ATRP depends on many factors including the solubility of activator and deactivator, their possible interactions, and variations of their structures and reactivities with concentrations and composition of the reaction medium. The development and progress of controlled radical polymerization has been exhaustively covered in several review articles.³⁶⁻⁴³

1.6.3. Tuning in ATRP – a multicomponent System

Monomer, catalyst, initiator, ligand, solvent and temperature, all together, form a multicomponent ATRP. All these components have their specific role in the mechanism of polymerization. A change in any one component will cause considerable variation in the properties of the obtained polymer. Therefore, to obtain the best results careful tuning of all these parameters are required.

1.6.3.1 Catalysts

Transition metal complexes serve as catalysts in ATRP. These complexes are formed by the reaction of a metal salt in appropriate oxidation state with a donor ligand. The requirements of a good catalyst are,

- Existence of two rapidly interconvertible oxidation states separated by one electron. It determines equilibrium (K_{eq}) constant and dynamics of exchange that in turns gives polydispersity index, (M_w/M_n).
- Highly selective for halogen transfer that involves cleavage of C-X bond homolytically and forms Cu-X.
- Design of new improved catalyst requires the expansion of the coordination sphere to accommodate atom (halogen or pseudo halogen) transfer.
- Steric and electronic effects should selectively favor inner sphere electron transfer (ISET) over any other (outer sphere ET, β -H abstraction, formation of organometallic species, etc.) processes.
- The metal should not be a strong Lewis acid that ionizes certain end-groups to carbocations.
- Cost of catalyst is also important for commercialization of a process.

Copper catalyzed ATRP is the most studied system.^{37,38} The properties of the complex basically depend upon the choice of the transition metal and its electronic configuration. The electronic configuration of the two ions is Cu^+ [$3d^{10}$] & Cu^{2+} [$3d^9$]. The crystal field stabilization energy is zero (i.e., $\text{CFSE} = 0$) for d^{10} configuration whether the complex is octahedral or tetrahedral. The activity of a catalyst depends dramatically on the nature of ligands, which are preferably polydentate in nature. The copper based initiating system was first reported for styrene polymerization by Wang *et al.* and Percec *et al.*^{30,44} The polymerization was heterogeneous with CuCl and 2,2'-bipyridine. However, good conversions as well as lower PDI were attained. In an effort to attain homogeneous polymerization, long-chain alkyl groups on 4,4'-positions of bipyridine were introduced. Narrow MWD ($M_w/M_n < 1.10$) polystyrene could be obtained with such ligands.^{45,46} Similarly, Collins *et al.* polymerized styrene using even longer alkyl chains ($> C_9$) but the results was comparable to that obtained using shorter alkyl chain ($< C_9$).⁴⁷ Polymerization under homogeneous conditions was faster than those under heterogeneous conditions. It was difficult to isolate the copper complex when bipyridine ligands with long alkyl chains are used.

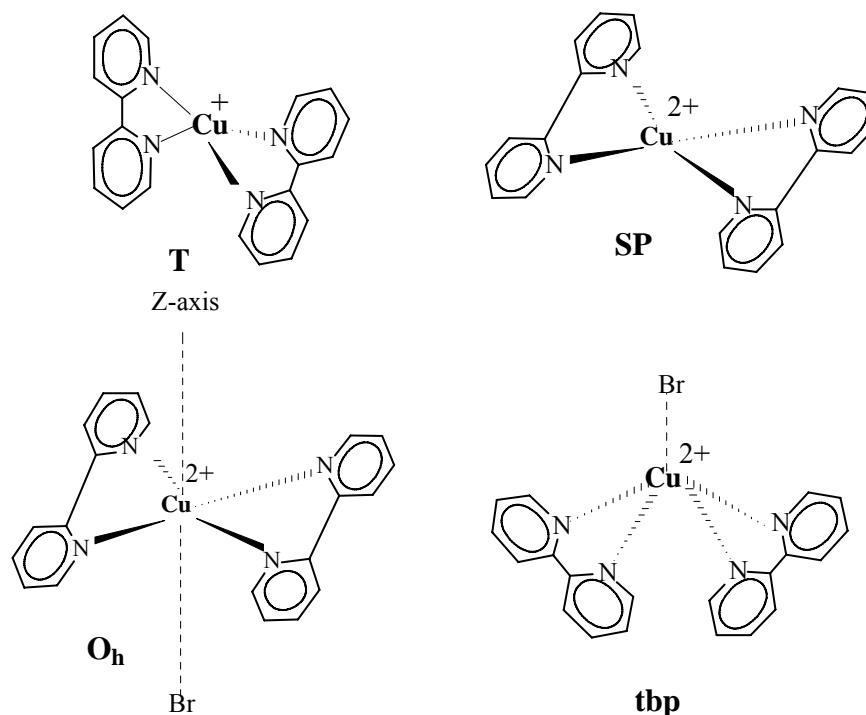
Recently, it was observed that the addition of copper metal to ATRP produced significant rate enhancements.³⁷ The possible geometries of the complex in dormant and active state are shown in Scheme 1.8, i.e., before and after the atom transfer. The deactivator, or the Cu^{II} species, is important for molecular weight control in ATRP. However, the rate of polymerization is of inverse order with respect to the concentration of Cu^{II} . Therefore too high a concentration of this reagent will lead to rather slow rates of polymerization. Upon the addition of copper metal to the polymerization, a disproportionation of the Cu^0 takes place and Cu^{2+} species re-forms the starting Cu^+ complex (equation 1.2) given as,



This equilibrium reaction is probably driven by the presence of the electron donating ligands, which serve to stabilize copper in its 1+ oxidation state. An additional advantage to using copper metal in ATRP is that any Cu^{2+} species formed from the oxidation of Cu^+ by dioxygen will also be removed via disproportionation with Cu^0 .

1.6.3.2 Ligands

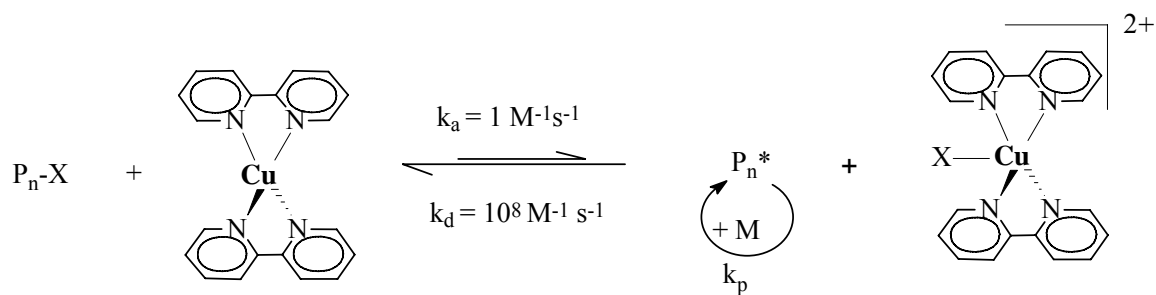
The most important factor that controls the reactivity of the catalyst is the nature of the ligand. The ligand should be capable of conferring sufficient stability to Cu^+ in order to keep the concentration of radicals low enough to minimize termination relative to propagation. At the same time, it should not raise the redox potential in such a way that no halogen can be abstracted from alkyl halide species.



Scheme 1.8: Possible geometries of the copper bipyridine complex in two different oxidation states. (a) T: *Tetrahedral*, (b) SP: *Square planar*, (c) Oh: *Octahedral*, and (d) tbp: *Trigonal bipyramidal*.⁴⁸

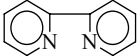
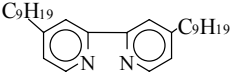
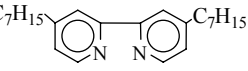
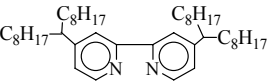
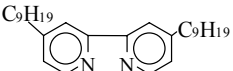
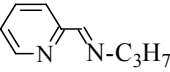
In general, ligands that are good σ -donors and π -acceptors, lower the electron density on the copper center and, therefore, preferably stabilize the lower oxidation state. For example, in most of ATRP systems bipyridines and Schiff's bases act as suitable ligands for Cu^+ . Although they both possess comparable σ -bonding capabilities, the latter has lower lying LUMO⁴⁹ and is, therefore, superior in stabilizing Cu^{I} as compared to bipyridines. However, electron withdrawing groups on para position of bipyridine lowers the energy of vacant π^* -

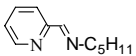
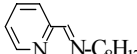
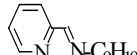
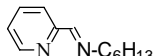
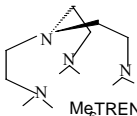
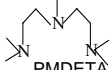
significantly, thereby favoring stabilization. This electronic effect is in addition to the possible steric effects of the substituents on the redox potential, i.e., 2,2'-bipyridine ligand not only stabilizes Cu^{I} by π -electron back donation from the metal, but also helps the interchange between tetrahedral Cu^{I} and distorted square based pyramidal Cu^{II} (Scheme 1.9). The active species in other ATRP catalyst systems are still under investigation. Thus, any shift in the redox potential affects the electron transfer and equilibrium dynamics.⁴³ Ligand should complex strongly, unless catalytic activity requires its dissociation from coordination sphere and should allow its expansion⁵⁰ to accept halogen atom from the dormant species (Scheme 1.9). It was also observed that the activity of N-based ligands in ATRP decreases with the number of coordinating sites i.e. $\text{N}_4 > \text{N}_3 > \text{N}_2 \gg \text{N}_1$ and with the increasing number of linking C-atoms i.e., $\text{C}_2 > \text{C}_3 \gg \text{C}_4$. Activity is usually higher for bridged and cyclic systems than for linear analogues. Ligand also undergoes side reactions such as the reaction of amines (especially aliphatic) and phosphines with alkyl halides. These side reactions are reduced when tertiary amines are used as ligands and are minimum when the ligands are complexed to CuBr .³⁷ Nitrogen ligands have been used in copper- and iron-mediated ATRP. Sulfur, oxygen, or phosphorus, ligands are less effective due to inappropriate electronic effects or unfavorable binding constants.



Scheme 1.9: ATRP equilibrium with a copper halide complex containing two 2,2'-bipyridine units as ligands.

Table 1.3: Copper Based N-donors employed in CRP

Ligand Structure complexed with CuBr	Monomer used	Initiator	Mole Ratios C: L: I (Solvent used)	Time (h) (Yield, %)	M _{n,SEC}	MWD	I _{eff}
 2,2'-bipyridine (bpy) ³⁰	MMA	EBiB	1:3:1 (EAc 50 % sol)	3 (85)	9,800	1.40	1.02
 4,4'-bis-(5-nonyl) 2,2'-bipyridine (dNbpy) ³⁷	MMA	(<i>p</i> -TsCl)	1:2:2 (Ph ₂ O 50% in vol)	24 (82)	1,69,000	1.40	1.02
 4,4' di- <i>n</i> -heptyl 2,2'-bipyridine (dHbpy) ⁴⁵	Sty	1-PEBr	1:2:1 (bulk)	4 (80)	8,800	1.05	0.91
 4,4'-di- <i>n</i> -octyl-2,2'-bipyridine (dHDbpy) ^{37,38}	BMA	EBiB	1:2 (water borne)	2.2 (83)	27,800	1.21	0.85
 4,4'-di- <i>n</i> -nonyl 2,2'-bipyridine (dNbpy) ⁴⁴	MMA	<i>p</i> -methoxy phenylsulfonyl chloride	1:2:1 (<i>p</i> -xylene)	74 (63)	6,200	1.18	1.01
 N-(<i>n</i> -propyl)-2-pyridylmethanimine (NPPI) ³⁷	MMA	EBiB	1:2:1 (xylene, 50 vol %)	4(82)	8,300	1.18	0.99

Ligand Structure complexed with CuBr	Monomer used	Initiator	Mole Ratios C: L : I (Solvent used)	Time (h) (Yield, %)	M _{n,SEC}	MWD	I _{eff}
 N-(<i>n</i> -pentyl)-2-Pyridylmethanimine ³⁷	do	EBiB	1:2:1 (xylene, 50 vol %)	4 (85)	8,900	1.23	0.95
 N-(<i>n</i> -octyl)-2-pyridyl methanimine ³⁷	do	EBiB	1:2:1 (xylene, 50 vol %)	4 (80)	9,800	1.24	0.82
 N-(<i>n</i> -nonyl)-2-pyridyl methanimine ³⁷	do	EBiB	1:2:1 (xylene, 50 vol %)	4 (70)	10,900	1.27	0.64
 N-(<i>n</i> -hexyl)-2-pyridyl methanimine ³⁷	do	EBiB	1:2:1 (xylene, 50 vol %)	4 (84)	7,600	1.19	1.09
 tris[2-(dimethylamino) ethyl] amine ³⁷	MMA	EBiB	1:1:1 (ethylene carbonate) (Cu ^{II} Cl ₂ added, 20%)	5 (50)	32,000	2.20	1.60
 N,N,N',N'',N'''-penta methyldiethylenetriamine ³⁷	MMA	EBiB	1:1:1 (anisole soln)	6 (78)	15,700	1.18	0.78

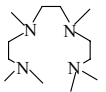
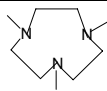
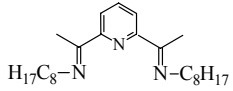
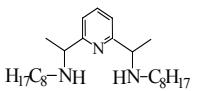
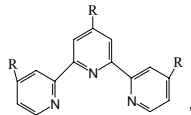
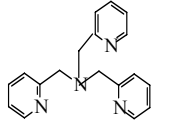
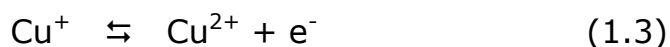
Ligand Structure complexed with CuBr	Monomer used	Initiator	Mole Ratios C : L : I (Solvent used)	Time (h) (Yield ,%)	M _{n,SEC}	MWD	I _{eff}
 HMTETA hexa- methyltriethylenetetramine ³⁷	MMA	<i>p</i> -TsCl	1:1:1 (anisole soln)	6 (75)	18,500	1.13	0.92
 TACN 1,4,7-triazacyclononane ³⁷	Sty	1-PEBr	1:1:1 (bulk)	1.25 (65)	18,000	1.23	0.72
 H ₁₇ C ₈ -N N-C ₈ H ₁₇ 2,6-bis[1-(octyl imino)ethyl]pyridine(DOIP) ³⁷	MMA	2-BPN	1:1:1 (Anisole 50 vol %)	3.5 (68)	14,300	1.23	0.95
 H ₁₇ C ₈ -NH HN-C ₈ H ₁₇ 2,6-bis[1-(octyl amino)ethyl]pyridine (DOAP) ³⁷	MMA	2-BPN	do	7.25 (64)	24,000	1.56	0.54
 TERPY ^{37,38}	Sty	1-PEBr	1:2	50 (31)	30,600	1.57	0.37
 TPMA ^{37,38} tris(2-pyridyl)methylamine	MMA	1-PEBr	1:1:1 (50 vol% in Anisole)	1.0 (<5)	10,500	1.12	0.10

Table 1.3 provides an overview of few of the successful N-donor ligands employed in controlled radical polymerization. It is seen that the use of long chain alkyl groups reduces the polarity and, thereby, increases the solubility of the complex. The most efficient ligand in ATRP are HMTETA and Me₆TREN. The latter appears to be more attractive since it promotes very fast activation as well as sufficiently fast deactivation. However, the more commonly used and inexpensive ligand employed in ATRP is PMDETA. The redox potential of Cu⁺ ion in aqueous solution is -153 mV,⁵¹ as shown in equation 1.3, whereas upon complexation with 2,2'-bipyridine the redox potential increases to + 120 mV,⁵² indicative of the stabilizing effect of the ligand. If the redox potential rises beyond this value then cationic polymerization occurs.⁵³



Similarly, Grubbs and Louie used FeL₂X₂ [X = Cl, Br; L = 1,3-diisopropyl-4,5-dimethyl imidazol-2-ylidene] complexes as catalysts for the ATRP of styrene and methyl methacrylate.⁵⁴ Acar and Bicac used a ligand having *n*-hexyl chains over four N-donor atoms (hexahexyl triethylenetetramine: HHTETA) to polymerize MMA and styrene using CuBr and EB/B at 75 °C and 110 °C respectively. The reaction was reported to be homogeneous giving polydispersity (M_w/M_n) below 1.2.⁵⁵ Iovu *et al.*⁵⁶ used a C2 bridged bisiminopyridine as ligand for copper catalyzed ATRP of MMA. Poor control was obtained when reaction was performed in bulk. Even in 33% acetonitrile the obtained polydispersities (M_w/M_n) were high. In an effort to design effective ligands for late transition metal catalyst, Lee *et al.* reported copper(I) pyridine-2-carboximidates as novel catalyst for ATRP of MMA.⁵⁷ More recently, 1,8-diazabicyclo[5.4.0]undec-7-ene was used as an effective ligand for ATRP of MMA at 65 °C, yielding polymer with a polydispersity of 1.19 and molecular weight, M_{n,SEC} ~16,000, obtained in 7.5 h with 70 % conversion.⁵⁸ However, author failed to obtain control with other monomers like styrene and methyl acrylate

1.6.3.3 Monomers

In contrast to ionic polymerization, a wide variety of monomers have been successfully polymerized by ATRP. They include styrenes,^{37,38} acrylates,^{59,60} and methacrylates,^{37,61-66} and several other relatively reactive monomers such as acrylamides,⁶⁷ vinyl pyridines,^{37,38}

and acrylonitrile, 2-hydroxyethyl acrylate (HEA) and 2-hydroxyethyl methacrylate (HEMA).^{37,38} Munirasu and Dhamodharan performed ATRP of benzyl methacrylate (BnMA) at room temperature using PMDETA as ligand, and EBiB as initiator to obtain a high molecular weight ($M_{n,SEC} = 1,72,850$; $I_{eff} = 0.85$) polymers narrow polydispersity ($M_w/M_n=1.06$). The reaction was very fast and the polymerization of BnMA is comparable to (*t*-butyl methacrylate) *t*-BMA.⁶⁸ Later, Beers and Matyjaszewski reported that 2-hydroxyethyl methacrylate can be polymerized in mixed solvent in a controlled manner.⁵⁹ More recently, successful demonstration of metal catalyzed living radical polymerization of vinyl chloride in aqueous media has been reported.⁶⁹ The application of controlled radical polymerization to vinyl acetate (VAc) had proven to be relatively more difficult. Cunningham and coworkers polymerized vinyl acetate (VAc) using a RAFT process using both dithiocarbamates and xanthates.⁷⁰⁻⁷³

In general, the dynamics of equilibrium between an active and dormant species also depend upon the propagation rate constant of the monomer. Thus, for a specific monomer, the concentration of propagating radicals needs to be adjusted to get controlled polymerization. Acrylic and methacrylic acids cannot be polymerized with currently available ATRP catalysts since during the reaction the monomers form inefficient deactivators, which cannot be reduced back to active ATRP catalysts. Halogenated alkenes, alkyl-substituted olefins, and vinyl esters are presently resistant to polymerization by ATRP due to inherently low reactivity in radical polymerization.

1.6.3.4 Initiators

The efficiency of the initiator is of prime importance for successful ATRP. If initiation is fast and transfer and termination rates are negligible, then the number of growing chains is constant and is equal to the initial concentration of the initiator.

In ATRP, alkyl halides (R-X) are typically used as initiators. Control on molecular weight is better when 'X' is Br or Cl. Iodine works well for acrylate monomers and fluorine is not used due to the stronger bond strength of C-F bond. In general, any alkyl halide with activating substituents on the α carbon atom, such as polyhalogenated alkanes (CCl₄ and

CHCl_3),^{72,74} primary/ secondary benzyl halide, a α -haloester, α -haloketone, α halonitrile, arenesulfonyl halide, conventional radical initiators and compounds with a weak bond, such as, N-X, S-X, and O-X can be used as ATRP initiators.^{37,38} The stabilizing group order in the initiator is roughly $\text{CN} > \text{C(O)R} > \text{C(O)OR} > \text{Ph} > \text{Cl} > \text{Me}$. Multiple functional groups may increase the activity of the alkyl halide. Tertiary halides are better initiators than secondary ones, which are in turn better than primary alkyl halides. When an initiating moiety is attached to the macromolecular species, macroinitiators are formed and can be used to synthesize block/graft copolymers.

1.6.4. Reverse ATRP

ATRP has two major problems: the halide species RX are limited in number and the catalysts employed are unstable in air and in presence of moisture. It is important to find new initiators and new catalytic systems for reverse ATRP that obviates the above problems. Conventional radical initiators, such as 2,2'-azobisisobutyronitrile (AIBN), in the presence of transition metal complexes in higher oxidation state, have been used in ATRP. This reaction is termed as "reverse" or "alternative" ATRP, abbreviated as RATRP.³⁷ The only difference between normal ATRP and reverse ATRP is the initiation step. After the formation of active radicals by the initiator, oxidized catalyst $\text{X-M}^{(n+1)+}$ rapidly establishes the equilibrium between the radicals and the dormant species by halogen atom back-transfer. Thus, low radical concentration is maintained, and the propagation proceeds in the same fashion as normal ATRP. Under proper conditions, good control on polydispersity can be achieved. End-group analysis of the polymer obtained shows that the polymerization is indeed initiated by AIBN.³⁷ As an interesting extension of ATRP, reverse ATRP may change some conventional radical polymerizations into controlled polymerization simply by adding transition metal catalysts without changing initiators. Several monomers including styrene,³⁷ MMA,^{75,76} MA and *n*-butyl methacrylate (*n*BA)³⁸ were successfully polymerized by this process. Recently reverse ATRP is reported to occur in miniemulsion system at 70 °C with a reasonable solid content ($\geq 20\%$) using much lower concentration of non-ionic surfactant.⁷⁷ Using the concept of reverse ATRP Wang *et al.* prepared structurally well-

defined polymer grafted nanocomposite by introducing the peroxide groups on the surface of ultrafine silica.⁷⁸

1.6.5. Perspectives and future prospects

Copper catalyzed ATRP is a robust reaction; yet there is a need for more efficient and cost effective catalysts. The solubility, structure, concentration in solution, aggregation, and effect of ion pairing, etc., may change not only with the overall catalyst composition and preparation method but also for each monomer, solvent, and temperature. One of the big advantages of controlled radical polymerization is the absence of Trommsdorf (gel) effect that enables one to carry out polymerization even in absence of a solvent.

Mechanistically, the most exciting area involves insights in the atom transfer step during activation-deactivation equilibrium. Synthetically, it is important to expand the range of monomers and initiators and better understand cross-propagation processes as well as ability to end functionalize the polymer. Extensive research has been devoted to achieve controlled radical polymerization with much greater efficiencies. New nitroxide mediated polymerization (NMP) mediators have been developed that allows efficient polymerization of acrylates. New ligands for various transition metals have increased the catalyst activity in ATRP by 10,000 fold.^{37,38} New methodologies have been developed to reduce the amount of catalyst used in ATRP. Supported and hybrid catalyst systems have been developed that reduces the residual metal to less than 5 ppm.⁷⁹ Over 7000 papers, and 500 patents have been published since 1995 in CRP which is indicative of the interest generated by this field.

41

1.7. Scope and Objective of this thesis

- To investigate the effect of a tridentate ligand, namely 2,6-bis[1-(2,6-diisopropyl phenyl imino) ethyl] pyridine (BPIEP) on ATRP of MMA. The work involves identification of most suitable reaction conditions for controlled polymerization of MMA in non-polar as well as polar solvent. The extent of control on reverse equilibrium will also be studied by reverse ATRP. The kinetics of polymerization will be studied and compared with other well-known ligands.

- To study the steric and electronic effects around metal center in atom transfer radical polymerization of methylmethacrylate at 90 °C using *bis(imino)* pyridine ligand. This involves synthesis of various tridentate N-donor ligands and their study as ligands for controlled polymerization of methyl methacrylates.
- To examine the efficiency of various ligands (bidentate and multidentate amines and imines) with copper (I) halide ($\text{Cu}^{\text{I}}\text{X}$: $\text{X} = \text{Br}$) along with ethyl-2-bromoisobutyrate (EBiB) as initiator on ATRP of methacrylates.
- Synthesis of novel initiators for ATRP of methacrylates. The initiators chosen for the study are 3-bromo-3-methyl-butanone-2 (MBB) and 3-(bromomethyl)-4-methylfuran-2,5-dione (BMFD). Moreover, the efficacy of standard initiator like 2-bromopropionitrile (BPN) along with above two mentioned will be examined by performing the polymerization under different conditions.
- To study the efficacy of softer pseudo halogen (SCN^-) as counterion in the initiator (R-X) as well as for catalyst ($\text{Cu}^{\text{I}}\text{-X}$) in copper catalyzed ATRP of MMA. The chemistry of using thiocyanate both as counter ion for copper salt, CuSCN , and initiator, R-SCN , was based on the premise that CuSCN forms stable complexes with bidentate ligands. Therefore, ethyl-2-methyl-2-thiocyanatopropanoate (EMTP) was synthesized and used in conjunction with CuSCN for ATRP of styrene and methylmethacrylate. Moreover, different unconjugated α -diimines to be utilized as ligands were also synthesized.
- To examine the feasibility of performing the ATRP of methylvinylketone. The polymerization of this new monomer, both in bulk and solution, will be attempted by varying the type of ligands as well as initiators.

1.8. References

1. *Early Plastics, Perspectives*, Mossman, S. (Ed.), **1997**, Leicester University Press, London, 1850-1950.
2. Meikle, J. L., *American Plastic, A Cultural History* **1995**, Rutgers University Press, New Brunswick, New Jersey.
3. www.plasticsresources.com
4. Hocking, M. B. *Science* **1991**, 251, 504.

5. Moad, G.; Solomon, D. H. *The chemistry of Free Radical Polymerization*; 1st ed.; Elsevier Science Ltd.: Oxford, **1995**.
6. Otsu, T. *J. Polym. Sci., Part A Polym. Chem.* **2000**, 38, 2121.
7. Szwarc, M. *Nature* **1956**, 178, 1168.
8. Szwarc, M. *Carbanions, Living Polymers, and Electron Transfer Processes*. Wiley, New York, 1968.
9. Matyjaszewski, K. *J. Phys. Org. Chem.* **1995**, 8, 197.
10. Matyjaszewski, K. Ed. *Cationic Polym.: Mechanisms, Synthesis and Applications*; Marcel Dekker, New York, **1996**.
11. Müller A, R.; Zhuang, R. D.; Litvinienko, G. *Macromolecules* **1995**, 28, 4326.
12. Flory, P. J. "*Principles of Polymer Chemistry*", Cornell University Press: Ithaca, New York 1953.
13. (a) Greszta, D.; Mandare, D.; Matyjaszewski, K. *Macromolecules* **1994**, 27, 638. (b) Goto, A.; Fukuda, T. *Prog. Polym. Sci.* **2004**, 29, 329.
14. Colombani, D. *Prog. Polym. Sci.* **1997**, 22, 1649.
15. Borsig, E.; Lazar, M.; Capla, M. *Makromol. Chem.* **1967**, 105, 212 (b) Borsig, E.; Lazar, M.; Capla, M. *Coll. Czech. Chem. Commun.* **1968**, 33, 4264.
16. Borsig, E.; Lazar, M.; Capla, M.; Florian, S. *Angew. Makromol. Chem.* **1969**, 9, 89.
17. (a) Lee, M.; Utsumi, K.; Minoura, Y. *J. Chem. Soc., Faraday Trans. I* **1979**, 75, 1821. (b) Lee, M.; Minoura, Y. *J. Chem. Soc., Faraday Trans. I* **1978**, 74, 1726.
18. Fischer, H. *J. Am. Chem. Soc.* **1986**, 108, 3925.
19. Fischer, H. *Macromolecules* **1997**, 30, 5666.
20. Mandare, D.; Matyjaszewski, K. *Macromolecules* **1994**, 27, 645.
21. Otsu, T.; Yoshida, M. *Makromol. Chem., Rapid Commun.* **1982**, 3, 127
22. Nair, C. P. R.; Chaumont, P.; Clouet, G. *J. Macromol. Sci., Chem.* **1990**, A27, 791.
23. Turner, S. R.; Blevins, R. W. *Macromolecules* **1990**, 23, 1856.
24. Druliner, J. D. *Macromolecules* **1991**, 24, 6079.
25. Harwood, H. J.; Arvanitopoulos, L. D.; Greuel, M. P. *J. Polym. Prepr. (Am. Chem. Soc., Div. Polym. Chem.)* **1994**, 35 (2), 549.
26. Wayland, B. B.; Poszmik, G.; Mukerjee, S. L. Fryd, M. *J. Am. Chem. Soc.* **1994**, 116, 7943.
27. Solomon, D. H.; Rizzardo, E.; Cacioli, P. *U.S. Patent* **1986**, 4, 581,429.
28. Georges, M. K.; Veregin, R. P. N.; Kazmaier, P. M.; Hamer, G. K. *Macromolecules* **1993**, 26, 2987; *ibid* **1993**, 26, 5316.
29. Chiefari, J.; Chong, Y. K.; Ercole, F.; Krstina, J.; Jeffery, J.; Le, T. P. T.; Mayadunne, R. T. A.; Meijs, G. F.; Moad, C. L.; Moad, G.; Rizzardo, E.; Thang, S. H. *Macromolecules* **1998**, 31, 5559.
30. (a) Wang, J.-S.; Matyjaszewski, K. *J. Am. Chem. Soc.* **1995**, 117, 5614. (b) Wang, J. - S.; Matyjaszewski, K. *Macromolecules* **1995**, 28, 7901.
31. Kato, M.; Kamigato, M.; Sawamoto, M.; Higashimura, T. *Macromolecules* **1995**, 28, 1721.
32. Yamago, S.; Iida, K.; Yoshida, J. I. *J. Am. Chem. Soc.* **2002**, 124, 2874.
33. Gilbert, R. G. *Pure Appl. Chem.* **1996**, 68, 1491.
34. (a) Curran, D. P. *Comprehensive Organic Synthesis*: Trost, B. M., Fleming, I., Eds.: Pergamon Press, Oxford, **1991**; Vol. 4, p715. (b) Kharasch, M. S.; Jensen, E. V.; Urry, W. H. *Science* **1945**, 102, 128

35. Iqbal, J.; Bhatia, B.; Nayyar, N. *Chem. Rev.* **1994**, 94, 519.
36. Sivaram, S. *J. Sci. Ind. Res.* **1997**, 56, 1.
37. Matyjaszewski, K.; Xia, J. *Chem. Rev.* **2001**, 101, 2921.
38. Kamigaito, M.; Ando, T.; Sawamoto, M. *Chem. Rev.* **2001**, 101, 3689.
39. *Advances in controlled / Living Radical Polymerization* Ed. Matyjaszewski, K., ACS Symposium Series Vol. 864. ACS, Washington, DC, **2003**.
40. Pintauer, T.; Matyjaszewski, K. *Coordination Chemistry Reviews* **2005**, 249, 1155.
41. Matyjaszewski, K.; Spanswick, J. *Materials Today* **2005**, 3, 26.
42. Shipp, D. A. *J. Macromol. Sci., Part C: Polym. Rev.* **2005**, 45, 171.
43. Matyjaszewski, K. *Macromolecules* **1998**, 31, 4710.
44. Percec, V.; Barboiu, B.; Kim, H.-J. *J. Am. Chem. Soc.* **1998**, 120, 305.
45. Patten, T. E.; Xia, J.; Abernathy, T.; Matyjaszewski, K. *Science* **1996**, 272, 866.
46. Percec, V.; Barboiu, B.; Neumann, A.; Ronda, J. C.; Zhao, M. *Macromolecules* **1996**, 29, 3665.
47. Collins, J. E.; Fraser, C. L. *Macromolecules* **1998**, 31, 6715.
48. Kickelbick, G.; Reinohl, U.; Ertel, T. S.; Weber, A.; Bertagnolli, H.; Matyjaszewski, K. *Inorg. Chem.* **2001**, 40, 6.
49. Reinhold, J.; Benedix, R.; Birner, P.; Henning, H. *Inorg. Chim. Acta* **1979**, 33, 209.
50. Wang, X. S.; Malet, F. L. G.; Armes, S. P.; Haddleton, D. M.; Perrier, S. *Macromolecules* **2001**, 34, 162.
51. Latimer, W. M. *The Oxidation States of the Elements and their Potentials in Aqueous Solution*, 2nd Ed., Prentice Hall: New York, **1952**.
52. (a) James, B. R.; Williams, R. J. P. *J. Chem. Soc.* **1961**, 2007. (b) Bernhardt, P. V. *J. Am. Chem. Soc.* **1997**, 119, 771.
53. Haddleton, D. M.; Shooter, A. J.; Hannon, M. J.; Barker, J. *Polym. Prepr. (Am. Chem. Soc., Div. Polym. Chem.)* **1997**, 38(1), 679.
54. Louie, J.; Grubbs, R. H. *Chem. Commun.* **2000**, 1479.
55. Acar, M. H.; Bicak, N. *J. Polym. Sci., Part A: Polym. Chem.* **2003**, 41, 1677.
56. Iovu, M. C.; Mithufi, N. G.; Mapolie, S. F. *Polym. Int.* **2003**, 52, 899.
57. Lee, D. W.; Seo, E. Y.; Cho, S. I.; Yi, C. S. *J. Polym. Sci., Part A: Polym. Chem.* **2004**, 42, 2747.
58. Fournier, D.; Romage, M.-L.; Pascual, S.; Montembault, V.; Fontaine, L. *Eur. Polym. J.* **2005**, 41, 1576.
59. Beers, K. L.; Matyjaszewski, K. *J. Macromol. Sci. Pure Appl. Chem.* **2001**, A38, 731.
60. Wakioka, M.; Baek, K.-Y.; Ando, T.; Kamigaito, M.; Sawamoto, M. *Macromolecules* **2002**, 35, 330.
61. Snijder, A.; Klumperman, B.; van der Linde, R. *Macromolecules* **2002**, 35, 4785.
62. Zhang, H.; Klumperman, B.; van der Linde, R. *Macromolecules* **2002**, 35, 2261.
63. Luis de la Fuente, J.; Fernández-García, M.; Fernández-Sanz, M.; Madruga, E. L. *Macromol. Rapid Commun.* **2001**, 22, 1415.
64. Raghunadh, V.; Baskaran, D.; Sivaram, S. *Polymer* **2004**, 45, 3149.
65. Krishnan, R.; Srinivasan, K. S. V. *Eur. Polym. J.* **2004**, 40, 2269.
66. Narain, R.; Armes, S. P. *Chem. Commun.* **2002**, 2776.
67. Jewrajka, S. K.; Mandal, B. M. *J. Polym. Sci., Part A: Polym. Chem.* **2004**, 42, 2483.
68. Munirasu, S.; Dhamodharan, R. *J. Polym. Sci., Part A: Polym. Chem.* **2004**, 42, 1053.

69. Percec, V.; Popov, A. V.; Ramirez-Castillo, E.; Monteiro, M.; Barboiu, B.; Weichold, O.; Asandei, A. D.; Mitchell, C. M. *J. Am. Chem. Soc.* **2002**, 124, 4940.
70. Simms, R. W.; Davis, T. P.; Cunningham, M. F. *Macromol. Rapid Commun.* **2005**, 26, 592.
71. Coote, M. L.; Radom, L. *Macromolecules* **2004**, 37, 590.
72. Favier, A.; Kowollik, B. C.; Davis, T. P.; Stenzel, M. H. *Macromol. Chem. Phys.* **2004**, 205, 925.
73. Stenzel, M. H.; Davis, T. P.; Kowollik, B. C. *Chem. Commun.* **2004**, 1546.
74. Destarac, M.; Boutvein, B.; Matyjaszewski, K. In *Controlled / Living Radical Polymerization: Progress in ATRP, NMP, and RAFT*, Ed. Matyjaszewski, K., ACS Symposium Series 768. ACS, Washington, DC, **2000**, Chapter 17, pp 234.
75. Qin, D.-Q.; Qin, S.-H.; Qiu, K.-Y. *J. App. Polym. Sci.* **2001**, 81, 2237.
76. Chen, G.; Zhu, X.; Cheng, Z.; Xu, W.; Lu, J. *Rad. Phys. Chem.* **2004**, 69, 129.
77. Li, M.; Matyjaszewski, K. *Macromolecules* **2003**, 36, 6028.
78. Wang, Y. -P.; Pei, X. -W.; Yuan, K. *Mater. Lett.* **2005**, 59, 520.
79. Shen, Y.; Tang, H.; Ding, S. *Prog. Polym. Sci.* **2004**, 29, 1053.

Chapter 2. Experimental methods

This chapter describes the synthesis of ligands, initiators, general experimental procedures as well as purification and characterization techniques used in the course of this work. All the reactions were conducted under an inert atmosphere of nitrogen or argon gas, which were made free of oxygen and other reactive impurities.

2.1. Materials

All manipulations were performed using standard Schlenk or syringe techniques under an atmosphere of nitrogen. *n*-propylamine (S.d.Fine Ltd. Mumbai), *n*-pentylamine (E. Merck), *n*-nonylamine (E. Merck), *n*-butylamine (E. Merck), and pyridine-2-carboxaldehyde (Aldrich) were freshly distilled prior to use. Methylmethacrylate (Aldrich, 99%), Styrene (S.d.Fine, Mumbai), Glycidylmethacrylate (Aldrich), Methylacrylate (Aldrich), and *t*-Butylacrylate (Aldrich,) were distilled over calcium hydride. 2,6-diacetylpyridine (Aldrich), 2,6-pyridinedicarboxaldehyde (Aldrich) was used as received. Copper(I) bromide (Aldrich, 98%), Copper(I) thiocyanate (Aldrich, 99%), and Copper(I) Chloride (Aldrich, 99%) were purified according to the method of Keller and Wycoff.¹ CuBr₂, CuCl₂, *p*-toluene sulfonylchloride (*p*TsCl), and 3-methyl-2-butanone were purchased from Aldrich and used directly. Ethyl-2-bromoisobutyrate (EBiB, Aldrich) and 2,6-diisopropylaniline (Aldrich, 97%) was vacuum distilled before use. Solvents like, toluene (S.d. Fine, sulfur free), diphenylether (Aldrich), Anisole (Aldrich), dimethylformamide (Aldrich) were distilled before use. 4,5-diazafluoren-9-one (DAFONE) was procured from Aldrich. 2,2'-azobisisobutyronitrile (AIBN), N-bromosuccinimide (NBS), benzoylperoxide (BPO), CCl₄, CaCl₂ and others were purchased from E. Merck (India) and used after purification. Anhydrous magnesium sulfate (E. Merck, Germany) was used as procured. Silica gel (200-400 mesh) from SRL, Mumbai was used as received. KSCN was obtained from S.d. Fine Mumbai and used after drying under vacuum for 5 days at 160° C. Unless mentioned otherwise all other reagents were distilled/crystallize before use.

2.2. Purification

2.2.1. Nitrogen or argon gas

Nitrogen gas obtained from INOX (IOC, Mumbai) contains traces of moisture and, oxygen. Nitrogen was passed through three columns containing activated 4 Å molecular sieves and two columns containing active Cu deposited on kieselguhr kept at ~200 °C. The purified N₂ was then passed through a dark red solution of a tetramer or pentamer of poly (styryl) lithium in toluene. The moisture in N₂, if present, quenches the living oligomers, rendering the gas free of moisture. This pure nitrogen is then connected to manifold through rubber tubing for use in reaction.

Activation of molecular sieves and Cu columns were performed from time to time. Cu columns are activated by passing H₂ gas at 180 °C/ 7-8 h and the water formed by the reaction of H₂ and CuO was removed under vacuum. Molecular sieves are activated by heating at ~200 °C under vacuum for 6 h and cooled under nitrogen. The activated copper catalyst is dark brown in color while the catalyst before activation is pale green in color. This acts as the visual indicator for determining the appropriate time for reactivation.

2.2.2. Solvents

Toluene (S.d. Fine Ltd., Mumbai) was first refluxed and then fractionally distilled over CaH₂ and stored over hot activated molecular sieves. The fractionated solvent was further refluxed over K-metal or Na-benzophenone complex for 2-3 days and then distilled. The distilled solvent was stored (after proper degassing) in solvent storage flasks under high vacuum and kept continuously stirred over Na-K alloy. Required amount of solvent was distilled out into ampoules just prior to performing polymerization reactions. Ethanol (LR grade, E. Merck, Germany) was dried using MgSO₄, stirred over calcium hydride for 4 h and then distilled. It was stored in a round bottom flask over molecular sieves (type 4A) under nitrogen. N,N-dimethylformamide (Aldrich, USA), chlorobenzene (Aldrich, USA) and diphenyl ether (DPE) (Aldrich, USA) were stirred over CaH₂ for 6 h and then flash distilled in vacuo. They were stored in an ampoule under nitrogen.

2.2.3. Monomers

Methylmethacrylate (MMA), styrene, glycidylmethacrylate (GMA), methylacrylate (MA), and *t*-butylacrylate (*t*-BA) were first stirred over CaH₂ for almost 4-5 h and then distilled under vacuum and stored under N₂ in refrigerator. Prior to polymerization required amount of pre-purified monomer was taken in the reaction flask for polymerization reaction.

2.2.4. Copper (I) halides ¹

Copper salt was taken in a sintered crucible and following steps were performed

- A semi-solid paste was made with conc. H₂SO₄ and was treated with 10-15 mL of glacial acetic acid three times.
- The 20-30 mL washings of ethanol were given to the remaining mixture in crucible.
- Finally, the salt was washed with diethyl ether several times. The process was repeated three times. The resulting product was dried at 60 oC under vacuum. The catalyst was kept in a glove box under nitrogen pressure.

2.3. Synthesis of Ligands

The general structure of various N-donors from sections 2.3.1 to 2.3.5 are given in Fig. 2.1.

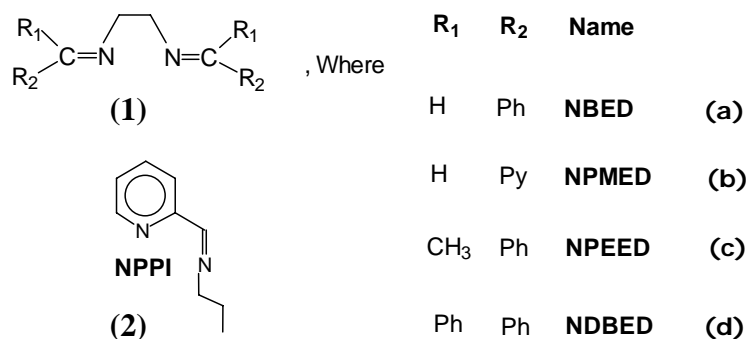


Fig. 2.1: Structures of bidentate Schiff base imines

2.3.1. N- (*n*-propyl)-2-pyridylmethanimine (NPPI) ² (2)

A solution of 2-pyridinecarboxaldehyde in 100 mL of diethyl ether was placed into a 250 mL flask under dry nitrogen together with 2-3 g of anhydrous MgSO₄. Appropriate amount of *n*-propyl amine was added dropwise to this solution with gentle cooling of the flask. After addition of amine was complete, the reaction was stirred for 4 h. The solvent was removed

by rotary evaporation and the residual oil was purified by vacuum distillation. The product was isolated as a pale yellow liquid, yield 90%. bp 60 °C/0.4 Torr. FTIR (KBr, ν , C=N): 1654 cm^{-1} . ^1H NMR (CDCl_3): δ = 8.60 (m, 1H), 8.34 (s, 1H), 7.95 (m, 1H), 7.69 (m, 1H), 7.23 (m, 1H), 3.60 (t, 2H), 1.71 (m, 2H), 0.92 (t, 3H) (Fig. 2.2). ^{13}C -NMR (CDCl_3): δ = 161.7, 154.6, 149.3, 36.4, 124.5, 121.1, 63.3, 23.8, 11.8. Anal. Calcd. for $\text{C}_9\text{H}_{12}\text{N}_2$: C, 72.9; H, 8.2; N, 18.9. Found: C, 71.85; H, 8.18; N, 19.17.

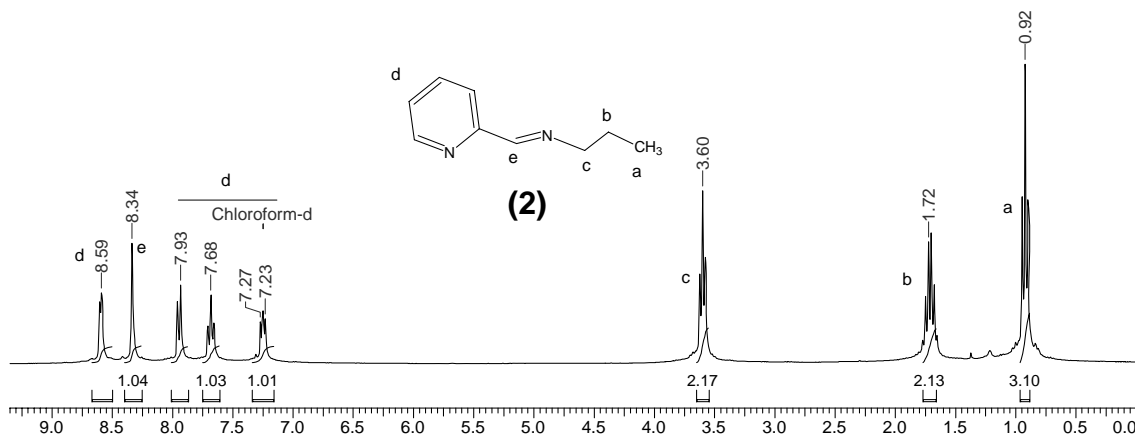


Fig 2.2: ^1H -NMR spectrum of N-(n-propyl)-2-pyridylmethanimine in CDCl_3

2.3.2. N, N'-dibenzylidene-ethane-1, 2-diamine (NBED)³ (1a)

Dry methanol (75 mL) was taken in a two-neck r.b attached with septum adapter and reflux condenser. The flask was flushed with nitrogen and 15 mL of benzaldehyde (148 mmol) was added followed by addition of 5 mL (74 mmol) of distilled ethylene diamine to the ice-cooled mixture. The solution was refluxed for 6 h over an oil bath kept at 60 °C. After 1 h anhydrous sodium sulphate was added to the reaction flask. Then the reaction mixture was evaporated on a water bath until the volume reduced to 20 mL to obtain a viscous liquid. The product was cooled in a refrigerator overnight to obtain a yellowish wax like compound. The product was recrystallized two times from n-hexane to obtain large pale yellow needle shaped crystals. Yield ~58% (9.0 g). FTIR (KBr, ν , C=N): 1650 cm^{-1} . ^1H -NMR (CDCl_3): δ = 8.3 (s, 1H, CH=N), 7.6 (m, 3H), 7.3 (m, 2H), 3.9 (t, 2H) (Fig. 2.3). Anal. Calcd. for $\text{C}_6\text{H}_{16}\text{N}_2$; C, 81.36; H, 6.78; N, 11.86. Found: C, 81.11; H, 6.98; N, 11.81.

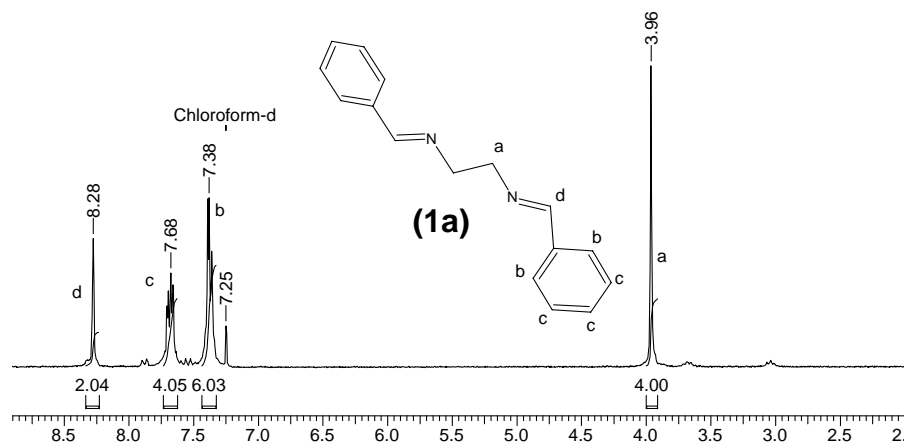


Fig 2.3: $^1\text{H-NMR}$ spectrum of N, N' -dibenzylidene-ethane-1, 2-diamine in CDCl_3

2.3.3. N, N' -bis-pyridin-2-yl-methylene-ethane-1,2-diamine⁴ (NPMED) (1b)

To a flame dried two-neck 100-mL round bottom flask containing 4 g of anhydrous MgSO_4 equipped with septum adapter, 50 mL of dichloromethane (DCM) was transferred through a cannula using dry nitrogen pressure. 6 mL (63 mmol) of freshly distilled pyridine-2-carboxaldehyde was added followed by the addition of 2.1 mL (31 mmol) of ethylene diamine at room temperature. Thereafter, the flask was stirred at room temperature for 2.25 h. Initially, white fumes were observed and later the solution turned orange yellow. After filtering, the residue was washed four times with dichloromethane. The solvent was pumped off and the orange yellow oil was cooled. The dark orange and yellow color crystals were washed several times with cold *n*-hexane till a uniform yellow color was obtained for all crystals. Recrystallization was done using hot *n*-hexane followed by treatment with activated charcoal. Yield ~ 64%. FT-IR (KBr, ν , C=N): 1650 cm^{-1} . $^1\text{H-NMR}$ (CDCl_3): $\delta = 8.59$ (d, 1H, Ar-H), 8.4 (s, 2H, N=CH), 7.95 (d, 1H, Ar-H), 7.68 (dd, 2H, Ar-H), 7.29 (m, 2H, Ar-H), 3.74 (s, 4H, $-\text{CH}_2-\text{CH}_2-$) (Fig. 2.4). *Anal. Calcd.* for $\text{C}_{14}\text{H}_{14}\text{N}_4$: C 70.6; H 5.9 ; N 23.5 ; *Found:* C 70.9 ; H 5.2 ; N 23.6.

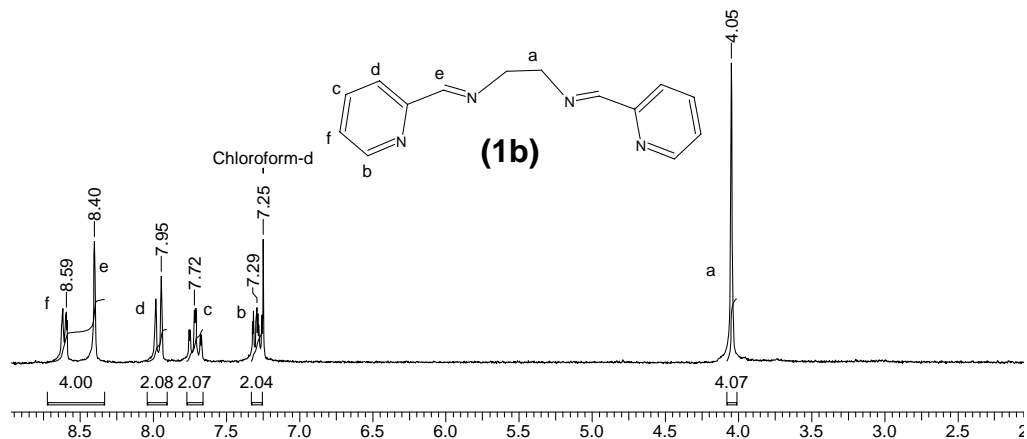


Fig 2.4: $^1\text{H-NMR}$ spectrum N,N' -bis-pyridin-2-yl-methylene-ethane-1,2-diamine in CDCl_3

2.3.4. N,N' -bis(1-phenylethylidene)-1,2-ethanediamine⁵ (NPEED) (1c)

Into a flame dried two-neck 250 mL r.b flask equipped with a Dean-Stark assembly on one side and a septum adapter to the other, was transferred 125 mL of toluene. 15.5 mL (~130 mmol) of acetophenone followed by 4.3 mL (64.4 mmol) of ethylenediamine was added to the flask at room temperature. The contents of the flask were refluxed for 3.5 h under N_2 . The reaction mixture was evaporated and cooled. The solid compound obtained was washed four times with cold *n*-hexane and finally recrystallized using benzene-hexane (1:1) mixture. Yield ~ 52%. FT-IR (KBr, ν , $\text{C}=\text{N}$): 1652 cm^{-1} . $^1\text{H-NMR}$ (CDCl_3): $\delta = 7.75$ (m, 4H, Ar- H_o), 7.35 (m, 6H, Ar- H_m , Ar- H_p), 3.92 (s, 4H, $-\text{CH}_2-\text{CH}_2-$), 2.30 (s, 6H, $-\text{CH}_3$) (Fig. 2.5). *Anal. Calcd.* for $\text{C}_{18}\text{H}_{20}\text{N}_2$: C 81.2; H 7.6; N 10.6; *Found*: C 80.3; H 7.1; N 9.9.

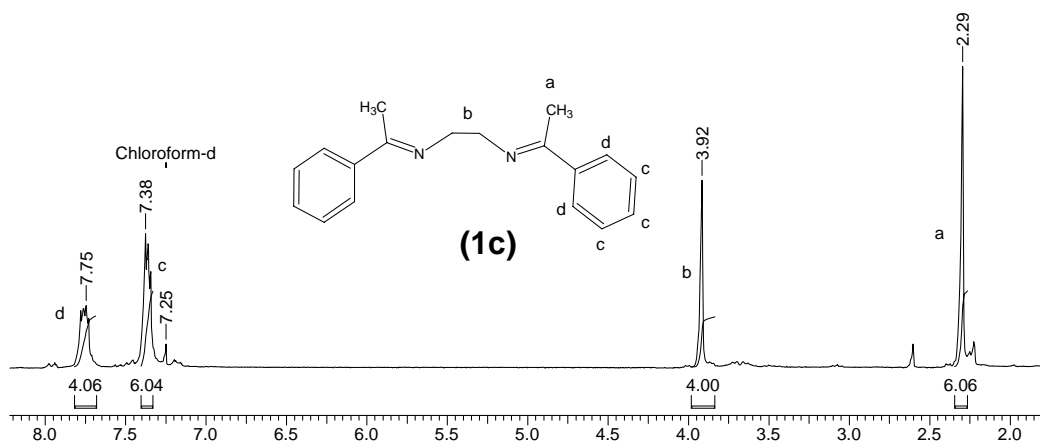


Fig 2.5: $^1\text{H-NMR}$ spectrum N,N' -bis(1-phenylethylidene)-1,2-ethanediamine in CDCl_3

2.3.5. N, N'-dibenzhydrylidene-ethane-1,2-diamine ³ (NDBED) (1d)

5.44 g of benzophenone (30 mmol) and 1 mL of distilled ethylene diamine (15 mmol) followed by addition of 1 mole % of PTSA were refluxed in 125 mL of toluene in two-neck 250 mL r.b flask for 6 h. The reaction mixture was evaporated on a water bath kept at 65°C. It was cooled to room temperature and kept overnight in a refrigerator to get a white waxy solid. The compound was recrystallized first from *n*-hexane and then in carbon tetrachloride. Yield ~ 85 %. FT-IR (KBr, ν , C=N): 1651 cm^{-1} . ¹H-NMR (CD₃COCD₃): δ = 7.57 (m, 8H, Ar-H_o), 7.32 (m, 8H, Ar-H_m), 7.1 (m, 4H, Ar-H_p), 3.74 (s, 4H, -CH₂-CH₂-) (Fig. 2.6). *Anal. Calcd.* for C₂₈H₂₄N₂: C 86.6 ; H 6.18 ; N 7.22 ; *Found:* C 86.6; H 6.15 ; N 7.13.

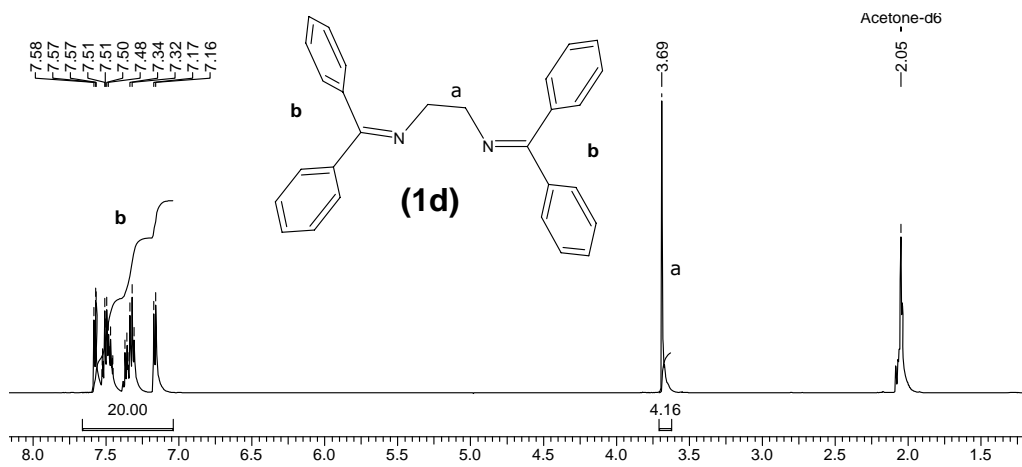


Fig 2.6: ¹H-NMR spectrum N, N'-dibenzhydrylidene-ethane-1, 2-diamine in acetone-D₆

2.3.6. N, N'-bis-(*n*-pentyl)-2,6-pyridylmethanimine (NBPPI)

To a flame dried two-neck 100 mL r.b. flask fitted with a septum adapter and an inverted ampoule (containing 2-3 g of MgSO₄, closed by a rotaflow stop-cock, using two-way BF19 joint) was transferred 100 mg (0.74 mmol) of 2,6-pyridinedicarboxaldehyde under positive pressure of nitrogen followed by 100 mL of degassed diethyl ether. To the stirred solution was added dropwise two equivalents of *n*-pentyl amine (0.22 mL; 1.48 mmol) with gentle cooling of the flask with iced water. After the addition of amine was complete, the reaction was brought to room temperature (27 °C) and stirred for 4 h. The solvent was removed by rotary evaporation and the residual oil was purified by vacuum distillation. The product was isolated as pale yellow liquid, Yield 85%, FT-IR (neat, ν , NaCl, cm^{-1}) 1650 (C=N), 1660

(C=O). $^1\text{H-NMR}$ (500MHz, CDCl_3) δ = 0.90 (s, 6, CH_3), 1.35 (bs, 8, $\text{Me}(\text{CH}_2)_2$), 1.72 (bs, 4, PropCH_2), 3.67 (m, 4, N-CH_2), 7.78 (m, 1, Py-H_p), 7.98 (s, 2, Py-H_m), 8.40 (s, 2, N=CH) (Fig. 2.7). $^{13}\text{C-NMR}$ (125 MHz, CDCl_3) δ = 161.4 (HC=N), 154.5 (HC-CH=N), 137.0 (Py-C_p), 122.1 (Py-C_m), 61.6 (N-CH_2), 30.4 (PropCH_2), 29.55 (EtCH_2), 22.46 (MeCH_2), 13.96 ($-\text{CH}_3$). Anal. Calcd for $\text{C}_{17}\text{H}_{27}\text{N}_3$: C, 74.73; H 9.89; N, 15.38. Found: C, 74.33; H, 9.96; N, 15.64.

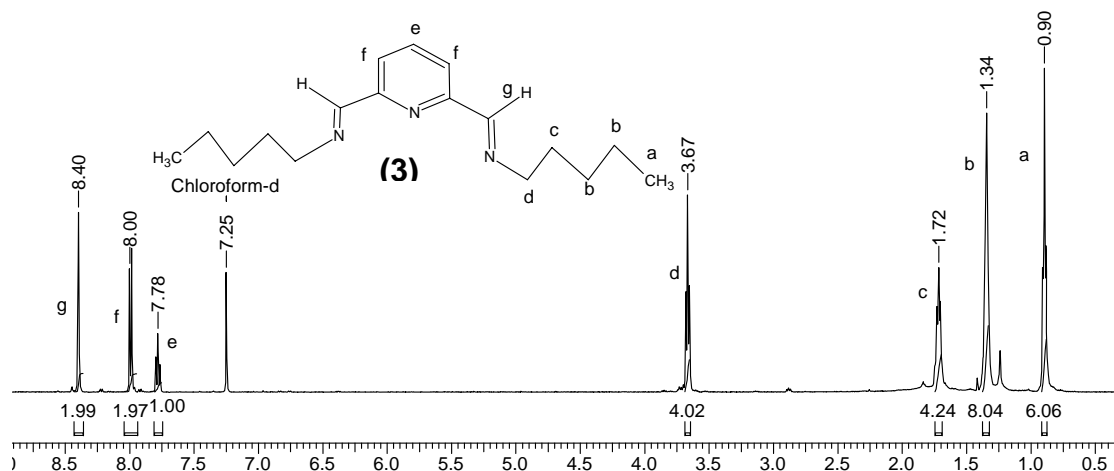
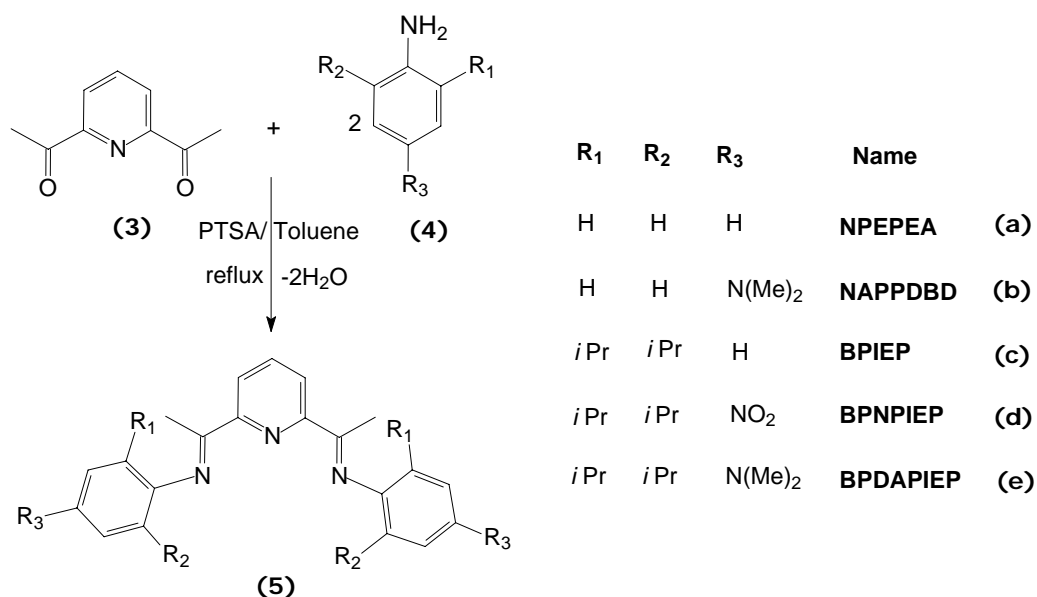


Fig 2.7: $^1\text{H-NMR}$ spectrum $\text{N, N}'$ -bis-(*n*-pentyl)-2,6-pyridylmethanimine in CDCl_3

2.3.7. 2,6-bis[1-(2,6-diisopropylphenylimino)ethyl]pyridine⁶ (BPIEP) (6c)

The general reaction for the preparation of tridentate N-donors is in Scheme 2.1. The reaction apparatus employed for the syntheses is shown in Fig. 2.8. To a 250 mL one neck round bottom flask was transferred 4.39 g (26.9 mmol) of 2,6-diacetylpyridine (**4**), 100 mL toluene, catalytic amount of PTSA (10 mol % wrt diacetyl pyridine) followed by dropwise addition of 10.5 mL of 2,6-diisopropylaniline (DIPA). The contents were refluxed (130 °C) for 24 h. Toluene was removed in vacuo and the solid obtained was washed thoroughly with methanol followed with hexane and finally with cold hexane and dried in vacuo for 8 h at 27 °C.



Scheme 2.1: Structures of tridentate Schiff base imines

Product yield 80 %. FT-IR (neat, ν , NaCl, cm^{-1}) 1630 (C=N). $^1\text{H-NMR}$ (CDCl_3): $\delta = 8.53$ (d, 2H, $\text{P}_Y\text{-H}_m$), 7.93 (t, 1H, $\text{P}_Y\text{-H}_p$), 7.20 (m, 6H, H_{aryl}), 2.79 (septet, 4H, HCMe_2), 2.25 (s, 6H, N=CCH_3), 1.18 (d, 24H, $\text{CH}(\text{CH}_3)_2$) (Fig. 2.9). $^{13}\text{C-NMR}$ (125 MHz, CDCl_3) $\delta = 167.2$ (HC=N), 155.1 (Py-C_o), 146.2 (HC-Ar) 136.9 (Ar-C_o) 135.9 (Py-C_p), 123.7 (Py-C_m) 123 (Ar-C_m) 122.4 (Ar-C_p) 28.38 ($\text{CH}(\text{Me})_2$) 22.8 ($\text{C}(\text{CH}_3)_2$) 17.15 (N=C-CH_3). *Anal. Calcd.* for $\text{C}_{33}\text{H}_{44}\text{N}_3$: C 82.16; H 9.13; N 8.71; *Found*: C 82.26; H 9.35; N 8.80.

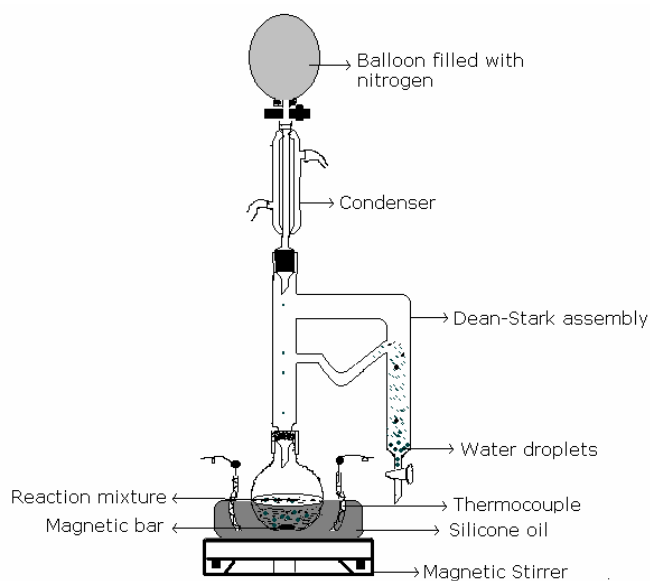


Fig. 2.8: Schiff base imine condensation using Dean Stark apparatus.

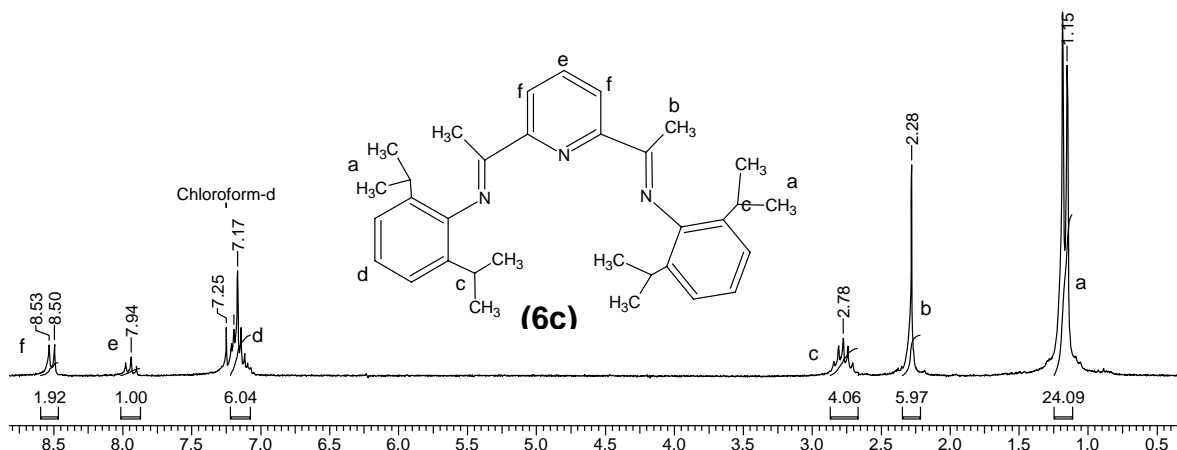


Fig 2.9: ¹H-NMR spectrum 2,6-bis[1-(2,6-diisopropylphenylimino)ethyl]pyridine in CDCl₃

2.3.8. N-((1E)-1-{6-[(1E)-N-phenylethanimidoyl]pyridin-2-yl} ethylidene) aniline (NPEPEA) (**6a**)

1g of **3** (6.13 mmol) and 1.5 mL of distilled aniline (12.3 mmol) were dissolved in 50 mL of absolute ethanol in a round bottom flask (100mL). Six drops of 97% formic acid were added, and solution was refluxed (90 °C) for 24h. Ethanol was removed in vacuo, and the solid obtained was washed with cold ethanol followed by cold hexane and dried under reduced pressure for 8 h. Yellow brown solid obtained was washed thrice with hexane followed by cold EtOH and finally cold hexane and dried in vacuo for 6 h. Yield ~24 %.

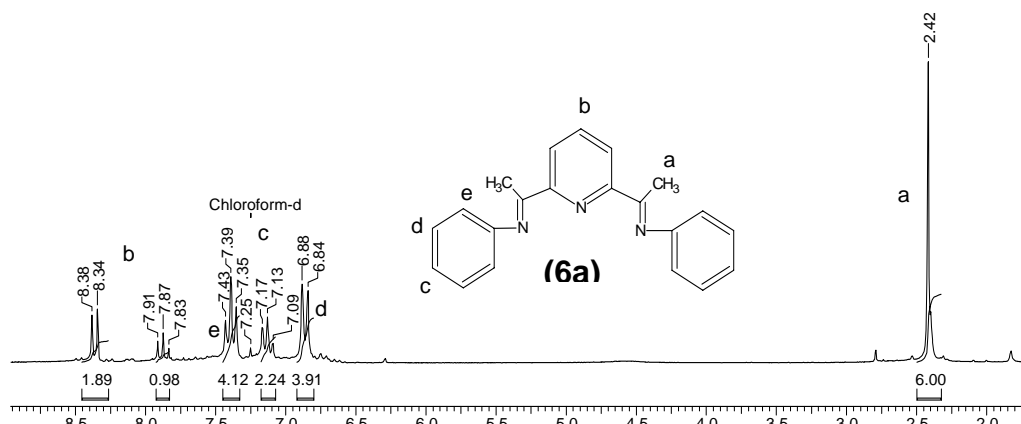


Fig 2.10: ¹H-NMR spectrum of N-((1E)-1-{6-[(1E)-N-phenylethanimidoyl]pyridin-2-yl} ethylidene) aniline in CDCl₃.

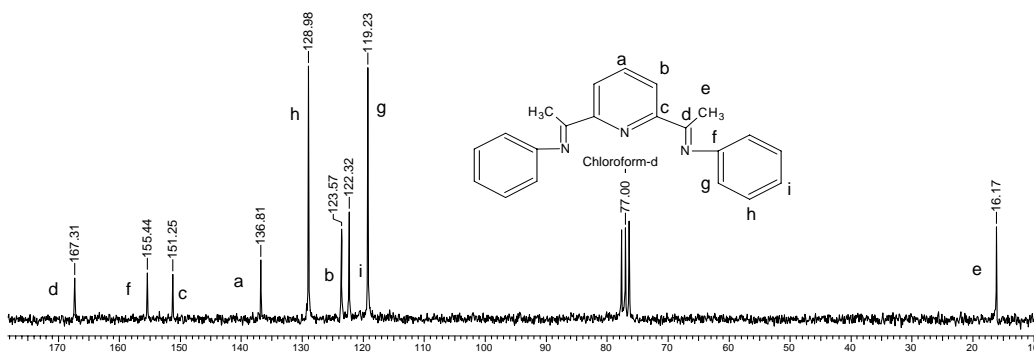


Fig 2.11: ¹³C-NMR spectrum of N-((1E)-1-{6-[(1E)-N-phenylethanimidoyl] pyridin-2-yl} ethylidene) aniline in CDCl₃.

FT-IR (neat, ν , NaCl, cm^{-1}) 1635 (C=N). ¹H-NMR (CDCl₃): δ = 8.34 (d, 2H, Py-H_m), 7.87 (t, 1H, Py-H_p), 6.84-7.43 (m, 6H, H_{aryl}), 2.42 (s, 6H, N=CCH₃) (Fig. 2.10). ¹³C-NMR (125 MHz, CDCl₃) δ = 167.3 (HC=N), 155.4 (HC-Ar), 151.2 (Py-C_o), 136.8 (Py-C_p), 128.5 (Ar-C_m), 123.5 (Py-C_m), 122.3 (Ar-C_p), 119.2 (Ar-C_o), 16.17 (-CH₃) (Fig. 2.11). *Anal. Calcd.* for C₂₁H₂₀N₃: C 80.48; H 6.11; N 13.41; *Found:* C 80.18; H 6.28; N 13.27.

2.3.9. N-((1E)-1-{6-[N-(aminophenyl)ethanimidylpyridin-2-yl]ethylidene)-N'-dimethylbenzene-1,4-diamine (NAPPDBD) (6b)

12.26 mmol of 4 (2 g) and 24.51 mmol of N,N-dimethyl-1,4-phenylenediamine (NDPA) (3.33 mL) along with 20 mg of PTSA was refluxed (140 °C) for 12h in 100 mL toluene using a Dean-Stark apparatus to separate the water of reaction. The reaction turned dark brown in color. Toluene was removed in vacuo and the solid obtained was washed thoroughly with methanol followed with hexane and finally with cold hexane and dried in vacuo for 4 h at 27 °C. The compound was crystallized using CCl₄: CHCl₃ mixture (3:1) to give yellow crystals. Yield (30 %, 1.43 g). ¹H-NMR (CDCl₃): δ = 8.29 (d, 2H, Py-H_m), 7.82 (t, 1H, Py-H_p), 6.81(m, 8H, H_{aryl}), 2.96 (s, 12 H, N(CH₃)₂), 2.47 (s, 6H, N=CCH₃) (Fig. 2.12). ¹³C-NMR (125 MHz, CDCl₃) δ = 166.4 (HC=N), 155.9 (HC=N)_{Ar}, 147.6 (Ar-C_p-N), 141.0 (CH-Ar), 136.5 (Py-C_p), 121.3 (Py-C_m), 116.5 (Ar-C_o), 113.2 (Ar-C_m), 41.01 (Ar-C_p-N(CH₃)₂), 16.17 (N=C-CH₃) (Fig. 2.13). *Anal. Calcd.* for C₂₅H₂₉N₅: C 75.15; H 7.32; N 17.53; *Found:* C 75.86; H 7.30; N 17.16.

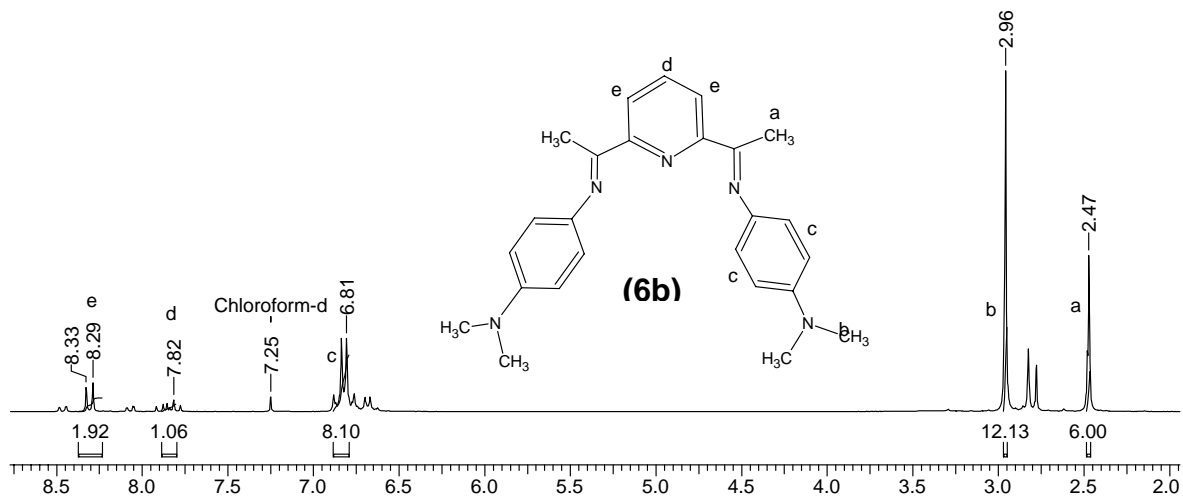


Fig 2.12: $^1\text{H-NMR}$ spectrum of (N-((1E)-1-{6-[N-(aminophenyl)ethanimidoyl]pyridin-2-yl} ethylidene)-N',N'-dimethyl benzene -1,4-diamine) in CDCl_3 .

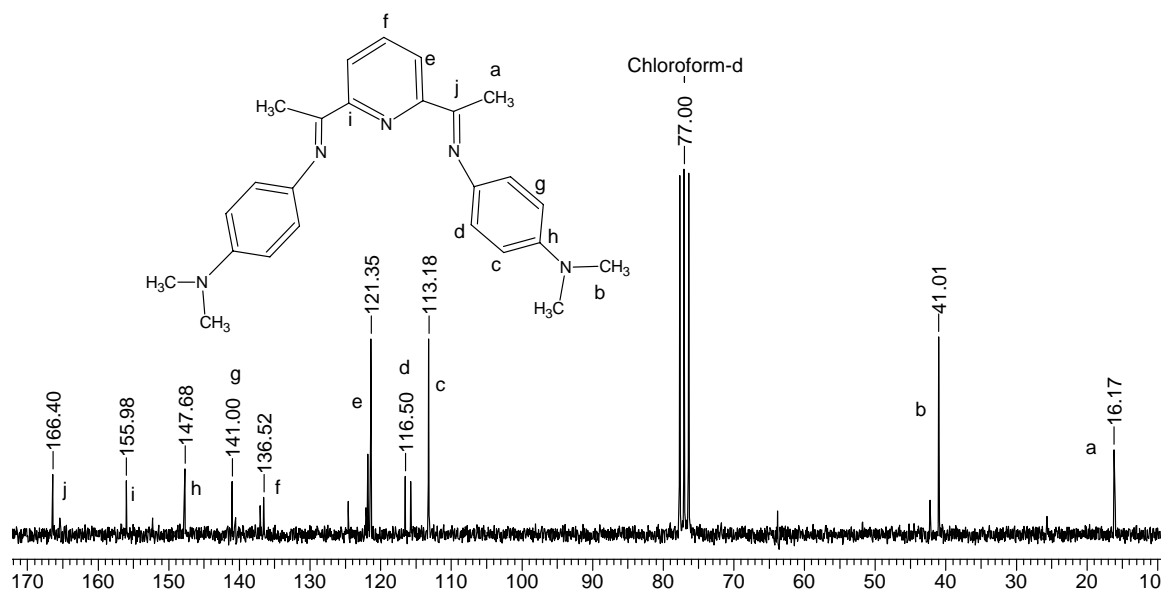


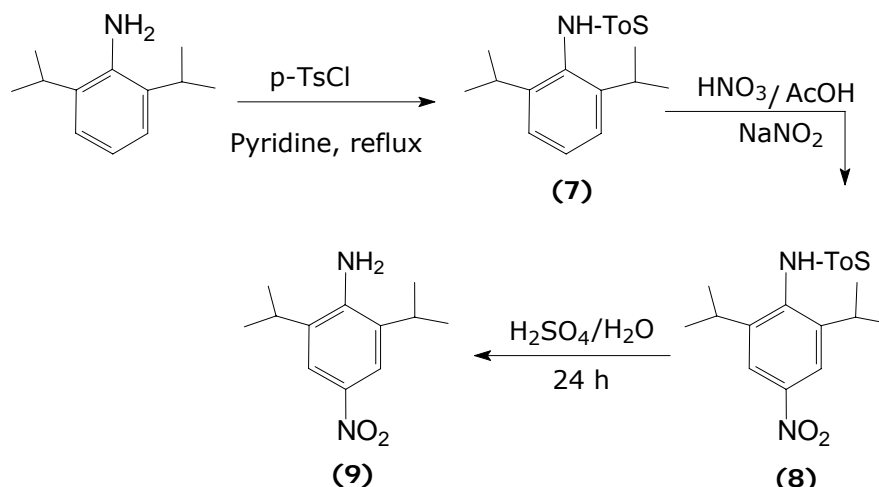
Fig 2.13: $^{13}\text{C-NMR}$ spectrum of (N-((1E)-1-{6-[N-(aminophenyl)ethanimidoyl]pyridin-2-yl} ethylidene)-N',N'-dimethyl benzene -1,4-diamine) in CDCl_3

2.3.10. 2,6-bis[1-(2,6-diisopropyl-4-nitrophenylimino)ethyl]pyridine (BPNPIEP) (6d)

The reaction steps used for the synthesis of BPNPIEP is given in Scheme 2.2

2.3.10.1. Protection of amino group of 2,6-diisopropylaniline ⁷

4-Toluene sulphonyl chloride (40.5g, 0.21 mol) was added to a stirred solution of 2,6-diisopropyl aniline (36.0 mL, 0.19 mol) in dry pyridine (75mL) and the mixture refluxed for 4 h at 146 °C under nitrogen atmosphere. The reaction mixture was poured, with stirring, into 2M HCl (250 mL) producing an orange/brown solution containing a pink solid which formed as the solution cooled.



Scheme 2.2: Synthesis of 4-nitro-2,6-diisopropyl aniline

The solid **7** was removed by filtration and recrystallised from hot ethanol as pale pink crystals (29.40 g, 51%). m.p. 158-162 °C; ¹H NMR (200 MHz, [D₆] DMSO, 21 °C): δ = 9.36 (s, 1H), 7.60 (d, 2 H), 7.40 (d, 2 H), 7.28 (t, 1H), 7.10 (d, 2H), 3.14 (sep, 2 H), 2.35 (s, 3H), 0.95 (d, 12H) (Fig. 2.14). ¹³C NMR (50 MHz, [D₆]DMSO, 21°C): δ = 148.38, 143.49, 137.43, 129.52, 128.71, 129.26, 127.41, 123.92, 28.50, 23.86, 21.51.

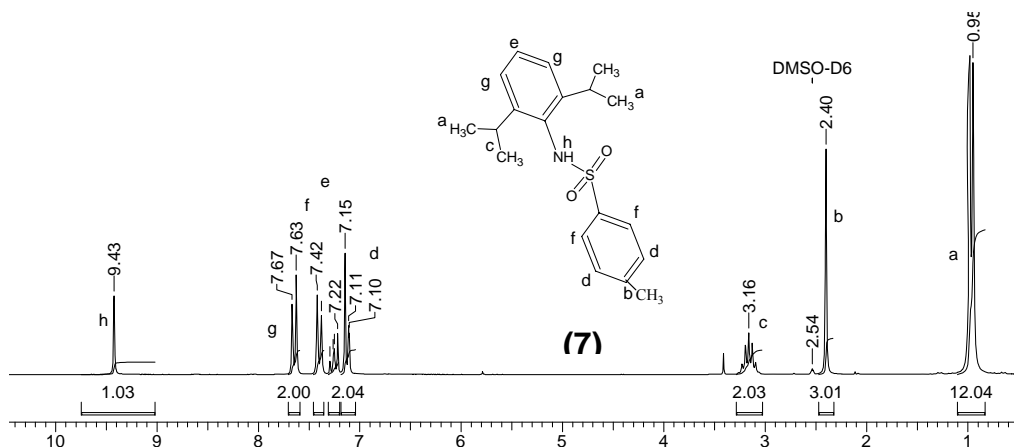


Fig 2.14: ¹H-NMR spectrum of protected amino of 2,6-DIPA in DMSO-D₆

2.3.10.2. Nitration of protected amine

7 (7.01 g, 0.021 mol), glacial acetic acid (140 mL) and sodium nitrite (2.23 g, 0.032 mol) were added successively to a stirred solution of nitric acid (30 mL) in water (140 mL). The mixture was heated at reflux for 12 h and allowed to cool to room temperature before pouring into distilled water (400 mL) where upon the product crystallized as a white solid (5.21 g, 65%) which was collected by filtration. m.p. 149-153 °C; ^1H NMR (200 MHz, CDCl_3 , 21 °C): δ = 8.00 (s, 2 H), 7.60 (d, 2 H), 7.28 (d, 2H), 6.27 (s, 1H), 3.20 (sep, 2H), 2.44 (s, 3H), 1.06 (d, 12H) (Fig. 2.15). ^{13}C NMR (50 MHz, CDCl_3 , 21°C): δ = 150.43, 147.80, 144.35, 136.72, 135.33, 129.82, 127.29, 119.72, 29.04, 23.56, 21.55; elemental analysis calcd (%) for $\text{C}_{19}\text{H}_{24}\text{N}_2\text{O}_4\text{S}$: C 60.62, H 6.43, N 7.44, S 8.52; found: C 60.27, H 6.42, N 7.10, S 8.75.

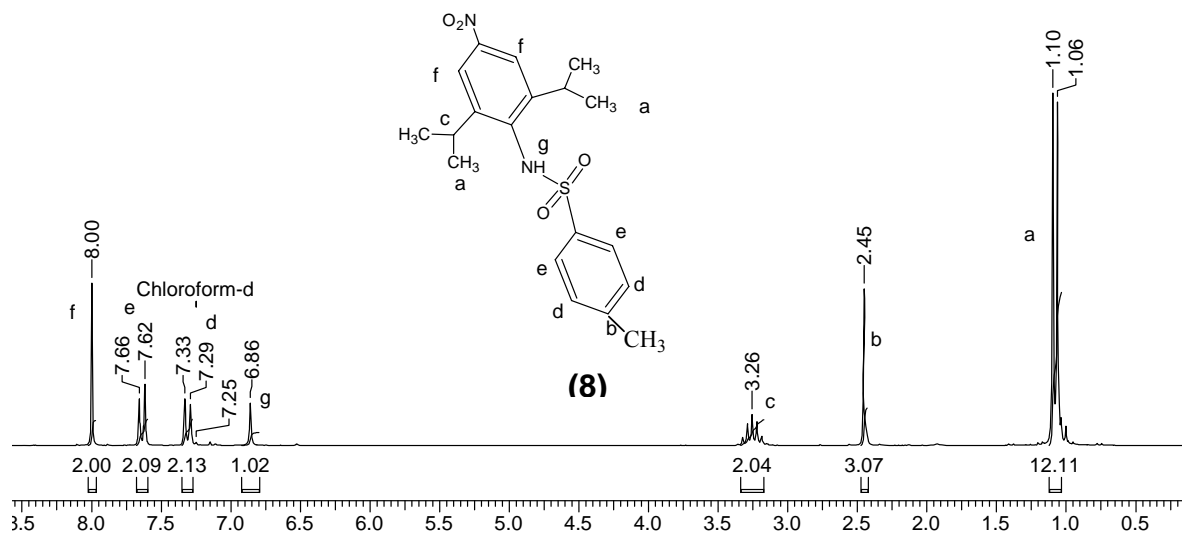


Fig 2.15: ^1H -NMR spectrum of **8** in CDCl_3

2.3.10.3. Hydrolysis of protected amine ⁷

8 (1.00 g, 2.91 mmol) was added to a solution of $\text{H}_2\text{SO}_4/\text{H}_2\text{O}$ (95:5) and the mixture was stirred at room temperature for 24 h. The resulting brown solution was poured onto ice and the mixture was made basic by the addition of NaOH pellets. The resulting yellow suspension was extracted into dichloromethane. After drying over anhydrous Na_2SO_4 , solvent was removed under reduced pressure yielding a yellow solid, which was recrystallised from dichloromethane/petroleum ether 40-60 (0.60 g, 93%). m.p. 105± 108 °C; ^1H NMR (200 MHz, CDCl_3 , 21°C): δ = 7.90 (s, 2H), 4.40 (br s, 2H), 2.80 (sep, 2 H),

1.24 (d, 12H) (Fig. 2.16). ^{13}C NMR (50 MHz, CDCl_3 , 21°C): $\delta = 146.95, 139.21, 131.43, 119.83, 28.02, 21.97$.

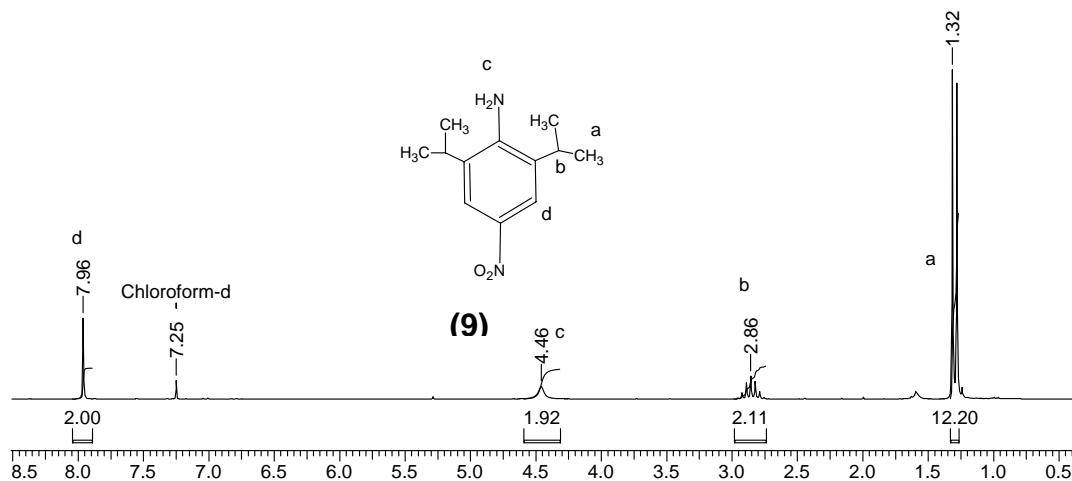


Fig 2.16: ^1H -NMR spectrum after hydrolysis of *p*-nitro-protected-2,6-DIPA in CDCl_3

2.3.10.4. Synthesis of imine ligand (BPNPIEP) (**6d**)

To a 250 mL one neck round bottom flask was transferred 0.74 g (4.5 mmol) of 2,6-diacetyl pyridine, 100 mL toluene, catalytic amount of PTSA (10 mol % wrt DAP) followed by slow addition of 2 g of **9**. The contents were refluxed (140°C) for 48 h.

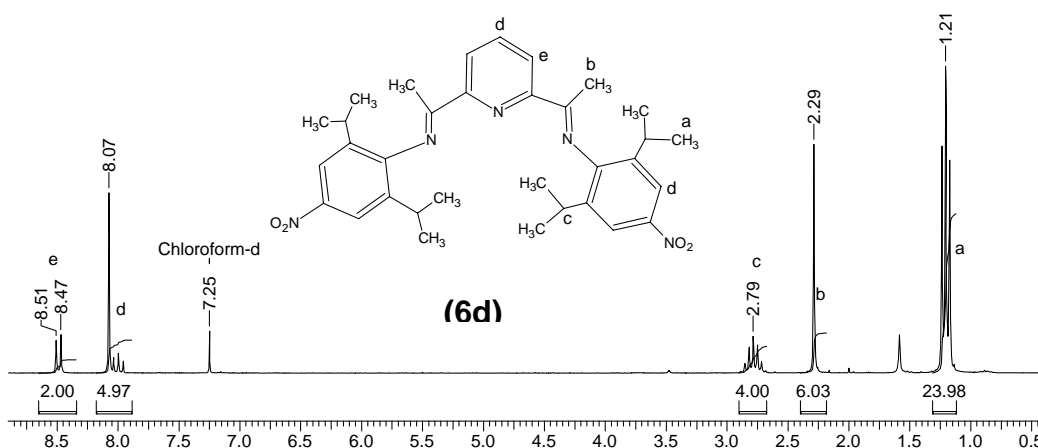


Fig. 2.17: ^1H -NMR spectrum of 2,6-bis[1-(2,6-diisopropyl-4-nitrophenylimino)ethyl] pyridine in CDCl_3

Toluene was removed in vacuo and the green solid obtained was washed thoroughly with methanol followed with hexane and finally with cold hexane and dried in vacuo for 4 h at 27°C . Yield (85 %, 2.22g). ^1H NMR (200 MHz, CDCl_3 , 21°C): $\delta = 8.5$ (d, 2H), 8.07 (s, 5H),

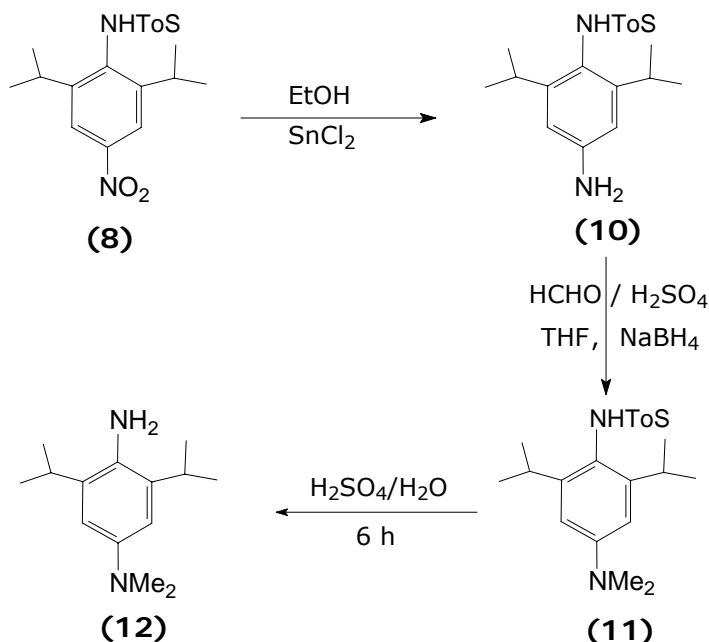
2.79 (sep, 2 H), 2.29 (s, 6H), 1.21 (d, 24H) (Fig. 2.17). ^{13}C NMR (50MHz, CDCl_3 , 21°C): δ = 16.0, 23.4, 27.0, 119.9, 126.2, 136.2, 139.2, 146.3, 149.4, 154.9, 164.6.

2.3.11. 2,6-bis[1-(2,6-diisopropyl,4-(N,N'-dimethylamino) phenylimino) ethyl] pyridine (BPDAPIEP) (6e)

The reaction steps used for the synthesis of BPNPIEP is shown in Scheme 2.3.

2.3.11.1. Reduction of protected nitro amine (10)⁷

Compound **8** (1.42 g, 3.78 mmol) was added to a solution of anhydrous SnCl_2 (4.25g, 18.9 mmol) in ethanol (20 mL) and the mixture heated at reflux (110°C) for 90 minutes. The reaction mixture was allowed to cool to room temperature and then poured onto ice and made strongly basic by the addition of solid NaOH. The resulting yellow solution was extracted into dichloromethane and the organic layer dried over anhydrous Na_2SO_4 . The solvent was removed under reduced pressure.



Scheme 2.3: Synthetic route to prepare 4-N,N-dimethyl- 2,6-diisopropyl aniline

The product **10** was isolated as a yellow solid after recrystallization from dichloromethane and petroleum ether 40-60 (1.25g, 96%). m.p. $186\text{-}187^\circ\text{C}$; ^1H NMR (200 MHz, CDCl_3 , 21°C): δ = 7.60 (d, 2H), 7.23 (d, 2H), 6.40 (s, 2 H), 5.78 (s, 1H), 3.65 (br s, 2H), 3.05 (sep, 2H), 2.44 (s, 3 H), 1.06 (d, 12H) (Fig. 2.18). ^{13}C NMR (50 MHz, CDCl_3 , 21°C): δ = 149.68,

146.50, 143.24, 137.53, 129.42, 127.42, 120.16, 110.60, 28.38, 23.70, 21.48. Elemental analysis calcd (%) C₁₈H₂₆N₂O₂S: C 65.86, H 7.56, N 8.08, S 9.25; found: C 65.48, H 7.64, N 7.77, S 9.01.

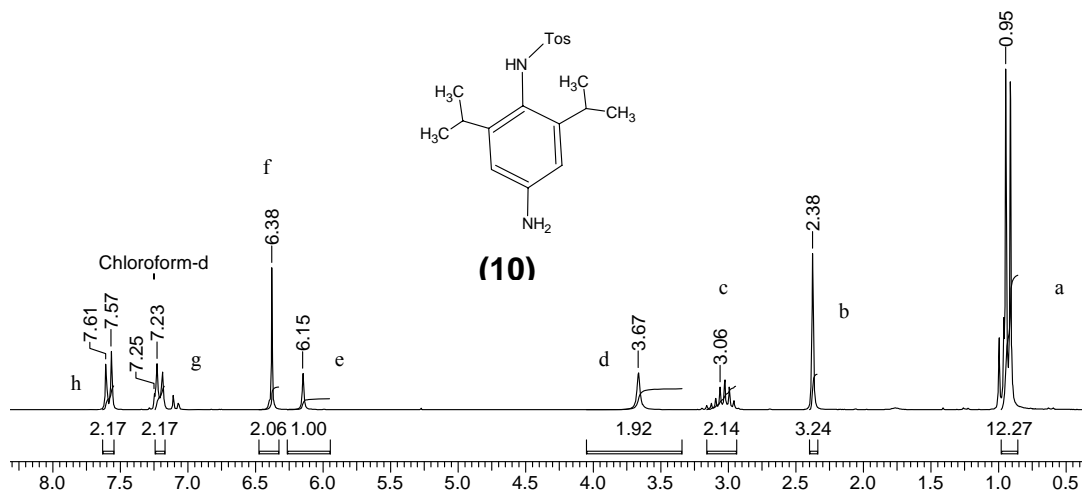


Fig 2.18: ¹H-NMR spectrum of **10** in CDCl₃

2.3.11.2. N-alkylation of protected nitro amine

A THF slurry of compound **10** (1.25g, 3.62 mmol) and finely ground NaBH₄ (0.96 g, 25 mmol) were added dropwise to a stirred solution of 3 M H₂SO₄ (2.93 mL, 9.03 mmol) and 36% aqueous formaldehyde (1.84 mL, 22 mmol) in a conical flask keeping the temperature between -10 °C and +20 °C. When the addition was complete the mixture was made strongly basic by the addition of solid NaOH. The yellow supernatant liquid was decanted and kept aside. The residue remaining in the flask was treated with distilled water (20 mL) producing a grey solution which was extracted with diethyl ether. The organic extracts were combined, washed with brine and dried over anhydrous Na₂SO₄. The solvent was removed under reduced pressure resulting in yellow oil. The oil was crystallized from dichloromethane and petroleum ether 40-60 to give a pale yellow solid (1.09 g, 81%). m.p. 177-178 °C; ¹H NMR (200 MHz, CDCl₃, 21 °C): δ = 7.60 (d, 2H), 7.23 (d, 2H), 6.40 (s, 2H), 5.85 (s, 1 H), 3.10 (sep, 2H), 2.98 (s, 6 H), 2.40 (s, 3H), 1.00 (d, 12H) (Fig. 2.19). ¹³C NMR (50 MHz, CDCl₃, 21 °C): δ = 150.2, 149.1, 143.2, 137.7, 129.4, 127.4, 118.5, 40.5, 28.6, 23.8, 21.5.

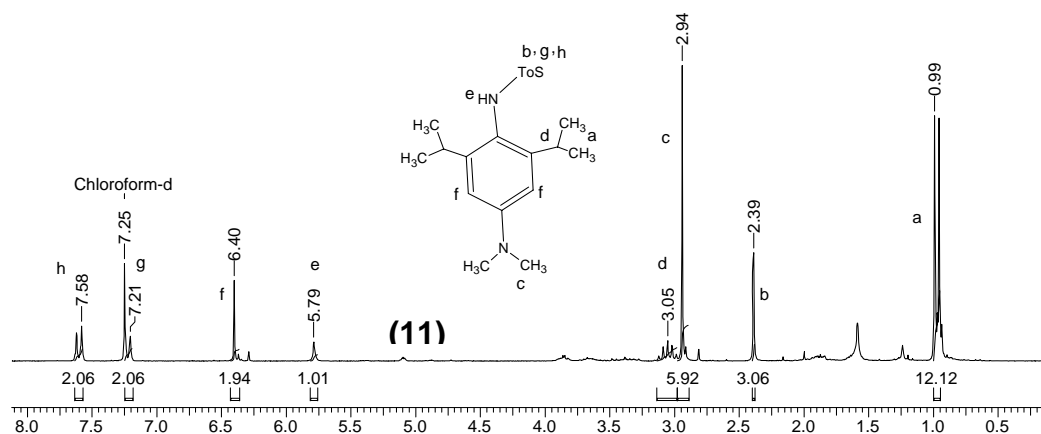


Fig 2.19: $^1\text{H-NMR}$ spectrum of **11** in CDCl_3

2.3.11.3. Hydrolysis of protected N-alkylated amine

Compound **11** (1.09 g, 2.91 mmol) was added to a solution of $\text{H}_2\text{SO}_4/\text{H}_2\text{O}$ (95:5) and the mixture warmed gently at 40°C for 6 h. After this time the brown solution was poured onto ice and the mixture made basic by the addition of NaOH pellets. The solution was extracted into dichloromethane and dried over anhydrous Na_2SO_4 before removal of the solvent under reduced pressure yielding purple oil, which was dried in vacuo for 1 h. Thin-layer chromatography showed the presence of a trace impurity. (0.52 g, 81%). $^1\text{H NMR}$ (200 MHz, CDCl_3 , 21°C): $\delta = 6.65(\text{s}, 2\text{H}), 3.75(\text{br s}, 2\text{H}), 3.00(\text{sep}, 2\text{H}), 2.90(\text{s}, 6\text{H}), 1.24(\text{d}, 12\text{H})$ (Fig. 2.20). $^{13}\text{C NMR}$ (50 MHz, CDCl_3 , 21°C): $\delta = 144.7, 134.0, 132.4, 101.1, 42.5, 28.3, 22.6$.

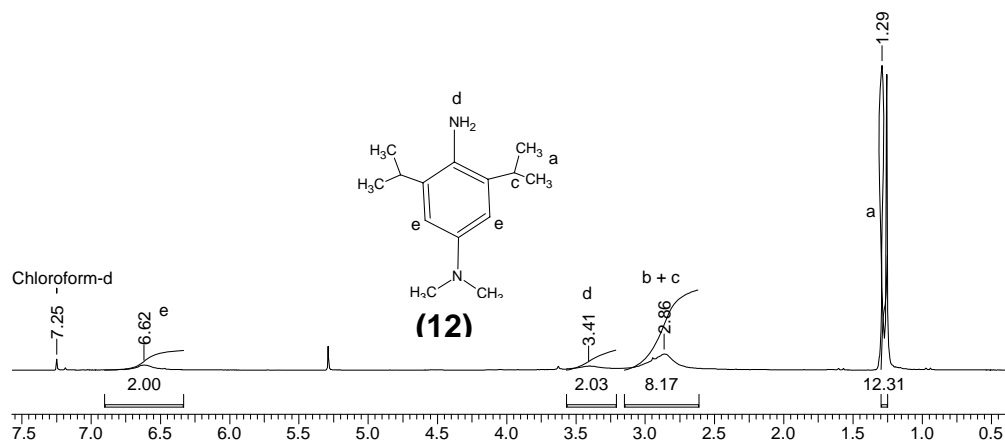


Fig 2.20: $^1\text{H-NMR}$ of **12** in CDCl_3

2.3.11.4. Synthesis of imine ligand (BPDAPIEP) (6e)

To a 250 mL one neck round bottom flask was transferred 4.39 g (26.9 mmol) of 2,6-diacetyl pyridine, 100mL toluene, catalytic amount of PTSA (10 mol % wrt DAP) followed by dropwise addition of 2 g of compound **11**. The contents were refluxed (130 °C) for 12 h. Toluene was removed in vacuo, and the dark tan color viscous liquid obtained was washed thoroughly with methanol followed with hexane and finally with cold hexane and dried in vacuo for 8 h at 27 °C. Yield (85 %, 2.22 g). ¹H NMR (200 MHz, CDCl₃, 21°C): δ = 8.5 (d, 2H), 8.19 (s, 1H), 6.63 (s, 4H), 2.95 (s, 12 H), 2.79 (s, 6 H), 2.26 (s, 6H), 1.16 (d, 24H) (Fig. 2.21). ¹³C NMR (50MHz, CDCl₃, 21°C): δ = 16.0, 23.4, 28.0, 40.3, 109.6, 126.2, 132.8, 139.2, 147.2, 154.9, 164.6.

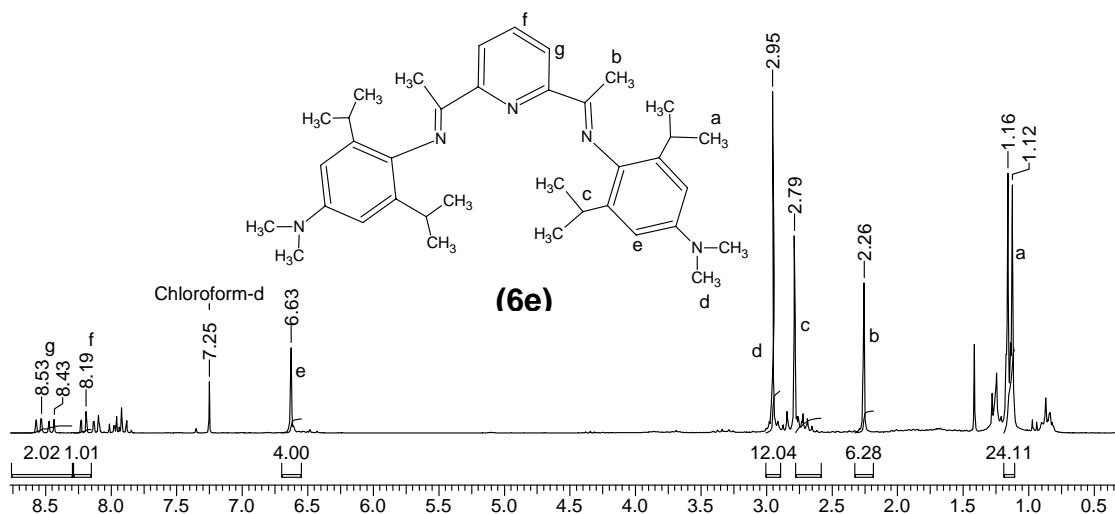


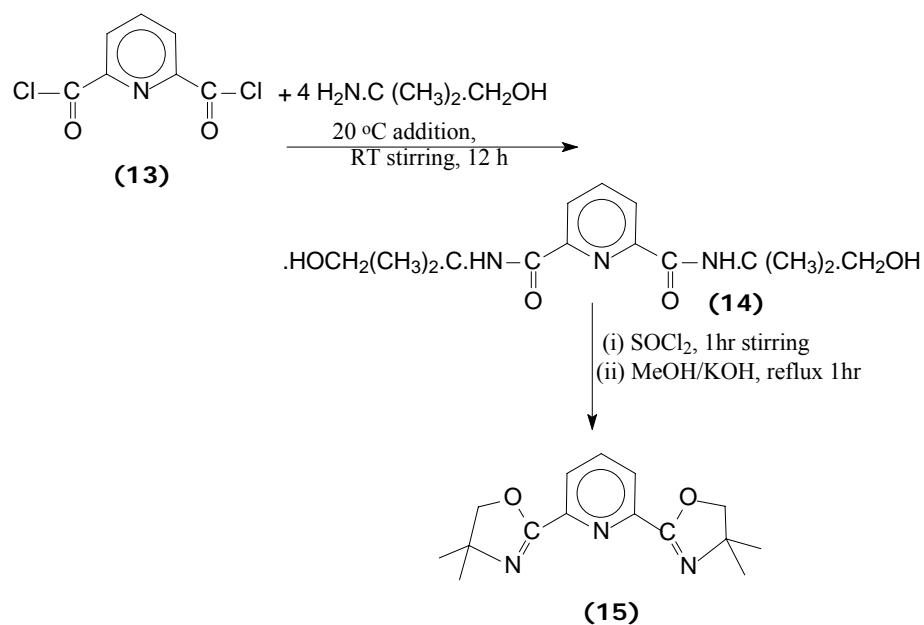
Fig. 2.21: ¹H-NMR spectrum of 2,6-bis[1-(2,6-diisopropyl-4-(N,N'-dimethylamino)phenylimino) ethyl] pyridine in CDCl₃

2.3.12. 2,6-bis(4,4-dimethyl-2-oxazolin-2-yl)pyridine ⁸ (dmPYBOX) (15)

Synthetic scheme for 2,6-bis(4,4-dimethyl-2-oxazolin-2-yl)pyridine is shown in Scheme 2.4.

2.3.12.1. Synthesis of N,N'-(1,1-dimethyl-2-hydroxyethyl) pyridine-2,6-dicarbox amide (14): 2,6-pyridinedicarbonyl dichloride (**13**) (8 g, 39.2 mmol) dissolved in dichloromethane (75 mL) was added dropwise on 2-amino-2-methyl propan-1-ol (15 g, 157 mmol) in dichloromethane (140 mL) at 0 °C.

The mixture was stirred at room temperature for 12 h. The white solid that separated from the solution was filtered, and the organic layer was washed thoroughly with water (500 mL) followed by saturated solution (200 mL) of NaHCO₃. The organic layer was dried over anhydrous Na₂SO₄. The solvent was evaporated in a rotavapor to afford a white powder. Yield (10.9g, 90 %). m.p. = 134 °C. ¹H-NMR (CDCl₃): δ = 8.43 (s, 2H, NH-CO), 8.27 (d, 2H, Py-H_m), 8.00 (t, 1H, Py-H_p), 3.65 (s, 4H, -CH₂-OH), 1.43 (s, 12H, C(CH₃)₂) (Fig. 2.22). ¹³C-NMR (125 MHz, CDCl₃) δ = 162.9 (CONH), 148.7 (Py-C_o), 139.1 (Py-C_p), 124.1 (Py-C_m), 70.1 (CH₂-OH). 55.0 (-C(CH₃)₂), 23.7 (C(CH₃)₂). *Anal. Calcd.* for C₁₅H₂₃N₃O₄: C 58.1; H 7.7; *Found*: C 57.5; H 7.8.



Scheme 2.4: Synthetic route to 2,6-bis(4,4-dimethyl-2-oxazolin-2-yl)pyridine (15)

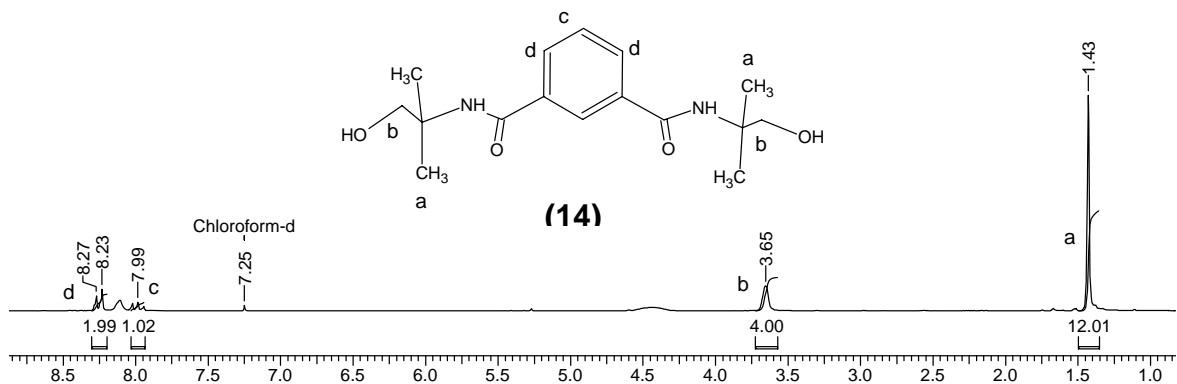


Fig. 2.22: ¹H-NMR spectrum of N,N'-(1,1-dimethyl-2-hydroxyethyl)pyridine-2,6-dicarboxamide in CDCl₃

2.3.12.2. Synthesis of bisoxazoline

3.0 mL (39.4 mmol) of dry and distilled SOCl_2 was added to N,N' -(1,1-dimethyl-2-hydroxyethyl)pyridine-2,6-dicarbox amide) (**14**) (3.6 g, 13.18 mmol). The reaction mixture was homogeneous and pale yellow in color. After one hour of stirring, excess of SOCl_2 was evaporated and 30 mL of 2 M KOH solution in methanol was added. The salt was precipitated out from solution and the mixture was further refluxed for 1 h resulting in a pale pink color solution. The reaction temperature was raised to room temperature and the solvent evaporated. The colorless viscous paste was dried in vacuo for 5 h. Upon cooling the flask a white solid was obtained.

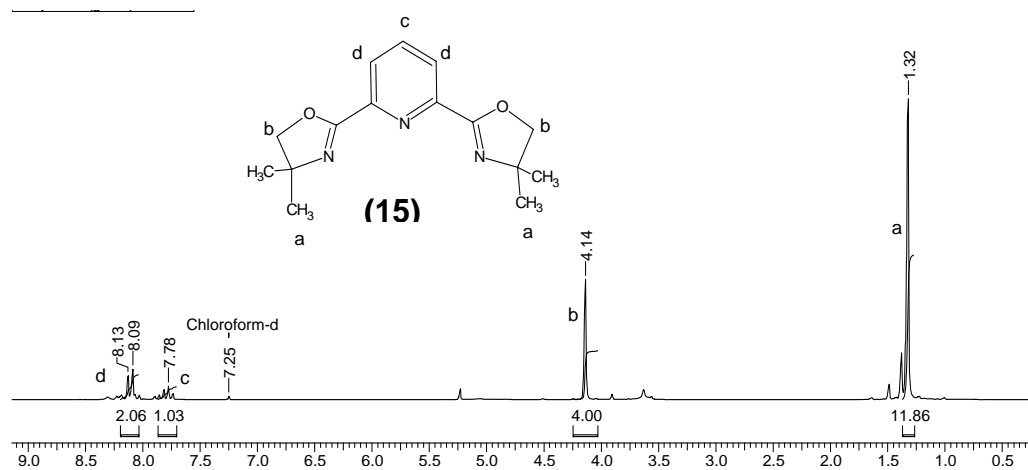


Fig. 2.23: ^1H -NMR spectrum of 2,6-bis(4,4-dimethyl-2-oxazolin-2-yl)pyridine in CDCl_3

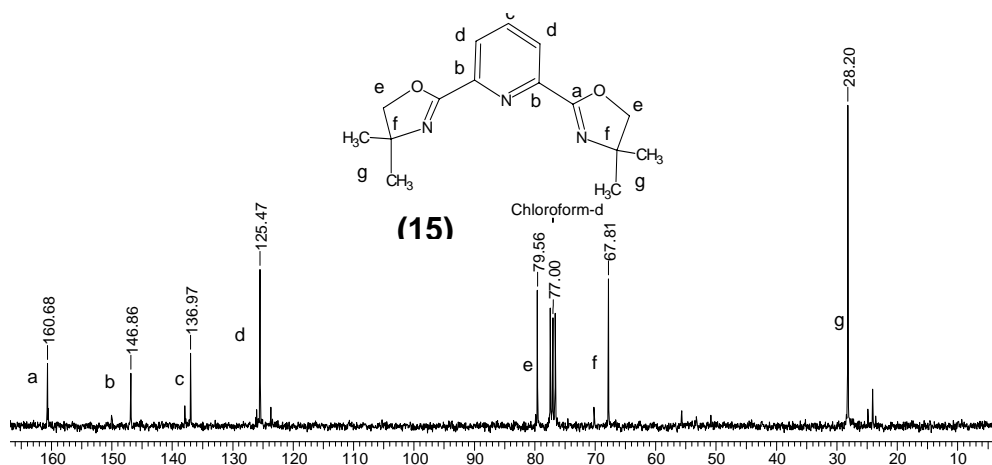


Fig. 2.24: ^{13}C -NMR spectrum of 2,6-bis(4,4-dimethyl-2-oxazolin-2-yl)pyridine in CDCl_3

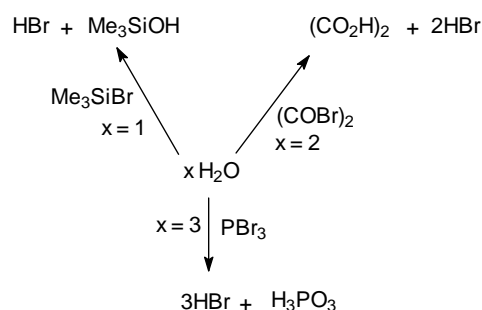
Product yield (2.7 g, 75 %). m.p. = 130 °C. FT-IR (KBr, ν , cm^{-1}) 1673 (C=N, O_{xz} ring), 1572 (C=N, Py), 1100 (C-O, O_{xz} ring), 1073-949 (C=C, Py). $^1\text{H-NMR}$ (CDCl_3): δ = 8.13 (d, 2H, Py- H_{m}), 7.78 (t, 1H, Py- H_{p}), 4.14 (s, 4H, $-\text{CH}_2-\text{O}_{\text{xz}}$ ring), 1.32 (s, 12H, $\text{C}(\text{CH}_3)_2$) (Fig. 2.23). $^{13}\text{C-NMR}$ (125 MHz, CDCl_3) δ = 160.6 (C=N, O_{xz} ring), 146.8 (Py- C_{o}), 136.9 (Py- C_{p}), 125.4 (Py- C_{m}), 79.5 ($\text{CH}_2-\text{O}_{\text{xz}}$ ring), 67.8 ($-\text{C}(\text{CH}_3)_2$, O_{xz} ring), 28.2 ($\text{C}(\text{CH}_3)_2$, O_{xz} ring) (Fig. 2.24). *Anal. Calcd.* for $\text{C}_{15}\text{H}_{19}\text{N}_3\text{O}_2$: C 65.93; H 6.96; N 15.38; *Found*: C 65.8; H 7.08; N 15.95.

2.4. Synthesis of Initiators

2.4.1. 1-Phenylethyl bromide (1-PEBr) ⁹

To a suspension of styrene (6.9 mL, 60 mmol) and SiO_2 (30 g) in dichloromethane (150 mL), a solution of PBr_3 (2.3 mL, 24 mmol) in dichloromethane (60 mL) was slowly added at 27 °C. The reaction was more efficient in terms of stoichiometry because HBr used for the reaction is prepared insitu. One mole of PBr_3 produces 3 moles of HBr by reaction with water (Scheme 2.5).

After complete addition the suspension was stirred for 20 min and then filtered. The SiO_2 was washed with 15 mL of dichloromethane, and the combined liquid was washed with 10 % NaHCO_3 followed by two brine washings. The organic extract was dried using anhydrous Na_2SO_4 . The solvent was evaporated in a rotary evaporator at reduced pressure to give pure 1-PEBr. Yield (95 %), b.p 200 °C. $^1\text{H-NMR}$ (CDCl_3): δ = 7.22-7.40 (m, 5H), 5.11 (q, 1H), 1.97 (d, 3 H) (Fig. 2.25).



Scheme 2.5: Reaction of water with phosphorous tribromide

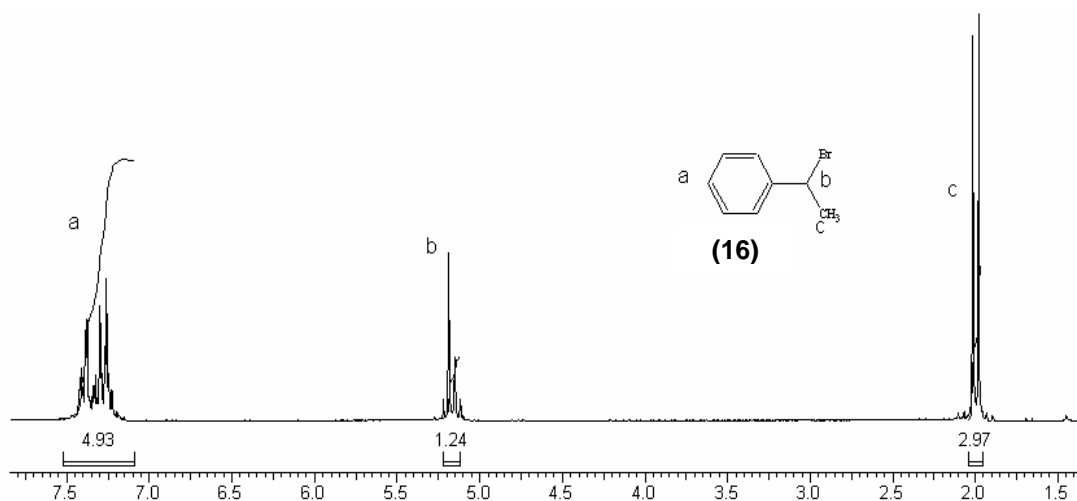


Fig. 2.25: ¹H-NMR spectrum of 1-phenylethyl bromide in CDCl₃.

2.4.2. Benzyl thiocyanate (BzSCN) ¹¹

A 100 mL round bottom flask was charged with KSCN (9.76 g, 100 mmol) dissolved in distilled water (15 mL) and silica gel (10 g, 100-200 mesh) was added in one portion. The flask was then connected to a rotatory evaporator and the water was removed in vacuo keeping the bath temperature at 50 °C. The resulting silica supported thiocyanate was dried for 4 h under dynamic vacuum at 55 °C.

Into the round bottom flask containing KSCN supported on silica was added approximately 4.00 mL (4.27 g, 33.7 mmol) of benzyl chloride. The reactants adsorbed on the solid support were mixed thoroughly and left at 30° C for 4 h with occasional shaking. The reaction mixture was dissolved in benzene and the inorganic support is separated by filtration. Removal of filtrate under reduced pressure gave BzSCN. Yield (3.84 g, 90 %), m.p 39-40° C (Lit ¹¹ m.p. 39 °C). ¹H-NMR (CDCl₃): δ = 7.35-7.52 (m, 5H), 4.13 (s, 2H) (Fig. 2.26).

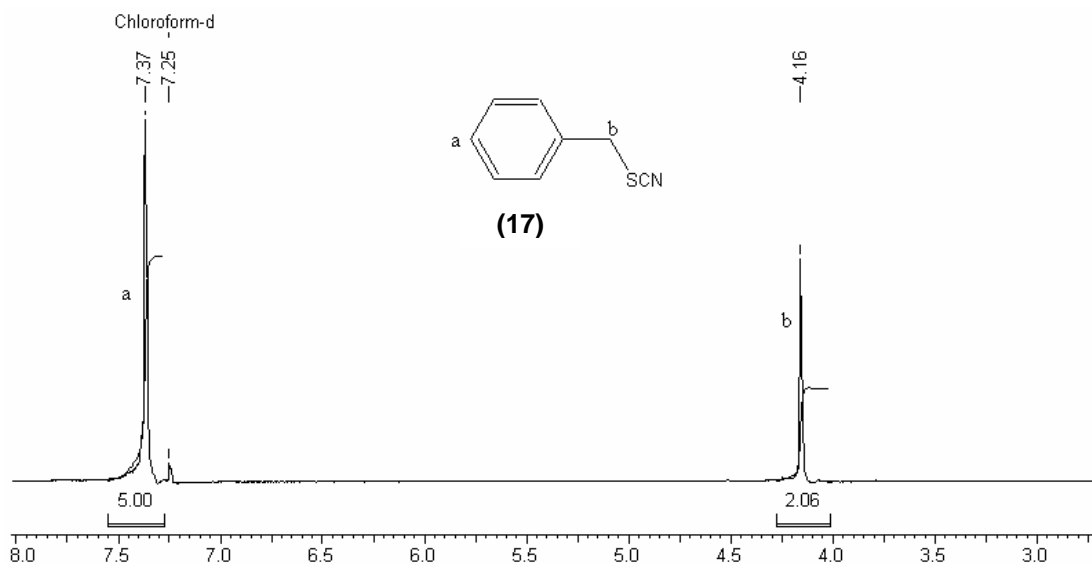


Fig. 2.26: ¹H-NMR spectrum of benzyl thiocyanate (BzSCN) in CDCl₃.

2.4.3. Ethyl-2-methyl-2-thiocyanatopropanoate (EMTP) ¹¹

EMTP was prepared using KSCN supported over silica gel (> 200 mesh). It is reported that when the loading (mmol of salt/grams of support) is 3 the yields are high. The support was made as follows: Into a 250 mL two-neck round bottom flask fitted with a septum adapter and a reflux condenser was placed 28.87 g of silica-gel 8.261 g (85.17 mmol) of KSCN and 40 mL of water (water/ mmol of salt = 0.2 -3.0). The mixture was dried in vacuo at 50 °C 12 h till a free flowing powder was formed. To this powder was added 125 mL of distilled cyclohexane and 5 mL (34.07 mmol) of ethyl-2-bromoisobutyrate with stirring. The slurry was gently refluxed at 90 °C for 24 h. The warm mixture was filtered through MgSO₄ followed by activated charcoal and the solid further washed with diethylether. Evaporation of the combined filtrates afforded the required compound as a liquid, yield 85 %, d = 1.060, b.p. 213-215 °C; IR (neat, v, NaCl, cm⁻¹) 2150 (s, SCN), 1720 (C=O) cm⁻¹. ¹H-NMR (CDCl₃) δ 1.33 (t, 3H), 1.77 (s, 6H), 4.28 (q, 2H) (Fig. 2.27). ¹³C-NMR (CDCl₃) δ: 171.1 (s, C=O), 110.7 (s, SCN), 62.8 (t, CH₂), 55.1 (s, C(Me)₂), 26.7 (qt, C(Me)₃), 13.9 (qt, EtCH₂). Anal. Calcd for C₇H₁₁NO₂S: C, 48.53; H 6.40; S, 18.51. Found: C, 48.05; H, 6.99; S, 18.66.

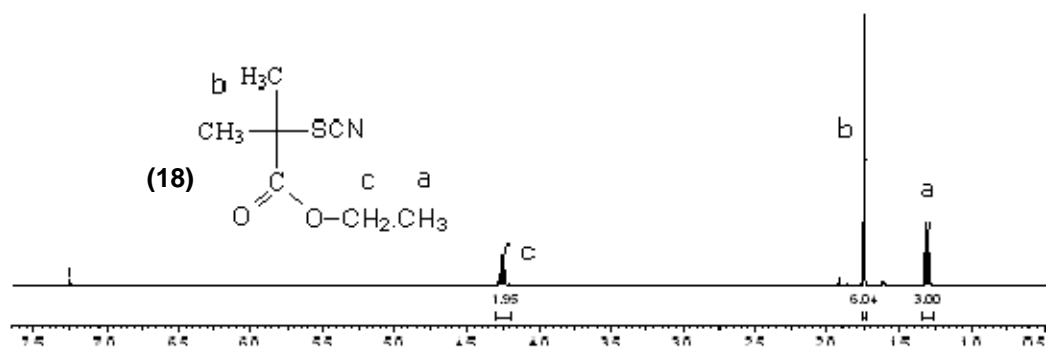
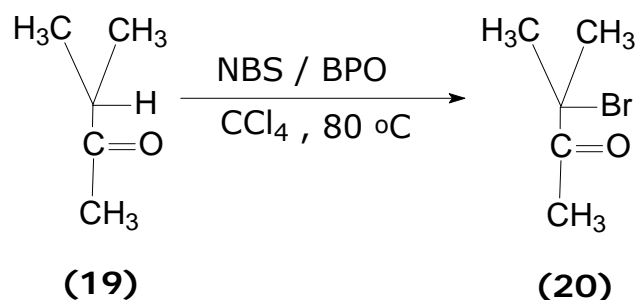


Fig. 2.27: $^1\text{H-NMR}$ spectrum of ethyl 2-methyl-2-thiocyanatopropanoate in CDCl_3 .

2.4.4. 3-Bromo-3-methyl-butanone-2 (MBB) ¹²

A mixture of 3-methyl-2-butanone (**19**) (9.4 mL, 0.0882 mmol), N-bromosuccinimide (15.7 g, 0.0882 mmol), benzoylperoxide (1.62 g, 6.67 mmol), and CCl_4 (100 mL) was heated under reflux for 6 hours (Scheme 2.6). The mixture was filtered, washed with water (4 x 50 mL) and brine (3 x 50 mL), dried over CaCl_2 , and then concentrated in vacuo.



Scheme 2.6: Synthesis of 3-bromo-3-methyl-butanone-2

The resulting oil was subjected to vacuum distillation to give the desired product. Yield (12 g, 84 %). density = 1.339 g/cc. $^1\text{H-NMR}$ (CDCl_3) δ 1.80 (s, 3H), 2.37 (s, 6H) (Fig.2.28). $^{13}\text{C-NMR}$ (CDCl_3) δ : 203 (s, C=O), 63.6 (s, C(Me₂)), 29.4(s, Br(CH₃)), 2.39(s, CH₃) (Fig. 2.29). UV (λ_{max} = 298). HPLC purity (99.5 using UV detector). IR (neat, v, NaCl, cm^{-1}) 1720 (C=O) cm^{-1} . Anal. Calcd for $\text{C}_5\text{H}_9\text{BrO}$: C, 36.36; H 5.45; Br, 48.48 Found: C, 36.23; H 5.49; Br, 48.82.

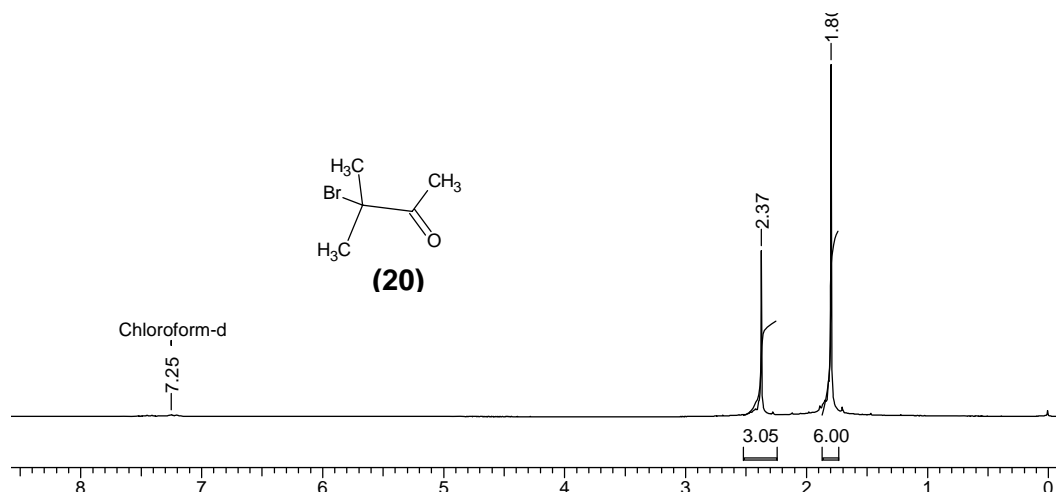


Fig. 2.28: $^1\text{H-NMR}$ of 3-bromo-3-methyl-2-butanone in CDCl_3 .

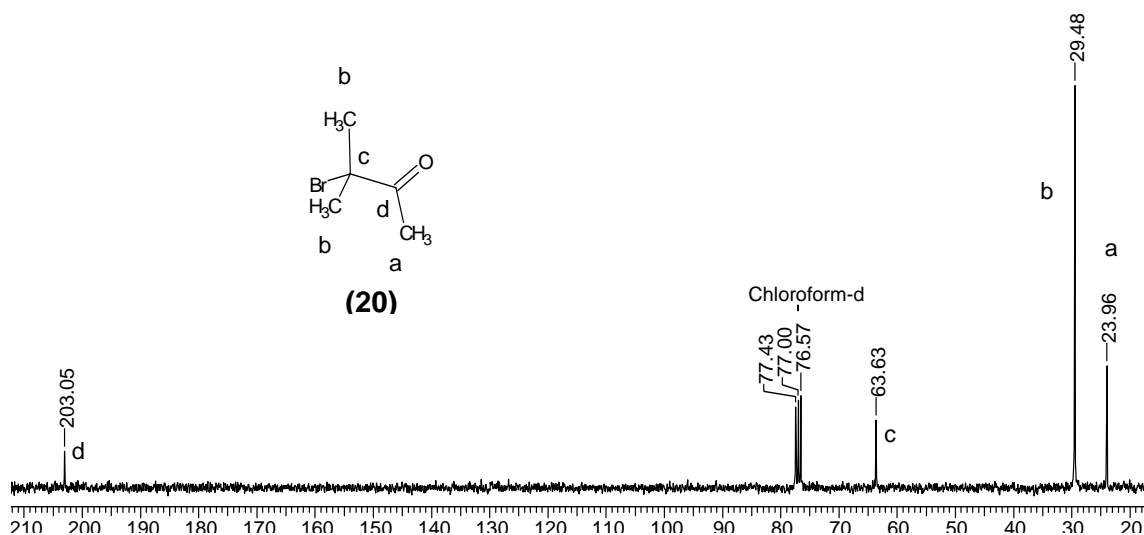


Fig. 2.29: $^{13}\text{C-NMR}$ of 3-bromo-3-methyl-2-butanone in CDCl_3

2.4.5. 3-(Bromomethyl)-4-methylfuran-2,5-dione (BMFD) ¹³

A mixture of 2 g (15.9 mmol) of 3,4-dimethyl maleic anhydride, 2.83g (15.9 mmol) of N-bromosuccinimide, 0.1g (0.4 mmol) of benzoyl peroxide and 75 mL of carbon tetrachloride was stirred and refluxed for 24 h. A second lot of 0.15 g of benzoyl peroxide was added after 10 h of reflux. The mixture was cooled to room temperature and filtered, giving 1.6g of succinimide (expected, 1.57 g). The filtrate was diluted with 20 mL of *n*-hexane, lower layer separated and evaporated, giving 2.97 g (90 mole %) of orange viscous oil as product. It was distilled in vacuo to obtain a pale yellow viscous oil, b.p. 105 °C (0.35 mm). density 1.672

g/cc. $^1\text{H-NMR}$ (CDCl_3 , 500 MHz): δ 4.15 (s, 2H); 2.12 (s, 3H) (Fig. 2.30). $^{13}\text{C-NMR}$ (CDCl_3 , 125 MHz): δ 164.9; 163.6; 143.8; 139.0; 16.0; 9.83 (Fig. 2.31). FT-IR (ν , cm^{-1} : KBr pellet): 1830 cm^{-1} and 1771 (s, C=O stretching); 1675 (m, C=C stretching); 1278 (m, C-O-C stretching). Anal. Calcd. for $\text{C}_6\text{H}_5\text{BrO}_3$: C 35.2; H 2.46; Br 38.9. Found: C 35.4; H 2.28; Br 39.5.

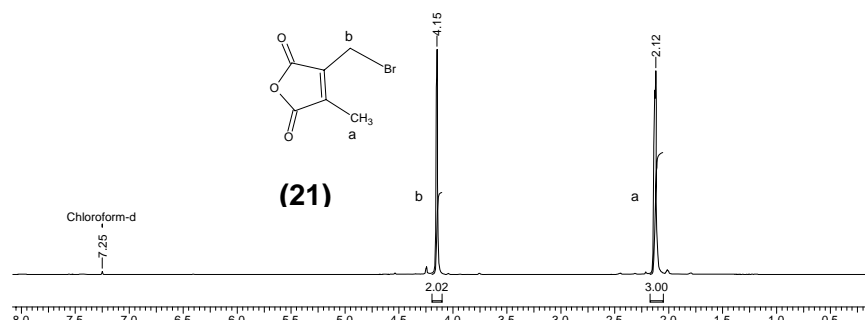


Fig. 2.30: $^1\text{H-NMR}$ of 3-(bromomethyl)-4-methylfuran-2,5-dione in CDCl_3 .

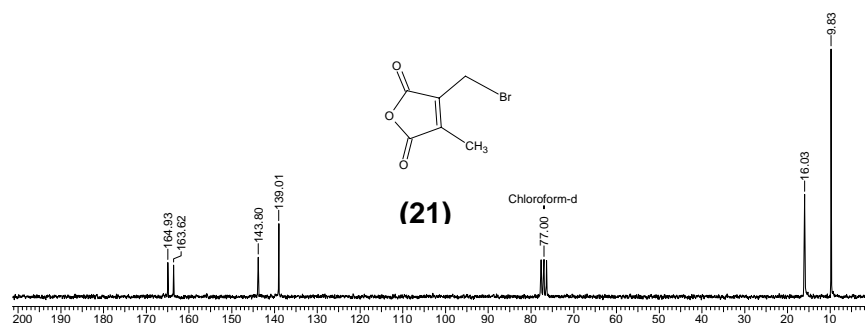


Fig. 2.31: $^{13}\text{C-NMR}$ of 3-(bromomethyl)-4-methylfuran-2,5-dione in CDCl_3 .

2.5. Electrochemical studies of copper complexes

Complexes were synthesized in acetonitrile under a positive pressure of nitrogen. The molar ratio of copper salt to the ligand was 1:2. The solution containing the complexes was degassed thrice-using freeze-pump-thaw cycles and kept stirring at 27 °C for 3 h. The complexes were soluble in acetonitrile solution. Therefore, the same solvent was used for cyclic voltammetric studies of different ligands (**1a**, **1b**, **1c**, and **1d**). The concentration of the copper complexes was kept at 0.01M in all the measurements.

2.6. General procedure for ATRP

2.6.1. Polymerization of methylmethacrylate (MMA) in toluene

A typical ATRP was carried out as follows: CuBr (68 mg, 0.468 mmol) was placed in a flame dried round-bottom flask (50 mL), which was capped by a three-way stopcock and was repetitively purged with nitrogen and evacuated for 30 minutes. MMA (5 mL, 46.8 mmol) and toluene (5 mL) were transferred to the flask using a syringe. The mixture was stirred rapidly under nitrogen and N-(*n*-propyl)-2-pyridyl-methanimine) (0.14 mL, 0.935 mmol: NPPI), was added resulting in a deep reddish-brown color solution. The required amount of ethyl-2-bromoisobutyrate (0.0686 mL, 0.468 mmol: EB*i*B) was diluted in 5 mL of toluene and transferred to the reaction flask and, finally, the solution was degassed three times using freeze-pump-thaw cycles. The resulting mixture was immersed in an oil bath maintained at 90 °C. After 4h, the reaction was quenched by cooling the flask under liquid nitrogen and diluting the final mixture with tetrahydrofuran. The polymer mixture was precipitated in excess of hexane. The polymer was redissolved in THF and passed through neutral alumina column to remove the catalyst, re-precipitated, dried in vacuo and then analyzed by GPC.

2.6.2. Polymerization of styrene

A flame dried round bottom flask equipped with a magnetic stir bar was charged with CuBr (68 mg, 0.468 mmol), BPIEP (0.450 g, 0.935 mmol), styrene (5.36 mL, 46.8 mmol) and diphenylether (1.7 mL). The flask was capped by a three-way stopcock and repetitively purged with nitrogen and evacuated for 30 minutes. The required amount of 1-phenylethylbromide (0.0638 mL, 0.468 mmol: 1-PEBr) was diluted in 1 mL of diphenylether and transferred to reaction flask and finally, the solution was degassed thrice using freeze-pump-thaw cycles. The flask was immersed in an oil bath maintained at 110 °C. After 24 h, the reaction was quenched by cooling the flask under liquid nitrogen and diluting the final mixture with tetrahydrofuran. The polymer mixture was precipitated in excess of methanol. The polymer was redissolved in THF and passed through neutral alumina column to remove the catalyst, re-precipitated again, dried in vacuo and then analyzed by GPC.

2.6.3. Polymerization of *t*-butylacrylate (*t*-BA)

CuBr (68 mg, 0.468 mmol), CuBr₂ (6 mg, 0.0234 mmol) and BPIEP (0.450 g, 0.935 mmol) were placed in a flame dried round-bottom flask equipped with a three-way stopcock connected to manifold. The flask repetitively purged with nitrogen and evacuated to remove oxygen. Monomer (*t*-BA: 6.7 mL, 46.8 mmol) and initiator (MBP: 0.104 mL, 0.468 mmol) were transferred and degassed thrice using freeze-pump-thaw cycles. The flask was immersed in an oil bath maintained at 60 °C. After 12 h, the reaction was quenched by cooling the flask and diluting the final mixture with tetrahydrofuran. The polymer was precipitated in excess of hexane. The polymer obtained was redissolved in THF and passed through neutral alumina column to remove the catalyst, re-precipitated again, dried under vacuum and then analyzed by GPC.

2.6.4. Polymerization of glycidyl methacrylate (GMA)

BPIEP (0.450 g, 0.935 mmol) degassed monomer, (GMA, 6.4 mL, 46.8 mmol) and solvent (diphenylether, 5 mL) were transferred to a flame dried round –bottom flask containing CuBr (68 mg, 0.468 mmol). The polymerization mixture was carefully degassed once using freeze-pump-thaw cycle and the initiator (BPN, 0.405 mL, 0.468 mmol) was introduced into the flask using a syringe. The solution was degassed thrice using freeze-pump-thaw cycles. The reaction flask was placed in an oil bath maintained at 60 °C. After 3 h, the reaction was quenched by cooling the flask under liquid nitrogen and diluting the final mixture with tetrahydrofuran. The polymer mixture was precipitated in excess of hexane. The obtained polymer was redissolved in THF and passed through neutral alumina column to remove the catalyst, re-precipitated again, dried under vacuum and then analyzed by GPC.

2.6.5. Bulk polymerization of methylmethacrylate (MMA)

In glove box, CuBr (134 mg, 0.936 mmol) and BPIEP (0.90 g, 1.8 mmol) were added to a flame dried round-bottom flask equipped with a three-way stopcock. The flask was then connected to the manifold and repetitively cycled between vacuum/nitrogen. Monomer (MMA: 10 mL, 93.6 mmol) and pre-distilled initiator (EB/B: 0.13 mL, 0.936 mmol) were transferred and degassed thrice using freeze-pump-thaw cycles. The flask was immersed in an oil bath preset at 90 °C and stirred at about 500 rpm for 5.5 h. Polymer was removed as before.

2.6.6. Reverse ATRP of MMA

CuBr₂ (0.468 mmol, 105 mg), Schiff base (BPIEP, 450 mg, 2-mol equivalent to CuBr), MMA (46.8 mmol, 5 mL), AIBN 0.234 mmol, 39 mg), and diphenylether (5 mL) were added under a positive pressure of nitrogen using a cannula in the order mentioned. The ligand was a light yellow color solid compound. The color of reaction mixture changed from pale yellow to dark brown upon heating indicating the change from Cu²⁺ to Cu⁺ in solution. Three freeze-pump-thaw cycles were performed to remove molecular oxygen from the polymerization mixture. Thereafter the flask was filled with nitrogen prior to placing it in an oil bath preset at 70 °C. After 24 h, the reaction was quenched by cooling the flask under liquid nitrogen and diluting the final mixture with tetrahydrofuran. The polymer mixture was precipitated in excess of hexane. The polymer was redissolved in THF and passed through neutral alumina column to remove the catalyst, re-precipitated again, dried in vacuo and then analyzed by GPC.

2.6.7. Kinetics of polymerization and estimation of rate constants

From experiment described in para 2.6.1, aliquots were withdrawn periodically using a degassed syringe. The aliquot was further diluted by addition of 5 mL of tetrahydrofuran and samples were stored at 0 °C. These samples were used for gas chromatography (GC) measurements to determine monomer conversion. *n*-Octane was used as an internal standard. Monomer conversion at time (t) with respect to that at t=0 was determined using equation 2.1,

$$p = 1 - \frac{\left(\frac{M_t}{I_t}\right)}{\left(\frac{M_o}{I_o}\right)} \quad (2.1)$$

where *p* is the conversion at time *t*, *M_t* and *M_o* are the molar concentration of MMA at time *t* and 0 respectively. *I_t* and *I_o* are the molar concentration of *n*-octane at time *t* and 0 respectively. The slope of the plot between $\ln\left(\frac{[M_o]}{[M_t]}\right)$ vs *time* gives apparent rate constant,

k_{app}, of polymerization. The rest of the sample solution remaining after GC analysis was

passed through a column of neutral alumina and subjected to GPC measurements. After 5.5 h, the reaction was quenched by cooling the flask under liquid nitrogen and diluting the final mixture with tetrahydrofuran. The polymer was precipitated in excess of hexane. The polymer was redissolved in THF and passed through neutral alumina column to remove the catalyst, re-precipitated again, dried in vacuo and analyzed by GPC.

2.6.8. Free radical polymerization of methylvinylketone (MVK)

AIBN (200 mg, 1.205 mmol), distilled and degassed MVK (120.5 mmol, 10 mL), and THF (15 mL) were placed in a flame dried round-bottom flask equipped with a three-way stopcock connected to manifold. The contents of the flask were cycled thrice between vacuum and nitrogen to remove oxygen. Thereafter, the flask was degassed twice using freeze-pump-thaw cycles. The flask was immersed in an oil bath maintained at 70 °C. After 30 h, the reaction was quenched by cooling the flask and diluting the final mixture with tetrahydrofuran. The polymer was precipitated in excess of hexane, dried in vacuo and analyzed by GPC.

2.6.9. ATRP of MVK

In a glove box, CuBr (68 mg, 0.4744 mmol) was placed in a flame dried round-bottom flask equipped with a three-way stopcock. The flask was then connected to the manifold and cycled repetitively between vacuum/nitrogen. MVK (5 mL, 60.25 mmol) and toluene (5 mL) were transferred to the flask using a syringe. The mixture was stirred rapidly under nitrogen and NPPI (0.14 mL, 0.95 mmol), was added resulting in a deep reddish-brown color solution. The required amount of EBiB (0.069 mL, 0.4744 mmol) was transferred to the reaction flask and finally, the solution was degassed thrice using freeze-pump-thaw cycles. The flask was immersed in an oil bath preset at 90 °C. After 4 h, the reaction was quenched by cooling the flask under liquid nitrogen and diluting the contents with tetrahydrofuran. The polymer was precipitated using an excess of hexane.

2.6.10. Reverse ATRP of MVK

CuBr₂ (0.468 mmol, 105 mg), Schiff base (bipyridyl, 160 mg, 2-mol equivalent to CuBr), MVK (46.8 mmol, 5 mL), AIBN (0.234 mmol, 39 mg), and anisole (5 mL) were added

under a positive pressure of nitrogen using a cannula in the order stated above. The ligand was a pale yellow color compound. The color of the reaction mixture turned from pale yellow to brown after degassing and then to dark brown upon heating indicating the change from Cu^{2+} to Cu^+ in solution. Three freeze-pump-thaw cycles were performed to remove molecular oxygen and the reaction flask was placed in an oil bath preset at 70 °C. After 20 h the reaction was quenched by cooling the flask under liquid nitrogen and diluting the final mixture with tetrahydrofuran. The polymer was precipitated using an excess of hexane.

2.6.11. Copolymerization of MVK and MMA by reverse ATRP

CuCl_2 (63 mg, 0.468 mmol), 2,2-bipyridine (bpy: 160 mg, 0.935 mmol) and AIBN (0.234 mmol, 39 mg) were placed in a flame dried round-bottom flask equipped with a three-way stopcock. The flask was then connected to the manifold and repetitively cycled between vacuum/nitrogen. MMA (1.84 mL, 17.55 mmol) and MVK (0.5 mL, 0.60 mmol) were added to the flask using a syringe. The mixture was stirred rapidly under nitrogen resulting in a dark dirty green colored solution. The solution was degassed three times using freeze-pump-thaw cycles. Thereafter, the flask was immersed in an oil bath preset at 70 °C. After 24 h, the reaction was quenched by cooling the flask under liquid nitrogen and diluting the final reaction mixture with tetrahydrofuran. The polymer was precipitated using an excess of hexane.

2.7. Characterization techniques

Polymer samples were analyzed by SEC. Molecular weights and MWD were determined using a GPC-TQ with two 60 cm PSS SDV-gel columns: 1 x 10 μ /100 Å, and 1x 10 μ /linear: 10²-10⁵Å columns connected in series, using an RI and UV detector and tetrahydrofuran as an eluent for mobile phase (flow rate of 1mL min⁻¹). Monodisperse PMMA standards from PSS Germany were used for calibration. For kinetic experiments, monomer conversions were determined using a Perkin Elmer XL gas chromatograph equipped with FID detector and a BP1 (non-polar) column. FT-IR spectra were recorded in the solid state as KBr disc in the range 4400-400 cm⁻¹ on a Perkin Elmer Spectrum GX spectrometer. UV spectra of samples were recorded using HPLC grade chloroform on UV-1601PC, Shimadzu spectrophotometer. Elemental analyses were performed using CHNS-O EA11008 elemental

analyzer, Carlo Erba Instruments, Germany. $^1\text{H-NMR}$ & $^{13}\text{C-NMR}$ were obtained in CDCl_3 using a 200/300/500 MHz Brüker MSL spectrometer. Thermogravimetric analysis was performed using a TA instruments TGA Q5000 RI analyzer in N_2 at $10\text{ }^\circ\text{C}/\text{min}$. Cyclic voltammograms of all the complexes were recorded in acetonitrile solution on a Bioanalytical System BAS CV-27 from USA with an XY recorder. A three electrode configuration composed of a Pt disc, 2 mm diameter, working electrode, a Pt wire counter / auxiliary electrode, and a saturated calomel as reference electrode filled with a solution by a bridge (4 mL) filled with a 0.1 M tetraethyl ammonium perchlorate (TEAP) in acetonitrile.

2.8. References

1. Keller, R. N.; Wycoff, H. D. *Inorg. Synth.* 1947, 2, 1.
2. Haddelton D. M.; Duncalf D. J.; Kukulj D.; Crossman M. C.; Jackson, S. G.; Bon, S. A. F.; Clark, A. J.; Shooter A. J. *Eur. J. Inorg. Chem.* **1998**, 1799.
3. Chowdhury S.; Patra, G. K.; Drew, M. G. B.; Chattopadhyay, N.; Datta, D. *J. Chem. Soc., Dalton Trans.*, **2000**, 235-237.
4. Ng, C.; Sabat, M.; Fraser, C. L. *Inorg. Chem.* **1999**, 38, 5545.
5. Tidjani-Rahmouni, N.; Adjebbar-Sidd, S.; Hamrit, H.; Benali-Baitich, O. *J. Soc. Alger. Chim.* **2001**, 11, 121.
6. Britovsek, G. J. P.; Gibson, V. C.; Kimberley, B. S.; Maddox, P. J.; McTavish, S. J.; Solan, G. A.; White, A. J. P.; Williams, D. J. *Chem Commun.* **1998**, 849.
7. Carver, F. J.; Hunter, C. A.; Livingstone, D. J.; McCabe, J. F.; Seward, E. M. *Chem. Eur. J.* **2002**, 8, 2847.
8. Chevallier, P.; Soutif, J.-C.; Brosse, J.-C. *Eur. Polym. J.* **1998**, 34, 767.
9. Sanseverino A. M.; de Mattos, M. C. S. *J. Braz. Chem. Soc.* **2001**, 12, 685.
10. Kodomari, M.; Kuzuoka, T.; Yoshitomo, S. *Synthesis* **1979**, 141.
11. Brimeyer, M. O.; Mehrota, Quici, S.; Nigam, A.; Regen, S. L. *J. Org. Chem.* **1980**, 45, 4254.
12. Takashi, S.; Eiichiro, A.; Kazuyoshi, M.; Masanori, U. Akira, T. *Bull. Chem. Soc. Jpn.* **1987**, 60, 1945.
13. Fields, E. K.; Winzenburg, M. L. *US4526986* **1985**, 5p.

Chapter 3. Atom transfer radical polymerization of methyl methacrylate using 2,6-bis[1-(2,6-diisopropylphenylimino)ethyl]pyridine - A tridentate ligand

3.1. Introduction

Since its discovery, copper mediated ATRP has become one of the most powerful tools for controlled polymer synthesis by radical method.¹ Recent studies have been aimed at developing new ligands and metals that increase the activity and selectivity of the catalyst.²⁻⁵ The ligand plays a crucial role in solubilizing the transition metal salt, and adjusts the redox potential of the metal center for the atom transfer.⁶⁻⁸ The copper(I) catalytic systems based on bidentate (2,2'-bipyridine derivatives) and multidentate nitrogen ligands have been shown to be very effective for producing relatively high molecular weight polymers and for controlling the polydispersity. In general, Schiff based ligands are more effective for the polymerization of (meth)acrylates⁹⁻¹¹ in toluene or xylene solution in conjunction with copper halides along with suitable alkyl halide initiators over a range of temperatures, even, as low as $-15\text{ }^{\circ}\text{C}$ (68 % conversion in 116 h, $M_n = 10,200$, $M_w/M_n = 1.28$).¹²

Increasing the polarity of the solvent influences the solubility of the catalyst.^{13,14} A careful consideration of the solvent with regard to the coordination of various species that may be present in the reaction and its ability to solubilize a monomer, polymer, and catalyst is always required. Therefore, it has been considered that an increase in the solvent polarity and the associated increase in the rate of reaction would enable the catalyst level to be reduced in addition to lowering the reaction temperature.¹⁵ In addition to solvent, the temperature has a significant effect on thermodynamic parameters like activation energy ($\Delta E_{app}^{\ddagger}$) as well as equilibrium constant (K_{eq}) and molecular weights.¹⁶

This chapter explores the utility of a tridentate ligand possessing bulky aryl groups, namely, 2,6-bis [1-(2,6-diisopropylphenylimino) ethyl] pyridine (BPIEP), copper (I) bromide as the catalyst and ethyl-2-bromoisobutyrate (EBiB) as the initiator for the controlled polymerization of methyl methacrylate (MMA). Similar ligands have found extensive use

with late transition metals in ethylene polymerization by Brookhart¹⁷ and Gibson¹⁸. However, there is no prior report of such tridentate ligands in ATRP. The only report of the use of a similar class of tridentate ligand in ATRP is due to Göbelt and Matyjaszewski¹⁹ who used a dialkylimino- and dialkylaminopyridine complexes of CuBr and FeBr₂ in ATRP of MMA, styrene and methylacrylate in anisole at 90 °C with 2-bromo propionitrile as initiator. However, the polymerization of MMA was uncontrolled with dialkyl imino-/FeBr₂ catalyst (42 % conversion in 9 h, $M_n = 8,400$, $M_w/M_n = 1.68$) and somewhat better controlled with CuBr as catalyst (68 % conversion in 3.5 h, $M_n = 13,600$, $M_w/M_n = 1.23$).

3.2. Results and discussion

3.2.1. ATRP of MMA using BPIEP as ligand and EB*i*B as initiator

A bulky schiff base imine having three N-donors was employed as a ligand for ATRP of MMA. The polymerization was conducted in a non-polar medium (i.e., 66 % v/v toluene wrt monomer) at 95-85 °C with DP = 100. The mole ratios of various components of ATRP were kept as [MMA]: [EB*i*B]: [CuBr]: [BPIEP] = 100: 1: 1: 2.

Table 3.1: ATRP of MMA in toluene using 2,6-bis[1-(2,6-diisopropyl phenyl imino) ethyl] pyridine (BPIEP) as ligand

Run	[M] ₀ ^{a)} (mmol)	[I] ₀ ^{b)} (mmol)	Temp (°C)	Conv ^{c)} (%)	M _{n,cal} ^{d)}	M _{n,SEC}	PDI
1	46.8	0.477	85	64	6,300	12,300	1.21
2	46.8	0.474	85	55	5,400	11,400	1.22
3 ^{e)}	46.8	0.477	95	55	5,400	11,900	1.26
4 ^{e)}	46.8	0.477	95	64	6,300	13,900	1.22

^{a)} [M]₀ = 3.12M, [MMA]: [EB*i*B]: [CuBr]: [Ligand] = 100: 1: 1: 2, toluene (50 %, v/v) wrt monomer and reaction time = 5 h; ^{b)} [I]₀: initiator; ^{c)} gravimetrically, ^{d)} M_{n,cal} = % conversion (grams of monomer / moles of initiator), ^{e)} reaction for 4.5 h.

All the batch experiments (Table 3.1) using the tridentate ligand (BPIEP) were performed under nitrogen atmosphere. The color of the complex changed from pale yellow to dark yellow after 1 h and finally reaching to dark red brown. The rate of color change at higher temperature (95 °C) was faster as compared to lower temperature (85 °C). The initiator

efficiency was ~ 0.5 in all the runs. Low initiator efficiency could be due to the temperature variation or the effect of bulky ligand employed in the reaction, thereby, causing more termination by radical coupling. The reaction was conducted at $90\text{ }^{\circ}\text{C}$ to get better results.

3.2.2. Kinetics of bulk polymerization of MMA with BPIEP ligand

Kinetics of bulk ATRP of MMA at $90\text{ }^{\circ}\text{C}$ was performed using CuBr as catalyst, EBiB as initiator and a tridentate ligand (BPIEP) bearing a central pyridine unit and two peripheral imine coordination sites. The mole ratios of various components utilized are $[\text{MMA}]:[\text{EBiB}]:[\text{CuBr}]:[\text{L}] = 100:1:1:2$.

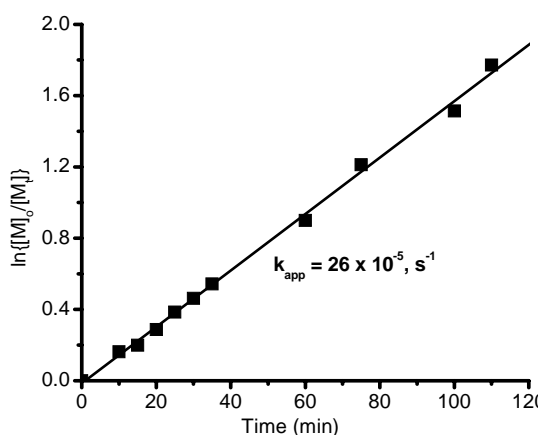


Fig. 3.1: First order kinetic plot for the bulk ATRP of MMA at $90\text{ }^{\circ}\text{C}$. $[\text{MMA}] = 3.12\text{ M}$. $[\text{MMA}]:[\text{EBiB}]:[\text{CuBr}]:[\text{BPIEP}] = 100:1:1:2$.

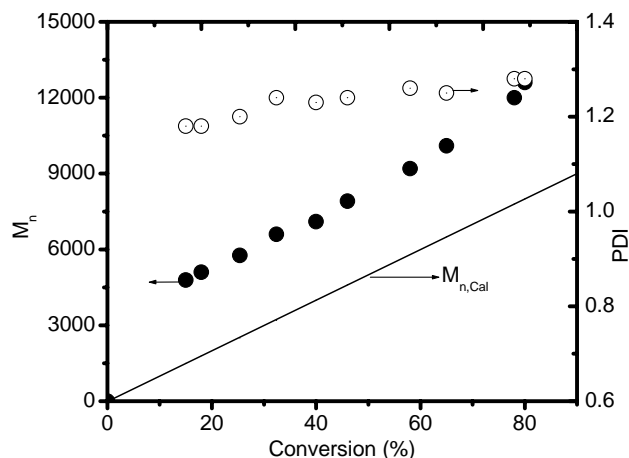


Fig. 3.2: Dependence of molecular weight and polydispersity on conversion for the bulk ATRP of MMA at $90\text{ }^{\circ}\text{C}$ with $[\text{EBiB}] = 0.0312\text{ M}$. Open symbols represent polydispersities and filled symbol represents M_n -(GPC).

Initially the polydispersities remained constant but increased with higher monomer conversion. This could be attributed to faster reaction in bulk, thereby, increasing the viscosity of the solution within 3 h. No pick-out could be withdrawn after 1.83 h. The reaction was quenched after 2.15 h. The reaction attained 90 % conversion with a polydispersity of 1.28 ($M_{n,\text{SEC}} = 12,800$) as shown in Table 3.2. The initiator efficiency was 0.73. The plot of $\ln\{[\text{M}]_0/[\text{M}]_t\}$ vs time was linear (Fig. 3.1) giving a k_{app} value of $26 \times 10^{-5}\text{ s}^{-1}$, whereas the molecular weight obtained were higher than calculated as seen from plot of M_n vs conversion (Fig. 3.2).

Table 3.2: Kinetic data of bulk ATRP of MMA at 90 °C using BPIEP as ligand ^{a)}

Run	Time (min)	Conv ^{b)} (%)	M _{n cal} ^{c)}	M _{n SEC}	PDI	I _{eff} ^{d)}
1	0	0	0	0	-	-
1.1	10	15	1,500	4,500	1.18	0.33
1.2	15	18	1,800	5,100	1.18	0.35
1.3	20	25	2,500	6,200	1.20	0.40
1.4	25	32	3,200	6,600	1.24	0.48
1.5	30	40	4,000	7,100	1.23	0.56
1.6	35	46	4,600	7,600	1.24	0.60
1.7	60	58	5,800	9,200	1.26	0.63
1.8	75	65	6,500	10,100	1.25	0.64
1.9	100	80	8,000	12,000	1.28	0.67
1.10	110	90	9,000	12,800	1.28	0.70

^{a)} [MMA] = 9.36 M; ^{b)} by GC; ^{c)} M_{n cal} = %conversion (grams of monomer / moles of initiator) ^{d)} Initiator efficiency (I_{eff}) = M_{n, cal} / M_{n, SEC}

3.2.3. Kinetics of polymerization of MMA with BPIEP ligand

The kinetics of MMA polymerization was studied in toluene at 90 °C using CuBr as the catalyst, EBiB as the initiator and, BPIEP as the ligand. Unless otherwise specified, the general concentration of the solvent was kept at 66 % v/v with respect to monomer. The mole ratios of the components utilized in the present study are [MMA]: [EBiB]: [CuBr]: [BPIEP] = 100: 1: 1: 2.

3.2.3.1. Effect of ligand concentration

The dependence of the rate of polymerization of MMA with catalyst concentration was investigated. The plot of $\ln k_{app}$ versus $[BPIEP]_0$: $[CuBr]_0$ (Fig. 3.3) shows the dependence of the apparent rate constant of polymerization as a function of [ligand]: [CuBr] ratio. The most favourable ratio was found to be 2:1 (Fig. 3.4). Typically ATRP is carried out with 2 times

molar excess of Schiff base ligand with respect to $\text{Cu}^{\text{I}}\text{X}$ irrespective of the coordinating ability of the ligand. Only in case of linear branched multidentate amines like PMDETA ($\text{N,N,N,N,N}'$ -pentamethyldiethylenetriamine) and Me_6TREN (*tris*(dimethylaminoethyl) amine) lower ligand concentration gives better results.²⁰ This mole ratio is consistent with X-ray crystal structures in which $\text{Cu}(\text{I})$ prefers a tetrahedral geometry which can be achieved by the coordination of two moles of bidentate ligands.²¹

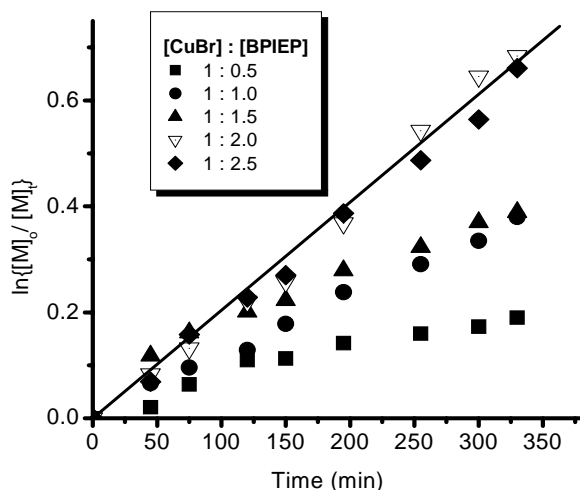


Fig. 3.3: Semi logarithmic kinetic plots for the ATRP of MMA at 90 °C in toluene (66 %, v/v). $[\text{MMA}] = 3.12 \text{ M}$. $[\text{MMA}]: [\text{EBiB}]: [\text{CuBr}]: [\text{BPIEP}] = 100: 1: 1: \text{X}$

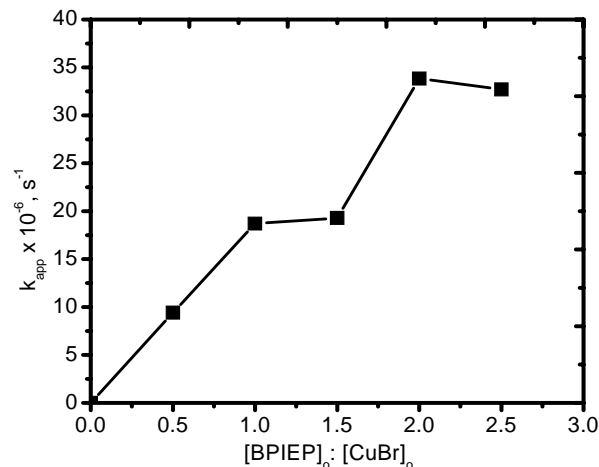


Fig. 3.4: Plot of k_{app} as a function of increasing ligand concentration (BPIEP) at constant CuBr concentration for the solution ATRP of MMA in toluene at 90 °C. $[\text{EBiB}] = [\text{CuBr}] = 0.0312 \text{ M}$

The reason behind the decrease of the rate constant in the presence of higher ligand concentration ($[\text{C}]: [\text{L}] = 1: 2.5$) is not clear. However, further coordination of the ligand to the metal center may hinder the activity of the catalyst resulting in a slight decrease in the rate of polymerization. The different geometries of the active complex that are in equilibrium are also predicted by the change of color during the reaction.⁵ In the present study the color of CuBr/BPIEP changes from pale yellow at room temperature to orange in freeze state and reddish brown on heating.

Table 3.3: Effect of ligand concentration in ATRP of MMA^{a)} in toluene^{b)} at 90 °C

[Ligand]/ [CuBr]	Conv ^{c)} (%)	M _{n,SEC}	PDI	I _{eff} ^{d)}	k _{app} ^{e)} (× 10 ⁻⁵ , s ⁻¹)	[P*] ^{f)} (× 10 ⁻⁸ s ⁻¹)	k _t ^{g)} (× 10 ⁻⁵ , s ⁻¹)
0.5	18	7,600	1.25	0.24	1.67	1.04	6.42
1.0	32	9,700	1.26	0.40	2.07	1.29	9.33
1.5	32	26,700	1.23	0.13	3.74	2.34	7.75
2.0	55	10,200	1.23	0.60	3.41 ^{h)}	2.13	-
2.5	48	8,100	1.25	0.60	3.27 ^{h)}	2.04	-

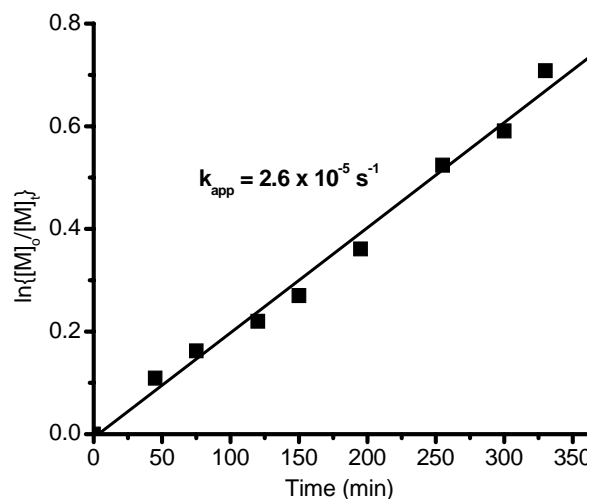
a) [MMA]₀ = 3.12 M; [MMA]: [EBiB]: [CuBr]: [L] = 100: 1: 1: 2 and reaction time 5.5 h; ^{b)} 66 % v/v with respect to monomer; ^{c)} from GC, ^{d)} I_{eff} = M_{n,Cal}/ M_{n,SEC}, ^{e)} Slope of ln[M₀/M_t] vs time plot; ^{f)} [P*] = k_{app}/k_p; ^{g)} Non-linear curve fit; ^{h)} First order plot with no termination reactions.

Table 3.3 shows the various termination rate constants (k_t) and active radical concentration [P*] at concentrations of ligand other than optimum is calculated using non-linear fit. In addition, the initiator efficiencies were found to be lower than obtained for bulk ATRP under similar experimental conditions. This is attributed to the side reactions that occur at the onset of polymerization due to labile C-Br bond. M_{n,SEC} obtained increased linearly with conversion but were higher than the M_{n,Cal} values, whereas, the polydispersity of the obtained PMMA remained narrow, i.e., M_w/M_n ≤ 1.23.

3.2.3.2. Effect of initiator concentration

The effect was studied by changing the concentration of initiator with respect to catalyst, i.e., [CuBr]: [EBiB] = 1: 1 and [CuBr]: [EBiB] = 1: 0.5. In general, the propagation rate was found to be directly proportional to the concentration of EBiB for the solution ATRP of MMA (k_{app} = 3.4 × 10⁻⁵ s⁻¹) for [Cu^IBr]: [EBiB] = 1:1 vs 2.6 × 10⁻⁵ s⁻¹ for [Cu^IBr]: [EBiB] = 1: 0.5 as shown in Fig. 3.5.

Fig. 3.5 Semi logarithmic kinetic plot for the solution ATRP of MMA at 90 °C where [MMA] = 3.12 M. [MMA]: [EBiB]: [CuBr]: [BPIEP] = 100: 0.5: 1: 2



From Table 3.4, a plot between $\ln k_{app}$ and $\ln[EBiB]$ tells that the rate of polymerization is pseudo order (0.5) with respect to concentration of initiator. Thus, a 1:1 ratio of $[Cu^I Br]$: $[EBiB]$ was found to be an optimum ratio for the solution ATRP of MMA in toluene at 90 °C.

Table 3.4: ATRP of MMA^{a)} in toluene^{b)} at 90 °C

$[CuBr]:$ $[EBiB]$	$[EBiB] \times 10^4$ (mmol)	$\ln[EBiB]$	$k_{app} \times 10^{-5}$ (s ⁻¹)	$\ln(k_{app})$
1:1	9.35	-7.667	3.40	-10.2921
1:0.5	4.68	-6.975	2.55	-10.5768

^{a)} [MMA] = 3.12 M; ^{b)} toluene (66 %, v/v) wrt monomer;

3.2.3.3. Effect of solvent

ATRP is very often performed in solution so as to keep the viscosity of the solution low. Non-polar solvents (like, xylene,¹⁰ toluene,¹⁰ and diphenylether^{11,22}) and polar solvents²³ have been utilized for ATRP extensively. Polar solvents such as ethylene or propylene carbonate,²⁴ 2-propanol,²⁵ acetone,²⁶ and ethanol²⁷ fully solublize the catalyst under conditions employed. A prerequisite of the solvent is that it should not interact with the catalyst. Diphenylether and anisole were found to be the most suitable solvent among the common organic solvents. ATRP of MMA was conducted in four different solvents²⁸ i.e., ϵ_{DMF} (37.6, 20 °C), $\epsilon_{anisole}$ (4.33, 25 °C), $\epsilon_{diphenylether}$ (3.87, 25 °C) and $\epsilon_{toluene}$ (2.39, 20 °C) of varying polarity keeping toluene as reference solvent. However, it is known in literature

that polar solvents such as anisole or phenyl ether produce high activity for ATRP of MMA because of their ability to form a homogeneous solution during the entire polymerization period.

Table 3.5: Effect of solvents in batch ATRP of MMA at 90 °C ^{a)}

	Solvent (%, v/v)	Conv ^{b)} (%)	M_{n,SEC}	PDI	I_{eff} ^{c)}
Toluene	66	55	10,600	1.24	0.60
	50	90	14,000	1.27	0.60
	33	90	12,400	1.22	0.73
DMF	66	20	4,000	1.20	0.50
	50	32	4,600	1.21	0.70
	33	53	5,800	1.21	0.80
Anisole	66	80	9,600	1.30	0.80
	50	90	11,700	1.24	0.76
	33	90	10,500	1.24	0.85
Diphenyl ether	66	82	9,900	1.29	0.80
	50	90	12,800	1.22	0.70
	33	90	11,300	1.23	0.80

^{a)} [MMA]₀ = 3.12 M and reaction time = 5.5 h; [MMA]: [EBiB]: [CuBr]: [BPIEP] = 100: 1: 1: 2; ^{b)} from gravimetry; ^{c)} I_{eff} = M_{n,CaI}/ M_{n,SEC}

The result of ATRP of MMA in different solvents and monomer concentration is shown in Table 3.5. In toluene, the system is heterogeneous at all reaction conditions, whereas, in other solvents the reaction becomes homogeneous at the reaction temperature. The effect of solvents on the initiator efficiency and yield of the polymer obtained are summarized in Table 3.5. It was observed that lower the solvent concentration gave better results, i.e., 33 % v/v concentration resulted in better initiator efficiency and conversion compared to 50 % v/v, which in turn is better than 66 % v/v. DMF behaved as a coordinating solvent and, hence, was not used further. This fact is also supported by Pascual *et al.*¹³ who found that

solvents like DMF makes the system homogeneous but also acts as a coordinating solvent for the catalyst and monomer, yielding polymers with higher polydispersity. Coordinating solvents displace the ligands from the complex and saturate the coordination sphere around Cu^I species. Also side reactions like outer sphere ET or elimination of halogen²⁹ by coordinating ligand may take place. This leads to the loss of functionality during the polymerization. However, the coordinating ability of DMF was reduced at lower concentration of solvent (Table 3.5) leading to better initiator efficiency (0.8) and lower polydispersity (1.21). The reaction mixture was highly viscous when the monomer concentration was high. However, the reaction in 66 % toluene possesses lower I_{eff} and conversion as compared to anisole, which could be attributed to slower initiation in the former case. Thus, further kinetic study of ATRP of MMA was performed at 90 °C in toluene and anisole (33% v/v with respect to monomer concentration).

3.2.3.4. Effect of solvent volume

Chambard *et al.*³⁰ reported that besides its effect on catalyst solubility solvent influences activation rate constant, k_{act}, in case of styrene and butyl acrylate through its polarity and coordinating ability. The polarity of the solvents may also affect the induction period of the polymerization reaction as observed in the case of lauryl methacrylates.³¹ Less polar solvents like toluene and xylene were incapable of producing a polymer of glycidyl methacrylate (GMA) by ATRP. However, good control and high conversions was observed when polymerization was performed in diphenylether.^{11,32,33}

Table 3.6: Kinetic study of the effect of solvents in ATRP of MMA at 90 °C^{a)}

Solvent (33%, v/v)	Time (min)	Conv ^{b)} (%)	M _{n,SEC}	PDI	I _{eff} ^{c)}	k _{app} (× 10 ⁻⁵ , s ⁻¹)
Toluene	110	55	8,200	1.20	0.70	12.97
Anisole	110	51	8,000	1.20	0.70	10.96

^{a)} [MMA]₀ = 3.12 M; [MMA]: [EBiB]: [CuBr]: [BPIEP] = 100: 1: 1: 2; ^{b)} from GC; ^{c)} I_{eff} = M_{n,Cal}/M_{n,SEC}.

At similar monomer conversions, lower experimental molecular weights were obtained with increase in the polarity of the solvent. In the polymerization of MMA using *p*TsCl/CuBr/pentylimine systems, the rate increased in the order xylene < dimethoxybenzene < diphenylether, probably due to the differences between the dielectric constants and coordinating ability of the solvents.³⁴ Table 3.6 gives the results of kinetic study of MMA polymerization in toluene and anisole. Although the reaction was controlled in both solvents, but it was observed that the k_{app} of the reaction in 33 % v/v toluene was 1.2 times higher than in anisole. This behavior is just the opposite to what is expected, considering that, as the polymerization conditions approach almost bulk reaction conditions, an increase of initiator and catalyst concentration will occur and, as a result, the polymerization rate should be faster.³⁵ A similar trend was observed when butyl acrylate was polymerized by R-Br/Cu^IBr /bpy in ethylene carbonate.²⁴ The author stated that the reduction of the amount of solvent gives rise to a decrease in the polarity of the reaction mixture resulting in a lower concentration of Cu^I in solution and consequently, the rate of polymerization is reduced. Apparently, the solubility of Cu^{II} is not strongly affected since the polydispersity indexes are lower when less solvent proportion is used. As shown in Fig. 3.6, $\ln\{[M_o]/[M]_t\}$ versus time (t) remained linear indicating that polymerization obeyed first order kinetics with negligible termination. The molecular weights (M_n) increased linearly with respect to conversion but were higher, when 66 % v/v solvent was used when compared to $M_{n,Cal}$ (Fig. 3.7). The polydispersities remained constant (≤ 1.21) at higher monomer concentration. This could be attributed to faster rate of reaction at a solvent (toluene and anisole) concentration of 33 % v/v, thereby, increasing the viscosity of the solution within 3 h. No pick-out could be withdrawn after 1.83 h.

The reaction mixture was highly viscous before it was quenched. Overall, it was found that the rate of polymerization was higher at lower volume (v/v) for non-polar solvent as compared to polar solvent (Table 3.5). The rate constant of polymerization in bulk was roughly twice as compared to that in 33 % v/v toluene, and about eight times faster as compared to that in 66 % v/v toluene. Hence, solvent polarity as well as its volume plays an important role in determining the course of polymerization reaction.

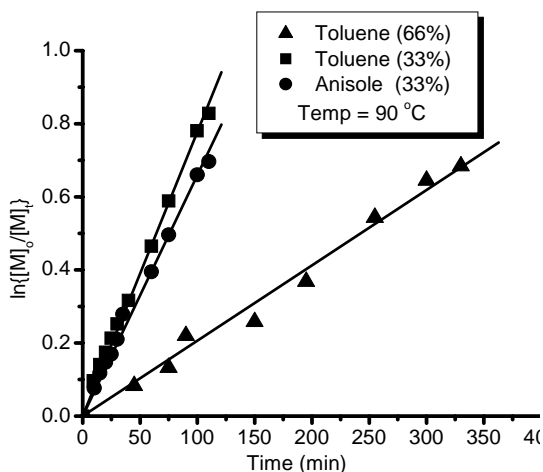


Fig. 3.6: Semi logarithmic kinetic plots for the ATRP of MMA at 90 °C in toluene and anisole. [MMA] = 3.12 M. [MMA]: [EBiB]: [CuBr]: [BPIEP] = 100: 1: 1: 2

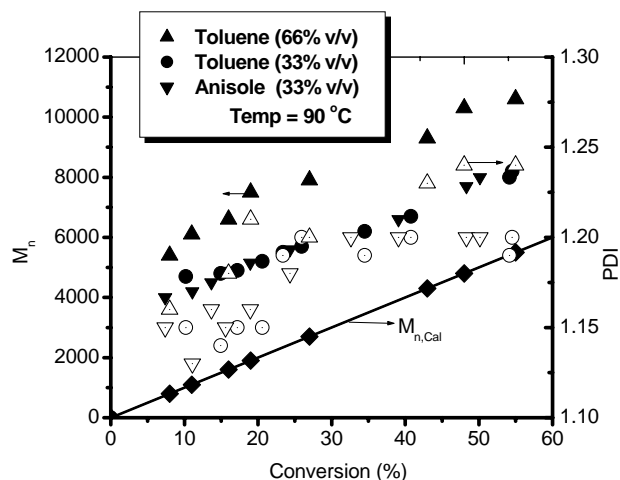


Fig. 3.7: Dependence of molecular weight and polydispersity on conversion for the bulk ATRP of MMA at 90 °C with [EBiB] = 0.0312M. Open symbols represent polydispersities and filled symbol represents M_n -(GPC).

3.2.3.5. Effect of temperature

The effect of reaction temperature was studied in toluene (33%, v/v) at 30 °C, 50 °C, and 90 °C. Fig. 3.8 shows a good linear relationship between $\ln\{[M]_0/[M]_t\}$ and polymerization time. The rate of polymerization increases with increasing temperature, and the induction period becomes zero when polymerization temperature is increased to 90 °C. Fig. 3.9 gives the effect of temperature on the molecular weight and polydispersity of the obtained PMMA by ATRP.

Table 3.7: Kinetic data for ATRP of MMA^a in toluene (33%, v/v) at different polymerization temperatures

Temp (°C)	Time (h)	k_{app}^b ($\times 10^{-5}, s^{-1}$)	k_p^c ($\times 10^3, Lmol^{-1} s^{-1}$)	$M_{n,SEC}$	PDI	$[P^*]^d$ ($\times 10^{-8}, mol L^{-1}$)
30	46	0.474	0.374	8,500	1.22	1.27
50	23	1.640	0.647	10,200	1.18	2.54
90	1.84	13.10	1.620	8,200	1.22	8.27

^{a)} [MMA]₀ = 3.12 M; [MMA]: [EBiB]: [CuBr]: [BPIEP] = 100: 1: 1: 2; ^{b)} Slope of $\ln\{[M]_0/[M]_t\}$ vs time plot;

^{c)} calculated according to reference 36; ^{d)} $[P^*] = k_{app}/k_p$.

It is seen that the reaction is very slow at room temperature with an induction period of almost 10 h. The stationary concentration of the propagating radicals during the solution ATRP of MMA can be estimated by combination of values of k_{app} in equation (3.1) and rate constant of radical propagation for MMA calculated according to the equation (3.2) and presented in Table 3.7.

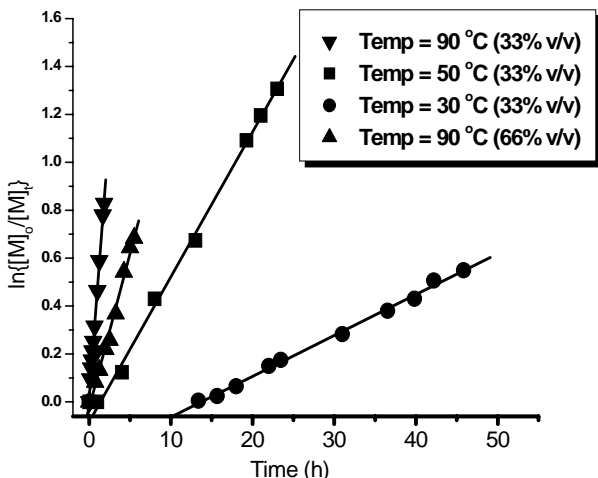


Fig 3.8. First order kinetic plots showing the effect of the polymerization temperature on ATRP of MMA in toluene. $[MMA] = 3.12 \text{ M}$; $[MMA]:[EBiB]:[CuBr]:[BPIEP] = 100: 1: 1: 2$

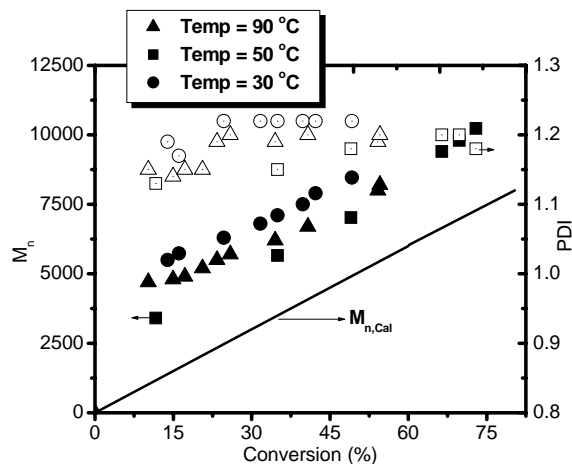


Fig. 3.9. Temperature effect on the molecular weight and polydispersity with respect to conversion in the solution ATRP of MMA at 90 °C with $[EBiB] = 0.0312\text{M}$. Open symbols represent polydispersities and filled symbol represents M_n -(GPC).

In addition, from Table 3.7, it can be seen that the rate of polymerization increases with increasing polymerization temperature because of increase in, both, the rate constant of propagation and atom transfer equilibrium constant.

$$R_p = k_{app} [M] = k_p [M] [P^*] \quad (3.1)$$

$$\ln k_p = 14.8 \text{ Lmol}^{-1} \text{ s}^{-1} - 22.36 \text{ KJ mol}^{-1} / RT \quad (3.2)$$

$$\Delta H_{eq}^{\circ} = \Delta E_{app}^{\ddagger} - \Delta E_{prop}^{\ddagger} \quad (3.3)$$

The Arrhenius plot, of $\ln k_{app}$ versus $1/T$, for CuBr/BPIEP catalyzed polymerization of MMA is plotted in Fig. 3.10. Based on the slope, an apparent energy of activation, $\Delta E_{app}^{\ddagger} = 50.96 \text{ KJ mol}^{-1}$, is calculated. According to Equation (3.3), the enthalpy of pre-equilibrium (ΔH_{eq}°) is calculated as the difference between apparent energy ($\Delta E_{app}^{\ddagger}$) of activation (Fig. 3.10) and activation energy of MMA (our case) propagation ($\Delta E_{prop}^{\ddagger}$)³⁶. Now with $\Delta E_{prop}^{\ddagger}$

= 22.15 KJ mol⁻¹ for MMA, a value of $\Delta H^{\circ}_{eq} = 28.8$ KJ mol⁻¹ can be calculated for Br-mediated ATRP of MMA.

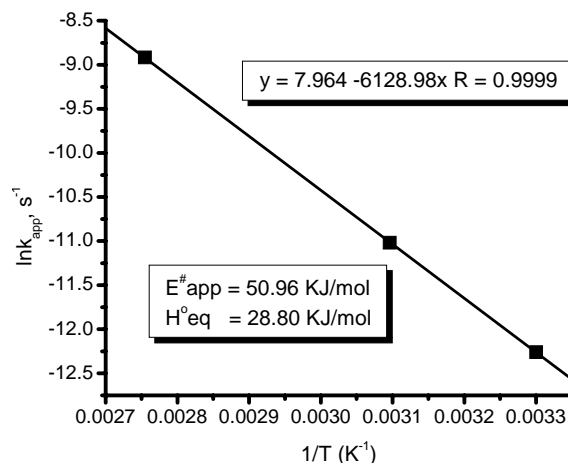


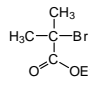
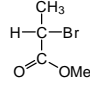
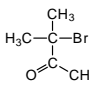
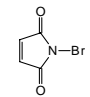
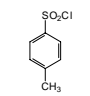
Fig. 3.10 Plot of $\ln k_{app}$ vs $1/T$ for ATRP of MMA initiated by EB*i*B with CuBr/BPIEP as ligand in toluene. [MMA] = 3.12 M. [MMA]: [EB*i*B]: [CuBr]: [BPIEP] = 100: 1: 1: 2

This value is much lower than the corresponding values for MMA ($\Delta E^{\ddagger}_{app}$ from 62.9 KJ mol⁻¹ ¹⁶ and 52.8 KJ/mol ³⁷) reported previously by Haddleton *et al.* ³⁸ The rate of polymerization in non-polar solvent in the present case is nearly four times higher than that reported by Matyjaszewski ³⁹ using CuCl/bipyridyloctylamine system in anisole and 1.5 times higher than reported by Haddleton using CuBr/ N-alkyl-2-pyridylmethanimine system in xylene. ¹⁰

3.2.3.6. Effect of initiator structure

Various α -bromo active organic compounds, viz., EB*i*B (ethyl-2-bromoisobutyrate), MBP³⁵ (methyl-2-bromopropionate) and MBB ⁴⁰ (3-bromo-3-methyl-2-butanone), having structural similarities to that of growing polymer chain were used as initiators for ATRP of MMA. Jiang *et al.* has recently utilized NBS (N-bromosuccinimide) as initiator for ATRP of MMA in anisole ⁴¹ at 90 °C. The use of NBS as an initiator for MMA polymerization was first introduced by Otsu ⁴² with reduced nickel and later by Percec. ⁴³ However, polymers with high polydispersities (~1.8) and negligible initiator efficiencies (0.017) were reported. Similarly, Matyjaszewski ⁴⁴ and Percec ⁴⁵ also reported fast initiation of ATRP of MMA using arenesulfonyl chlorides as initiators and substituted bipyridine as ligand giving polydispersities close to 1.10. Thus, both, the initiators, namely, N-bromosuccinimide (NBS) and *p*-toluenesulfonyl chloride (*p*TsCl), were employed in the present study. The mole ratios of various components used were [MMA]: [Initiator]: [CuBr]: [BPIEP] = 100: 1: 1: 2. The results of are shown in Table 3.8.

Table 3.8: Effect of initiators in ATRP of MMA in toluene (66%, v/v) using CuBr/BPIEP as catalyst system at 90 °C/ 5.5h^{a)}

Initiator Structure	Time (h)	Conv (%) ^{b)}	M _{n,SEC}	PDI	I _{eff} ^{c)}	
	EBiB	5.5	65	9,300	1.23	0.70
	MBP	5.5	74	13,400	1.82	0.74
	MBB ^{d)}	5.5	75	9,300	1.26	0.81
	NBS	5.5	5	4,300	1.17	0.12
	pTsCl	5.5	46	5,400	1.12	0.85

^{a)} [MMA]₀ = 3.12 M; [MMA]: [I]: [CuBr]: [BPIEP] = 100: 1: 1: 2; ^{b)} gravimetric; ^{c)} I_{eff} = M_{n,Cal}/ M_{n,SEC}; **EBiB**: ethyl-2-bromoisobutyrate, **MBP**: methyl-2-bromo propionate, ^{d)} **MBB**: 3-bromo-3-methyl-2-butanone, reaction at 50 % v/v with respect to monomer, **NBS**: N-bromosuccinimide, **pTsCl**: *p*-toluenesulfonyl chloride.

The polymerization was faster with α -bromoalkyl initiators in comparison to *p*TsCl and NBS. This can be explained on the basis of differences in bond energies of C-Br and C-Cl bond. The reaction was controlled with EBiB, MBB and *p*TsCl, whereas, uncontrolled with MBP and NBS. This result is in accordance with prior reports wherein EBiB/CuBr couple exhibited a higher polymerization rate as compared to *p*TsCl/CuBr.⁴⁶ The polymer conversion was in the range of 60-70 %. The polymerization initiated by NBS resulted in lower polydispersity (1.13) in 2.5 h and 34 % conversion. However, the initiator efficiency was only 0.17. This lower value is a consequence of the fact that molecular bromine produced undergoes side reaction, i.e., it brominates the monomer. On the other hand polydispersities were narrow with *p*TsCl when compared to other initiators. Also, the initiator efficiency varied as *p*TsCl > MBP > EBiB > MBB > NBS. Thus, in order to prepare PMMA with high chain-end functionalities as starting material for the synthesis of block copolymer, the *p*TsCl/CuBr couple appears to be the best choice with BPIEP a tridentate ligand.

3.2.3.7. Effect of catalyst concentration

The ATRP of MMA at 90 °C in toluene (66%, v/v) was conducted with various catalyst to initiator mole ratios wherein [MMA]: [EBiB]: = 100 and [CuBr]: [BPIEP] = 1: 2. The concentration of catalyst was increased in steps of 0.5 thereby keeping the initiator concentration constant. As seen from the Table 3.9, the polymerization was slower with lower catalyst concentration resulting in higher PDI with low initiator efficiency. On the other hand when [C]: [I] = 2, higher conversion was obtained with higher initiator efficiency but broader molecular weight distribution.

Table 3.9: ATRP of MMA in toluene (66%, v/v) with different catalyst concentration ^{a)}

[C]/[I] ^{b)}	Time (h)	Conv ^{c)} (%)	M _{n,SEC} (× 10 ⁻³)	PDI	I _{eff} ^{d)}
0.5	5.5	50	7.60	1.33	0.66
1.0	5.5	60	8.30	1.21	0.72
1.5	5.5	95	11.6	1.24	0.82
2.0	5.5	95	11.1	1.28	0.86

^{a)} [MMA]₀ = 3.12 M; ^{b)} [C]/[I]: catalyst/initiator where [MMA]: [EBiB]: = 100; [CuBr]:[BPIEP] = 1: 2; ^{c)} gravimetric; ^{d)} I_{eff} = M_{n,cal}/ M_{n,SEC}

3.2.3.8. Effect of [M]/ [I] ratios

The kinetics of higher M_n range is of interest because persistent radical effect is minimum at low initiator concentrations.^{47,48} Though MMA is among the most studied monomers for ATRP, past kinetics studies are limited to system with targeted molecular weights less than 40,000 in a single step. Matyjaszewski *et al.*³⁵ showed that the PDI increases rapidly beyond 1.2 when number average molecular weight (M_n) exceeds 100,000. Later, Grimaud and Matyjaszewski⁴⁴ reported MMA polymerization, yielding PMMA with M_w/M_n = 1.18 for M_n = 83,000 and PDI increased to 1.4 for M_n = 1,69,000. Xue *et al.* recently reported linear PMMA ([M]₀/[I]₀ = 6400) by ATRP leading to high molecular weight (M_n ≈ 3,67,000) and polydispersity as low as 1.2.⁴⁹ Our objective was to examine the extent of control of molecular weight and polydispersity with the bulky tridentate ligand, BPIEP, system coupled with CuBr as catalyst. The effect of monomer to initiator concentration on

the ATRP of MMA using BPIEP/CuBr system was examined. The results obtained are tabulated in Table 3.10. The polymerization reaction was very slow. The conversion decreased while initiator efficiency increased with higher $[M]/[I]$ values. However, the polydispersity remains relatively narrow.

Table 3.10: ATRP of MMA^{a)} at different DP values

$[M]/[I]$ ^{b)}	Time (h)	Conv ^{c)} (%)	$M_{n,SEC}$	PDI	I_{eff} ^{d)}
100	5.5	60	8,300	1.21	0.70
200	5.5	60	14,600	1.21	0.82
400	5.5	40	16,200	1.19	0.98
800	5.5	30	26,500	1.20	0.91

^{a)} $[MMA]_0 = 3.12$ M, in toluene (66%, v/v); ^{b)} $[M]/[I]$: monomer/ initiator where $[CuBr]: [BPIEP]: [EBiB]: [MMA] = 1: 2: X: 100$, ^{c)} gravimetric, ^{d)} $I_{eff} = M_{n,cal}/ M_{n,SEC}$,

3.2.3.9. Effect of ageing of the catalyst

The conversion obtained in ATRP of MMA in toluene at 90 °C after 2 h of reaction was ≤ 20 %. The lower value was attributed to the slow rate of formation of the required complex or the slow equilibrium dynamics actually required to give controlled polymerization.

Table 3.11: Ageing of the BPIEP/CuBr complex using different concentration of solvent in ATRP of MMA^{a)} at 90 °C

Solvent (% _{v/v})	Time (h)	Conv ^{b)} (%)	$M_{n,SEC}$	PDI	I_{eff} ^{c)}	
Toluene	66	5.5	65	9,300	1.23	0.70
	33	5.5	95	13,800	1.18	0.69
Anisole	33	5.5	95	13,000	1.23	0.73
Diphenyl ether	33	5.5	90	12,400	1.23	0.73

^{a)} $[MMA]_0 = 4.68$ M; $[MMA]: [EBiB]: [CuBr]: [L] = 100: 1: 1: 2$; ^{b)} gravimetric; ^{c)} $I_{eff} = M_{n,Cal}/ M_{n,SEC}$

Therefore, attempts were made to form the complex *insitu* prior to reaction. The mole ratio of ligand with respect to copper halide was 2:1. A 2:1 molar ratio of ligand to copper chloride was aged at 25 °C/ 12 h, followed by heating to 90 °C for an additional 1.5 h. The reddish brown colored catalyst complex was cooled to room temperature followed by addition of monomer, degassing three times using freeze-pump-thaw and initiation of polymerization at 90 °C. The color of the complex changed from brown to reddish brown when initiator was added. As shown in Table 3.11, higher conversions of the polymer were obtained with good control over molecular weight and polydispersities. This particular effect was more pronounced when solvent concentration of 33 % (v/v) was used. Thus, ageing of the complex has a positive effect on initiator efficiency as well as polymer conversion.

3.2.3.10. Polymerization of glycidylmethacrylate (GMA), methyl acrylate (MA), styrene, and *t*-butylacrylate (*t*-BA)

The efficacy of CuBr/BPIEP catalyst system was further examined by polymerizing other vinyl monomers including styrene. The results obtained are shown in Table 3.12. All polymerizations were performed in diphenylether or bulk. The reaction condition used in the study of each monomer is well established in the literature, with ligands like *dn*Nbpy (bidentate) or PMDETA (tridentate).

Table 3.12 indicates that the conversion obtained in all runs was very low except in the case of GMA (run number 1). The polymerization of GMA was performed at 60 °C in diphenylether that resulted in a very-very viscous liquid in just 2.5 h. The polymerization of GMA is reported to be very fast using pyridylalkyl imine type and/or PMDETA ligand along with CuBr as catalyst at room temperature.^{11,32} Therefore, polymerization of GMA was performed in solution rather than bulk. The catalyst system used was active for polymerizing all the monomers except *t*-BA. The polymerization of *t*-BA did not occur when a well-known ATRP initiator, namely, 2-bromopropionitrile (BPN), was used along with BPIEP ligand at 60 °C (run number 2). Low conversions with negligible initiator efficiency were obtained in bulk polymerization of *t*-BA. This indicates that initially most of the initiator was consumed due to some side reactions and the remaining initiator was involved in producing polymer in low conversion (run number 3).

Table 3.12: ATRP of different monomers using BPIEP as ligand, CuBr as catalyst and α -bromo compounds as initiators ^{a)}

Run	M	Solvent (50%, v/v) /Bulk	Time (h)	T (°C)	[I] ^{b)}	Conv ^{c)} (%)	M _{n,Cal} ^{d)}	M _{n,SEC}	PDI
1	GMA ^{e)}	DPE	3	60	BPN	70	9,940	7,384	1.23
2	<i>t</i> -BA ^{f)}	DPE ⁱ⁾	3	60	BPN	-	-	NP	-
3		Bulk	12		MBP	5	640	5,504	1.13
4	MA ^{g)}	DPE ^{j)}	5.5	90	BPN	1	172	1,806	1.16
5		Bulk	21		MBP	62	7,740	8,084	1.21
6	Sty ^{h)}	DPE ⁱ⁾	24	110	PEBr	15	1,498	4,680	1.35

^{a)} [M]₀ = 3.12M; ^{b)} [I]: initiator; ^{c)} gravimetric; ^{d)} M_{n,cal} = % conversion (grams of monomer / moles of initiator); ^{e)} **GMA**: Glycidyl methacrylate, [GMA]: [BPN]: [CuBr]: [BPIEP] = 100: 1: 1: 2; ^{f)} ***t*-BA**: *tert* butylacrylate, [*t*BA]: [X]: [CuBr]: [BPIEP]: [CuBr₂] = 100: 1: 1: 2: 0.05; ^{g)} **MA**: Methylacrylate, [MA]: [X]: [CuBr]: [BPIEP] = 150: 1: 1: 2; ^{h)} **Sty**: Styrene, [Sty]: [X]: [CuBr]: [BPIEP] = 96: 1: 1: 2; ⁱ⁾ 33 % toluene v/v, with respect to monomer, ^{j)} 5 % CuBr₂ added wrt CuBr, **BPN**: 2-bromopropionitrile; **MBP**: methyl-2-bromopropionate; **EBiB**: ethyl-2-bromoiso butyrate; **1-PEBr**: 1-phenylethyl bromide; **NP**: no polymer.

Similarly, no polymer was obtained in solution polymerization of MA whereas bulk polymerization resulted in a polymer with good control as seen from Table 3.12. This could be attributed to the slower rates of initiation in solution than in bulk (run number 4 & 5). In addition, the catalyst system when used for styrene polymerization resulted in a polymer with low conversion and higher polydispersity. Thus, the catalyst system employed is effective in polymerizing GMA and MA under defined conditions.

3.2.3.11. Chain extension experiments

The controlled nature of the CuBr/BPIEP system was confirmed by adding a fresh aliquot of monomer in a chain extension experiment. Thus, the isolated PMMA (M_{n,SEC} = 14,600, M_w/M_n = 1.21) was further utilized as macroinitiator to initiate polymerization of fresh MMA at 90 °C in toluene using CuBr as catalyst and BPIEP as ligand for 5.5 h. The GPC of the PMMA obtained from this study is shown in Fig. 3.11.

The formation of high molecular weight PMMA ($M_{n,SEC} = 90,000$ $M_w/M_n = 1.10$) clearly establishes that the reaction is well controlled and that essentially all the end groups of the macroinitiator are available for chain extension. The initiator efficiency (I_{eff}) of the macroinitiator for generating the second block was 0.7.

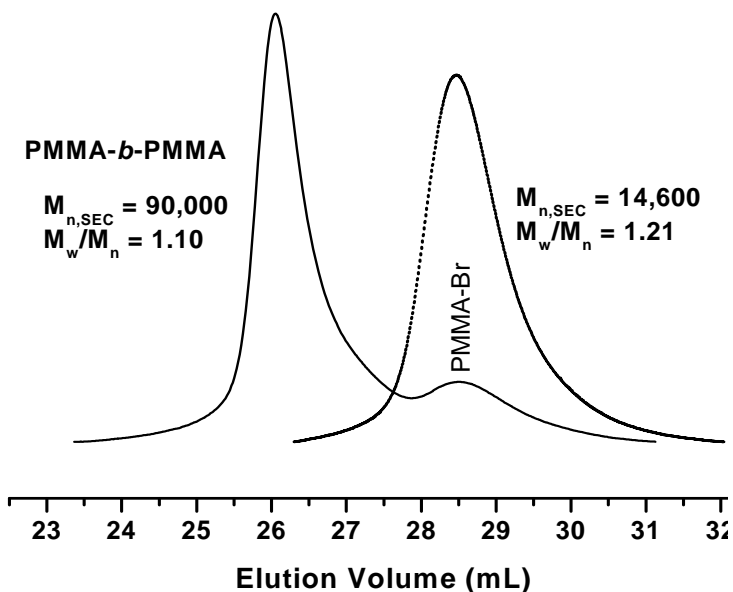


Fig. 3.11. Gel Permeation chromatograms of PMMA-Br (before and after chain extension) by ATRP initiated by EB*i*B with CuBr/BPIEP as catalyst in toluene. [MMA] = 3.12 M. [MMA]: [EB*i*B]: [CuBr]: [BPIEP] = 100: 1: 1: 2

3.2.4. Kinetics of ATRP of MMA using bidentate and tridentate Schiff base imines

Kinetic studies of ATRP of MMA in toluene at 90 °C were performed using CuBr as catalyst, EB*i*B as initiator and NPPI (N-(*n*-propyl)-2-pyridylmethanimine) as bidentate and BPIEP as a tridentate ligand. The mole ratios of various components utilized are [MMA]: [EB*i*B]: [CuBr]: [L] = 100: 1: 1: 2. The kinetic data (Table 3.13) for NPPI ligand showed that the reaction was controlled as evident from a linear first-order plot (Fig. 3.12) of $\ln \{[M_0]/[M]_t\}$ vs time, increment of M_n with conversion and narrow MWD with conversion (Fig. 3.13). The linear first order time-conversion plot indicates that growing radical concentration is low and is constant.

Table 3.13: Kinetic studies of ATRP of MMA at 90 °C using CuBr/ N-(*n*-propyl)-2-pyridylmethanimine as ligand ^{a)}

Run	Time (min)	Conv ^{b)} (%)	M _{n,cal}	M _{n,SEC}	PDI
1	0	0	-	-	-
1.1	30	16	1,600	4,700	1.15
1.2	60	29	2,900	6,000	1.21
1.3	105	46	4,600	7,700	1.23
1.4	150	56	5,600	9,100	1.19
1.5	195	66	6,600	9,900	1.19
1.6	240	72	7,200	10,500	1.20

^{a)} [MMA] = 3.12M in toluene (66% v/v); [MMA]: [EBiB]: [CuBr]: [Ligand] = 100: 1: 1: 2, ^{b)} by GC.

The actual values of M_n are slightly higher than the theoretical value suggesting that the initiator efficiency is less than unity i.e., the initiator is involved in secondary, as yet undetermined reactions such as coupling of carbon-centered radicals in the initial stages of the reaction. The molecular weight distribution was narrow in beginning of the reaction, but slowly increases as the reaction proceeds (Table 3.13). This indicates the presence of transfer reactions in the system. The value of apparent rate constant, k_{app}, of MMA using NPPI was found to be 0.9 x 10⁻⁴ s⁻¹. Haddleton and coworkers reported a value of 0.75 x 10⁻⁴ s⁻¹.⁵⁰ The apparent rate constant shown in Table 3.3 (Section 3.2.3.1) using, tridentate ligand, BPIEP, was found to be lower than NPPI ligand (k_{app} = 0.34 x 10⁻⁴ s⁻¹). However, similar rates of polymerization are reported in literature for well known bidentate and tridentate ligands (Table 3.14). Thus, the lower rate observed with tridentate BPIEP ligand can be attributed to the relative coordinating ability of the two ligands (BPIEP and NPPI) with CuBr in ATRP.

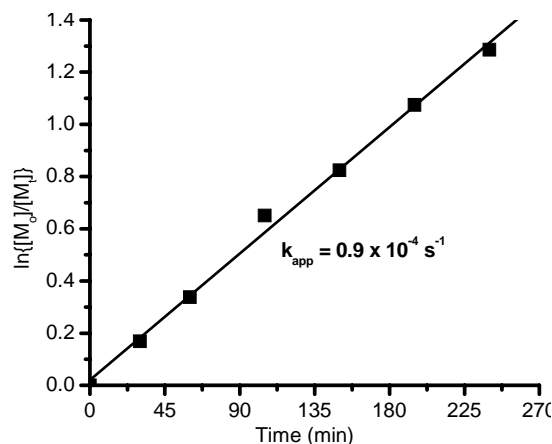


Fig. 3.12: Semi logarithmic kinetic plot for the ATRP of MMA in toluene (66 %, v/v) at 90 °C. [MMA] = 3.12 M. [MMA]: [EBiB]: [CuBr]: [NPPI] = 100: 1: 1: 2.

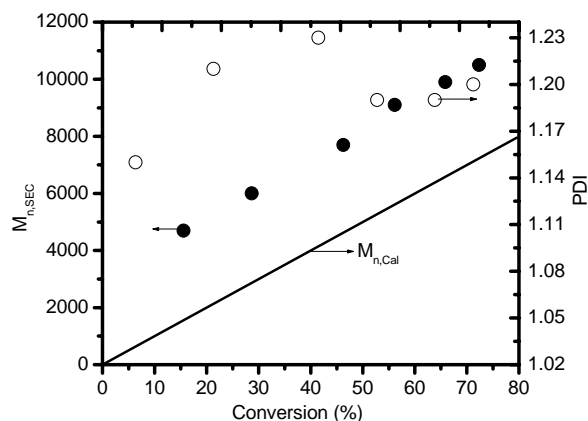


Fig. 3.13: Dependence of molecular weight and polydispersity on conversion for the ATRP of MMA in toluene (66 %, v/v) at 90 °C with [EBiB] = 0.0312M. Open symbols represent polydispersities and filled symbol represents M_n -GPC).

The slow rate with BPIEP can be attributed to the presence of bulky isopropyl groups in the ligand environment surrounding the metal. In addition, the tridentate ligand (BPIEP) possesses two symmetrical imine (-C=N-Ar) units around central pyridine unit whereas, only one imine unit (-C=N-R, R = C₃) is present in case of the bidentate imine ligand (NPPI). Therefore, the coordination of copper with tridentate ligand might be better as compared to bidentate ligand, thereby, causing more hindrance to the expansion of coordination sphere during ATRP equilibrium dynamics. On the contrary, the rate of polymerization with BPIEP as ligand is higher as compared to CuCl/BPMOA in diphenylether³⁹ and CuBr/NPPI system in xylene (Table 3.14).¹⁰

Table 3.14: Comparison of type of ligands in ATRP of MMA in different solvents

Nature	Ligand /CuBr	Solvent (% , v/v)	$k_{app} \times 10^4 (s^{-1})$	Temp (°C)	[I]	PDI	I_{eff}	Ref
Bidentate Ligand	bpy	50 %, anisole	0.43	90	NBS	1.14	0.17	41
		50 %, Tol	1.40	100	MBP	1.50	0.35	51
	dNbipy	50 %, DPE	2.67	90	EBiB	1.20	1.04	14
	NPPI	33 %, xylene	0.78	90	EBiB	1.23	0.72	10
		50 %, Tol	0.71	90	EBiB	1.19	0.72	50
		66 %, Tol	1.28	90	EBiB	1.20	0.89	10
	NOPI	66 %, xylene	0.97	90	EBiB	1.18	1.05	52
CPPC	50 wt %, veratrole	1.19	60	EBiB	1.14	0.80	53	
Tridentate Ligand	PMDETA	50 wt %, veratrole	0.91	60	EBiB	1.15	0.62	53
	DOIP	50 %, anisole	0.90	90	BPN	1.23	0.95	19
	BPMOA	50 %, anisole	0.46	50	EBiB	1.22	0.62	39

bpy (2,2'-bipyridine); **dNbipy** (4,4-di-(5-nonyl)-2,2'-bipyridine); **NPPI** (N-(*n*-propyl)-2-pyridylmethanimine); **NOPI** (N-(*n*-octyl)-2-pyridyl methanimine); **CPPC** (cyclopentyl-pyridine-2-carboximidate); **PMDETA** (N,N,N',N',N''-pentamethyldiethylenetriamine); **DOIP** (2-6-bis[1-(octylimino)ethyl]pyridine); **BPMOA** (N,N-bis(2-pyridylmethyl)octylamine); **BPIEP** (2-6-bis[1-(2,6-diisopropyl phenylimino)ethyl] pyridine), **MBP** (methyl-2-bromopropionate); **NBS** (N-bromosuccinimide); **EBiB** (ethyl-2-bromo isobutyrate); **BPN** (2-bromopropionitrile); **MBB** (3-methyl-3-bromo-butanone-2).

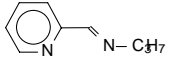
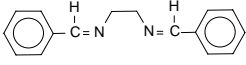
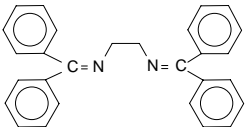
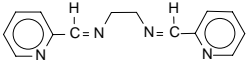
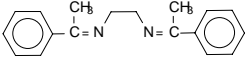
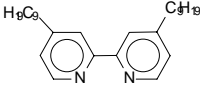
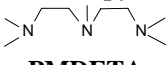
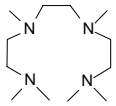
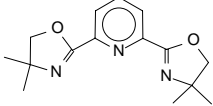
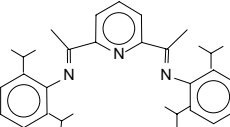

3.2.5. Reverse ATRP of MMA in solution and bulk using BPIEP as ligand, CuX₂ as catalyst and AIBN as initiator

Since more active catalytic systems are generated by less oxidatively stable Cu^I complexes, reverse ATRP, using more stabilized Cu^{II} complexes, is an alternative approach to controlled radical polymerization. Wang and Matyjaszewski reported that “living”/controlled radical polymerization is also observed when a conventional radical initiator (e.g. AIBN) is associated with a transition metal compound of higher oxidation state (e.g. CuCl₂ or CuBr₂) complexed with suitable ligands (e.g. 2,2'-bipyridine)^{54,55} the process is termed as reverse ATRP.

Matyjaszewski and coworkers⁵⁶ reported that benzoyl peroxide (BPO)/CuBr/dNbpy could be used as a reverse ATRP initiating system for bulk polymerization of styrene at higher temperature (110 °C). More recently, Wang and Yan⁵⁷ developed a new procedure for reverse ATRP of methyl acrylate (MA) styrene using AIBN/Cu^{II}/bpy as initiating systems under heterogeneous conditions. Later Yan and Jérôme⁵⁸ reported the polymerization of MMA using BPO/ Cu^IBr in methyl ethyl ketone gave $M_n = 35,000$, PDI = 1.20 with good initiator efficiency (0.92). However, the reaction time was 100 h. The polymerizations were generally carried out at lower temperature, where initiator decomposes more slowly, so better control could be realized. However the low temperature usually causes long induction time and slow polymerization rate. Thus the time scale in literature for RATRP of MMA is in the range of 50-100 h. The microwave methodology in reverse ATRP of MMA accelerated the rate of reaction but led very poor initiator efficiencies.⁵⁹ The general conditions for successful reverse ATRP are $Cu(II)_o / [AIBN]_o \geq 1$ and rather high polymerization temperature for rapid decomposition of initiator provided the half-life of AIBN ($t_{1/2} = 4.8$ h at 70 °C, and 74 h at 50 °C)⁶⁰ at that temperature is known.

We have examined the efficacy of polar solvents and various N-donors for RATRP of MMA. For DP of 100, the mole ratios of different components taken are [MMA]: [AIBN]: [CuBr₂]: [L] = 100: 0.5: 1: 2. In all cases except PMDETA and HMTETA the color of reaction mixture turned from pale yellow to brown or brick red upon heating indicating the change from Cu²⁺ to Cu⁺ in solution. The color change indicates that the dynamics of reverse ATRP is followed. However, in toluene (run number 10) the cupric complex is insoluble, which is detrimental to the occurrence of redox reaction and formation of dormant and active species in equilibrium. Therefore, no controlled polymerization was observed. Table 3.15 shows that when reaction was performed in polar solvents using a tridentate ligand, BPIEP, fairly good control was observed within 24 h giving a conversion of 95 % with PDI < 1.20. Reverse ATRP of MMA was successful in both solution and bulk. Among the other N-donors the reaction is slow in case of NPPI and NDBED yielding polymers with PDI < 1.18.

Table 3.15: Reverse ATRP of MMA using different N-donors at 70 °C ^{a)}

Run	Ligand		Time (h)	Conv ^{b)} (%)	M _{n,SEC} (x 10 ⁻³)	PDI	I _{eff} ^{c)}
	Structure	Solvent (50 %, v./v)					
1	 NPPI	Anisole	24	5	1.60	1.04	0.21
2	 NBED	Anisole	24	NP ^{d)}	-	-	-
3	 NDBED	Anisole	24	5	3.50	1.14	0.14
4	 NPMED	Anisole	24	90	52.4	1.59	0.17
5	 NPEED	Anisole	24	NP	-	-	-
6	 dnN bpy	Anisole	24	85	9.2	1.09	0.42
7	 PMDETA	Anisole	24	90	30.0	1.46	0.15
8	 HMTETA	Anisole	24	90	27.0	1.36	0.20
9	 dmPYBOX	bulk	27	50	7,300	1.61	0.68
10		DMF	20	10	4.60	1.36	0.22
11		DPE	20	95	17.6	1.10	0.54
12		Anisole	20	84	23.1	1.21	0.37
13	BPIEP	Bulk ^{e)}	12	98	16.5	1.19	0.60

^{a)} [MMA]₀ = 4.68 M and 50 % v/v of solvent wrt monomer; [MMA]: [AIBN]: [CuBr₂]: [Ligand] = 100: 0.5: 1: 2, **NPPI**: N-(*n*-propyl)-2-pyridylmethanimine; **NBED**: N,N'-dibenzylidene-ethane-1,2-diamine; **NDBED**: N,N'-dibenzylidene-ethane-1,2-diamine; **NPMED**: N,N'-bis-pyridin-2-yl-methylene-ethane-1,2-diamine; **NPEED**: N,N'-bis(1-phenylethylidene)-1,2-ethanediamine; **dnN bpy**: 4,4'-di(*n*-nonyl)-2,2'-bipyridine; **PMDETA**: N,N,N',N',N''-pentamethyldiethylenetriamine; **HMTETA**: (N,N,N,N,N,N-hexamethyltriethylene

tetramine; **dmPYBOX**: 2,6-bis(4,4-dimethyl-2-oxazolin-2-yl)pyridine; ^{b)} gravimetric, ^{c)} $I_{\text{eff}} = M_{n,\text{cal}} / M_{n,\text{SEC}}$, ^{d)} NP: no polymer; ^{e)} RATRP of MMA (9.36 M) using CuCl₂.

There was no polymerization observed with NBED and NPEED ligand. All other ligands except **dmPYBOX** resulted in uncontrolled polymerization (Table 3.15). Ligand, **dmPYBOX**, shows reasonable initiator efficiencies and broader polydispersities. RATRP was extended to methyl acrylate using BPIEP as ligand resulting in poly (methyl acrylate) with $M_{n,\text{SEC}} = 8,600$ and narrow polydispersity (1.18).

3.3. Conclusions

The diiminoarylpyridine ligand, BPIEP, was successfully employed in ATRP of MMA. In addition to CuBr-mediated ATRP, it was also used in combination with CuCl forming an active catalyst for the polymerization of MMA.

Table 3.16: Summarized kinetic data for bidentate and tridentate ligand in ATRP of MMA

Entry No	Ligand /CuBr	Solvent (v/v)	Time (h)	$k_{\text{app}} \times 10^4$ (s ⁻¹)	Temp (°C)	[I]	PDI	I_{eff}
1	NPPI	66 %, Tol	4.0	0.90	90	EBiB	1.20	0.80
2		33 %, Tol	1.84	1.30	90	EBiB	1.20	0.70
3		33 %, Tol	23	0.16	50	EBiB	1.18	0.72
4		33 %, Tol	46	0.047	30	EBiB	1.22	0.60
5	BPIEP	33 %, anisole	1.84	1.10	90	EBiB	1.20	0.70
6 ^{a)}		50 %, Tol	5.5	0.97	90	BPN	1.10	0.84
7 ^{a)}		50 %, Tol	5.5	0.72	90	MBB	1.26	0.80
8		66 %, Tol	5.5	0.34	90	EBiB	1.24	0.60

^{a)} Data collected from chapter 6, section 6.2.3.1, Table 6.7; **NPPI**: (N-(*n*-propyl)-2-pyridylmethanimine); **BPIEP** (2-6-bis[1-(2,6-diisopropyl phenylimino)ethyl] pyridine); **EBiB**: ethyl-2-bromoisobutyrate; **BPN**: 2-bromopropionitrile; **MBB**: 3-bromo-3-methyl-butanone-2

In all the cases, the rate of polymerization follows first order kinetics, indicating the presence of low radical concentration throughout the reaction. Polymerization rate attains a maximum at a ligand-to-metal ratio of 2:1 in toluene at 90 °C. Solvent volume has a

significant effect on polymerization kinetics. Polymerization is faster in polar solvents like, diphenylether, and anisole, as compared to toluene. However, at constant solvent volume the decrease in temperature results in lowering of the rate of polymerization. The apparent activation energy (ΔE_{app}^\ddagger) = 50.96 KJ mol⁻¹ and enthalpy of equilibrium (ΔH_{eq}°) = 28.8 KJ/mol for polymerization of MMA. Controlled nature of the polymerization was confirmed by the formation of high molecular weight PMMA ($M_{n,SEC} = 90,000$ $M_w/M_n = 1.10$) using a pre-formed PMMA macroinitiator in a chain extension experiment.

The rate of polymerization in ATRP of MMA with tridentate ligand (BPIEP) is lower than a bidentate ligand (NPPI) under similar conditions (Table 3.16). This can be attributed to the hindered nature of the ligand. The tridentate ligand (BPIEP) possesses two symmetrical imine (-C=N-Ar) units around central pyridine unit, whereas, only one imine unit (-C=N-R, R = C₃) is present in case of the bidentate imine ligand (NPPI). Therefore, the coordination of copper with tridentate ligand might be more efficient compared to bidentate ligand, thereby, causing greater hindrance to the expansion of coordination sphere during ATRP equilibrium dynamics.

The other key features exhibited by the tridentate ligand are, (a) the ageing of the copper salt complexed with BPIEP has a beneficial effect on polydispersities and conversion, (b) reverse ATRP of MMA using Cu^{II}/AIBN system shows good control, both, in solution as well as in bulk and (c) the tridentate ligand is also equally effective for ATRP of monomers like methylacrylate and glycidyl methacrylate.

3.4. References

1. Matyjaszewski, K.; Spanswick, J. *Materials Today* **2005**, 3, 26.
2. Matyjaszewski, K. *Chem. Eur. J.* **1999**, 5, 3095; *Polym. Mater. Sci. Eng.* **2001**, 84, 52.
3. Britovsek, G. J. P.; Bruce, M.; Gibson, V. C.; Kimberly, B. S.; Maddox, P. J.; Mastroianni, S.; McTavish, S. J.; Redshaw, C.; Solan, G. A.; Stromberg, S.; White, A. J. P.; Williams, D. J. *J. Am. Chem. Soc.* **1999**, 121, 8728.
4. Gibson, V. C.; O'Reilly, R. K.; Reed, W.; Wass, D. F.; White, A. J. P.; Williams, D. J. *Macromolecules* **2003**, 36, 2591.
5. Pintauer, T.; Matyjaszewski, K. *Coord. Chem. Rev.* **2005**, 249, 1155.
6. Xia, J.; Zhang, X.; Matyjaszewski, K. *ACS Symp. Ser.* **2000**, 760, 207.

7. Matyjaszewski, K.; Göbelt, B.; Paik, H. J.; Horwitz, C. P. *Macromolecules* **2001**, 34, 430.
8. Qui, J.; Matyjaszewski, K.; Thouin, L.; Amatore, C. *Macromol Chem. Phys.* **2000**, 201, 1625.
9. Haddleton, D. M.; Crossman, M. C.; Hunt, K. H.; Topping, C.; Waterson, C.; Suddaby, K. G. *Macromolecules* **1997**, 30, 3992.
10. Haddleton, D. M.; Martin, C. C.; Dana, B. H.; Duncalf, D. J.; Heming, A. M.; Kukulj, D.; Shooter, A. J. *Macromolecules* **1999**, 32, 2110.
11. Krishnan, R.; Srinivasan, K. S. V. *Macromolecules* **2004**, 37, 3614.
12. Haddleton, D. M.; Duncalf, D. J.; Kukulj, D.; Heming, A. M.; Shooter, A. J.; Clark, A. J. *J. Mater. Chem.* **1998**, 1525.
13. Pascual, S.; Coutin, B.; Tardi, M.; Polton, A.; Vairon, J.-P. *Macromolecules* **1999**, 32, 1432.
14. Matyjaszewski, K.; Wang, J.; Grimaud, T.; Shipp, D. *Macromolecules* **1998**, 31, 1527.
15. Perrier, S.; Armes, S. P.; Wang, X. S.; Malet, F.; Haddleton, D. M. *J. Polym. Sci.: A., Polym. Chem.* **2001**, 39, 1696.
16. Wang, J.-L.; Grimaud, T.; Matyjaszewski, K. *Macromolecules* **1997**, 30, 6507.
17. Small, B. L.; Brookhart, M.; Bennett, A. M. A. *J. Am. Chem. Soc.* **1998**, 120, 4049.
18. Britovsek, G. J. P.; Gibson, V. C.; Kimberley, B. S.; Maddox, P. J.; McTavish, S. J.; Solan, G. A.; White, A. J. P.; Williams, D. J. *Chem. Commun.* **1998**, 849.
19. Göbelt, B.; Matyjaszewski, K. *Macromol. Chem. Phys.* **2000**, 201, 1619.
20. Xia, J.; Matyjaszewski, K. *Macromolecules* **1997**, 30, 7697.
21. Nagle, P.; O'Sullivan, E.; Hathaway, P. J.; Muller, E. J. *J. Chem. Soc., Dalton Trans.* **1990**, 3399.
22. Matyjaszewski, K.; Patten, T. E.; Xia, J. *J. Am. Chem. Soc.* **1997**, 119, 674.
23. Jo, S. M.; Paik, H. J.; Matyjaszewski, K. *Polym. Prepr. (Am. Chem. Soc., Div. Polym. Chem.)* **1997**, 38(1), 697.
24. Matyjaszewski, K.; Nakagawa, Y.; Jasieczek, C. B. *Macromolecules* **1998**, 31, 1535.
25. Xia, J.; Zhang, X.; Matyjaszewski, K. *Macromolecules* **1999**, 32, 3531.
26. Destarac, M.; Matyjaszewski, K.; Silverman, E.; Ameduri, B.; Boutvein, B. *Macromolecules* **2000**, 33, 4613.
27. Jewrajka, S. K.; Chatterjee, U.; Mandal, B. M. *Macromolecules* **2004**, 37, 4325.
28. Lide, D. R.; Frederikse, H. P. R. *CRC Handbook of Chemistry and Physics*, 78th ed., CRC Press, New York 1997.
29. Wei, M.; Matyjaszewski, K.; Patten, T. E. *Polym. Prepr. (Am. Chem. Soc., Div. Polym. Chem.)* **1997**, 38 (1), 683.
30. Chambard, G.; Klumperman, B.; German, A. L. *Macromolecules* **2000**, 33, 4417.
31. Xu, W.; Zhu, X.; Cheng, Z.; Chen, J. *J. Appl. Polym. Sci.* **2003**, 90, 1117.
32. Krishnan, R.; Srinivasan, K. S. V. *Macromolecules* **2003**, 36, 1769.
33. Cañamero, P. F.; Luis de la Fuente, J.; Madruga, E. L.; Fernández-García, M. *Macromol. Chem. Phys.* **2004**, 205, 2221.
34. Destarac, M.; Jerome, A.; Boutvein, B. *Macromol. Rapid Commun.* **2000**, 21, 1337.
35. Matyjaszewski, K.; Xia, J. *Chem. Rev.* **2001**, 101, 2921.

36. Beuermann, S.; Michael Buback, M.; Davis, T. P.; Gilbert, R. G.; Hutchinson, R. A.; Olaj, O. F.; Russell, G. T.; Schweer, J.; van Herk, A. M. *Macromol. Chem. Phys.* **1997**, 198, 1545.
37. Zhang, H.; van der Linde, R. *J. Polym. Sci. A: Polym. Chem.* **2002**, 40, 3549.
38. Haddleton, D. M.; Kukulj, D.; Duncalf, D. J.; Heming, A. M.; Shooter, A. J. *Macromolecules* **1998**, 31, 5201.
39. Xia, J.; Matyjaszewski, K. *Macromolecules* **1999**, 32, 2434.
40. Mittal, A. *Ph.D. Thesis* **2006**, Chapter 2.
41. Jiang, J.; Zhang, K.; Zhou, H. *J. Polym. Sci.: A, Polym. Chem.* **2004**, 42, 5811.
42. Otsu, T.; Aoki, S.; Nishimura, M.; Yamaguchi, M.; Kusuki, Y. *J. Polym. Sci.: B, Polym. Lett.* **1967**, 5, 835.
43. Percec, V.; Grigoras, C. *Polym. Prepr., ACS Polym. Div.* **2002**, 43 (2), 171.
44. Grimaud, T.; Matyjaszewski, K. *Macromolecules* 1997, 30, 2216.
45. Percec, V.; Barboiu, B. *Macromolecules* **1995**, 28, 7970.
46. Matyjaszewski, K.; Wang, J-L.; Grimaud, T.; Shipp, D.A. *Macromolecules* **1998**, 31, 1527.
47. Shipp, D. A.; Matyjaszewski, K. *Macromolecules* **2000**, 33, 1553.
48. Davis, K.; Paik, H. -J.; Matyjaszewski, K. *Macromolecules* **1999**, 32, 1767.
49. Xue, L.; Agarwal, U. S.; Lemstra, P. J. *Macromolecules* **2002**, 35, 8650.
50. Haddleton, D. M.; Duncalf, D. J.; Kukulj, D.; Crossman, M. C.; Jakson, S. G.; Bon, S. A. F.; Clark, A. J.; Shooter, A. J. *Eur. J. Inorg. Chem.* **1998**, 1799.
51. de la Fuente, J. L.; Fernández-Sanz, M.; Fernández-García, M.; Madruga, E. L. *Macromol. Chem. Phys.* **2001**, 202, 2565.
52. Haddleton, D. M.; Waterson, C. *Macromolecules* **1999**, 32, 8732.
53. Lee, Do W.; Seo, Eun Y.; Cho, Sung I.; Yi, Chae S. *J. Polym. Sci.: A, Polym. Chem.* **2004**, 42, 2747.
54. Wang, J. S.; Matyjaszewski, K. *Macromolecules* **1995**, 28, 7572.
55. Xia, J. Matyjaszewski, K. *Macromolecules* **1997**, 30, 7692.
56. Xia, J. Matyjaszewski, K. *Macromolecules* **1999**, 32, 5199.
57. Wang, W.; Yan, D.; Jiang, X.; Detrembleur, C.; Lecomte, P.; Jérôme, R. *Macromol. Rapid Commun.* **2001**, 22, 439.
58. Zhu, S.; Wang, W.; Tu, W.; Yan, D. *Acta Polym.* **1999**, 50, 267.
59. G. Chen; X. Zhu; Z. Cheng; W. Xu; J. Lu *Radiation Phys. and Chem.* **2004**, 69, 129.
60. Odian, G. *Principles of Polymerization*, 2nd ed., Wiley: New York, **1981**, 196.

Chapter 4. Influence of steric and electronic effects around the metal center in ATRP of MMA using *bis*(iminopyridine) ligand and EB/B as initiator.

4.1. Introduction

Dieck tom *et al.*¹ showed that π -back bonding, a stability factor for lower oxidation state metals, is twice as strong for α -diimines compared to 2,2'-bipyridines. This phenomena was later validated by Reinhold *et al.* using quantum chemical investigations.² A good π -acceptor efficiently stabilizes the lower oxidation state of the metal. Alkyl amines are better π -acceptor than pyridines or imines³⁻⁵ since they possess low lying π^* LUMO that binds with metal strongly. Matyjaszewski *et al.*⁶ reported that the rate of activation depends upon the nature of N-binding site of the ligand. The phenyl substituted ligands forms very slowly activating and very rapidly deactivating catalysts. Generally, a slowly activating catalyst deactivates quickly, and a rapidly activating catalyst deactivates slowly. An ideal catalyst should have very large k_{deact} and appropriate k_{act} in order to get the optimum value of equilibrium constant of reaction dynamics.

Bidentate ligands from *n*-alkyl substituted bipyridine results in homogeneous polymerization compared to bipyridine giving better control over MW and MWD.^{7,8} This apart, bidentate ligands derived from condensation of an aldehyde or ketone with an appropriate amine have also received wide spread attention.⁹ Although bipyridines and Schiff bases possess comparable σ -bonding capabilities, the latter has lower lying LUMO² and is therefore superior in stabilizing Cu^{I} as compared to bipyridines. However, electron withdrawing groups on para position of bipyridine lowers the vacant π^* -significantly, thereby, favoring stabilization. This electronic effect is in addition to the possible steric effects of the substituents on the redox potential, i.e., 2,2'-bipyridine ligand not only stabilizes Cu^{I} by π -electron back donation from the metal, but also helps the interchange between tetrahedral Cu^{I} and distorted square based pyramidal Cu^{II} .¹⁰

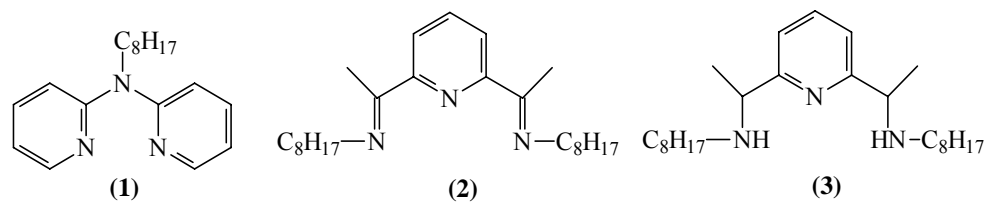
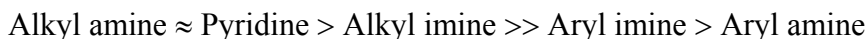


Fig. 4.1: Tridentate imines as N-donors in ATRP

Similarly, a tridentate ligand with two pyridines, and one amine (**1**) gave narrow MWD polymers using styrene, MA and MMA as monomers. However, M_n values for PMMA were slightly higher than calculated values.¹¹ Also, diminopyridine (**2**) can be employed for controlled polymerization of MMA ($M_w/M_n < 1.3$), while diaminopyridine (**3**) is effective for MA and styrene ($M_w/M_n < 1.3$).¹² In general, Schiff base ligands based on central pyridine moiety are more effective for the polymerization of (meth)acrylates⁷⁻⁹ and styrene.¹³ However, a similar ligand, diazabutadiene or diimine, which has no pyridine moiety, does not induce controlled polymerization because of high stability of Cu^I complexes with regard to oxidation.⁹ Similarly, diamine compounds like TMEDA (N,N,N',N'-tetramethylethylenediamine) coordinate to copper species, but their use for MA, MMA, and styrene results in slower polymerization and broader MWDs ($M_w/M_n = 1.3-2.5$) than those with bipyridine based bidentate ligands.¹⁴ Slower deactivation rates were found for catalysts with central pyridine unit in the ligand as compared to the catalysts derived from ligands with a central amine unit. Therefore, the decrease in π -accepting ability of various diimines is



Recently, ligands containing imine donors, especially tridentate *bis*(imino) pyridines have been widely explored as olefin polymerization catalysts. It has been reported that five coordinate iron (II) complexes containing *bis* (imino) pyridines have limited potential for Fe-based ATRP catalysts, most probably due to steric crowding within the metal coordination sphere.¹² Most recently, Gibson *et al.* utilized a stable class of four-coordinate iron complexes, containing bidentate α -diimine ligands, first described by Dieck and coworkers to polymerize styrene.¹⁵ Among the various substituents studied, cyclohexyl was identified to be the best for ATRP of styrene. Polymerization was slow, reaching 93 % conversion in 8 h. However, fairly good control over molecular weight and polydispersity ($M_w/M_n = 1.3$)

was observed. Aryl substituents favored β -hydrogen chain transfer processes.¹⁶ Later, α -diimine ligands containing pyridine nitrogen and imine nitrogen were employed as bidentate ligands for ATRP of styrene and methyl methacrylate. In the latter case, a monomeric iron complex with cyclododecyl (C₁₂H₂₃) substituent on imine nitrogen was structurally identified for the polymerization of MMA. Although molecular weight control could be achieved, the polydispersities ($M_w/M_n = 1.49$) remained very high.¹⁷

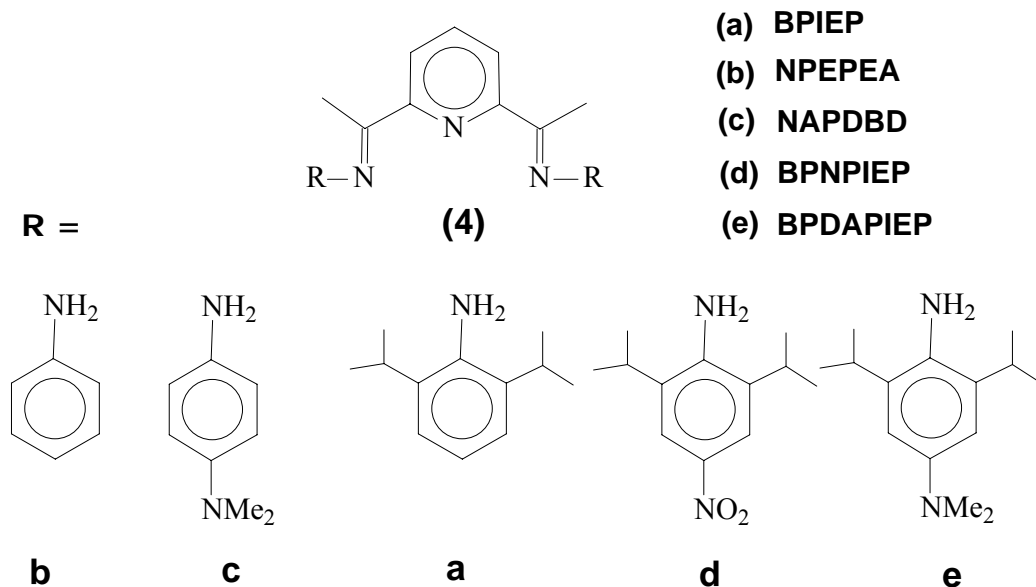
A diiminoarylpyridine ligand namely, 2,6-*bis* [1-(2,6-diisopropylphenylimino)ethyl]pyridine (BPIEP), was successfully employed for ATRP of MMA (Chapter 3). Therefore, it was of interest to explore structural variants of the ligand in the course of ATRP. Thus, two different diiminoarylpyridine ligand were synthesized having different electronic and steric property around the central metal atom. This chapter discusses the results of ATRP of MMA in toluene at 90 °C using various N-donors as ligands, CuBr as catalyst and EB*i*B as initiator.

4.2. Results and discussion

4.2.1. Nature of tridentate ligand

The simplest tridentate ligand of the series (Scheme 4.1), NPEPEA: {(N-((1E)-1-{6-[(1E)-N-phenylethanimidoyl]pyridine-2-yl}ethylidene)aniline, (**4b**), was explored. **4b** differed from **4a** in the extent of steric crowding around the metal center. In addition, the electronic effects on **4a** and **4b** were studied by varying the substituents on para position. The N(Me)₂ substituent acts as an electron donating whereas NO₂ at *para* position acts as an electron-withdrawing group. **4d** and **4e** differ from **4a** in terms of electronic properties. **4c** differs from **V** in terms of steric bulk around the metal center. Thus, the basicity of the amines employed in this study increases in the following order:





Scheme 4.1: Structures of various Schiff base imines utilized for ATRP of MMA

4.2.2. Influence of steric crowding around metal center on the ATRP of MMA

Scheme 4.1 shows the structures of various N-donors with different steric bulk employed for ATRP of MMA. In this section, the results of polymerization with ligands namely, **4a**, **4b**, **4c** and **4e** will be discussed.

4.2.2.1. ATRP of MMA in toluene at 90 °C using tridentate N-donor as ligands and EBiB as initiator

ATRP of MMA in toluene at 90 °C was performed using CuBr as catalyst, EBiB as initiator and **4a**, **4b**, **4c** and **4e** as ligands. The mole ratios of the different components utilized in present study are [MMA]: [EBiB]: [CuBr]: [L] = 100: 1: 1: 2. Table 4.1 shows the results of polymerization of MMA as a function of ligand structure. The polymerization resulted in uncontrolled molecular weight in case of **4b** and **4c** with polydispersities higher than 1.6, lower initiator efficiencies and good polymer conversion. Presence of isopropyl groups in 2,6-position resulted in better control of molecular weight along with higher initiator efficiency (entry 1 and 4). This can be attributed to the ability of bulky isopropyl groups to stabilize the copper complex during the atom transfer step, thereby, leading to better

dynamics of equilibrium. Thus, steric crowding around central metal atom helps in attaining better polymerization control and lower polydispersity.

Table 4.1: Effect of steric bulk in ligand structure and catalyst in ATRP of MMA^{a)}

Entry	Ligands/ CuX	Time (h)	Conv ^{b)} (%)	M _{n,Cal} ^{c)}	M _{n,SEC}	PDI	I _{eff} ^{d)}
1	4a / CuBr	5.5	60	6,000	8,300	1.21	0.70
2	4b ^{e)} / CuBr	5.5	43	4,300	18,400	1.63	0.24
3	4c ^{f)} / CuBr	5.5	52	5,200	16,000	1.82	0.32
4	4e ^{g)} / CuBr	5.5	50	5,000	7,500	1.24	0.67

[MMA]₀ = 3.12 M, in toluene (66 %, v/v) at 90 °C, reaction time = 5.5 h; [MMA]: [EBiB]: [CuBr]: [L] = 100: 1: 1: 2; ^{b)} gravimetrically; ^{c)} M_{n,cal} = % conversion (grams of monomer / moles of initiator); ^{d)} I_{eff} = M_{n,Cal} / M_{n,SEC}; ^{e)} **4b**: N-((1E)-1-{6-[(1E)-N-phenylethanimidoyl]pyridin-2-yl}ethylidene) aniline, ^{f)} **4c**: {(N-((1E)-1-{6-[N-(aminophenyl)ethanimidoyl]pyridin-2-yl}ethylidene)-N'-dimethylbenzene-1,4-di amine)}; ^{g)} **4e**: 2,6-bis[1-(2,6-diisopropyl,4-(N,N'-dimethylamino) phenylimino)ethyl] pyridine.

4.2.3. Influence of electronic effects around metal center on the ATRP of MMA

In this section, polymerization results with ligands, namely, **4d**, **4e**, **4b** and **4c** are discussed.

4.2.3.1. ATRP of MMA in toluene at 90 °C using tridentate N-donor as ligands and EBiB as initiator

The polymerization of MMA was performed in toluene at 90 °C using CuBr/N-donor catalyst system along with EBiB as initiator and **4a**, **4d**, and **4e** as ligands. The mole ratios of the different components utilized in present study are [MMA]: [EBiB]: [CuBr]: [L] = 100: 1: 1: 2. Table 4.2 shows the results of ATRP of MMA as a function of ligand structure with varying electronic property. A very slow polymerization with **4d** was seen resulting in molecular weights much higher than calculated thereby leading to poor initiator efficiency (0.29). The lower polydispersity indicates that the deactivation kinetics is slow as compared to activation step.⁶

Table 4.2: Effect of electronic properties of ligand on ATRP of MMA^{a)}

Entry	Ligands/ CuX	Time (h)	Conv ^{b)} (%)	M _{n,Cal} ^{c)}	M _{n,SEC}	PDI	I _{eff} ^{d)}
1	4a / CuBr	5.5	60	6,000	8,300	1.21	0.70
2	4d ^{e)} /CuBr	5.5	4	4,00	1,400	1.21	0.29
3	4e ^{f)} /CuBr	5.5	50	5,000	7,500	1.24	0.67

^{a)} [MMA]₀ = 3.12 M, in toluene at 90 °C, reaction time = 5.5 h; [MMA]: [EBiB]: [CuBr]: [L] = 100: 1: 1: 2;

^{b)} gravimetrically; ^{c)} M_{n,cal} = % conversion (grams of monomer / moles of initiator); ^{d)} I_{eff} = M_{n,Cal}/ M_{n,SEC}; ^{e)} **4d**: 2,6-bis[1-(2,6-diisopropyl,4-nitrophenylimino)ethyl] pyridine; ^{f)} **4e**: 2,6-bis[1-(2,6-diisopropyl,4-(N,N'-dimethylamino) phenylimino)ethyl] pyridine.

However, **4e** and **4a** resulted in better control on molecular weight and higher initiator efficiency. Thus, presence of sterically bulky isopropyl groups as well as electron donating groups stabilize the copper complex during the atom transfer step, thereby, leading to better dynamics of equilibrium. The effect of monomer to initiator concentration on the ATRP of MMA using different N-donors complexed with CuBr was examined. The results obtained are tabulated in Table 4.3.

Table 4.3: Electronic effect of ligands on ATRP of MMA at different [M]/[I] ratios^{a)}

Ligands/ CuX	[M]/[I] ^{b)}	Conv ^{c)} (%)	M _{n,SEC}	PDI	I _{eff} ^{d)}
4a ^{e)} / CuBr	200	60	14,600	1.21	0.82
	400	40	16,200	1.19	0.98
	800	30	26,500	1.20	0.91
4d ^{f)} / CuBr	200	4	2,600	1.14	0.31
	400	6	3,700	1.24	0.65
	800	6	6,300	1.37	0.76
	1000	5	6,500	1.38	0.76
4e ^{g)} / CuBr	200	40	10,650	1.23	0.75
	400	30	16,200	1.23	0.74

Contd

4e ^{g)} / CuBr	800	18	15,600	1.16	0.85
	1000	20	22,900	1.18	0.87

^{a)} $[MMA]_0 = 4.68$ M, in toluene (50 %, v/v); ^{b)} $[M]/[I]$: monomer/ initiator where $[I]$ is constant and $[M]$ is varied; ^{c)} gravimetric; ^{d)} $I_{eff} = M_{n, cal} / M_{n, SEC}$; ^{e)} Chapter 3: Section 3.2.3.8: **4a**: 2,6-bis[1-(2,6-diisopropyl phenyl imino)ethyl] pyridine ^{f)} **4d**: 2,6-bis[1-(2,6-diisopropyl,4-nitro phenylimino)ethyl]pyridine; ^{g)} **4e**: 2,6-bis[1-(2,6-diisopropyl ,4-(N,N'-dimethylamino) phenylimino)ethyl]pyridine;

The conversion obtained using **4d**/CuBr catalyst system generally remained very low. Lower values of polydispersity and higher initiator efficiency was obtained with higher $[M]/[I]$ values. These results are best understood based on the relative basicity of the amine in the ligand **4d** and **4e**. Better stabilization of copper complex occurred leading to slower activation and faster deactivation during ATRP dynamics,⁶ when an amine of higher basicity was used.

4.2.4. Kinetic study of ATRP of MMA in toluene at 90 °C using NPEPEA as ligand and EB/B as initiator

Kinetics of ATRP of MMA in toluene at 90 °C was performed using CuBr as catalyst, EBiB as initiator and ligands **4a** or **4b**. Table 4.4 shows the results of the study. In case of polymerization with CuBr/**4a** and CuCl/**4a** the concentration of growing radicals ($[P^*] \sim 10^{-8}$) is constant at 90 °C as observed by linear plot of $\ln\{[M]_0/[M]_t\}$ versus time (t). From Table 4.4 the apparent rate constant of the polymerization (k_{app}) was found to be in the order, CuBr/**4b** > CuCl/**4a** > CuBr/**4a**. The $\ln\{[M]_0/[M]_t\}$ versus time (t) plot was found to be linear (Fig. 4.2). Molecular weights of PMMA increased linearly with conversion, but, were much higher than predicted, indicating lower efficiency of the initiator system employed in this study (Fig. 4.3). Hence, low initiator efficiency must be caused by the consumption of some of the initiator due to side reactions that could have originated from the more labile C-Br bond end group¹⁸ at the beginning of polymerization.

Table 4.4: Effect of ligand structure complexed with CuX in ATRP of MMA^{a)}

Ligands/ CuX	Time (min)	Conv ^{b)} (%)	M _{n,SEC}	PDI	k _{app} ^{c)} (× 10 ⁵ , s ⁻¹)	[P*] ^{d)} (× 10 ⁸ s ⁻¹)
4a ^{e)} / CuBr	45	8	5,400	1.16	3.40	2.13
	120	16	6,600	1.18		
	195	27	7,900	1.20		
	330	55	10,200	1.23		
4a / CuCl	45	11	4,100	1.18	4.02	2.48
	120	26	6,100	1.17		
	195	38	7,600	1.18		
	330	50	9,300	1.15		
4b ^{f)} / CuBr	45	18	18,600	1.54	6.82 ^{g)}	4.21
	120	28	19,100	1.56		
	195	35	17,800	1.60		
	330	43	18,400	1.63		

^{a)} [MMA]₀ = 3.12 M, in toluene at 90 °C, reaction time = 5.5 h; [MMA]: [EBiB]: [CuBr]: [L] = 100: 1: 1: 2; ^{b)} from GC; ^{c)} slope of ln{[M₀]/[M_t]} vs time plot; ^{d)} [P*] = k_{app}/k_p, k_p = 1.62 × 10³ Lmol⁻¹s⁻¹; ^{e)} BPIEP: **4a**; ^{f)} **4b**: N-((1E)-1-{6-[(1E)-N-phenylethanimidoyl]-pyridin-2-yl}ethylidene) aniline; ^{g)} From non-linear curve fit, k_{app} and k_t = 1.13 × 10⁻³ s⁻¹.

Although both polymerization reactions are catalyzed at 90 °C, the monomer conversion is lower at early stage of reaction catalyzed by CuBr and higher at the end of reaction in comparison to CuCl. In addition, CuCl was found to be a better catalyst than CuBr in terms of giving a higher reaction rate (k_{app} = 4.02 × 10⁻⁵ s⁻¹ for CuCl vs 3.4 × 10⁻⁵ s⁻¹ for CuBr) and higher M_{n,SEC} at 50 % conversion (Table 4.4). In case of CuCl a curvature (Fig. 4.2) was observed in first order plot for longer reaction times (> 4 h), i.e., indicating occurrence of unavoidable termination reactions.

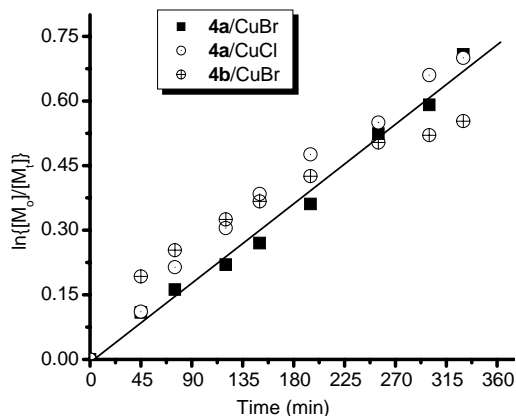


Fig. 4.2: Semi logarithmic kinetic plots for the ATRP of MMA at 90 °C in toluene. [MMA] = 3.12 M. [MMA]: [EBiB]: [CuBr]: [Ligand] = 100: 1: 1: 2.

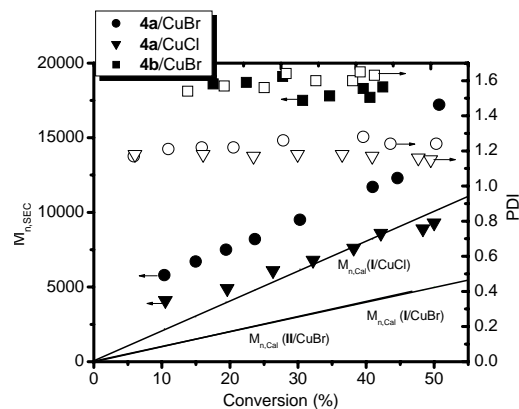


Fig. 4.3: Dependence of molecular weight and polydispersity on conversion in the solution ATRP of MMA at 90 °C with [EBiB] = 0.0312M.

4.3. Conclusions

The subtle effects, both steric and electronic, of the ligands on the efficiency of a tridentate ligand, namely **4a**, **4c**, **4d** and **4e**, on ATRP of MMA is evident from this study. Decreasing steric demand around the metal center substantially reduced the degree of control as well as the rate of polymerization. Similarly, decreasing electron density around the metal atom also proved detrimental to polymerization. However, increasing the electron density around the metal did not dramatically alter the course of ATRP of MMA, in terms of conversion, polydispersity and initiator efficiency. Probably, the choice of $-N(Me)_2$ substituent is not appropriate, since, the substituent itself can interact with the copper center. A more appropriate electron donating substituent which cannot, by itself, interact with Cu(II)/ Cu(I) pair may be more appropriate for unambiguously delineating the effect of electron donating substituent around the ligand.

4.4. References

1. tom Dieck, H.; Franz, K. D.; Hohmann, F. *Chem. Ber.* **1975**, 108, 163.
2. Reinhold, J.; Benedix, R.; Birner, P.; Hennig, H. *Inorg. Chim. Acta* **1979**, 33, 209.
3. van Koten, G.; Vrieze, K. *Adv. Organomet. Chem.* **1982**, 21, 151.
4. Vrieze, K. *J. Organomet. Chem.* **1986**, 300, 307.
5. Svoboda, M.; tom Dieck, H. *J. Organomet. Chem.* **1980**, 191, 321.
6. Matyjaszewski, K.; Göbelt, B.; Paik, H. J.; Horwitz, C. P. *Macromolecules* **2001**, 34, 430.
7. Matyjaszewski, K.; Xia, J. *Chem Rev.* **2001**, 101, 2921.

8. Kamigaito, M.; Ando, T.; Sawamoto, M. *Chem. Rev.* **2001**, 101, 3689.
9. Haddleton, D. M.; Martin, C. C.; Dana, B. H.; Duncalf, D. J.; Heming, A. M.; Kukulj, D.; Shooter, A. J. *Macromolecules* **1999**, 32, 2110.
10. Haddleton, D. M.; Jasieczek, C. B.; Hannon, M. J.; Shooter, A. J. *Macromolecules* **1997**, 30, 2190.
11. Xia, J.; Matyjaszewski, K. *Macromolecules* **1999**, 32, 2434.
12. Göbelt, B.; Matyjaszewski, K. *Macromol. Chem. Phys.* **2000**, 201, 1619.
13. Perrier, S.; Berthier, D.; Willoughby, I.; Batt-Coutrot, D.; Haddleton, D. M. *Macromolecules* **2002**, 35, 2941.
14. Xia, J.; Matyjaszewski, K. *Macromolecules* **1997**, 30, 7697.
15. Britovsek, G. J. P.; Bruce, M.; Gibson, V. C.; Kimberly, B. S.; Maddox, P. J.; Mastroianni, S.; McTavish, S. J.; Redshaw, C.; Solan, G. A.; Stromberg, S.; White, A. J. P.; Williams, D. J. *J. Am. Chem. Soc.* **1999**, 121, 8728.
16. Gibson, V. C.; O'Reilly, R. K.; Reed, W.; Wass, D. F.; White, A. J. P.; Williams, D. J. *Chem. Commun.* **2002**, 1850.
17. Gibson, V. C.; O'Reilly, R. K.; Reed, W.; Wass, D. F.; White, A. J. P.; Williams, D. J. *Macromolecules* **2003**, 36, 2591.
18. Matyjaszewski, K.; Wang, J.; Grimaud, T.; Shipp, D. *Macromolecules* **1998**, 31, 1527.

Chapter 5. Influence on the nature of ligands on ATRP of methyl methacrylate using Cu^IX as catalyst and EB/B as initiator

5.1. Introduction

Copper-catalyzed atom transfer radical polymerization (ATRP) is one of the most robust techniques for controlled radical polymerization. Recent studies in ATRP have explored the use of new ligands as well as new metals that influence the activity and selectivity of the catalysts.¹ The catalyst-ligand complex in ATRP plays a key role in controlling chain growth, polymerization rate and polydispersity. Nitrogen based ligands are effective for copper mediated ATRP². The structure of amine/imine ligand greatly affects the catalyst activity. Homogeneity of the catalyst-ligand complex results in high deactivator concentration and a fast deactivation rate leading to lower apparent rate constant and low polydispersity.³ A recent survey of nitrogen-based ligands revealed that the activity of a ligand increases with the number of coordinating nitrogen atoms and decreases with the number of carbon atoms in the spacer². Schiff bases have been shown to be very effective ligands for ATRP of methacrylates in toluene and xylene solutions (Table 5.1; references therein). Chiral Schiff bases were also employed as ligands for copper mediated ATRP of MMA but no effect on stereochemistry of the resulting polymers was observed¹⁴. Another feature of ATRP that is influenced by the ligand is the turn over number (TON), defined as the number of moles of polymer formed per mole of catalyst per hour. Typical TON reported in the literature for ATRP of methyl methacrylate (MMA) as a function of ligand is given in Table 5.2. A bidentate Schiff base (NPPI) gives a poor TON compared to substituted bipyridyl ligand (*dn*Nbpy).

Several factors have been considered as important in defining the efficiency of ligand in ATRP. These are, inter alia distance between the donor atoms, π -accepting and σ -donating ability, redox potential of the complex and conformational property of the ligand. Subtle changes in the σ -donating and π -accepting abilities can change the redox potential of oxidation half reaction in atom transfer equilibrium¹⁹.

Table 5.1: Literature data for ATRP of MMA using CuBr/L as catalyst system and EBiB as initiator.

Ligand /CuBr	Solvent (% , v/v)	Temp (°C)	M _{n,SEC}	PDI	I _{eff}	Ref
bpy	50 %, EAc	100	9,800	1.40	1.02	4
	50 %, Tol	100	79,000	1.50	0.35	5
dNbipy	50 %, DPE	90	12,000	1.20	1.04	6
	33 %, xylene	90	9,200	1.23	0.72	7
NPPI	50 %, xylene	90	9,200	1.19	0.72	8
	66 %, Tol	90	8,300	1.20	0.89	7
NOPI	66 %, xylene	90	7,300	1.18	1.05	9
CPPC	50 wt %, veratrole	60	39,100	1.14	0.80	10
PMDETA	50 wt %, anisole	90	15,700	1.18	0.78	3
DOIP	50 %, anisole	90	14,300	1.23	0.95	11
BPMOA	50 %, anisole	50	22,500	1.22	0.62	12
Me₆TREN	50 %, ethylene carbonate	90	32,000	2.20	1.60	13

bpy (2,2'-bipyridine); **dNbipy** (4,4-di-(5-nonyl)-2,2'-bipyridine); **NPPI** (N-(*n*-propyl)-2-pyridylmethanimine); **NOPI** (N-(*n*-octyl)-2-pyridyl methanimine); **CPPC** (cyclopentyl-pyridine-2-carboximidate); **PMDETA** (N,N,N',N',N''-pentamethyldiethylenetriamine); **DOIP** (2-6-bis[1-(octylimino)ethyl]pyridine); **BPMOA** (N,N-bis(2-pyridylmethyl)octylamine); **BPIEP** (2-6-bis[1-(2,6-diisopropylphenylimino)ethyl]pyridine); **MBP** (methyl-2-bromopropionate); **NBS** (N-bromosuccinimide); **EBiB** (ethyl-2-bromo isobutyrate); **BPN** (2-bromopropionitrile); **MBB** (3-methyl-3-bromo-butanone-2).

A good π -acceptor is likely to stabilize the lower oxidation state of the metal better. For example alkyl amines possess low lying π^* LUMO that binds with metal strongly²⁰⁻²² and are likely to be better π -acceptors compared to pyridines or imines (Fig.5.1). Hence, α -Diimines, $RN=C(R')-C(R')=NR$, have been widely used as ligands in transition metal complexes.²³⁻²⁹ Several of the α -diimine complexes have found their application as catalysts

for ethylene and α -alkenes.³⁰⁻³⁵ tom Dieck *et al.* showed that π -back bonding (a stability factor for lower oxidation state metals) is twice as strong for α -diimines than 2,2'-bipyridines.³⁶

Table 5.2: Literature data of TON obtained for PMMA by ATRP

Ligand/ Catalyst	T (h)/conv ^{a)} / temp (°C)	[M]/[I]	M _{n,SEC} (x 10 ⁻⁴)	PDI	I _{eff} ^{b)}	TON ^{c)}
RhCl(PPh ₃) ₃ ¹⁵	24/ 82/ 60	6000	24.9	1.70	0.8	206
Fe-isophthalic ¹⁶	4.5/ 9/ 90	500	4.8	1.50	0.9	101
PMDETA/ CuCl ¹⁷	1.2/ 27/ 90	800	2.7	1.28	0.8	180
dnNbpy/ CuCl ¹⁷	1.83/ 22/ 90	3200	7.2	1.23	1.0	393
dnNbpy/ CuCl ¹⁷	8.3/ 55/ 90	6400	37	1.20	0.9	424
dnNbpy/ CuCl ¹⁷	1.2/ 42/ 90	800	2.5	1.18	1.3	283
NPPI/ CuBr ⁷	4/ 83/ 90	100	0.8	1.18	1.0	21
PMDETA/ CuBr ¹⁸	17/ 55/ 30	1000	6.2	1.18	0.9	32
PMDETA/ CuBr ¹⁸	52/ 80/ 30	1000	9.4	1.25	0.6	15
HMTETA/CuBr ³	6/75/90	200	1.85	1.13	0.81	25
Octyliminobisethyl pyridine/ CuBr ¹¹	3.5/ 68/ 90	200	1.4	1.23	0.9	39

^{a)} Gravimetry, ^{b)} I_{eff} = M_{n,cal}/ M_{n,SEC}, ^{c)} moles of polymer per mole of catalyst per hour.

Although a large body of work has been reported on various nitrogen-containing ligands there have been few reports on mono and bi-functional α -diimines systems. This chapter examines a new class of unconjugated α -diimines³⁷ as N-donor ligands with decreasing order of π -accepting ability depending on the nature of the substituents (Fig. 5.1) in atom transfer radical polymerization. Apart from N-donors synthesized during the course of the present work, other known ligands such as NPPI, dnNbpy, PMDETA and HMTETA were studied for comparison. A new tridentate ligand, dmPYBOX, was also studied and results compared with BPIEP.

5.2. Results and discussion

5.2.1. ATRP of MMA in toluene at 90 °C with unconjugated α -diimines as ligands, CuBr as catalyst and EB*i*B as initiator

The ATRP of MMA was performed in toluene (66%, v/v) at 90 °C using different unconjugated α -diimines as N-donors ligands (Fig. 5.1), CuBr as catalyst and EB*i*B as initiator. The basic skeleton (C=N.CH₂-CH₂.N=C) in each of the ligand is similar but the substituents are different, thereby, changing the electron density on imine-N atom of the ligands. The increasing order of basicity of the imines is NDBED > NPEED > NBED > NPMED. The mole ratios of various components of ATRP employed in present study are [MMA]: [EB*i*B]: [CuBr]: [Ligand] = 100: 1: 1: 2. The results obtained were compared with a well known bidentate ligand, N-(*n*-propyl)-2-pyridylmethanimine (NPPI) in ATRP of MMA.

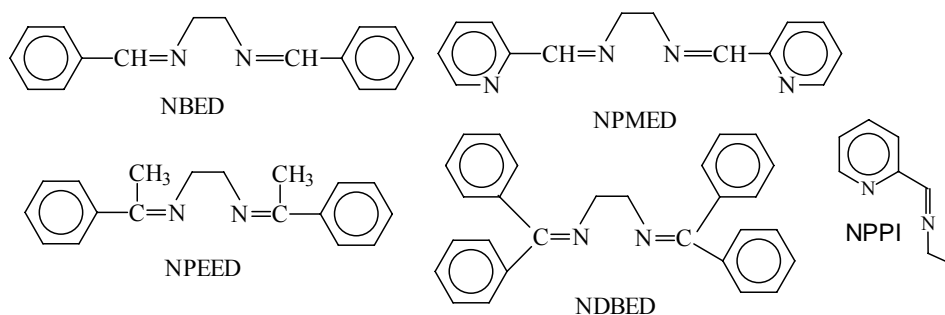


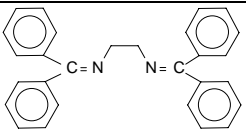
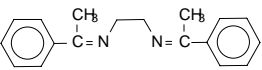
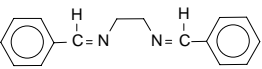
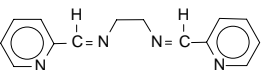
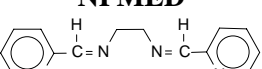
Fig. 5.1: Structures of various Schiff base imines used in ATRP

The color of the *insitu* copper(I) complex formed varied with the type of ligand, viz., yellow (NBED), orange (NPEED), red (NDBED), dark brown (NPMED), red-brown (DNDB), reddish-green (NDDDB), dark brown (DAFONE), no color (BDED), *dn*Nbpy (dark brown) PMDETA (dark green), HMTETA (dark violet), and *dm*PYBOX (blood red). The colors mentioned herein are the color of the complex obtained upon heating the mixture for 1 h at 90 °C. All polymerization reactions were heterogeneous in nature.

The results of the ATRP of MMA using unconjugated α -diimines as ligands are tabulated in Table 5.3. All ligands exhibit uncontrolled polymerization reaction in a non-polar solvent. Loss of catalytic activity and the consequential loss of control of polymerization can be due

to the high stability of the Cu^I complex, inability of the complex to expand the coordination sphere, solubility of the copper complex and redox potentials of the complexes.²¹

Table 5.3: ATRP of MMA with unconjugated α -diimines as ligands^{a)}

Run	Structure/Name	Conv ^{b)} (%)	M _{n,SEC}	PDI	I _{eff} ^{c)}	TON
1	 NDBED	66	44,000	1.71	0.15	17
2	 NPEED	51	16,600	1.76	0.31	13
3	 NBED	68	39,000	1.72	0.17	17
4	 NPMED	71	27,000	1.83	0.26	18
5 ^{d)}	 NPMED	55	25,000	1.41	0.22	14

^{a)} [MMA] = 3.12 M, [MMA]: [EBiB]: [CuBr]: [Ligand] = 100: 1: 1: 2. ^{b)} Gravimetry, ^{c)} I_{eff} = M_{n,cal}/ M_{n,SEC}, ^{d)} [C]: [L] = 1: 1.5.

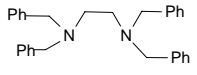
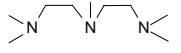
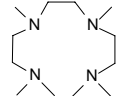
In case of α -diimines examined, we suspect ineffective stabilization of Cu^I by π -back donation from metal to ligand thereby disturbing the equilibrium dynamics between tetrahedral Cu^I and trigonal bipyramidal complex. Thus, without enough deactivator formation in organic phase, the polymerization proceeded like a classical free radical polymerization.

5.2.1.1. ATRP of MMA using multidentate amines as ligands, CuBr as catalyst and EB/B as initiator

bis-(N,N'-Dibenzyl) ethylenediamine (BDED) was examined as a ligand for ATRP of MMA and compared with N,N,N',N',N''-pentamethyldiethylenetriamine (PMDETA) and 1,1,4,7,10,10-hexamethyltriethylenetetramine (HMTETA). Results are shown in Table 5.4. The polymerization in case of BDED (*bis*-(N,N'-dibenzyl)ethylenediamine) followed a

classical free radical pathway. This could be due to the formation of highly stable Cu^I complex, which cannot expand the coordination sphere during atom transfer step.

Table 5.4: ATRP of MMA with multidentate amine as ligands ^{a)}

Run	Structure	Ligand	Conv ^{b)} (%)	M _{n,SEC}	PDI	I _{eff} ^{c)}	TON
1		BDED	19	46,300	1.82	0.04	5
2		PMDETA	80	14,900	1.41	0.54	20
3		HMTETA	95	13,900	1.52	0.68	24

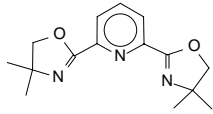
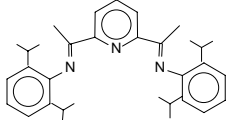
^{a)} [MMA] = 3.12 M, [MMA]: [EBiB]: [CuBr]: [Ligand] = 100: 1: 1: 2. ^{b)} Gravimetry, ^{c)} I_{eff} = M_{n,cal}/ M_{n,SEC}, **BDED**: *bis*-(N,N'-dibenzyl)ethylenediamine

Although the linear amine ligands do not possess π -electrons, yet they are able to stabilize Cu^I sufficiently to ensure control of polymerization. This could be due to the different hybridization of the N-atom present, i.e., sp² in case of imine (C=N) and sp³ in case of (C-N), the latter possessing greater electron donating capacity compared to the former. Polymerizations were also found to be uncontrolled with PMDETA and HMTETA.³⁸ This observation is contrary to what is reported in the literature, where, polymerization control has been reported for MMA using PMDETA and HMTETA as ligand and catalyst: ligand ratio of 1: 1 and 1: 0.5 respectively. However, at a catalyst: ligand ratio of 1: 2 used in our study, there was no control of polymerization.

5.2.1.2. ATRP of MMA in toluene at using tridentate N-donor as ligand, CuBr as catalyst and EB/B as initiator

In this study the behavior of 2,6-*bis*[1-(2,6-diisopropyl phenylimino)ethyl] pyridine (BPIEP) was compared with another tridentate ligand, namely, and 2,6-*bis*(4,4-dimethyl-2-oxazolin-2-yl) pyridine (*dm*PYBOX) for MMA polymerization. Both ligands possess a structural resemblance in terms of the nature of the coordination site. The ligands differ in their relative steric hindrance around the coordination site and the electron donating capacity of the nitrogen atoms.

Table 5.5: ATRP of MMA with different N-donor as ligand ^{a)}

Run	Structure	Toluene (%, v/v)	Conv ^{b)} (%)	M _{n,SEC}	PDI	I _{eff} ^{c)}	TON
1		66	17	6,200	1.27	0.27	4
2	dmPYBOX	50	40	6,900	1.23	0.58	10
3		50	90	14,000	1.27	0.60	23
	BPIEP						

^{a)} [MMA] = 3.12 M, reaction for 5.5 h, [MMA]: [EBiB]: [CuBr]: [Ligand] = 100: 1: 1: 2; ^{b)} Gravimetry; ^{c)} I_{eff} = M_{n,cal}/M_{n,SEC}

The results are shown in Table 5.5. The color of the complex using *dmPYBOX* is bright brick red and does not undergo any change during the reaction. The rate of polymerization with *dmPYBOX*/CuBr system is slower (Table 5.5, run number 2) compared to BPIEP/CuBr. These results indicate very slow initiation followed by deactivation. This can be due to higher stability of the Cu(I) complex with *dmPYBOX*.

5.3. Conclusions

Four bidentate unconjugated α -diimines, and a tridentate bisoxazoline were examined as ligands in the ATRP of MMA. None of the ligand-copper complexes gave adequate control on the polymerization. This is ascribed to the formation of very stable Cu^I complexes with these ligands and inadequate concentration of deactivator in the organic phase, thereby, disturbing the equilibrium dynamics. The tridentate ligand, *dmPYBOX* gave somewhat better results in toluene (50 %, v/v) at 90 °C in terms of conversion, polydispersity and I_{eff}. Further work is needed to fully optimize the performance of this ligand.

5.4. References

1. Patten, T. E.; Matyjaszewski, K. *Acc. Chem. Res.* **1999**, 32, 895.
2. Xia, J.; Zhang, X.; Matyjaszewski, K. In *Transition Metal Catalysis in Macromolecular Design*; Boffa, L. S., Novak, B. M., Eds.; ACS Symposium Series 760; American Chemical Society: Washington, DC, **2000**; Chapter 13, pp 207-223.
3. Xia, J.; Matyjaszewski, K. *Macromolecules* **1997**, 30, 7697.
4. Wang, J. -S.; Matyjaszewski, K. *Macromolecules* **1995**, 28, 7901.

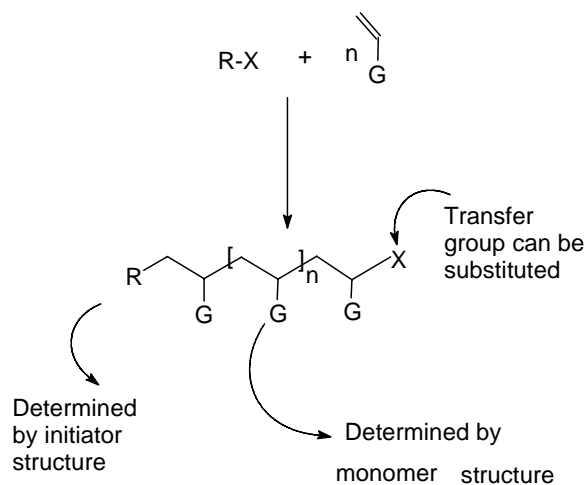
5. de la Fuente, J. L.; Fernández-Sanz, M.; Fernández-García, M.; Madruga, E. L. *Macromol. Chem. Phys.* **2001**, 202, 2565.
6. Matyjaszewski, K.; Wang, J.; Grimaud, T.; Shipp, D. *Macromolecules* **1998**, 31, 1527.
7. Haddleton, D. M.; Martin, C. C.; Dana, B. H.; Duncalf, D. J.; Heming, A. M.; Kukulj, D.; Shooter, A. J. *Macromolecules* **1999**, 32, 2110.
8. Haddleton, D. M.; Duncalf, D. J.; Kukulj, D.; Crossman, M. C.; Jakson, S. G.; Bon, S. A. F.; Clark, A. J.; Shooter, A. J. *Eur. J. Inorg. Chem.* **1998**, 1799.
9. Haddleton, D. M.; Waterson, C. *Macromolecules* **1999**, 32, 8732.
10. Lee, Do W.; Seo, Eun Y.; Cho, Sung I.; Yi, Chae S. *J. Polym. Sci.: A, Polym. Chem.* **2004**, 42, 2747.
11. Göbelt, B.; Matyjaszewski, K. *Macromol. Chem. Phys.* **2000**, 201, 1619.
12. Xia, J.; Matyjaszewski, K. *Macromolecules* **1999**, 32, 2434.
13. Queffelec, J.; Gaynor, S. G.; Matyjaszewski, K. *Macromolecules* **2000**, 33, 8629.
14. Haddleton, D. M.; Duncalf, D. J.; Kukulj, D.; Heming, A. M.; Shooter, A. J. *J. Mater. Chem.* **1998**, 8, 1525.
15. Moineau, G.; Granel, C.; Dubois, Ph.; Jerome, R.; Teyssie, Ph. *Macromolecules* **1998**, 31, 542.
16. Zhu, S.; Yan, D. *Macromol. Rapid Commun.* **2000**, 21, 1209.
17. Xue, L.; Agarwal, U. S.; Lemstra, P. J. *Macromolecules* **2002**, 35, 8650.
18. Ramakrishnan, A.; Dhamodharan, R. *Macromolecules* **2003**, 36, 1039.
19. Qui, J.; Matyjaszewski, K.; Thouin, L.; Amatore, C. *Macromol. Chem. Phys.* **2000**, 201, 1625.
20. Matyjaszewski, K.; Göbelt, B.; Paik, H. J.; Horwitz, C. P. *Macromolecules* **2001**, 34, 430.
21. Xia, J.; Zhang, X.; Matyjaszewski, K. *Polym. Mater. Sci. Eng.* **1999**, 80, 453.
22. Haddleton, D. M.; Shooter, A. J.; Morsley, S. R. *Controlled Radical Polymerization: Matyjaszewski, K., Ed.; ACS Symp. Ser.* **1998**, Vol. 685, p 284.
23. Koten, G. van; Vrieze, K. *Adv. Organomet. Chem.* **1982**, 21, 151.
24. Vonzelewsky, A.; Belser, P.; Hayoz, P.; Dux, R.; Hua, X.; Suckling, A.; Stoeckli-Evans, H. *Coord. Chem. Rev.* **1994**, 132, 75.
25. Paw, W.; Cummings, S. D.; Mansour, M. A.; Connick, W. B.; Geiger, D. K.; Eisenberg, R. *Coord. Chem. Rev.* **1998**, 171, 125.
26. Kaes, C.; Katz, A.; Hosseini, M. W. *Chem. Rev.* **2000**, 100, 3553.
27. Farrell, I. R.; Vlcek, A. *Coord. Chem. Rev.* **2000**, 208, 87.
28. Slageren, J.; van, Hartl, F.; Stufkens, D. J.; Martino, D. M.; van Willigen, H. *Coord. Chem. Rev.* **2000**, 208, 309.
29. Hicks, C.; Ye, G. Z.; Levi, C.; Gonzales, M.; Rutenburg, I.; Fan, J. W.; Helmy, R.; Kassis, A.; Gafney, H. D. *Coord. Chem. Rev.* **2001**, 211, 207.
30. Gottfried, A. C.; Brookhart, M. *Macromolecules* **2001**, 34, 1140.
31. Ittel, S. D.; Johnson, L. K.; Brookhart, M. *Chem. Rev.* **2000**, 100, 1169.
32. Tempel, D. J.; Johnson, L. K.; Huff, R. H.; White, P. S.; Brookhart, M. *J. Am. Chem. Soc.* **2000**, 122, 6686.
33. Liimatta, J.O.; Lofgren, B.; Miettinen, M.; Ahlgren, M.; Haukka, M.; Pakkanen, T. T. *J. Polym. Sci. Pol. Chem.* **2001**, 39, 1426.
34. Mecking, S. *Angew. Chem. Int. Ed.* **2001**, 40, 534.

35. Albietz, P. J.; Yang, K. Y.; Lachicotte, R. J.; Eisenberg, R. *Organometallics* **2000**, 19, 3543.
36. (a) Dieck, tom H.; Svoboda, M.; Grieser, T. *Z. Naturforsch., B*, **1981**, 36, 823. (b) Dieck, tom H.; Dietrich, J. *Chem. Ber.* **1984**, 694, 701.
37. Chowdhury S.; Patra, G. K.; Drew, M. G. B.; Chattopadhyay, N.; Datta, D. *J. Chem. Soc., Dalton Trans.*, **2000**, 235-237.
38. Nanda, A. K.; Matyjaszewski, K. *Macromolecules* **2003**, 36, 1487.

Chapter 6. Study of novel initiators in atom transfer radical polymerization of methyl methacrylate

6.1. Introduction

One of the most important characteristics of ATRP is the fact that initiation occurs through an alkyl halide initiator in presence of a catalyst (ligand/CuX) via a redox process and the polymers prepared by this process consists of a halogen atom at the macromolecular chain-end.¹⁻⁴ Several strategies are available in ATRP for the introduction of functional group, either in-chain or at either end of the polymer chain.⁵ This is shown schematically in Scheme 6.1. In order to obtain good control on the polymerization, it is necessary that the rate of initiation should be equal or faster than the rate of propagation. Hence, the selection of initiator is very important. Initiator provides the head group, whereas, the nature of monomer defines the in-chain functionality. The terminal group in ATRP is almost always a halogen group, which can be subsequently modified using standard procedures in organic chemistry.⁶⁻⁸



Scheme 6.1: Structural features of a polymer chain prepared by ATRP

Relatively less attention has been paid to the influence of initiator type on ATRP of methyl methacrylate. In this chapter we describe results of ATRP of methyl methacrylate (MMA)

with three initiators namely, 3-bromo-3-methyl-butanone-2 (MBB: **1**), 3-(bromomethyl)-4-methylfuran-2,5-dione (BMFD: **2**) and 2-bromopropionitrile (BPN: **3**) as shown in Fig. 6.1.

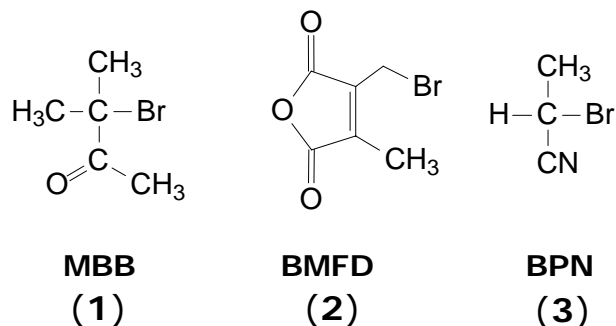


Fig. 6.1: Structure of the initiators employed in ATRP

6.2. Results and discussion

6.2.1. ATRP of MMA in toluene at 90 °C with different N-donors as ligands, CuBr as catalyst, and MBB as initiator

Different N-donors were employed in this study, such as, **NBED** (N, N'- dibenzylidene-1,2-ethanediamine), **NPEED** (N, N'- bis-(1-phenylethylidene)-1,2-ethanediamine), **NDBED** (N,N'-dibenzhydrylidene-ethane-1,2-diamine) and **NPMED** (N,N'-bis-pyridin-2-yl methylene ethane-1,2-diamine) were synthesized by Schiff base condensation of an aromatic carbonyl compound and ethylenediamine respectively.⁹ 2,6-bis(4,4-dimethyl-2-oxazolin-2-yl)pyridine (**dmPYBOX**)¹⁰ and 3-bromo-3-methyl-butanone-2 (**MBB**)¹¹ were synthesized by reported procedures. Bipyridine and multidentate N-donor ligands namely, **dnN bpy**: 4,4'-di (*n*-nonyl) 2,2'-bipyridine; **PMDETA**: N,N,N',N',N''-pentamethyldiethyl enetriamine; **HMTETA**: (N,N,N,N,N,N-hexamethyltriethylenetetra mine, were employed for ATRP of MMA in toluene at 90 °C using various initiating systems along with CuBr as catalyst.

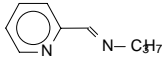
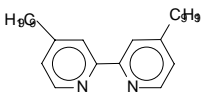
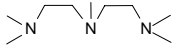
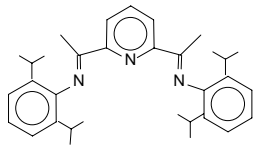
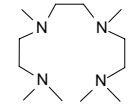
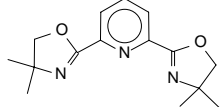
6.2.1.1. Influence of different N-donors as ligands on polymerization of MMA using MBB as initiator

α -Haloketone (for example, CCl₃COCH₃ and CHCl₂COPh) initiators are known for ruthenium^{12,13} and nickel catalyzed¹⁴ controlled radical polymerization of MMA with aluminum triisopropoxide [Al(O*i*Pr)₃] as additive. Typically ~ 90 % conversion was reported in 60-80 h reaction time yielding polymers with a polydispersity \leq 1.23. However,

control over polymerization is lost when mono α -haloketone (for example $(\text{CH}_3)_2\text{C}(\text{Br})\text{COPh}$) was used with copper catalyzed (CuBr) homogeneous systems.¹⁵ This is probably because of the stronger electron-withdrawing power of the ketone's carbonyl that results in the reduction of electrophilic radicals species into anions by highly active Cu(I) catalysts.

3-bromo-3-methyl-butanone-2 (**1**) was employed as an initiator for copper catalyzed ATRP of MMA at 90 °C in toluene. The effect of various N-donors was explored in a non-polar solvent like toluene. The mole ratio of various components used were [MMA]: [**1**]: [CuBr]: [Ligand] = 100: 1: 1: 2. Table 6.1 shows the results of polymerization of MMA.

Table 6.1: ATRP of MMA using MBB (**1**) as initiator at 90 °C/5.5 h ^{a)}

Run	Ligand		Conv ^{b)} (%)	M _{n,SEC} (x 10 ⁻³)	PDI	I _{eff} ^{c)}
	Structure	Notation				
1		NPPI	3	2.20	1.06	0.14
2		dnNbpy	<1	2.50	1.07	-
3		PMDETA	98	14.7	1.34	0.67
4		BPIEP	73	8.80	1.26	0.83
5 ^{d)}		HMTETA	98	18.7	1.41	0.52
6		dmPYBOX	20	5.40	1.36	0.40

^{a)} [M]₀ = 4.68 M and 50 % v/v of toluene wrt monomer; [MMA]: [MBB]: [CuBr]: [Ligand] = 100: 1: 2; ^{b)} gravimetric, ^{c)} I_{eff} = M_{n,Cal}/ M_{n,SEC}, ^{d)} bimodal distribution.

ATRP of MMA using **1** as initiator produces PMMA in the presence of all the N-donor ligands used in this study. However, initiation efficiency of **1** in the presence of bidentate ligands is relatively poor (Table 6.1: entry 1, 2). It has been previously reported that the

initiator efficiency of ethyl-2-bromoisobutyrate in the presence of a tridentate ligand, namely BPIEP, is high for MMA polymerization.¹¹ The difference in the reactivity of α -bromoketone (MBB) and α -bromoester (EBiB) initiators in ATRP could be attributed to the relative coordinating ability of the initiators with CuX in ATRP.

Polymerization of MMA using bidentate ligands (NPPI and *dn*Nbpy) is very slow resulting in low molecular weight PMMA with narrow molecular weight distribution. The reason for this behavior is attributed to an association between the copper complex and the initiator. However, the reaction is very fast and uncontrolled with multidentate linear amines (PMDETA and HMTETA). Nevertheless, initiator efficiencies are better as compared to the bidentate ligands. It is also evident from the Table 6.1 that **1** works efficiently with a sterically hindered tridentate N-donor ligand (BPIEP). This indicates that the α -bromoketone is not effectively coordinating with Cu^I in the presence of tridentate ligands with large steric hindrance around the coordination site. MBB (**1**) initiates the polymerization of MMA more efficiently (Table 6.1, run number 4) when compared to EBiB (Chapter 3, Table 3.5, entry 2: DP = 100, $M_{n,SEC}$ = 14,000, PDI = 1.27, I_{eff} = 0.60) when employed with BPIEP as ligand under similar experimental conditions.

In addition, a new N-donor ligand, namely, 2,6-*bis*(4,4-dimethyl-2-oxazolin-2-yl) pyridine (*dm*PYBOX) was also explored for the ATRP of MMA using **1** as initiator. The coordination site of the ligand (N=C-*py*-C=N) is similar for BPIEP and *dm*PYBOX, except, for the steric hindrance around the coordination site. The color of the complex is bright brick red and does not undergo any change during the reaction. The rate of polymerization is slower (run number 6) relative to BPIEP and PMDETA, but, higher than NPPI and *dn*Nbpy as ligands. The molecular weight is lower than targeted. These results indicate very slow initiation followed by deactivation. This is attributed to the fact that the copper (I) complex with *dm*PYBOX might be more stable thereby disturbing the equilibrium dynamics of the reaction. If the number of nitrogen atom increases beyond three in ligands, then an uncontrolled polymerization occurs resulting in bimodal distribution (table 6.1, run number 5).

6.2.1.2. Kinetic study of ATRP of MMA in toluene at 90 °C using BPIEP as ligand, CuBr as catalyst and MBB (1) as initiator

Kinetic study of ATRP of MMA in presence of BPIEP/ CuBr as catalyst system was performed in toluene at 90 °C and **1** as initiator. The following mole ratios were used: [MMA]: [MBB]: [CuBr]: [BPIEP] = 100: 1: 1: 2. The results obtained are tabulated in the Table 6.2.

Table 6.2: Kinetic study of ATRP of MMA at 90 °C using MBB (**1**)^{a)}

Run	Time (min)	Conv ^{b)} (%)	M _{n cal} ^{c)}	M _{n SEC}	PDI
6.2	0	0	0	-	-
6.2.1	45	20	2,000	2,800	1.24
6.2.2	75	32	3,200	4,300	1.23
6.2.3	120	42	4,200	6,200	1.26
6.2.4	150	50	5,000	7,100	1.26
6.2.5	195	59	5,900	8,200	1.27
6.2.6	255	68	6,800	9,100	1.26
6.2.7	300	72	7,200	9,400	1.25
6.2.8	330	76	7,600	9,500	1.26

^{a)} [MMA] = 9.36 M; ^{b)} by GC; ^{c)} M_{n cal} = %conversion (grams of monomer / moles of initiator).

The semi-logarithmic time conversion plot shows a straight line indicating absence of termination reaction in the polymerization (Fig. 6.2). An apparent rate constant of polymerization, k_{app} , was found to be $7.15 \times 10^{-5} \text{ s}^{-1}$. The rate of polymerization using MBB is faster as compared to a α -bromoester initiator (EBiB: $k_{app} 3.4 \times 10^{-5} \text{ s}^{-1}$).¹¹ The polymer conversion is high, i.e., 85 % in contrast to the aromatic α -haloketone initiators which gave 90 % conversion in 60-80 h.¹² Fig. 6.3 shows the dependence of M_{n,SEC} with conversion as well as molecular weight distribution of the polymer. It is seen that the molecular weight

data obtained from SEC had a curvature indicating the presence of transfer reactions during the polymerization.

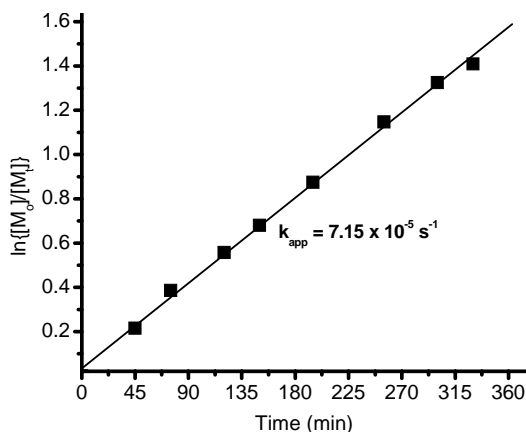


Fig. 6.2: Semi logarithmic kinetic plot for the ATRP of MMA in toluene at 90 °C using MBB as initiator. $[MMA]_0 = 4.68$ M. $[MMA]_t$: $[MBB]$: $[CuBr]$: $[BPIEP] = 100$: 1: 1: 2

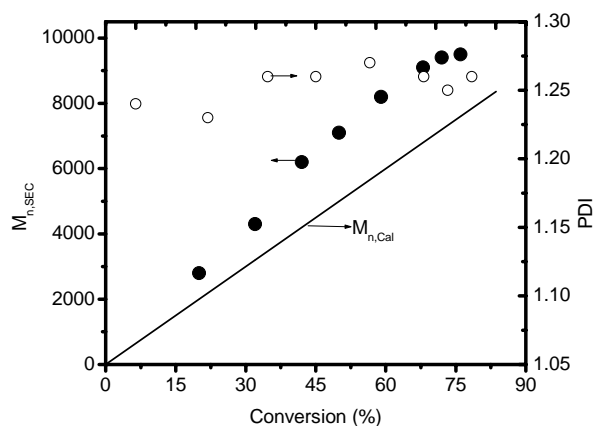


Fig. 6.3: Dependence of molecular weight and polydispersity on conversion in the solution ATRP of MMA at 90 °C with $[MBB] = 0.0468$ M. Open symbols represent polydispersities and filled symbol represents M_n -(GPC).

However, the molecular weight distribution of the polymer was relatively narrow, i.e., ≤ 1.26 as compared to the conventional (or redox initiated) radical polymerization. Thus, a strong electron withdrawing effect of keto carbonyl in MBB resulted in higher rate of initiation as compared to EB*i*B in ATRP.

6.2.2. ATRP of MMA in toluene at 90 °C with BPIEP/CuBr as catalyst system, and BMFD (2) as initiator

Only three methods for preparing anhydride functional polymers by ATRP have been reported in literature. Malz *et al.* employed ATRP initiator having anhydride moiety to polymerize styrene.¹⁶ The polydispersities of the polymer obtained was reported broad (1.31-1.43) and loss of anhydride functionality during workup. Using post polymerization method, Kallitsis and coworkers functionalized polystyrene with excess of maleic anhydride assuming that latter cannot form homopolymer under the conditions employed.¹⁷ The transformation of such type leads to the loss of functionality.

Recently, Moon *et al.* reported *end* and *mid* phthalic anhydride functional PS and PMMA by ATRP.¹⁸ However, the methodology used involves multiple steps to prepare a bromo functional initiator, which in turn is used as ATRP initiator. Post polymerization method involves pyrolysis of the functional polymer at a temperature (210 °C) where loss of some chains of polymer might occur.

In search of a simpler method to prepare anhydride functional PMMA, 3-(bromomethyl)-4-methyl-2,5-furandione (**2**) was examined as an initiator for ATRP of MMA. **2** can be readily prepared by NBS bromination of commercially available 3,4-dimethylmaleic anhydride.¹⁹ **2** was found to be an effective initiator for MMA polymerization in toluene at 90 °C using BPIEP/CuBr as catalyst system (Table 6.3).

Table 6.3: Batch ATRP of MMA using BMFD (**2**) as initiator^{a)}

Run	CuX/ Ligand	Conv^{b)} (%)	M_{n,SEC}	PDI	I_{eff}^{c)}
1	CuBr/BPIEP	85	7,500	1.15	0.9
2 ^{d)}		90	9,500	1.16	0.9
3 ^{e)}	CuBr/BPIEP	50	1,600	1.08	0.47
4 ^{f)}	CuCl/BPIEP	26	3,500	1.15	0.8
5 ^{g)}		55	6,000	1.12	0.9

^{a)} [M]₀ = 5.08 M, for 5.5 hat 90 °C and 50 % v/v of toluene wrt monomer; [MMA]: [BMFD]: [CuBr]: [BPIEP] = 100: 1: 1: 2, ^{b)} gravimetric, ^{c)} I_{eff} = M_{n,Cal}/ M_{n,SEC}; ^{d)} 66 % , v/v toluene wrt monomer, ^{e)} DP_{SEC} = 15 and DP_{NMR} = 14 (Fig. 6.6), ^{f)} Using toluene (66 %, v/v) at RT, ^{g)} Using toluene (66 %, v/v) at 90 °C.

Use of a mixed halogen system resulted in faster initiation, slower propagation and faster deactivation, thereby, yielding polymers with better molecular weight control and PDI. Therefore, ATRP of MMA in 66 % (v/v) toluene was performed using CuCl/BPIEP as catalyst (Table 6.3, run 4) and BMFD as initiator yielding PMMA (M_{n,SEC} = 6000 and PDI = 1.12, conversion = 55 %) and high initiator efficiency of 0.9. However, performing the latter

reaction at room temperature (Table 6.3, run 3) yielded PMMA with lower conversion and lower $M_{n,SEC}$ value.

6.2.2.1. ATRP of MMA in toluene at 90 °C using different N-donors as ligand, CuBr as catalyst, and BMFD (2) as initiator

The efficacy of the initiator (2) was also examined using other bidentate and multidentate amine systems. The mole ratio of various components utilized are [MMA]: [2]: [CuBr]: [Ligands] = 100: 1: 1: 2 (Table 6.4). The control over molecular weight and PDI is lost in case of linear amines (Table 6.4, run 4, and 5).

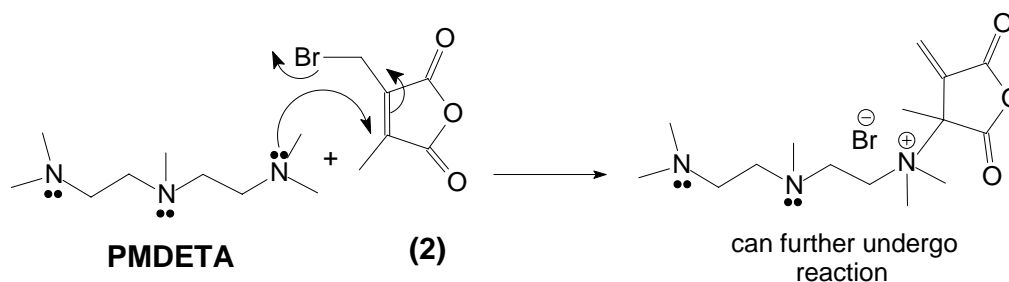
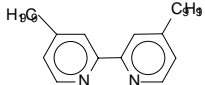
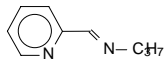
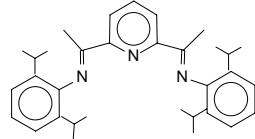
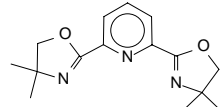
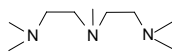
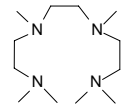


Fig. 6.4: Reaction of PMDETA with BMFD (2)²⁰

This is presumably due to the loss of most part of the initiator on account of the reaction with amines forming quaternary ammonium salts as shown in Fig. 6.4.²⁰⁻²² PMMA synthesized using 2 as initiator and CuBr/*dm*PYBOX as catalyst exhibited controlled molecular weight ($M_{n,SEC} = 5,000$) and narrow polydispersity (1.22). This can be due to the stronger complexation of the *bis*oxazoline ligand with the metal halide, involving all the three nitrogen atoms. Long chain-substituted bipyridine, generally considered as good ligand in ATRP failed to produce a polymer when employed with 2 as initiator (run1, Table 6.4). Pyridine based alkyl imine ligand also gave low conversion and poor I_{eff} (run 2, Table 6.4). The possible reason could be reaction between the Schiff base imine (NPPI) and the initiator (2) as revealed by the darker intensity of the reaction mixture and change in color of copper complex from reddish brown to dark violet or black.²⁰⁻²² Another reason could be the coordination of the monomer to the carbonyl group of the initiator.

Thus, the initiator system (2) resulted in a controlled polymerization with high initiator efficiency only when used along with a bulky ligand (BPIEP). A typical GPC eluogram of PMMA obtained using BPIEP/2 is shown in Fig. 6.5.

Table 6.4: ATRP of MMA using BMFD (2) as initiator at 90 °C / 5.5h^{a)}

Run	Ligand		Conv ^{b)} (%)	M _{n,SEC} (x 10 ³)	PDI	I _{eff} ^{c)}
	Structure	Notation				
1		dnNbpy	-	NP ^{d)}	-	-
2		NPPI	25	5,200	1.05	0.48
3		BPIEP	65	7,600	1.17	0.86
4		dmPYBOX	40	5,000	1.22	0.80
5		PMDETA	3	52,700	1.36	-
6		HMTETA	3	6,500	1.60	-

^{a)} [M]₀ = 4.68 M and 50 % v/v of toluene wrt monomer; [MMA]: [MBB]: [CuBr]: [Ligand] = 100: 1: 1: 2; ^{b)} gravimetric, ^{c)} I_{eff} = M_{n,Cal} / M_{n,SEC}; ^{d)} NP: no polymer.

6.2.2.2. Structure of PMMA obtained using BMFD (2) as initiator, BPIEP/CuBr as catalyst system

The structure of the polymer was determined by preparing a relatively low molecular weight PMMA using 2 as initiator. ATRP of MMA in toluene at 90 °C was performed using BPIEP/CuBr as catalyst system and BMFD as initiator. The mole ratio of various components utilized are [MMA]: [BMFD]: [CuBr]: [BPIEP] = 15: 1: 1: 2. The results are shown in run 3, Table 6.3 and the GPC eluogram of the polymer obtained is shown in Fig. 6.6.

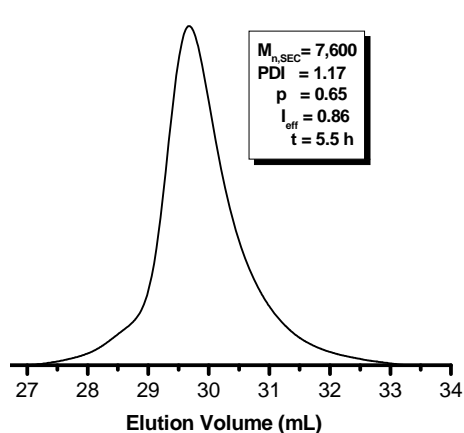


Fig. 6.5: GPC eluogram of PMMA (Run 3, Table 6.4)

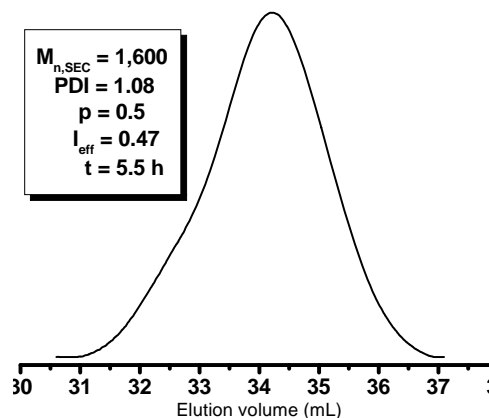


Fig. 6.6: GPC eluogram of PMMA (Run 3, Table 6.3)

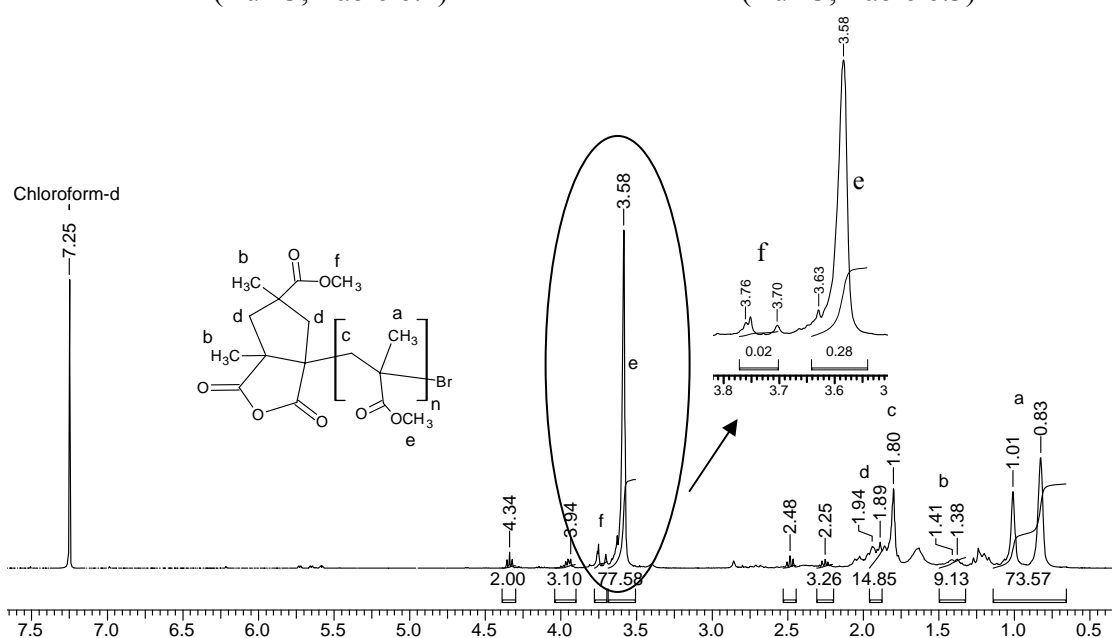


Fig. 6.7: ^1H NMR (500 MHz) spectrum of PMMA (Run 3, Table 6.3) in CDCl_3 .

The peak assignment in ^1H NMR of the PMMA (Fig. 6.7) obtained after removal of the catalyst resulted in the absence of methylene ($=\text{CH}_2$) functionality. The ratio of the protons arising out of the OCH_3 group (at $\delta = 3.76$ ppm) present in the head group to the protons arising out of OCH_3 group (at $\delta = 3.58$ ppm) present in the polymer chain, gave a value of $\text{DP} = 14$. The DP found by ^1H NMR was close to that determined by SEC ($\text{DP}_{\text{SEC}} = 15$), indicating the presence of a single end-group per molecule. Moreover, absence of peak due to methylene group ($=\text{CH}_2$) in the range (δ : 120-150 ppm) in ^{13}C -NMR (DEPT) clearly indicates that the polymer possesses a different end-group (Fig. 6.8 and Fig. 6.9) than

anticipated (Scheme 6.2 a). Thus, a probable end-group structure (**5**) was proposed as shown in Scheme 6.2 b.

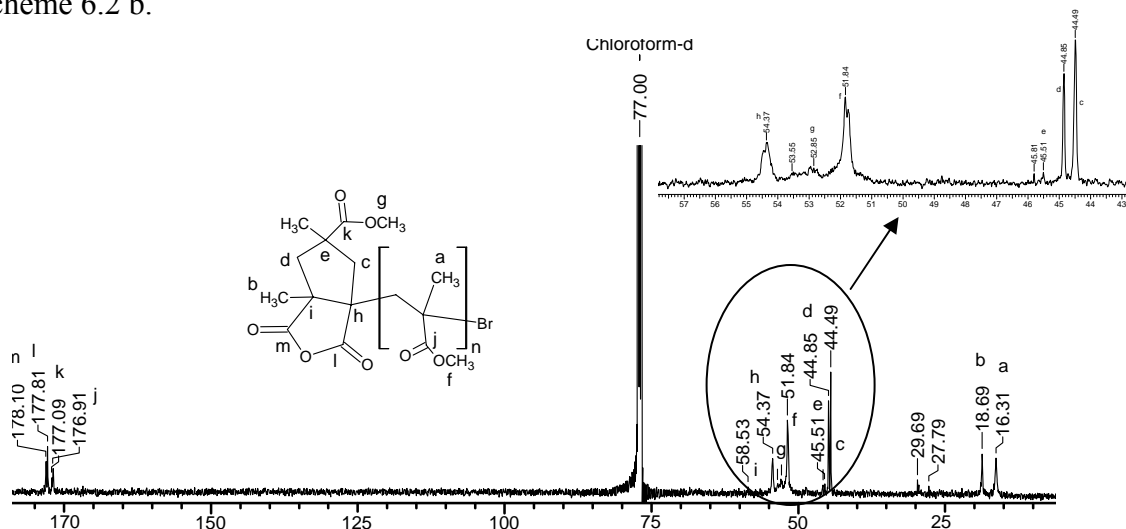


Fig. 6.8: ^{13}C NMR (125 MHz) in CDCl_3 of PMMA (Run 3, Table 6.3) obtained by ATRP

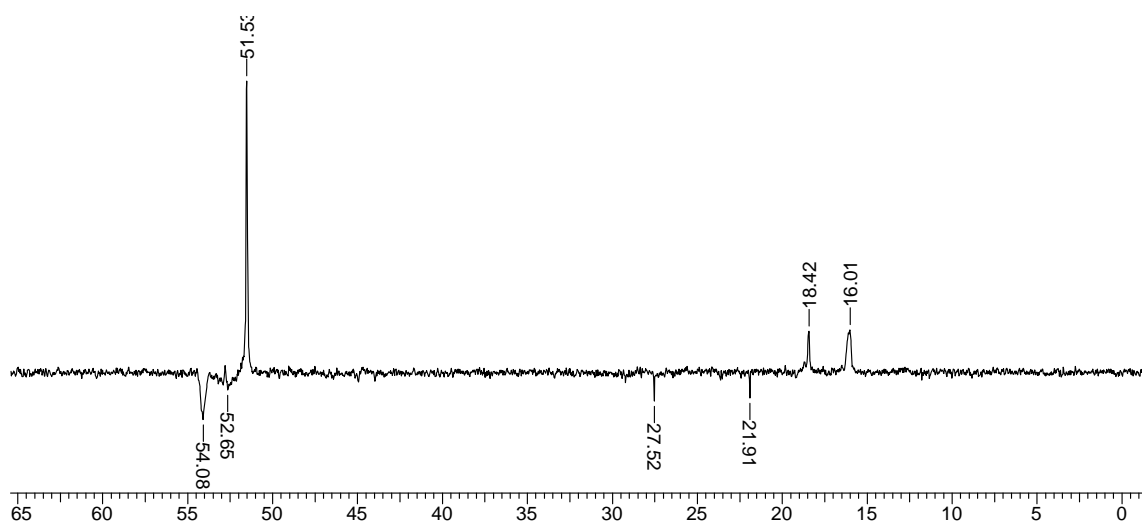
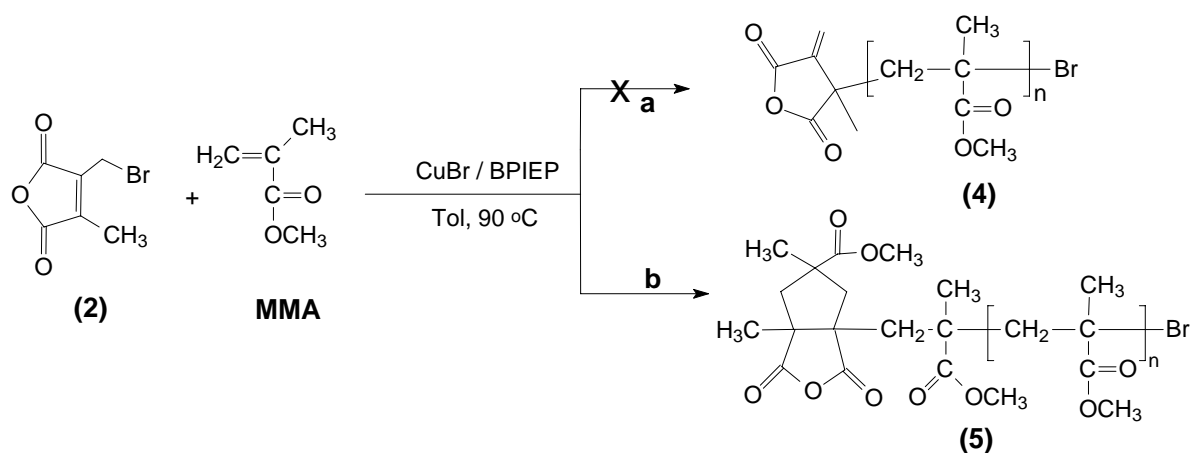


Fig. 6.9: DEPT spectrum of PMMA (Run 3, Table 6.3) obtained by ATRP in CDCl_3

Scheme 6.2 depicts the possible route of the ATRP of MMA using BMFD as initiator along with CuBr/BPIEP as catalyst. If the polymerization reaction proceeds by the anticipated route then the final polymer should have structure (**2**) as shown in Scheme 6.2. Based on this assumption, the structure of the low molecular weight polymer obtained using **2** as initiator was assigned as **5**. FT-IR (Fig. 6.10) of PMMA (Run 3, Table 6.3) also showed the presence of anhydride peak in the polymer.



Scheme 6.2: ATRP of MMA using BMFD (2) as initiator

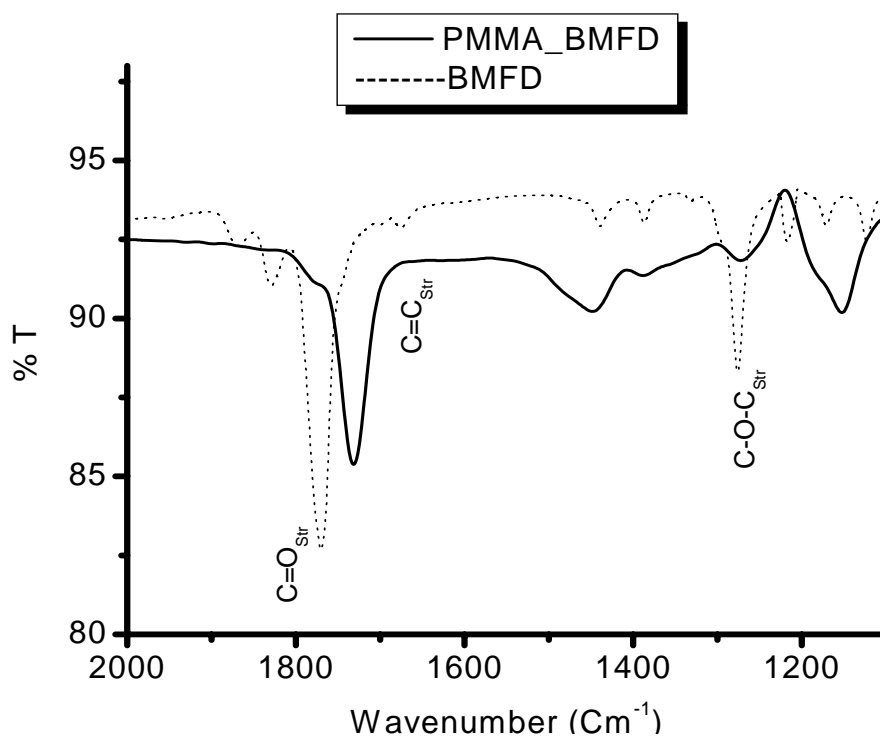
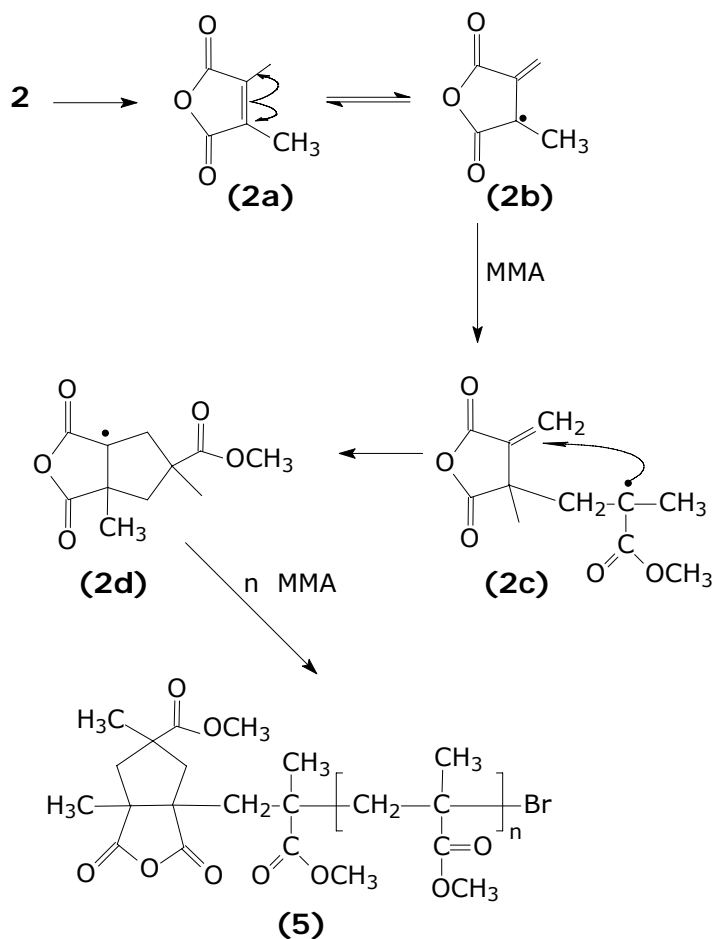


Fig. 6.10: FT-IR of PMMA (Run 3, Table 6.3) using KBr pellet.

A possible mechanistic pathway for the formation of the unusual end group in the polymer is shown in Scheme 6.3. The primary initiator radical (**2a**) rearranges to a stable tertiary radical (**2b**), which adds to a molecule of MMA resulting in an intermediate species (**2d**). We propose that **2c** undergoes a facile ring closure reaction to yield a radical species **2d**, which ultimately initiates the polymerization. The driving force for **2c** \rightarrow **2d** conversion is due to

the activation of the methylene group by the anhydride moiety, making the intramolecular ring closure more favorable than an intermolecular addition of **2c** to MMA. The resulting radical **2d** is a tertiary radical located at a bridgehead end α to an anhydride group. Apparently, this radical possesses a unique combination of stability and reactivity on account of both electronic and conformational factors.



Scheme 6.3: Mechanism of intramolecular ring closure

6.2.2.3. Analysis of the polymer end-groups

With a view to definitively characterize the end-group of the polymer, several strategies were explored. Initially atom transfer radical addition (ATRA) reaction was performed between **2** and MMA. ATRA was performed at three different (90 °C, 70 °C and 30 °C) temperatures for 5-48 h. The ^1H NMR of the product after work up did not show any peaks due to OCH_3 protons.

The polymer from run 3, Table 6.4 was subjected to MALDI-ToF analysis using matrices such as 2,5-dihydroxybenzoic acid (DHB), dithranol, and *trans*-indoleacetic acid (TAA) along with silver trifluoroacetate as well as potassium trifluoroacetate as cationic agents. The concentration ratio of matrix to polymer was varied from 3: 1; 10: 1; 20: 1; 100: 1 and 1: 1.²³⁻²⁵ However, under conditions, wherein, PMMA showed expected peak distribution, PMMA prepared using 2 as initiator (Run 3, Table 6.4) failed to exhibit a satisfactory spectra.

Hydrolysis of the putative anhydride group in PMMA (Run 3, Table 6.4) was attempted under acidic and basic conditions. The acid hydrolysis was performed using 1N HCl (aq) for 48 h, whereas, the base hydrolysis was performed using 1N THF solution of *tetrabutylammonium* fluoride (TBAF) for 48 h. The ¹H NMR of the product polymer obtained after hydrolysis was identical to that of the starting polymer prepared using BMFD as initiator, implying that no hydrolysis occurred under the conditions employed.

Anhydride functionality in the polystyrene can react with 2-fold molar excess of poly (ethylene glycol methyl ether) (PEG_OME)¹⁷ or amino functionalized polyethylene glycol (PEG) in DMF or THF respectively.²⁶ Consequently an attempt was made to react PMMA (Run 3, Table 6.4) with poly (ethylene glycol methyl ether) (PEG_OME: $M_{n,SEC} = 2,000$, PDI = 1.04) in refluxing DMF at 90 °C for 16 h and 48 h. After the reaction, the polymer was repeatedly washed with water to dissolve any unreacted PEG_OME. The reaction mixture was filtered and the product was dried in vacuo for 24 h. GPC showed the existence of unreacted PMMA and the appearance of new peak due to the formation of PEG_OME -*b*-PMMA (Fig. 6.11 and Fig. 6.12). The obtained polymer was analyzed by ¹H NMR spectroscopy (Fig. 6.13). Using the integral ratio of protons (H^b : $\delta = 3.58$ ppm) of the OCH₃ group of PMMA to the OCH₂ group of PEG_OME protons (H^a : $\delta = 3.73$ ppm). It was estimated that only ~ 13 % of the available anhydride group had reacted with the PEG_OME.

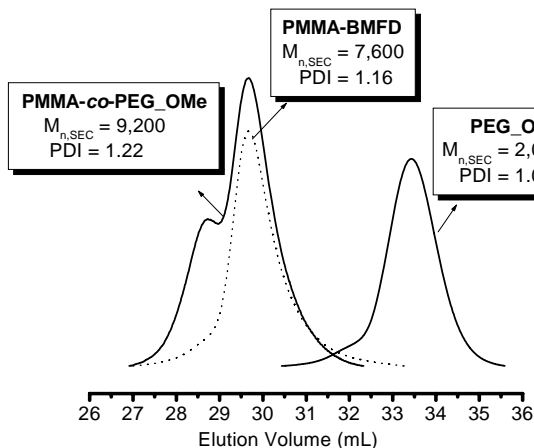


Fig. 6.11: GPC eluograms of the precursor PMMA, PEGM and PMMA-co-PEG_OMe after 48 h.

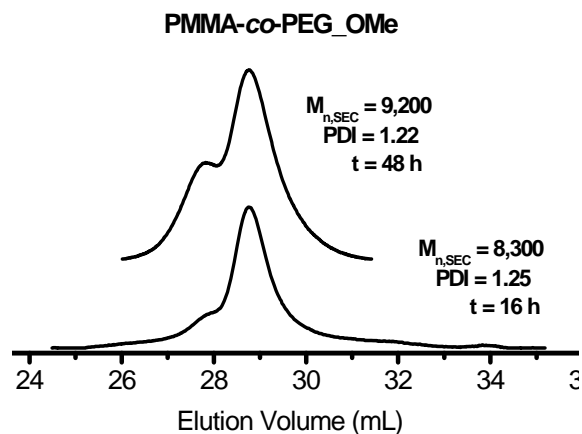


Fig. 6.12: GPC eluograms showing the formation of PMMA-co-PEG_OMe.

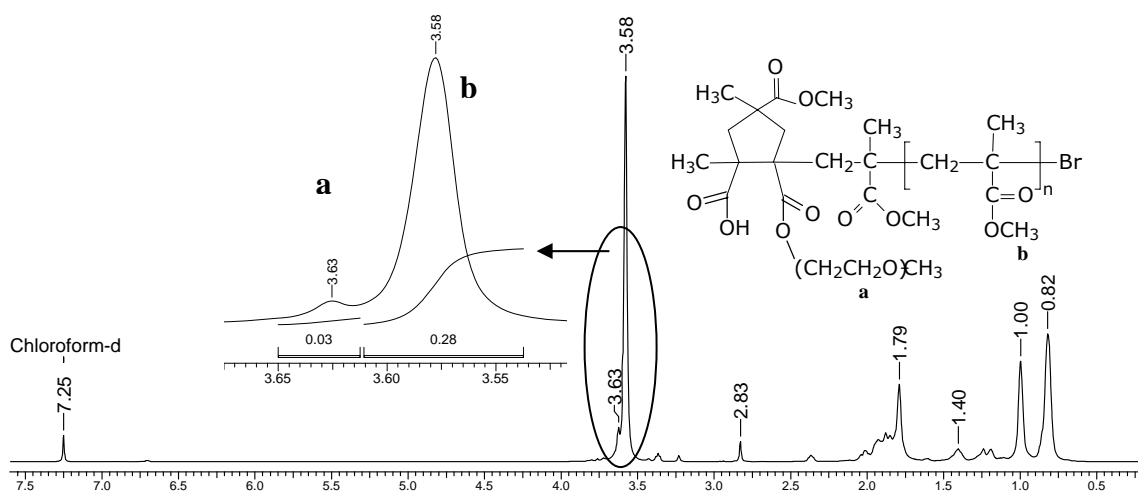


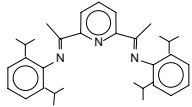
Fig. 6.13: ^1H NMR (500 MHz) of the PMMA-co-PEGM in CDCl_3

6.2.3. ATRP of MMA in toluene at 90 °C with BPIEP/CuBr as catalyst system, and BPN (3) as initiator

Batch ATRP of MMA in toluene at 90 °C was performed using CuBr as catalyst, EBiB as initiator and a tridentate ligand (BPIEP) as N-donor. The mole ratio of the components utilized in present study are $[\text{MMA}]: [\text{I}]: [\text{CuBr}]: [\text{BPIEP}] = 100: 1: 1: 2$. All the batch experiments (Table 6.5) using the tridentate ligand (BPIEP) were performed under nitrogen

atmosphere. The color of the complex changed from pale yellow to dark yellow after 1 h and finally reaching to dark red brown.

Table 6.5: Batch ATRP of MMA using BPN (**3**) as initiator ^{a)}

Run	Ligand	DP ^{b)}	Toluene (% _{v/v})	Conv ^{c)} (%)	M _{n,SEC}	PDI	I _{eff} ^{d)}
1		100	50	80	10,400	1.21	0.78
2		200	50	60	11,000	1.11	1.09
3		BPIEP	100	66	88	10,600	1.20

^{a)} [MMA] = 4.68 M, reaction performed for 5.5h, [MMA]: [BPN]: [CuBr]: [BPIEP] = 100: 1: 1: 2; ^{b)} DP = [M]/ [I₀]; ^{c)} gravimetric; ^{d)} I_{eff} = M_{n,Cal}/ M_{n,SEC}

The results obtained were reproducible except variation in the extent of polymer conversion. However, the better molecular weight control as well as high initiator efficiency was obtained in all the experiments. The PMMA molecular weights were little higher than predicted, indicating higher efficiency of the initiator system. The influence of concentration of solvent was very little as seen from the Table 6.5; therefore, a kinetic study was conducted at 90 °C in toluene (50 %, v/v) for further study.

6.2.3.1. Kinetic study of ATRP of MMA in toluene at 90 °C using BPIEP as ligand, CuBr as catalyst and BPN (**3**) as initiator

Kinetic study of ATRP of MMA in toluene at 90 °C was performed using BPIEP/ CuBr as catalyst system and EB*i*B as initiator. The mole ratios of various components utilized are [MMA]: [EB*i*B]: [CuBr]: [BPIEP] = 100: 1: 1: 2. The results are tabulated in Table 6.6.

Fig. 6.12 showed the first order kinetic plot for ATRP of MMA at 90 °C using BPIEP as ligand and **3** as initiator. The linear plot between ln{[M₀]/[M_t]} vs time indicates that the growing radical concentration is constant, indicating the absence of termination reaction. The apparent rate constant of polymerization, k_{app}, was found to be 9.7 x 10⁻⁵ s⁻¹ (Fig. 6.14). The rate of polymerization using **3** is faster compared to what is observed with EB*i*B/BPIEP system.

Table 6.6: Kinetic study of ATRP of MMA at 90 °C using BPN (3) ^{a)}

Run	Time (min)	Conv ^{b)} (%)	$M_{n,cal}$ ^{c)}	$M_{n,SEC}$	PDI
6.5	0	0	0	-	-
6.5.1	45	18	1,800	2,400	1.04
6.5.2	75	29	2,900	3,300	1.07
6.5.3	120	45	4,500	4,900	1.10
6.5.4	150	54	5,400	5,800	1.11
6.5.5	195	65	6,500	7,300	1.11
6.5.6	255	76	7,600	8,600	1.12
6.5.7	300	82	8,200	9,400	1.08
6.5.8	330	85	8,500	10,100	1.10

^{a)} [MMA] = 9.36 M; ^{b)} by GC; ^{c)} $M_{n,cal}$ = % conversion (grams of monomer / moles of initiator).

Fig. 6.15 shows the dependence of $M_{n,SEC}$ with conversion as well as polydispersity of the polymer. It is seen that the PMMA molecular weights increased linearly with conversion but were little higher than predicted. However, the polydispersity of the polymer was relatively narrow, i.e., ≤ 1.18 .

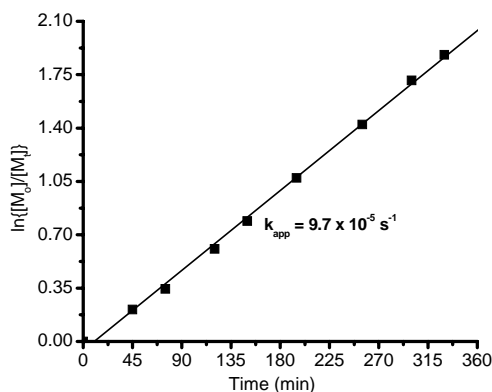


Fig. 6.14: Semi logarithmic kinetic plot for the ATRP of MMA in toluene at 90 °C using BPN as initiator. [MMA] = 4.68 M. [MMA]: [BPN]: [CuBr]: [BPIEP] = 100: 1: 1: 2

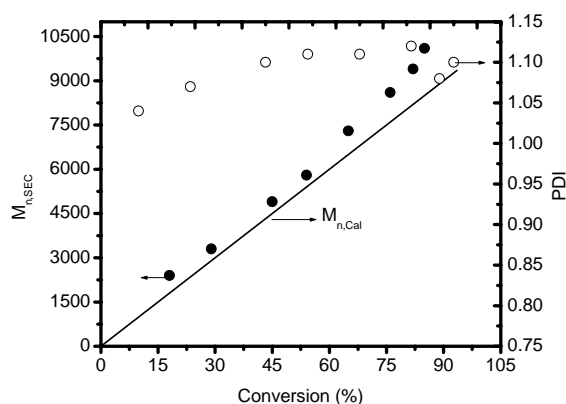


Fig. 6.15: Dependence of molecular weight and polydispersity on conversion in the solution ATRP of MMA at 90 °C with [BPN] = 0.0468 M. Open symbols represent polydispersities and filled symbol represents M_n -(GPC).

The plot between $\ln\{[M_o]/[M_t]\}$ vs time is linear. The rate of MMA polymerization using BPN (**3**) as initiator is higher as compared to EBiB.

Table 6.7: Comparison of apparent rate constant in ATRP of MMA ^{a)}

Run	Initiator	Solvent ^{b)} (%, v/v)	Conv ^{c)}	$M_{n,SEC}$ ($\times 10^3$)	PDI	I_{eff} ^{d)}	k_{app} ^{e)} ($\times 10^{-5}$), s^{-1}
1 ^{f)}	EBiB	66	55	10.2	1.23	0.60	3.40
2 ^{f)}	EBiB	bulk	90	12.8	1.28	0.70	10.96
3	1	50	76	9.5	1.26	0.80	7.15
4	3	50	88	10.1	1.10	0.84	9.70

^{a)} [MMA]: [I]: [CuBr]: [BPIEP] = 100: 1: 1: 2 at 90 °C for 5.5h; ^{b)} In toluene 50 (% v/v) with respect to monomer; ^{c)} from GC, ^{d)} $I_{eff} = M_{n,Cal} / M_{n,SEC}$, ^{e)} slope of $\ln\{[M_o]/[M_t]\}$ vs time plot, ^{f)} reference 15

6.3. Conclusions

Three different ATRP initiators (**1**, **2**, and **3**) were employed for controlled radical polymerization of MMA at 90 °C in toluene as solvent and BPIEP/CuBr as catalyst system. The reactions were well controlled with all the three initiators. The rate of polymerization followed first-order kinetics with all initiators indicating the presence of low radical concentration ($\leq 10^{-8}$) throughout the reaction. The apparent rate constant (k_{app}) and initiator efficiency (I_{eff}) decreased in the following order **3** > **1** > EBiB. Use of initiator **2** resulted in a polymer, which had an unusual end-group structure as determined by ¹H NMR and ¹³C NMR spectra. An unusual mechanism of initiation, involving an intramolecular radical ring closure reaction prior to propagation is proposed which results in a polymer with a cyclic anhydride group as the head group of the polymer.

6.4. References

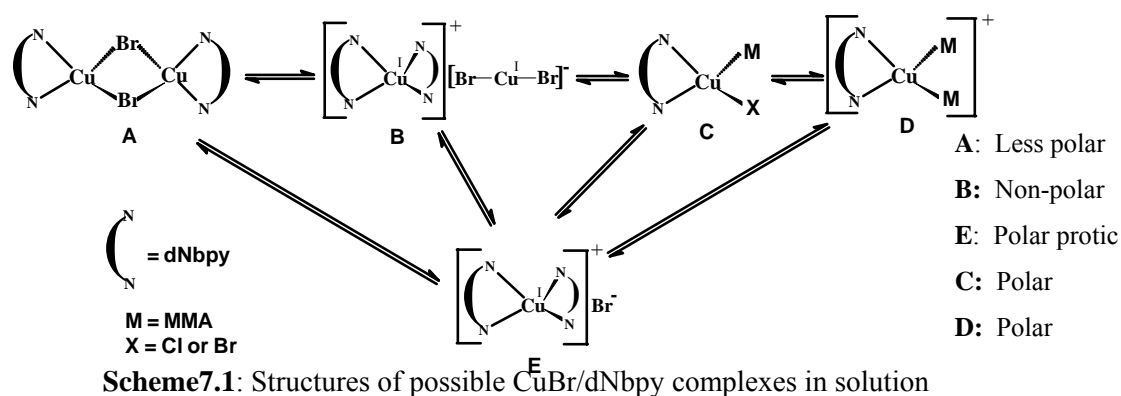
1. Matyjaszewski, K.; Xia, J. *Chem Rev.* **2001**, 101, 2921.
2. Patten, T. E.; Matyjaszewski, K. *Adv. Mater.* **1998**, 10, 901.
3. Matyjaszewski, K.; Gaynor, S. G. *ACS Symposium Series* Vol. 768. ACS, Washington, DC, **2000**, p. 396.

4. Gaynor, S. G.; Matyjaszewski, K. *ACS Symposium Series* Vol. 768. ACS, Washington, DC, **2000**, p. 347.
5. *Controlled Radical Polymerization*. Ed. Matyjaszewski, K., *ACS Symposium Series* Vol. 685. ACS, Washington, DC, **1998**.
6. Cossens, V.; Matyjaszewski, K. *J. Macromol. Sci., Pure Appl. Chem.* **1999**, A36, 811.
7. Cossens, V.; Pyun, J.; Miller, P. J.; Gaynor, S. G.; Matyjaszewski, K. *Macromol. Rapid Commun.* **2000**, 21, 103.
8. Beers, K. L.; Gaynor, S. G.; Matyjaszewski, K.; Sheiko, S. S.; Moller, M.; *Macromolecules* **1998**; 31, 9413.
9. Chowdhury S.; Patra, G. K.; Drew, M. G. B.; Chattopadhyay, N.; Datta, D. *J. Chem. Soc., Dalton Trans.*, **2000**, 235-237.
10. Chevallier, P.; Soutif, J.-C.; Brosse, J.-C. *Eur. Polym. J.* **1998**, 34, 767.
11. Mittal, A.; Sivaram, S. *J. Polym. Sci., Part A: Polym. Chem.* **2005**, 43, 4996.
12. Ando, T.; Kato, M.; Kamigaito, M.; Sawamoto, M. *Macromolecules* **1996**, 29, 1070.
13. Takahashi, H.; Ando, T.; Kamigaito, M.; Sawamoto, M. *Macromolecules* **1999**, 32, 3820.
14. Uegaki, H.; Kamigaito, M.; Sawamoto, M. *J. Polym. Sci., Part A: Polym. Chem.* **1999**, 37, 3003.
15. Matyjaszewski, K.; Wang, J.-L.; Grimaud, T.; Shipp, D. A. *Macromolecules* **1998**, 31, 1527.
16. Malz, H.; Komber, H.; Voigt, D.; Hopfe, I.; Pionteck, J. *Macromol. Chem. Phys.* **1999**, 200, 642.
17. Koulouri, E. G.; Kallitsis, J. K.; Hadziioannou, G. *Macromolecules* **1999**, 32, 6242.
18. Moon, B.; Hoyer, T. R.; Macosko, C. W. *Macromolecules* **2001**, 34, 7941.
19. Fields, E. K.; Winzenburg, M. L. *US 4526986 A*, **1985**, 5 p.
20. Deshpande, A. M.; Natu, A. A.; Argade, N. P. *Heterocycles* **1999**, 51, 2159.
21. Cushman, M.; Gentry, J.; Dekow, F. W. *J. Org. Chem.* **1977**, 42, 1111.
22. Cooke, E. P.; Walsh, O. M.; Meegan, M. J. *J. Chem. Res. (M)* **1994**, 2724.
23. Bednarek, M.; Biedron, T. Kubisa, P. *Macromol. Chem. Phys.* **2000**, 201, 58.
24. Cossens, V.; Matyjaszewski, K. *Macromol. Rapid Commun.* **1999**, 20, 66.
25. Singha, N. K.; Klumperman, B. *Macromol. Rapid Commun.* **2000**, 21, 1116.
26. Cernohous, J. J.; Macosko, C. W.; Hoyer, T. R. *Macromolecules* **1997**, 30, 5213.

Chapter 7. Atom transfer radical polymerization of methyl methacrylate using different N-donors as ligands, $\text{Cu}^{\text{I}}\text{X}$ ($\text{X} = \text{Br}, \text{Cl}, \text{SCN}$) as catalyst and ethyl-2-methyl-2-thiocyanatopropanoate as initiator

7.1. Introduction

In ATRP, copper(I) salts other than bromides and chlorides have also been employed as catalysts coupled with nitrogen based ligands. These salts seem to accelerate polymerization due to the formation of unbridged monomeric and highly active Cu^{I} species, whereas copper (I) halides generally form bridged dimeric complexes in organic solution. UV-Vis studies of Cu^{I} and Cu^{II} species suggest that the species in polymerization solution are more complex. Ligands on both the oxidation states are labile in solution and $^1\text{H-NMR}$ studies indicate that there is fast exchange with the free ligand in solution on the Cu^{I} coordinated by bipyridine. The absorption study on the complicated structures of CuBr complexes reveals the big differences in the values of molar absorption coefficient (ϵ) in solvents of different polarities.¹ Structure of CuBr/dNbpy complexes in polar H-bonding solvents as well as in non-polar solvent has been described in literature (Scheme 7.1).²



Most of the metal complexes in literature involve the use of counter anions like PF_6^- ,³ OTf^- ,⁴ OAc^- ,⁵ BF_4^- ,⁶ and SCN^- .^{7,8} Such anions are believed to stabilize the complex. However, in most of the above cases, polymers with broad polydispersity is obtained because the rate of

polymerization is faster than the rate of generation of the dormant species ($k_{\text{deact}} \lll k_a$), as well as irreversible termination via transfer of halogens from a polymer terminal to the complex. Copper(I) triflate [$\text{Cu}(\text{OTf})$, $\text{Tf} = \text{CF}_3\text{SO}_2$], generated *insitu* from $\text{Cu}(\text{OTf})_2$ and $\text{Cu}(0)$, induced fast polymerization of MA and styrene using PMDETA as ligand. A much faster polymerization of MA was attained with $\text{CuPF}_6/\text{dnNbpy}$ where the apparent polymerization rate constant is 40 times greater than that with CuBr , to give controlled molecular weight but broader MWDs ($M_w/M_n = 1.4-1.6$).³ Also, in ATRP the proportion of relatively less soluble Cu^{II} species increases with the increase in $[\text{Cu}^{\text{I}}]$ and $[\text{R-X}]$ thereby making reaction more heterogeneous and uncontrolled.² Thus, the concentration of $[\text{Cu}^{\text{II}}]$ species should be optimum such that $k_t (\text{P}\cdot)^2 \lll k_{\text{deact}} [\text{P}\cdot] [\text{Cu}^{\text{II}}]$. One approach to render Cu^{I} salts more soluble in hydrocarbon solvents is to use soft anions such as thiocyanates.⁹

Davis *et al.* reported the use of thiocyanate initiator for the polymerization of styrene and more recently methyl acrylate.³ Polymerization of styrene resulted in slow initiation and broader MWD (3.0) when benzyl thiocyanate was used as an initiator. Singha and Klumperman⁷ polymerized MMA using different ligands complexed with CuSCN and using EBiB and TsCl as initiators. The results were explained based on transfer of SCN group and an *insitu* exchange to form CuCl *insitu*, thereby, giving higher rates of polymerization and a broader polydispersity (1.6) of the polymer. The reason for higher MWD was attributed to the higher bond strength of C-SCN than C-Cl . Therefore, slower activation and higher deactivation was observed. However, neither a symmetrical system ($\text{R-SCN}/\text{CuSCN}$) nor a system that contained a non-exchangeable anion on the $\text{Cu}(\text{I})$ species (i.e., CuPF_6) was used to prove whether the polymerization was controlled in the absence of the halogen. Since the bond strength of C-X bond in initiator varies as $\text{R-Cl} > \text{R-Br} > \text{R-I}$,¹⁰ therefore, most frequently used initiators contain halogens, namely, chlorine and bromine. Recently, Davis and Matyjaszewski stated that thiocyanate group alone cannot control the polymerization of styrene or methyl acrylate effectively, instead a halogen is needed to impart better control and, in its absence the reaction rates are very slow with very poor initiator efficiency.¹¹

The present study examines a novel soft pseudo halogen (SCN^-) as head group in the initiator (R-SCN) as well as for catalyst ($\text{Cu}^{\text{I}}\text{-SCN}$) in copper catalyzed ATRP of MMA. The

chemistry of using thiocyanate both as counter ion for copper salt, CuSCN, and initiator, R-SCN, was based on the fact that CuSCN forms stable complexes with bidentate/ tridentate ligands.^{9,12,13} Therefore, ethyl-2-methyl-2-thiocyanatopropanoate (EMTP) was synthesized and used as an initiator along with CuSCN as catalyst for ATRP of MMA.

7.2. Results and discussion

7.2.1. Effect of nature of counterion

The softer ion SCN⁻ is a stronger field ligand than Cl⁻ or Br⁻. The electronic configuration of the two ions is Cu⁺ [3d¹⁰] & Cu²⁺ [3d⁹]. The former gives distorted tetrahedral complexes whereas the latter gives trigonal bipyramid structure. (CFSE = 0 for d¹⁰ configuration whether octahedral or tetrahedral). Hard Soft Acid Base principle classifies copper (I) cation as a soft Lewis acid. Therefore, coordination of copper to sulfur of the thiocyanate anion is favored.¹⁴ Also, the bond energy data for C-X bond available in literature^{15,16} for benzylic species are,

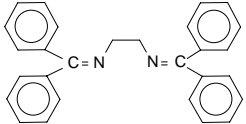
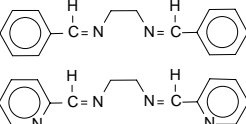
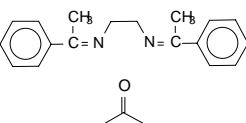
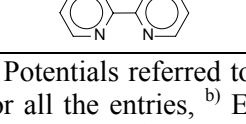
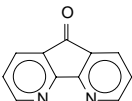
- Cu^{II}—Br = 293.7; Cu^{II}—Cl = 330.1 KJ/mol
- Cu^I—Br = 259 ; Cu^I—Cl = 360.7 ; Cu-S = 285 ± 17 KJ/mol.
- C₆H₅CH₂—X (Cl = 284.2; Br = 229.9; I = 167.2; CN = 418; CH₃ = 305.1; NH₂ = 300.9; H = 355.3 KJ/mol).

Based on available data in the literature the value of C-SCN bond energy was estimated to be 250.8 KJ/ mol, which lies in between that of chloride and bromide. Thus, it is of interest to explore the use of thiocyanate counterion for ATRP of MMA.

7.2.2. Cyclic Voltammetry studies of the Cu^I thiocyanate complexes in acetonitrile at room temperature

For a series of nitrogen-based ligands the Cu-based ATRP of methyl acrylate, a qualitative linear correlation between the polymerization rate and the redox potential of the complex in acetonitrile was found because of nearly similar bond strength of metal halogen bond.¹⁷ Therefore, electrochemical studies of CuSCN complexes were performed in acetonitrile to study their redox potentials (E_{1/2}) to enable a qualitative comparison with solution equilibrium dynamics of ATRP. Complexes were synthesized in acetonitrile under positive pressure of nitrogen.

Table 7.1: Redox potentials of Cu^ISCN- bidentate imine complexes in acetonitrile at 27 °C ^{a)}

Structure	Ligand	CuSCN			
		E _{p,c} ^{b)} /V	E _{p,a} ^{b)} /V	ΔE _p ^{c)} / (mV)	E _{1/2} ^{d)} /V
	NDBED	-0.410	-0.120	290	-0.260
	NBED	-0.350	-0.110	240	-0.230
	NPMED	-0.440	+0.050	390	-0.195
	NPEED	-0.440	+0.090	350	-0.175
	DAFONE	+0.130	+0.270	140	0.200

^{a)} Potentials referred to SCE electrode at a scan rate of 0.5 V s⁻¹. The ratio of salt /ligand is 1/2 for all the entries, ^{b)} E_{p,c} and E_{p,a} are the peak potentials of the reduction and oxidation waves, respectively, ^{c)} ΔE_p is the difference in mV between cathodic and anodic peak, ^{d)} E_{1/2} = 1/2 (E_{p,c} + E_{p,a})

The half-wave potential (E_{1/2}, V) provides information about the reducing ability of catalyst. Greater the E_{1/2} value (positive) poorer is the reducing ability of the catalyst and, hence, lower the catalyst activity. Peak-peak separation (ΔE_p, mV) indicates the extent of equilibrium between two oxidation states of the copper catalyst. Larger the ΔE_p value, higher is the life of the intermediate Cu(II) oxidation state and, consequently, higher is the activity for the catalyst. In general, E_{1/2} values of Cu^IBr complexes reported in literature are all negative (dNbpy:-0.05 V; dnNbpy:-0.06 V) except 2,2'-bipyridine which is +0.035 V.¹⁸ Therefore, negative E_{1/2} values are desirable for effective catalysis in case of substituted bipyridine ligands.

Table 7.1 corresponds to the one electron redox couple that is quasi-reversible in nature (ΔE > 60 mV) and the values of redox potentials of the CuSCN with α-unconjugated diimine complexes are negative, i.e., all the complexes can act as better reducing agents (easily oxidized) on the applied potential scale. The values obtained strictly depend upon the structures of the ligands. The more negative the value of redox potential easier it will be to oxidize that complex. The E_{1/2} value of a successful ligand (Me₆TREN) employed in ATRP

is -0.3 V, whereas the $E_{1/2}$ value of another well-studied system (NPPI) is 0.48 V. Matyjaszewski and coworkers proposed that metal complexes with redox potentials in the range between -0.3 V and +0.6 V (versus NHE) might prove to be useful ATRP catalysts for the polymerization of styrene and (meth)acrylates.¹⁸ Since the $E_{1/2}$ values of copper(I) thiocyanate complexes for the ligands NBED, NDBED, NPMED and NPEED are all negative and fall in the range. Therefore, they may be expected to show catalytic activity for ATRP of MMA.

7.2.3. ATRP of styrene in diphenylether using *dn*Nbpy as ligand, Cu^IX (X = Br, SCN) as catalyst and different initiation systems (R-SCN).

Polymerization of styrene was performed as described in Chapter 2. The mole ratios of various components of ATRP are [styrene]: [BzSCN]: [CuSCN]: [*dn*Nbpy] = 104: 1: 1: 2. The initiators employed in the study were benzyl bromide (BzBr), benzyl thiocyanate (BzSCN), and 1-PEBr (1-phenylethyl bromide) and *dn*Nbpy (4,4'-(*n*-nonyl)-2,2'-bipyridine) as ligand and CuX (X= SCN, Br, and Cl) as catalysts. For DP = 104, the amount taken was 5 mL monomer, 0.8404 mmol of *dn*Nbpy, 51 mg of CuSCN, 62.7 mg BzSCN and 10 mL of diphenylether. It is known that ATRP of styrene is heterogeneous in nature. An attempt was made to make it homogeneous by adding small (10-20 %, v/v) quantity of a slightly polar solvent such as chlorobenzene.

A known amount of an initiator, such as, BzSCN was dissolved in degassed DPE and stored over nitrogen in an ampoule. Similarly, the stock solution were prepared for ligands (DMDP: 4,4'-dimethyl-2, 2'-dipyridyl, *dn*Nbpy: 4,4'-(*n*-nonyl)-2,2'-bipyridine)) and other initiators employed in the study. The color of the reaction mixture changed from dark brown to leafy green and finally turning to greenish brown. Table 7.2 represents the results of polymerization of styrene. Run numbers 1 and 2, 7 and 8, and 5 represent the same terminal end of the catalyst and the initiator, whereas, run numbers 3, 4, and 9 represent different terminal ends of the initiator and the catalyst.

Table 7.2: ATRP of Styrene using Cu^IX (X = Br, SCN)/*dn*Nbpy as catalyst system ^{a)}

Run	C: L ^{a)}	C & I ^{a)}	Conv ^{b)} (%)	M _{n,cal} ^{c)}	M _{n,SEC}	PDI
1 ^{d)}	1: 0.5	CuBr/BzBr	21	2,200	2,300	1.31
2	1: 2	CuBr/BzBr	44	4,760	5,600	1.13
3	1: 0.5	CuBr/BzSCN	NP	-	-	-
4	1: 2	CuBr/BzSCN	< 3	312	7,000	1.69
5	1: 2	CuBr/1-PEBr	46	4,975	3,570	1.12
6 ^{e)}	1: 2	CuPF ₆ /BzSCN	75	31,200	52,000	3.20
7	1: 2	CuSCN/BzSCN	NP	-	-	-
8	1: 1.3	CuSCN/BzSCN	< 5	520	16,656	2.15
9	1: 2	CuSCN/BzBr	26	2,800	4,648	1.29

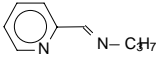
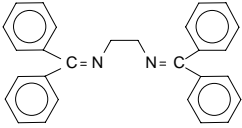
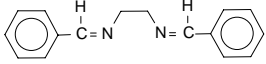
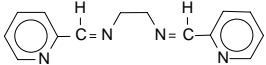
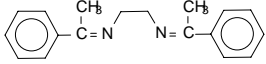
^{a)} [Styrene] = 2.92M; C: catalyst; L: ligand; I: initiator; [M]: [C]: [I] = 104: 1: 1; at 110 °C in DPE (66 %, v/v) wrt monomer, reaction time = 7h; ^{b)} gravimetrically, ^{c)} M_{n,cal} = % conversion (grams of monomer / moles of initiator), ^{d)} [CuBr]: [Ligand]: [benzyl bromide]: [Sty] = 1: 0.5: 1: 100 and Ligand = 4,4'-dimethyl-2, 2'-dipyridyl (DMDP), ^{e)} experimental results from reference 3.

Cu^IBr/ benzyl bromide and Cu^IBr/1-phenylethyl bromide systems gave controlled polymerization at a catalyst: ligand ratio of 1: 2, the ligand being 4,4'-(*n*-nonyl)-2,2'-bipyridine (Table 7.2, entry 2 and 5). However, when Cu^IBr was replaced by Cu^ISCN, loss of control in polymerization was evident (entry 9, Table 7.2). When benzyl bromide was replaced by benzyl thiocyanate, there was little or no polymerization (entry 3 and 4, Table 7.2) with poor control. When the system Cu^ISCN/ benzyl thiocyanate was used, the polymerization was uncontrolled. The results can be explained on the basis that radical generation from benzyl thiocyanate is too slow (because of larger C-SCN bond energy compared to C-Br) and, hence, causing ineffective initiation.

7.2.4. ATRP of MMA in toluene using unconjugated α -diimines, and NPPI as ligands, Cu^ISCN as catalyst and ethyl-2-methyl-2-thiocyanatopropanoate (EMTP) as initiator

ATRP of MMA was performed using mole ratios of various components as [MMA]: [EMTP]: [CuSCN]: [Ligand] = 100: 1: 1: 2. For DP = 100, the amount taken was 10 mL (93.5 mmol) monomer, 114 mg (0.935 mmol) of CuSCN, 20 mL of toluene under positive nitrogen pressure followed by two equivalents (0.935 mmol) of ligands (a) NDBED (726 mg); (b) NBED (441mg); (c) NPMED (222 mg); (d) NPEED (494 mg); (e) NPPI (0.14 mL) followed by 0.16 mL (0.935 mmol) of EMTP as initiator.

Table 7.3: ATRP of MMA using EMTP as initiator and CuSCN as catalyst and different ligands ^{a)}

Run	Structure	Ligand	Conv ^{b)} (%)	M _{n,cal} ^{c)}	M _{n,SEC}	PDI
1		NPPI	27	3,200	1,66,000	1.81
2			27	2,700	1,29,500	2.23
3			27	2,700	1,31,500	2.11
4		NDBED	NP	-	-	-
5		NBED	9	900	4,00,000	1.96
6		NPMED ^{d)}	13	1,300	3,95,000	1.88
7		NPEED	13	1,300	49,700	1.69

^{a)} [MMA] = 2.92M; [M]: [CuSCN]: [L]: [EMTP] = 100: 1: 2: 1; at 90 °C in toluene (66 %, v/v) wrt monomer; reaction time = 4 h, ^{b)} gravimetrically, ^{c)} M_{n,cal} = % conversion (grams of monomer / moles of initiator), ^{d)} NPMED (tetradentate ligand), [C]: [L] = 1: 1.

The results are shown in Table 7.3 (where C: L = 1: 2). No polymer is obtained when ligand used was NDBED (run number 4) whereas using other imine ligands highly uncontrolled polymerization ensued. The values of M_{n,SEC} is much higher than the targeted molecular weights. Apparently, the reaction proceeded via a conventional free radical mechanism. The GPC eluograms for all the reactions showed a high/ low molecular weight humps with broad

peaks that indicate the early termination of the initiator species via primary radical coupling reactions. The initiator efficiencies were very low indicating that the thiocyanate initiator is a poor source of initiating radicals. The color of the complexes formed with different concentration of catalyst to ligands is shown in Table 7.4.

Table 7.4: Color of the CuSCN Complex

Ligand/ CuSCN	[C]: [L] = 1: 1	[C]: [L] = 1: 2
NDBED	Milky white	Dark yellow/orange
NBED	Pale yellow	Pale yellow
NPMED	Reddish-Brown	Brown
NPEED	Dark yellow	Yellow

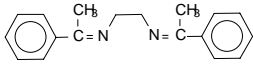
The results indicate that EMTP, once activated to form a tertiary radical, can initiate radical polymerization. However, the initiation efficiency is found to be very low. The lack of control in these systems can be attributed to either a low rate of activation of the initiator or inefficient deactivation by the $\text{Cu}(\text{SCN})_2$ species formed. However, if the binding of the thiocyanate group to the carbon occurs through the nitrogen instead of the sulfur, an inactive chain end will result.¹⁹ This may decrease the initiator efficiency as well. To test the effectiveness of the formed $\text{Cu}(\text{SCN})_2$ as a deactivator, unsymmetrical initiator/catalyst combinations were explored for the ATRP of MMA.

7.2.5. ATRP of MMA in toluene using NPEED as ligand, Cu^{X} (X = Br, Cl, SCN) and EB*i*B as initiator

The effect of copper salt on ATRP of MMA at 90 °C in toluene using unconjugated α -diimines as ligands was examined. ATRP of MMA at 90 °C was studied using NPEED as the ligand with copper halides (CuX , X = Br, Cl, and SCN) as catalysts and EB*i*B as initiator. It was found that all the polymerizations except with CuCl were heterogeneous in nature. However, unlike CuBr systems there was no change in the color when CuSCN or CuCl were used. The initiator efficiencies were better than that obtained in the case of R-SCN/ CuSCN (Table 7.5). The molecular weights obtained using GPC were almost double

than expected from them. This could be attributed to the occurrence of termination by coupling reactions.

Table 7.5: ATRP of MMA using NPEED as ligand, EBiB as initiator and various catalysts^{a)}

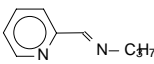
Run	CuX	Ligand	Conv ^{b)} (%)	M _{n,cal} ^{c)}	M _{n,SEC}	PDI
1	CuBr	 NPEED	51	5,100	16,600	1.76
2	CuSCN		83	8,300	19,500	1.82
3	CuCl		95	9,500	18,000	1.83

^{a)} [MMA] = 3.12 M; [M]: [C]: [NPEED]: [EBiB] = 100: 1: 2: 1; at 90 °C in toluene (66 %, v/v) wrt monomer; reaction time = 4 h, ^{b)} gravimetrically, ^{c)} M_{n,cal} = % conversion (grams of monomer / moles of initiator).

7.2.6. ATRP of MMA in toluene using NPPI as ligands, Cu^IX (X = Br, Cl, SCN) as catalyst and EMTP as initiator

The effect of copper salt on ATRP of MMA at 90 °C in toluene using unconjugated α -diimines as ligands was examined. A well-known Schiff base ligand, namely, N-(*n*-propyl)pyridylmethanimine (NPPI) was complexed with different copper halides (CuX, X = Br, Cl, and SCN) and used for the ATRP of MMA at 90 °C using EMTP as initiator. The effect of the nature of copper salt was studied (Table 7.6). The results indicate that EMTP is a poor source of initiating radicals. This is presumably in view of the stronger C-SCN bond relative to C-Br and C-Cl bonds.

Table 7.6: ATRP of MMA using NPPI as ligand, EMTP as initiator and various copper salts^{a)}

Run	CuX	Ligand	Conv ^{b)} (%)	M _{n,cal} ^{c)}	M _{n,SEC}	PDI
1	CuSCN	 NPPI	32	3,200	1,67,000	1.81
2	CuBr		34	3,400	1,03,600	1.40
3	CuCl		26	2,600	72,900	1.39

^{a)} [MMA] = 3.12 M; [M]: [C]: [NPPI]: [EMTP] = 100: 1: 2: 1; at 90 °C in toluene (66 %, v/v) wrt monomer; reaction time = 4 h, ^{b)} gravimetrically, ^{c)} M_{n,cal} = % conversion (grams of monomer / moles of initiator).

7.3. Conclusions

The salient conclusions from this study are as follows:

- † The redox potentials of copper (I) thiocyanate complexes with unconjugated α -diimines used in the present study were quasi-reversible ($\Delta E_p > 60$ mV) in the range of -0.3 V to +0.6 V. The observed negative $E_{1/2}$ values implied that these complexes might serve as useful catalysts for ATRP.
- † Uncontrolled polymerization of methyl methacrylate was observed with CuSCN/EMTP couple. The reason could be either a low rate of activation of the initiator or inefficient deactivation by the $\text{Cu}(\text{SCN})_2$ species during atom transfer step.
- † Styrene polymerization using CuSCN/BzSCN couple resulted in negligible activity. This could be due to the slow rate of radical generation by the initiator because of higher bond strength of C-SCN compared to copper (I) bromide.

Thus, it is concluded that thiocyanate group alone cannot control the polymerization of styrene, methylmethacrylate or methyl acrylate effectively. A halogen (non-exchangeable anion) is essential needed to impart better control on polymerization.

7.4. References

1. Qui, J.; Pintauer, T.; Gaynor, S.; Matyjaszewski, K. *Polym. Prepr. (Am. Chem. Soc., Div. Polym. Chem.)* **1999**, 40, 420.
2. Wang, J.-L.; Grimaud, T.; Matyjaszewski, K. *Macromolecules*, **1997**, 30, 6507.
3. Davis, K.; Paik, H. -J.; Matyjaszewski, K. *Macromolecules* **1999**, 32, 1767.
4. Woodworth, B. E.; Metzner, Z.; Matyjaszewski, K. *Macromolecules* **1998**, 31, 7999.
5. Matyjaszewski, K.; Wei, M.; Xia, J.; Gaynor, S. G. *Macromol. Chem. Phys.* **1998**, 199, 2289.
6. Haddleton, D. M.; Duncalf, D. J.; Kukulj, D.; Crossman, M. C.; Jakson, S. G.; Bon, S. A. F.; Clark, A. J.; Shooter, A. J. *Eur. J. Inorg. Chem.* **1998**, 1799.
7. Singha, N. K.; Klumperman, B. *Macromol. Rapid Commun.* **2000**, 21, 1116.
8. Davis, K.; O' Malley, J.; Paik, H.-J.; Matyjaszewski, K. *Polym. Prepr. (Am. Chem. Soc., Div. Polym. Chem.)* **1997**, 38 (1), 687.
9. Healy, P. C.; Pakawatchai, C.; Papisergio, R. I.; Patrick, V. A.; White, A. H. *Inorg. Chem.* **1984**, 23, 3769.
10. Matyjaszewski, K.; Shipp, D. A.; Wang, J.-L.; Grimaud, T.; Patten, T. E. *Macromolecules* **1998**, 31, 6836.
11. Davis, K.; Matyjaszewski, K. *J. Macromol. Sci. Part A: Pure and Appl. Chem.* **2005**, A41, 449.

12. Kickelbick, G.; Amirasr, M.; Khalaji, A. D.; Dehghanpour, S. *Aust. J. Chem.* **2003**, 56, 323.
13. You, Z. L. *Acta Cryst: Crystal Structure Communications* **2005**, C61, m406.
14. Braithwaite, A. C.; Rickard, C. E. F.; Waters, T. N. *Inorg. Chim. Acta* **1978**, 26, 63.
15. CRC Handbook of Chemistry and Physics. Ed. David R. Lide, 4th Edition, CRC Press, Vol 58, 1977/1978.
16. Huheey, J. E.; Keiter, E. A.; Keiter, R. L. " *Inorganic Chemistry: Principles of Structure and Reactivity*" Benjamin Cummings Publishing company, Inc. 4th Ed, 1997.
17. Matyjaszewski, K.; Göbelt, B.; Paik, H. J.; Horwitz, C. P. *Macromolecules* **2001**, 34, 430.
18. Qui, J.; Matyjaszewski, K.; Thouin, L.; Amatore, C. *Macromol Chem. Phys.* **2000**, 201, 1625.
19. Jenkins, C. L.; Kochi, J. K. I. *J. Org. Chem.* **1971**, 36, 3095.

Chapter 8. Atom transfer radical polymerization of methyl vinyl ketone

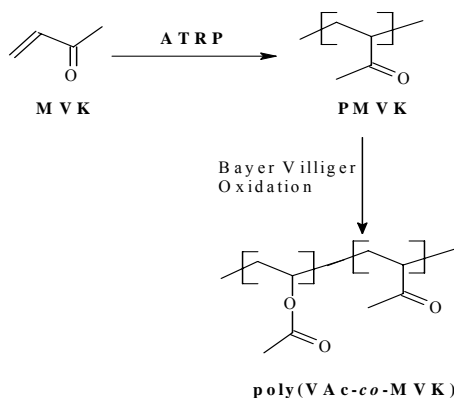
8.1. Introduction

Atom transfer radical polymerization (ATRP) has recently become one of the most rapidly developing areas of polymer science.¹ Matyjaszewski² and Sawamoto³ have used transition metal mediated atom transfer radical addition (ATRA) or Kharasch addition^{4,5} of alkyl halide with vinyl monomers and developed controlled radical polymerization of various alkyl(meth) acrylates and styrene. The technique rests in the transition metal catalyzed reversible cleavage of the carbon-halogen bond of an initiator or a dormant polymer chain-end leading to the formation of carbon centered radical through a redox process.⁶ Copper catalyzed ATRP is one of the robust techniques that provide tailor-made vinyl polymers through radical polymerization. Although, a wide range of monomers have been used in copper mediated ATRP,⁷ monomers such as vinyl acetate (VAc) and vinyl ketones are difficult to polymerize in a controlled manner.^{8,9}

Unlike methyl methacrylate (MMA) and styrene, VAc lacks conjugation and thus, its radicals are highly reactive, less stable and more prone to termination and transfer. The difficulty encountered in ATRP of VAc is also attributed to a low equilibrium constant (K_{eq}).¹⁰ Several attempts to polymerize VAc in a controlled manner by nitroxyl and copper mediated radical polymerizations have failed to provide adequate control of polymerization.¹¹⁻¹³ The cleavage of the carbon-halogen bond in the case of VAc is difficult. Therefore several side reactions, such as, decomposition of dormant species or the oxidation of the growing radicals by outer sphere electron transfer process to generate the corresponding carbocations are possible.

One of the strategies to synthesize a well-defined polyvinyl acetate (PVAc) is through post polymer analogous oxidation of poly(methyl vinyl ketone) (PMVK) (Scheme 8.1). This methodology can also be used to synthesize controlled molecular weight poly(vinyl alcohol) (PVA) by hydrolyzing PVAc.¹⁴ Therefore, synthesis of controlled molecular weight PVAc

from PMVK is of significant interest. Methyl vinyl ketone (MVK) has been polymerized using free radical,^{15,16} and ionic^{17,18} mechanisms in a stereo regulated addition.^{19,20} However, controlled polymerization of MVK has not been reported as yet. We, therefore, attempted to polymerize methyl vinyl ketone (MVK) using copper mediated ATRP.



Scheme 8.1. Synthesis of poly (vinyl acetate) copolymers with controlled molecular weight using post-polymer analogous reactions of poly (methyl vinyl ketone)

This chapter describes the issues associated with the polymerization of MVK under ATRP conditions and provides the evidence for the existence of coordination of MVK with copper halide using NMR, FT-IR, and UV-vis spectroscopy. The formation of copolymers of MVK and MMA using reverse ATRP is also discussed.

8.2. Results and discussions

8.2.1. Free radical polymerization of MVK using AIBN

The synthesis of PVAc and its copolymer through a post modification of PMVK using Baeyer Villiger oxidation and subsequent hydrolysis was attempted (Scheme 8.1). In order to validate the proposed strategy, MVK was polymerized using AIBN as initiator. After 4 h of the reaction, the polymer was precipitated in excess water and a colorless sticky poly (methyl vinyl ketone) (PMVK) was obtained in 60 % yield. The molecular weight of PMVK determined with respect to the PMMA standards is $M_{n,SEC} = 17,500$ g/mol with a broad molecular weight distribution ($M_w/M_n = 2.77$) (Fig. 8.1 a). The dried polymer was subjected to Baeyer Villiger oxidation²¹ using *m*-chloroperbenzoic acid in dichloroform at room

temperature for 10 days. This resulted in a partial oxidation and the formation of copolymer of poly (VAc-co-MVK) in 85:15 mole % as confirmed by ^{13}C -NMR spectrum (Fig. 8.1 b).

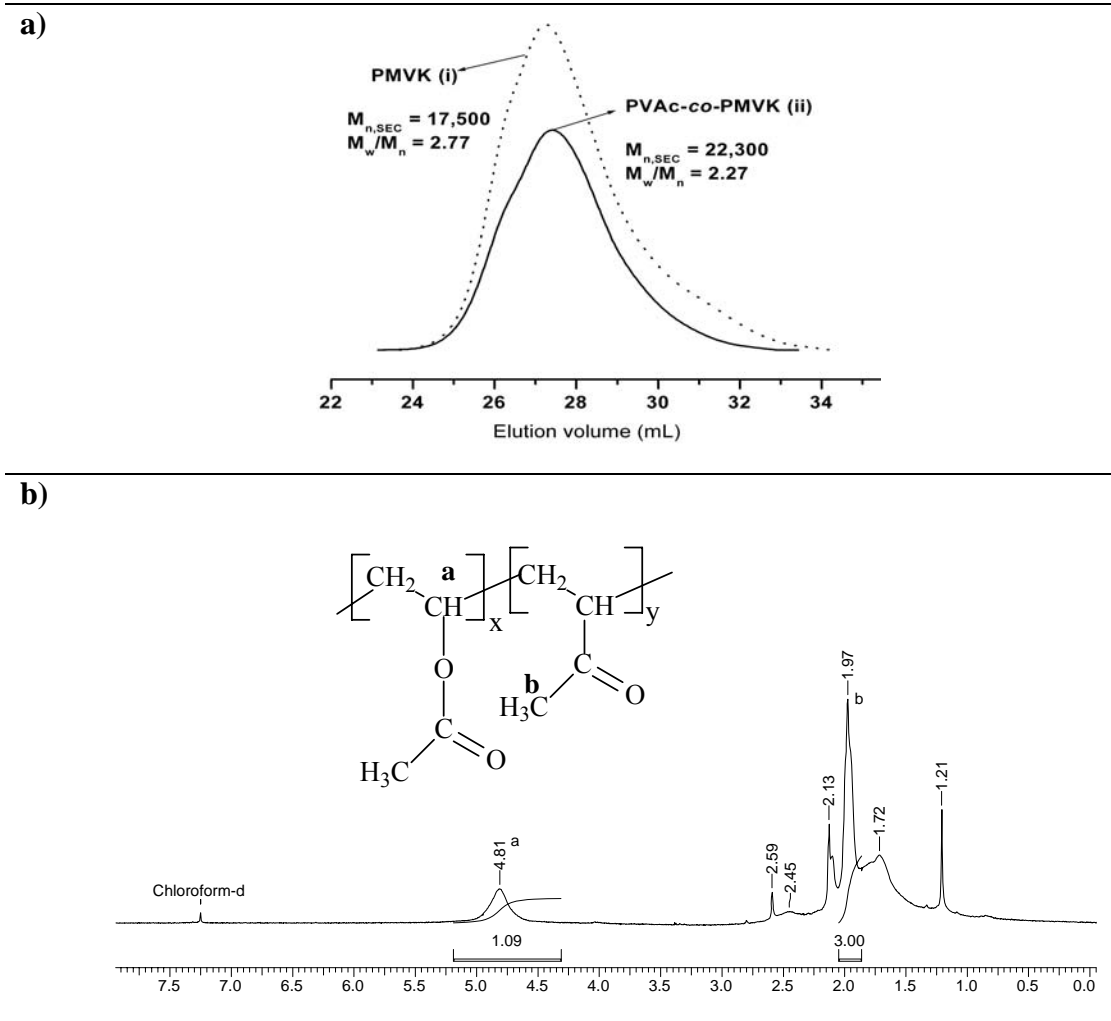


Fig. 8.1: Copolymer of poly (VAc-co-MVK) (a) SEC eluogram (i) before oxidation and (ii) after oxidation of PMVK and (b) ^1H NMR spectrum in CDCl_3

The ^1H and ^{13}C NMR of the copolymer of poly (VAc-co-MVK) show the presence of corresponding methine and carbonyl units of vinyl acetate and vinyl ketones. The apparent relative molecular weight of the copolymer was $M_{n,SEC} = 22,300$, $M_w/M_n = 2.27$ (Fig. 8.1 a). The results confirm that it is possible to synthesize PVAc copolymers from MVK using free radical polymerization and post-polymer analogous reactions.

8.2.2. Polymerization of MVK using ATRP and reverse ATRP

We, then, proceeded to study the polymerization of methyl vinyl ketone (MVK) via copper mediated ATRP using various initiator/CuX/ligand/solvent systems (Table 8.1). Ligands, such as, N,N,N',N',N''-pentamethyldiethylenetriamine (PMDETA), N-(*n*-propyl)-2-pyridyl methanimine (NPPI), 2,6-*bis*[1-(2,6-diisopropyl phenylimino)ethyl]pyridine (BPIEP), 4,4'-di(*n*-nonyl)2,2'-bipyridine (*dn*Nbpy), and 2,2'-bipyridine (bpy) were used in the presence of CuX (X = Cl or Br) with [MVK]: [I]: [CuX]: [Ligand] = 127: 1: 1: 2. Experiments were conducted in different solvents such as diphenyl ether, THF, anisole and also in bulk at 90 °C for several hours (3-24 h).

Table 8.1. Unsuccessful polymerization of methyl vinyl ketone using copper mediated ATRP and reverse ATRP processes

Run	I/C ^{a)}	L/S ^{b)}	T(°C)/ t (h)	Monomer		Yield ^{c)} (%)	M _{n,SEC}	PDI
				M ₁	M ₂			
1	AIBN ^{d)}	EtOH-bulk	70/4	MVK	-	30	38,623	1.66
2	EBiB/ CuX ^{e)}	NPPI/ Tol	90/8	MVK	-	NP ^{m)}	-	-
3		bpy/ Tol	90/6	MVK	-	NP	-	-
4		BPIEP-bulk	90/3	MVK	-	NP	-	-
5	MBB ^{f)} / CuBr	<i>dn</i> Nbpy ^{g)} /Tol	90/48	MVK	-	NP	-	-
6		PMDETA ^{g)} /Tol	90/48	MVK	-	NP	-	-
7		NPPI ^{g)} /Tol	90/48	MVK	-	NP	-	-
8 ^{h)}		PMDETA/THF	90/5.5	MVK	-	NP ^{k)}	-	-
9 ⁱ⁾	EBiB/ CuX	PMDETA /Tol	90/5.5	MVK	-	NP	-	-
10 ^{j)}		Tol	90/5.5	MVK	-	NP	-	-
11	AIBN/ CuX ₂ ^{g)}	bpy ^{g)} /THF	70/20	MVK	-	NP	-	-
12		bpy-bulk	70/20	MVK	-	NP	-	-
13	AIBN/ CuBr ₂	BPIEP-bulk	70/20	MVK	-	NP	-	-
14	AIBN/ CuX ₂	bpy -bulk	70/24	MMA (3)	MVK (1)	70 ^{l)}	7,400	1.71
15		BPIEP-bulk	70/24	MMA (3)	MVK (1)	< 1 ^{m)}	-	-

^{a)} Initiator/catalyst; ^{b)} Ligand/ solvent.; ^{c)} gravimetrically; ^{d)} free radical polymerization using 1 mole % of 2,2'-azobisisobutyronitrile (AIBN) wrt monomer; ^{e)} ATRP and RATRP using CuX and CuX₂ (X = Cl, Br); [MVK]: [I]: [CuX]: [L] = 127: 1: 1: 2 and [MVK]: [AIBN]: [CuX₂]: [L] = 100: 0.5: 1: 2; ^{f)} MBB: 3-bromo-3-methyl-butanone-2,

^{e)} *dn*Nbpy: 4,4'-di(*n*-nonyl)-2,2'-bipyridine; BPIEP: 2,6-bis[1-(2,6-diisopropylphenylimino)ethyl] pyridine; PMDETA: N,N,N',N',N''-pentamethyldiethylenetriamine; NPPI: N-(*n*-propyl)-2-pyridyl methanimine; bpy: 2,2'-bipyridine; ^{h)} reaction performed in polar solvent, THF, where [C]: [L] = 1: 2, DP = 127, ⁱ⁾ reaction performed using less concentration of ligand ([C]: [L] = 1: 0.5, DP = 127), ^{j)} reaction performed without ligand, ^{k)} NP: no polymer, ^{l)} Bulk copolymerization using 1.84 mL of MMA and 0.5 mL of MVK (DP = 50), [M]: [AIBN]: [CuX₂]: [L] = 100: 0.5: 1: 2); ^{m)} Very low conversion; the polymer was difficult to filter.

During the polymerization, the color of the reaction mixture changed to reddish-brown or green depending on the nature of ligands used for the reaction. However, the reaction mixture when poured into hexane after passing through a short alumina column did not produce any polymer. GC studies demonstrated that the reaction mixture contained a large amount of unreacted MVK in all the reactions. Disappointingly, no polymer could be obtained in all of the ATRP reactions. Experiments carried out in the presence of low concentration of ligand and in the absence of ligand have also failed to produce polymer (Table 8.1, entry 8-9). This clearly shows that the MVK is competing for complexation with CuBr. Upon scanning several initiating systems such as ethyl-2-bromoisobutyrate (EBiB), 3-bromo-3-methylbutanone-2 (MBB),¹⁴ and AIBN/CuX₂ (reverse ATRP), it was confirmed that none of the copper containing initiating systems could polymerize MVK. This confirms that MVK could not be polymerized using copper mediated ATRP. The fact that the radical polymerization of MVK produces polymer and the copper mediated ATRP initiating system does not produce polymer indicates that the copper catalyst is the cause for the inhibition of polymerization.²²

8.2.3. Evidences for the coordination of copper halide and MVK

Vinyl monomers having donor atoms such as N or O could coordinate with transition metal catalyst and could complicate the ATRP. Matyjaszewski and coworkers have shown that an interaction of monomer with copper having tetraphenylborate counterion led to the formation of π -complex.²³ Moreover, Haddleton and coworkers have shown that the reactivity of aminoethylmethacrylate differs significantly due to a strong monomer-coordination with catalyst in ATRP.²⁴ In an attempt to examine the complexation of copper with MVK, an admixture of MVK and copper halide was prepared by adding a small amount of CuBr (~10 mg) in 10 mL of MVK and kept the mixture stirring for 1 h at 30 °C. The CuBr completely dissolved in MVK and the solution becomes homogeneous. After an hour, excess MVK was pumped off under vacuum (10⁻⁴ torr) for 4-5 h. A transparent pale yellow viscous residue was obtained, which was subjected to FT-IR, NMR and UV-vis spectroscopic analysis.

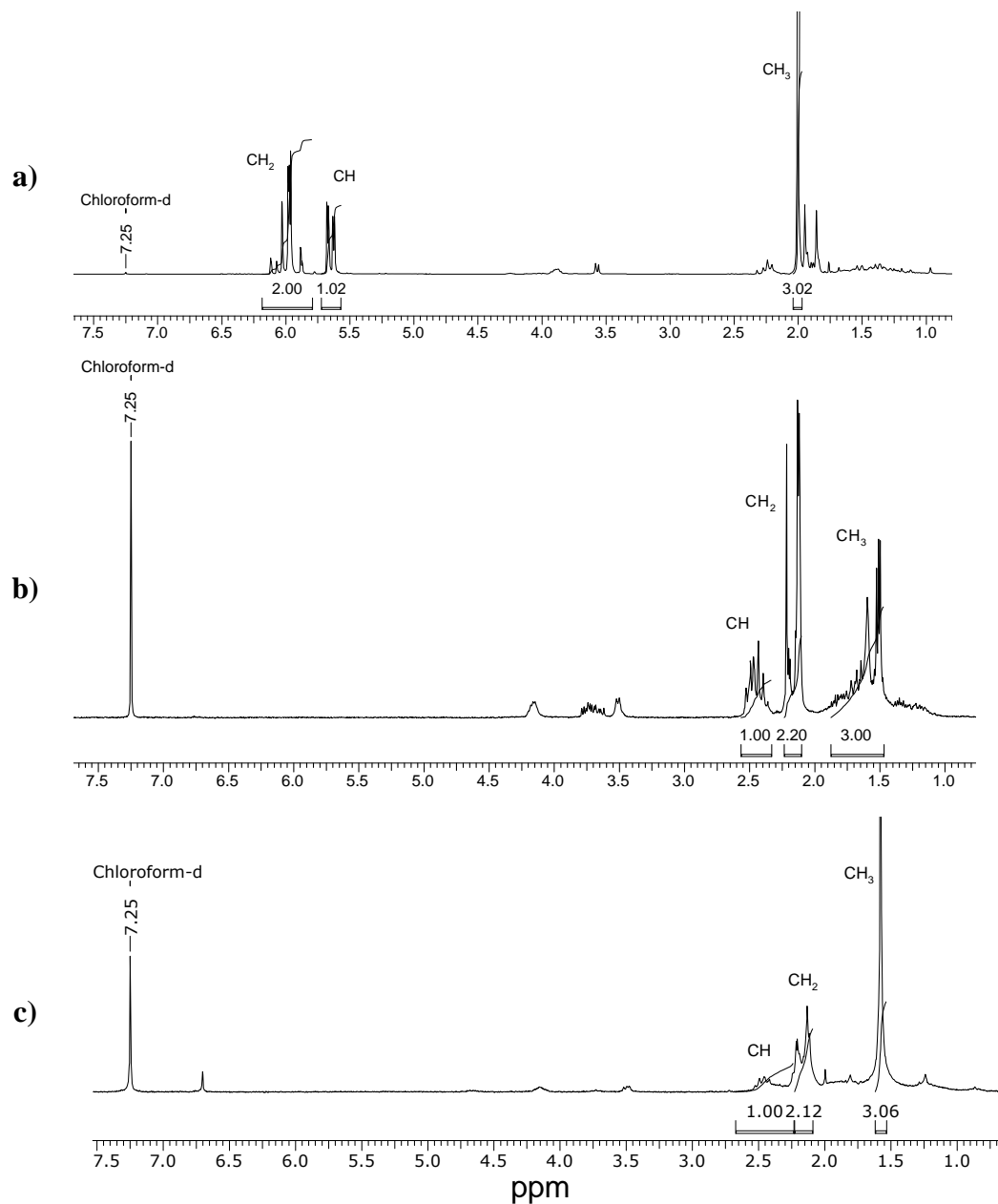


Fig. 8.2: $^1\text{H-NMR}$ spectra of the admixture residue after removing excess MVK in CDCl_3 (a) neat MVK, (b) residue of 1:1 mixture of MVK and CuBr, and (c) residue of CuBr mixed with excess of MVK.

If there were no interaction between CuBr and MVK, the residue should contain only CuBr free from MVK. However, the residue showed the presence of signals corresponding to MVK in IR and $^1\text{H NMR}$. The $^1\text{H NMR}$ spectrum of MVK-CuBr complex showed a huge

up-field shift of vinyl and CH₃ protons of MVK indicating an enhanced π -electron interaction of vinyl groups with copper (Fig. 8.2). The vinyl protons are shifted to 2.3 and 2.4 ppm from 5.2 and 6.0 ppm (Fig. 8.2c). Similarly, the methyl protons are seen at 1.6 ppm in the complexed MVK. The huge up-field shift of vinyl and methyl protons is attributed to the delocalization of π -electron participating in the coordinative complex formation with copper halide. In the case of 1:1 admixture of MVK-CuBr, the signals corresponding to the up-field splitting patterns of CH₂=CH- are also seen adjacent to -CH₃ signals at 1.5 ppm which support the coordination of copper with MVK is progressive in nature depending upon the concentration. The presence of coordinative complex between MVK and CuBr can also be seen in the FT-IR which showed the vinyl, carbonyl and CH₃ peaks of MVK had a substantial shift ($\Delta\nu$) -106, -12, and -27 cm⁻¹ respectively (Table 8.2).

Table 8.2: IR, UV and ¹H-NMR shifts on mixing methylvinyl ketone and copper bromide ^{a)}

Substrate	IR ^{b)} stretching (ν or $\Delta\nu$, cm ⁻¹)			UV ^{c)} (λ or $\Delta\lambda$, nm)	¹ H-NMR ^{d)} (δ or $\Delta\delta$ ^{e)} ppm)		
	C=C	C=O	C-H	C=O	CH ₂ =	CH=	COCH ₃
MVK	1618	1683	2925	325	5.91	6.19	2.25
MVK-CuBr	-106	-27 (1236) ^{f)}	-12	-4	+3.78	+3.73	+0.67
Me ₂ CO	-	1742	2977	Nd ^{g)}	-	-	2.16
Me ₂ CO-CuBr	-	+27	+50	Nd ^{g)}	-	-	+0.92

^{a)} Shift ($\Delta\nu$ or $\Delta\lambda$ or $\Delta\delta$) = value before complexing – value after complexing with CuBr; ^{b)} Performed using KBr pellet; ^{c)} UV performed in chloroform; ^{d)} ¹H-NMR recorded on 200 MHz spectrometer using CDCl₃ as solvent; ^{e)} Shift is calculated based on the δ value of an intense peak; ^{f)} New peak due C-O stretching ; ^{g)} Not done

In addition, a new peak at 1236 cm⁻¹ has appeared which corresponds to the C-O stretching frequency similar to the ones present in carboxylic acids.²⁵ This confirms the presence of extended coordinative complex between MVK and CuBr (Fig. 8.3). A similar shift in IR frequency was also observed in acetone-CuBr admixture suggesting the coordination of copper is present in all ketones (Table 8.2). In the case of MVK, the vinyl group also participates in the coordination as seen in ¹H NMR (Fig. 8.2).

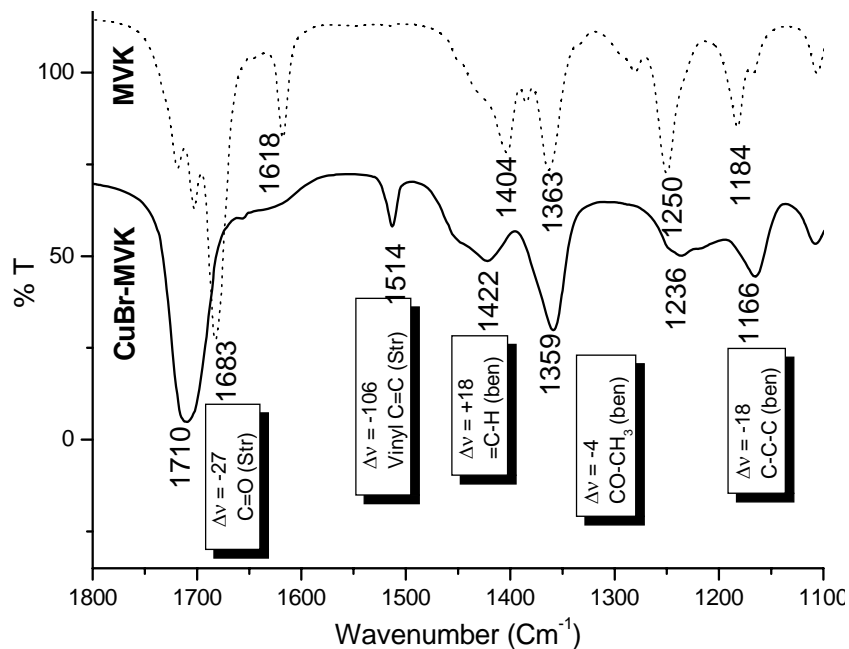


Fig. 8.3: (a) FTIR spectra showing stretching frequencies of MVK and (b) MVK-CuBr over KBr pellet

The UV-vis spectra of the MVK-CuBr complex in chloroform had a blue shift corresponding to $n \rightarrow \pi^*$ transition indicating a relatively strong interaction of carbonyl chromophore with copper (Table 8.2). The exact nature of the coordination of copper with vinyl and ketone of MVK is clearly not known.

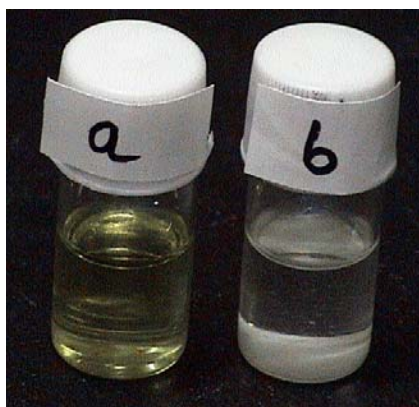


Fig. 8.4: Solutions of CuBr a) homogeneous in excess MVK (4 mg/mL) and b) heterogeneous in excess MMA (5 mg/mL).

A crystalline tetrameric complexes of MVK with copper(I) chloride has been reported at low temperature ($-100\text{ }^{\circ}\text{C}$).^{26,27} A physical mixture of CuBr in excess MVK and MMA produces

homogeneous and heterogeneous solutions respectively indicating the presence of a strong ketone-coordination as compared to ester-coordination in MMA (Fig. 8.4).

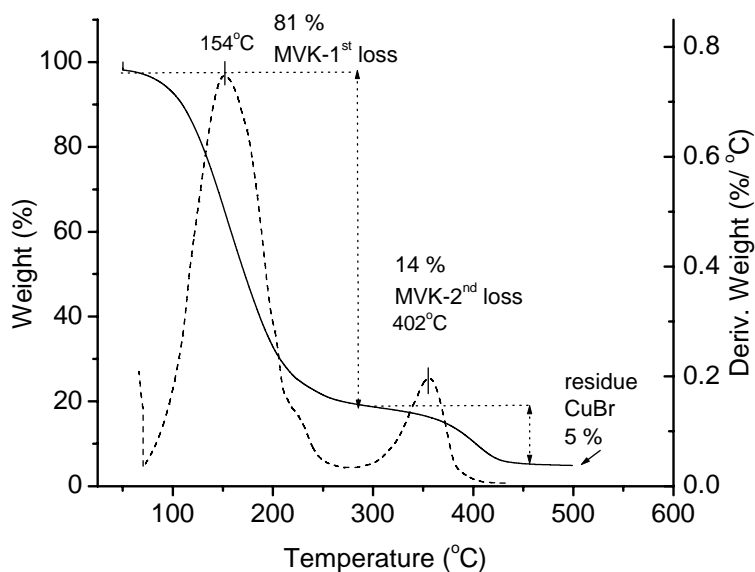


Fig. 8.5: TGA of viscous residue of $(\text{MVK})_m\text{-(CuBr)}_n$ admixture after removing all free MVK under vacuum. The calculation indicates 0.97:0.30 mole ratio of MVK:CuBr in the complex. This supports the extended coordination of MVK with CuBr through vinyl as well as carbonyl groups.

After removal of free MVK, the residual admixture of MVK-CuBr is viscous at room temperature, which also suggests that the nature the coordination with CuBr is non-stoichiometric and the coordination could be an extended network. Thermogravimetric analysis (TGA) of the residue showed 95 wt % loss at $T_{\text{max}} \sim 154 \text{ }^\circ\text{C}$ and $\sim 402 \text{ }^\circ\text{C}$ which were attributed to the decomposition of MVK and thermally polymerized MVK respectively. The residue at 500 °C was around 5 wt % corresponding to CuBr (Fig. 8.5). This indicates 0.97: 0.30 mole ratio of $(\text{MVK})_m\text{-(CuBr)}_n$ in the complex which confirms that the coordination of MVK to CuBr is non-stoichiometric in nature. On the basis of the results obtained through spectroscopy and the TGA, we propose an extended-coordination structure for $(\text{MVK})_m\text{-(CuBr)}_n$ (Fig. 8.6).

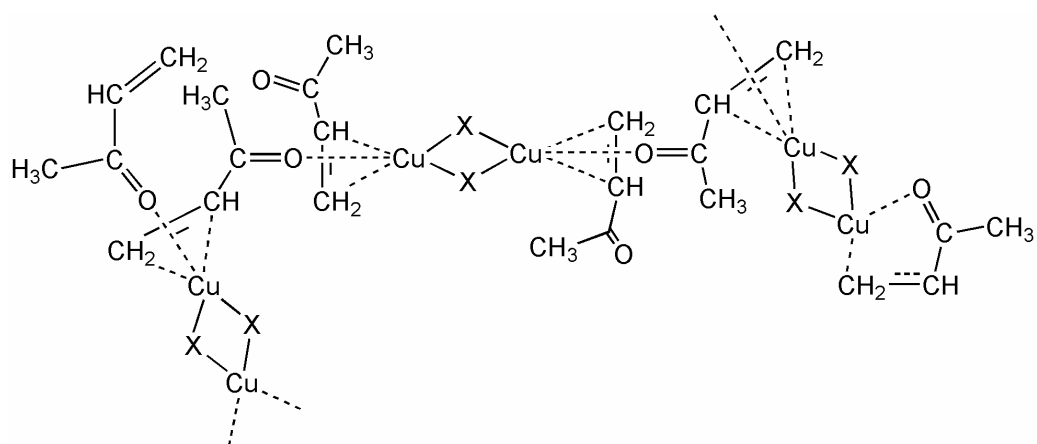


Fig. 8.6: Proposed extended-coordinative structure of $(\text{MVK})_m-(\text{CuBr})_n$ based on X-ray crystal structure of MVK-CuCl .^{26,27} Note that the structure shows both trans-conformation, inter and intra molecular MVK coordination with CuX dimer.

It has been reported by van Koten that a decrease in stretching frequency of $\text{C}=\text{O}$ was noticed in MMA from 1720 cm^{-1} to 1580 cm^{-1} due to a monomer-coordination with catalyst.²⁸ The presence of monomer-coordination has also been observed in ATRP of N,N-dimethylacrylamide (NDMA).^{29,30} In all these cases, the presence of monomer-coordination with metal catalyst did not suppress the polymerization. The coordination of copper with monomer would influence the equilibrium of activation and the deactivation processes in ATRP and, thus it could significantly alter the kinetics of the polymerization. In the case of MVK, the coordination of copper appears to be very strong, extensive and completely inhibited the polymerization. On the basis of the literature and the present study, the monomer coordination with copper catalyst in ATRP is very high in MVK than NDMA and MMA monomers (Fig. 8.7).

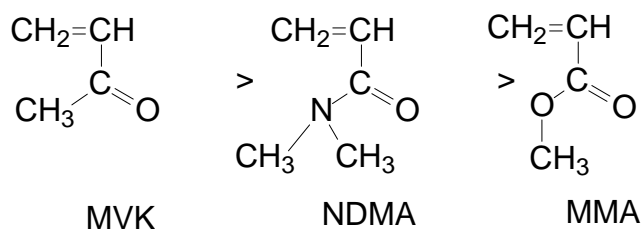


Fig. 8.7: The order of monomer coordination with copper halide

The extended coordination of copper with MVK renders the monomer non-reactive for the polymerization. In case of ATRP, it appears that the catalyst is not available for the redox process with the initiator due to the monomer coordination. In case of reverse ATRP, the

formed initial radicals (initiator or oligomeric) could have added to copper coordinated MVK and then become inactive either before or after undergoing a single redox cycle.

8.2.4. Copolymerization of MMA and MVK using reverse ATRP

Classical free radicals are generated in reverse ATRP, which subsequently gets transformed into dormant carbon-halide chain-ends in the presence of CuX_2 for a smooth controlled polymerization. Nevertheless, the copolymerization of MVK (0.5 mL) and MMA (1.8 mL) using AIBN (39 mg) as initiator and CuCl_2 (66 mg) as catalyst in bulk produced copolymer (Table 8.1, run 14 and run 15). It is believed that the copper coordinated MVK, after undergoing a single redox cycle, would have a different reactivity, which can undergo copolymerization with other reactive monomers.

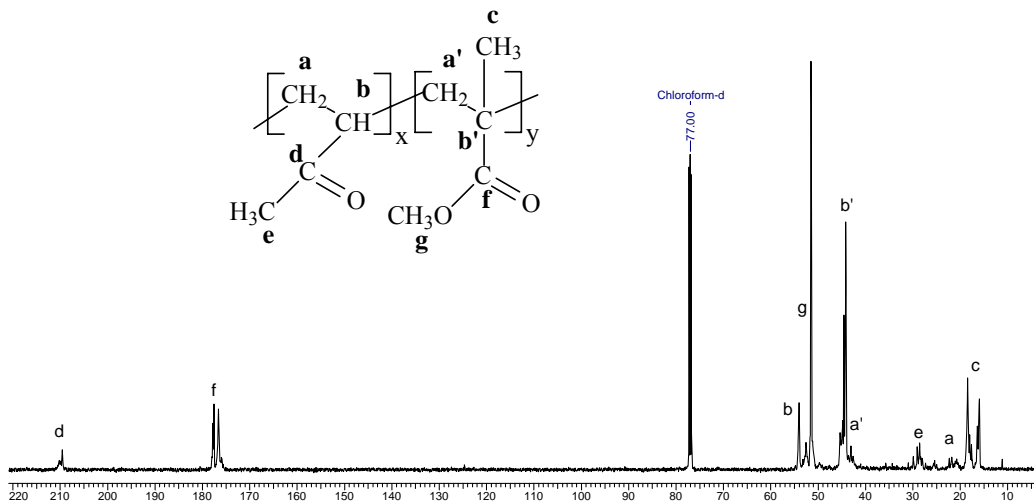


Fig. 8.8: ^{13}C NMR spectrum of the poly(MMA-*co*-MVK) obtained by reverse ATRP in CDCl_3

Unlike the homopolymerization, the copolymerization proceeded in bulk and produced polymer with $M_w/M_n = 1.7$ (70 % yield), which indeed, was a copolymer containing both MMA and MVK repeat units as confirmed by ^1H and ^{13}C NMR (Fig. 8.8). This indicates that the copper coordinated MVK may be in equilibrium with free MVK, which under goes copolymerization with MMA via reverse ATRP. However, the poly (MMA-*co*-MVK) showed that the content of MVK is very low. The composition of MMA in the copolymer was found to be six times higher than the composition of MVK as shown in Fig. 8.8.

8.3. Conclusions

The synthesis of PVAc and its copolymers through post analogous reaction of PMVK using Baeyer Villiger oxidation was performed using free radically polymerized MVK. Several attempts were made to polymerize MVK in a controlled manner using ATRP and reverse ATRP in the presence of copper catalyst. It was found that the copper mediated controlled polymerization of MVK failed to produce polymers through ATRP and reverse ATRP in the presence of different N-donors as ligands and using initiators like, ethyl-2-bromoisobutyrate (EBiB), and 3-bromo-3-methyl-butanone-2 (MBB), and AIBN. Unsuccessful polymerization of MVK in the presence of copper catalyst is attributed to the presence of extended coordination of MVK with copper as identified by the admixture complexes of MVK and CuBr in FT-IR, ¹H NMR, and UV-vis spectroscopic studies. However, the copper coordinated MVK was found to undergo copolymerization with MMA in reverse ATRP.

8.4. References

1. Matyjaszewski, K.; Spanswick, J. *Materials Today* **2005**, 3, 26.
2. (a) Wang, J.-S.; Matyjaszewski, K. *J. Am. Chem. Soc.* **1995**, 117, 5614. (b) Wang, J.-S.; Matyjaszewski, K. *Macromolecules* **1995**, 28, 7901.
3. Kato, M.; Kamigaito, M.; Sawamoto, M.; Higashimura, T. *Macromolecules* **1995**, 28, 1721.
4. (a) Kharasch, M. S.; Jensen, E. V.; Urry, W. H. *Science* **1945**, 102, 128. (b) Kharasch, M. S.; Jensen, E. V.; Urry, W. H. *J. Am. Chem. Soc.* **1945**, 67, 1626.
5. (a) Minisci, F. *Acc. Chem. Res.* **1975**, 8, 165. (b) Curran, D. P. *Synthesis* **1988**, 489. (c) Iqbal, J.; Bhatia, B.; Nayyar, N. *Chem. Rev.* **1994**, 94, 519.
6. (a) Patten, T. E.; Matyjaszewski, K. *Acc. Chem. Res.* **1999**, 32, 895. (b) Matyjaszewski, K. *Chem. Eur. J.* **1999**, 5, 3095. (c) Matyjaszewski, K.; Xia, J. *Chem. Rev.* **2001**, 101, 2921.
7. Coessens, V.; Pintauer, T.; Matyjaszewski, K. *Prog. Polym. Sci.* **2001**, 26, 337.
8. Mardare, D.; Matyjaszewski, K. *Macromolecules* **1994**, 27, 645.
9. Iovu, M. C.; Matyjaszewski, K. *Macromolecules* **2003**, 36, 9346.
10. Xia, J.; Paik, H.-J.; Matyjaszewski, K. *Macromolecules* **1999**, 32, 8310.
11. Simal, F.; Delfosse, S.; Demonceau, A.; Noels, A. F.; Denk, K.; Kohl, F. I.; Weskamp, T.; Herrmann, W. A. *Chem. Eur. J.* **2002**, 8, 3047.
12. Wakioka, M.; Baek, K. Y.; Ando, T.; Kamigaito, M.; Sawamoto, M. *Macromolecules* **2002**, 35, 330.
13. Mittal, A.; Sivaram, S. *J. Polym. Sci. Part A: Polym. Chem.* **2005**, 43, 4996.
14. Roychoudhury, R.; Kühn, S.; Schott, H.; Kössel, H. *FEBS Lett.* **1975**, 50, 140.
15. Marvel, C. S.; Levesque, C. L. *J. Am. Chem. Soc.* **1938**, 60, 280; **1939**, 61, 3234.
16. Lyons, A. R. *J. Polym. Sci., Macromol. Rev.* **1972**, 6, 251.
17. Schildknecht, C. E.; Zoss, A. O.; Grosser, F. *Ind. Eng. Chem.* **1949**, 41, 2891.

18. Webster, O. W.; Hertler, W. R.; Sogah, D. Y.; Farnham, W. B.; RajanBabu, T. V. *J. Am. Chem. Soc.* **1983**, 105, 5706.
19. Merle-Aubry, L.; Merle, Y. *Die Makromol. Chem.* **1975**, 176, 709.
20. Matsuzaki, K.; Kanai, T.; Aoki, Y. *Makromol. Chem.* **1981**, 182, 1027.
21. Kosaka, N.; Hiyama, T.; Nozaki, K. *Macromolecules* **2004**, 37, 4484.
22. Bulk polymerization of MVK was attempted using EBiB as initiator in the presence of FeCl₂ as catalyst and BPIEP as ligand. The ratio of the reagents was kept as [MVK]: [EBiB]: [FeCl₂]: [BPIEP] = 100: 1: 1: 2 and the polymerization was conducted at 90 °C for 18 h. This initiating system also failed to polymerize MVK indicating a strong coordination of MVK with FeCl₂.
23. Braunecker, W. A.; Pintauer, T.; Tsarevsky, N. V.; Kickelbick, G.; Matyjaszewski, K. *J. Organomet. Chem.* **2005**, 690, 916.
24. Lad, J.; Harrison, S.; Mantovani, G.; Haddleton, D. M. *Dalton Trans.* **2003**, 4175.
25. Gordon, A. J. *Chemists Companion: A Handbook of Practical Data, Techniques and References*; John Wiley & Sons, Inc., 1972.
26. Anderson, S.; Hakansson, M.; Jagner, S.; Nilsson, M.; Urso, F. *Acta Chem. Scand. A.* **1986**, 40, 194.
27. Hakansson, M.; Jagner, S. *J. Organomet. Chem.* **1989**, 361, 269.
28. van de Kuil, L. A.; Grove, D. M.; Gossage, R. A.; Zwikker, J. W.; Jenneskens, L. W.; Drenth, W.; van Koten, G. *Organometallics* **1997**, 16, 4985.
29. Teodorescu, M.; Matyjaszewski, K. *Macromolecules* **1999**, 32, 4826.
30. Rademacher, J. T.; Baum, M.; Mical, E.; Brittain, W. J.; Simonsick, W. J. *J. Macromolecules* **2000**, 33, 284.

Chapter 9. Summary and Conclusions

9.1. Summary and conclusions

The present thesis deals with the atom transfer radical polymerization (ATRP) of methyl methacrylate (MMA) and other acrylates as well as styrene using Schiff base imines as N-donor ligands complexed with copper halide in conjunction with suitable initiators in order to achieve controlled polymerization. The study involves a detailed investigation of a new tridentate N-donor ligand comprising batch, kinetics, solvent, temperature, aging and substituents effects differing in electronic and steric property, on the course of ATRP. The other part of the study involves the use of new initiators such as, 3-bromo-3-methylbutanone-2 (MBB), 3-(bromomethyl)-4-methylfuran-2,5-dione (BMFD) and 2-bromo propionitrile (BPN) for ATRP of MMA. In the course of this investigation, ATRP of a vinyl ketone monomer, namely, methyl vinyl ketone (MVK) was also examined using an initiator that has structural similarity to the propagating radical. The salient highlights of the present work as well as important conclusions are summarized below.

- † A tridentate ligand, 2,6-*bis* [1-(2,6-diisopropylphenylimino) ethyl] pyridine (BPIEP) Cu(I) halide complex was successfully employed in ATRP of MMA. Effect of various parameters, such as, solvent, temperature, and initiator, was studied using this ligand. In all the cases, the rate of polymerization followed first order kinetics. Controlled nature of the polymerization was confirmed by chain extension studies using a pre-formed polymer by ATRP. The ligand was also found to be very effective for reverse ATRP. Steric and electronic environment around the metal atom has a profound influence on the course of ATRP. Reducing the steric bulk of the ligand proved to be detrimental for controlled polymerization. In addition, a new N-donor ligand, 2,6-*bis*(4,4-dimethyl-2-oxazolin-2-yl) pyridine (*dm*PYBOX) was synthesized. When it was complexed with Cu(I)Br, the ligand caused controlled polymerization of MMA.

- † Three different ATRP initiators (MBB, BMFD, and BPN) resulted in controlled radical polymerization of MMA at 90 °C in toluene as solvent and BPIEP/CuBr as the catalyst system. The rate of polymerization followed first-order kinetics. Apparent rate constant (k_{app}) and initiator efficiency (I_{eff}) decreased in the following order BPN > MBB > EB/B. A simple cyclic anhydride (BMFD) proved to be an efficient initiator for ATRP of MMA. All the initiators works efficiently with tridentate N-donor ligand, BPIEP; other well-known ATRP ligands were inefficient. The mechanism of initiation with BMFD was elucidated. An interesting intramolecular radical ring closure, after the addition of the first monomer, preceded propagation reaction resulting in an unexpected head group.
- † In view of the structural resemblance between the initiator MBB and the propagating chain end of methylvinylketone (MVK). Polymerization of MVK was studied by ATRP as well as reverse ATRP. Surprisingly, there was no polymerization in both the processes. A detailed investigation for non-polymerizing nature of MVK was undertaken. Results established that a strong association exists between the monomer and the catalyst resulting in the deactivation of the catalytic cycle.

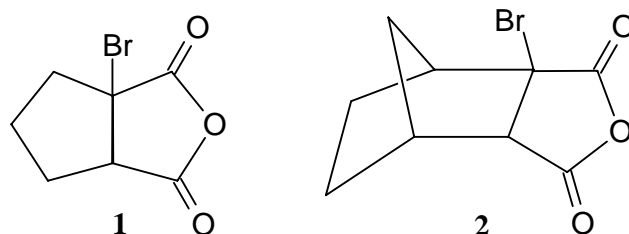
9.2. Scope for future work

The present research on controlled radical polymerization of methyl methacrylate has opened up many new prospects for future research.

- † Possibility of isolable Cu^I complexes derived from BPIEP and *dm*PYBOX should be explored. Well defined, isolable and structurally pure complexes are needed to establish the optimum geometry of the complex as well as reaction rate dependence on catalyst structure and stoichiometry.
- † A systematic investigation of the effect of varying the electronic environment around the metal, keeping the steric environment constant for a tridentate ligand on the rate of polymerization of MMA is worthy of investigation. For instance, instead of selecting $-N(Me)_2$ substituent a more appropriate electron donating substituent which cannot, by itself, interact with Cu(II)/ Cu(I) pair may be more appropriate for

unambiguously delineating the effect of electron donating substituent around the ligand.

- † The proposed mechanism of BMFD initiated ATRP of MMA, invokes a tertiary bridgehead C-Br bond α to an anhydride moiety. If this is true, it must be possible to use initiators of the type **1** and **2** for ATRP of MMA.



This may provide a convenient way to synthesize anhydride end functional PMMA.

- † It may be interesting to explore controlled polymerization of MVK *via* a radical addition chain-transfer termination (RAFT) approach.

Publications

- † "A novel tridentate N-donor as ligand for copper catalyzed ATRP of MMA" A. Mittal and S. Sivaram. (*J. Polym. Sci. Polym. Chem.*, **2005:43**, **4996**).
- † "Unfavorable Coordination of Copper with Methyl Vinyl Ketone in Atom Transfer Radical Polymerization". A. Mittal, D. Baskaran and S. Sivaram". (In press, *Macromolecules*, **39**, **5555**, **2006**)
- † "Copper Catalyzed ATRP of Methylmethacrylate Using Aliphatic Bromo Ketone Initiator" A. Mittal, D. Baskaran and S. Sivaram. (In press, *Macromolecular Symposia*, **240**, **238**, **2006**).
- † "Intramolecular ring closure followed by initiation of controlled radical polymerization: 3-(bromomethyl)-4-methylfuran-2,5-dione as a novel ATRP initiator", *Macromolecules*, A. Mittal and S. Sivaram (*Under Communication*).
- † "Influence of steric and electronic effects around the metal center in ATRP of methyl methacrylate using *bis*(iminopyridine) ligand", *J. Polym. Sci. Polym. Chem.*, A. Mittal and S. Sivaram (*Under Communication*).

Posters and Presentations

- † " *Studies in Atom Transfer Radical Polymerization Using a Tridentate N-Donor Ligand: New Monomers and Initiators* " **A. Mittal**, D. Baskaran and S. Sivaram, poster presented in "IP 2005" an international symposium on Ionic Polymerization (Under the auspices of International Union of Pure and Applied Chemistry-IUPAC), October 2005, held at Goa, India.
- † " *A novel tridentate nitrogen donor as ligand in copper catalyzed ATRP of methylmethacrylate: Influence of ligand concentration* " **A. Mittal** and S. Sivaram, poster presented in "Macro 2004" an international conference on

polymers for advanced technologies, December 2004, held at RRL Thiruvananthapuram, Kerala, India. *Dec. 15-17, 2004 (2004), PA.50/1-PA.50/5, CAN 144:70135*

- † "*Atom transfer radical polymerization: An approach to controlled radical polymerization*". **A. Mittal** and S. Sivaram, oral presentation in "Macro 2002" an international seminar on frontiers of polymer science and engineering, December, 2002 held at I.I.T Kharagpur, West Bengal, India.
- † "*Atom transfer radical polymerization: An approach to controlled radical polymerization*". **A. Mittal**, D. Baskaran and S. Sivaram, poster presentation at "*NCL-TU/e, Eindhoven*, Joint seminar at NCL, Pune, February, 2001.

Ph.D. Seminars Delivered

- † Electronically Conducting Polymers: Precise Length and Control
- † Matrix Assisted Laser Desorption Ionization-Time of Flight (MALDI-TOF) Analysis of Polymers
- † Atom Transfer Radical Polymerization: An approach to controlled radical polymerization.